University of Plymouth

PEARL **https://pearl.plymouth.ac.uk**

04 University of Plymouth Research Theses 01 Research Theses Main Collection

1995

DEVELOPMENT OF A TRACER TECHNIQUE FOR THE STUDY OF SUSPENDED SEDIMENT DYNAMICS IN AQUATIC ENVIRONMENTS

MARSH, JONATHAN K.

http://hdl.handle.net/10026.1/1795

http://dx.doi.org/10.24382/3618
University of Plymouth

All content in PEARL is protected by copyright law. Author manuscripts are made available in accordance with publisher policies. Please cite only the published version using the details provided on the item record or document. In the absence of an open licence (e.g. Creative Commons), permissions for further reuse of content should be sought from the publisher or author.

DEVELOPMENT OF A TRACER TECHNIQUE FOR THE STUDY OF SUSPENDED SEDIMENT DYNAMICS IN AQUATIC ENVIRONMENTS

JONATHAN K MARSH

LIBRARY

A thesis submitted to the University of Plymouth

in partial fulfilment for the degree of

DOCTOR OF PHILOSOPHY

Institute of Marine Sciences

University of Plymouth

In collaboration with Plymouth Marine Laboratory

Natural Environment Research Council

LIBRARY

February 1995

LIBRARY STORE

LIBRARY

UNIVERSITY OF
Item No. 900 2656995
Date 1 DEC 1998 S
Class No T 551.4609 M AR
Contl. No X703260900
LIBRARY SERVICES

90 0265699 5

REFERENCE ONLY

LIBRARY

LIBRARY STORE

This copy of the thesis has been supplied on condition that anyone who consults it is understood to recognise that its copyright rests with its author and that no quotation from the thesis and no information derived from it may be published without the author's prior written consent.

Signed .....

Date....28.12.95.....

DEVELOPMENT OF A TRACER TECHNIQUE FOR THE STUDY OF SUSPENDED SEDIMENT DYNAMICS IN AQUATIC ENVIRONMENTS

J. K. MARSH

ABSTRACT

The development and field testing of a particle tracing technique for the prediction and monitoring of cohesive sediment transport is described. Natural, chemical and water soluble dye tracers have been used for many years to determine water circulation in order to predict sediment transport. Radioactive and fluorescent particles have been used widely to predict sediment particle transport, but have been restricted mainly to non-cohesive sand and gravel transport studies due to the difficulties of preparation, handling, disassociation of the label from the particle and labour-intensive analysis. The development of a fine cohesive tracing technique therefore offered a significant advancement for the understanding and prediction of fine cohesive sediment and pollutant dynamics in aquatic environments if a sediment analogue could be developed.

The physical properties, including size, surface charge, fluorescence and settling velocity of natural fine cohesive sediment were analysed in order to passively and actively adsorb organic fluorescent dyes onto the sediment surface; the tests were largely unsuccessful. The physical properties of artificial fluorescent particles as sediment analogues were examined and found to have a close correlation to natural sediment. Analysis of the fluorescent particles in mud suspensions on an Analytical Flow Cytometer offered an automated and accurate method of tracer concentration determination at low dilutions. A preliminary field study was carried out in a small pool with encouraging results.

A study in a shallow freshwater lake was carried out to determine the sediment dynamics in the lake. A depth-averaged model of the wind-driven circulation within the lake was used to interpret the distribution of tracer. Secondary transport and deposition clearly led to an accumulation of sediment and internal loading in the lake driven by hydrodynamical forcing.

A study of the particle residence time and deposition-resuspension processes in the turbidity maximum of a macro-tidal estuary. Fluorescent particles were released into the turbidity maximum and were advected down-estuary on the ebb tide and up-estuary on the flood tide. The residual mass budgets indicated a significant deposition of the particles in the upper estuary at slack high water. The particles were detected in estuarine surface waters 1 week after release.

The fluorescent particles behaved in a similar way to the suspended sediment in both the lacustrine and estuarine study and were considered as sutiable tracers for cohesive sediment.

2.2 SEDIMENT TRACING - A REVIEW 21

2.2.1 Introduction 22
2.2.2 Photoluminescence: Phosphorescence and Fluorescence 22
2.2.3 Fluorescent Water Dyes 24

2.3 PARTICLE TRACERS 25

2.3.1 Introduction 25
2.3.2 Natural Tracers 26
2.3.3 Chemical Tracers 27
2.3.4 Radioactive Tracers 28

2.4 FLUORESCENT TRACER AND DETECTORS 29

2.4.1 Fluorescent Tracer Particle Studies 29
2.4.2 Analytical Flow Cytometry 31

CHAPTER 3 SEDIMENT PARTICLE CHARACTERISATION AND THE EVALUATION OF ADSORBING FLUORESCENCE ONTO THE SEDIMENT SURFACE.

3.1 INTRODUCTION 34

3.2 PHYSICAL ASPECTS 35

3.2.1 Introduction 35
3.2.2 Size and Density 35
3.3.3 Surface Charge 38
3.2.3.1 Previous Studies 38
3.2.3.2 Method and Results 40
3.2.4 Settling Velocity 41

CONTENTS

PAGE

CHAPTER 1 GENERAL INTRODUCTION

1.1 INTRODUCTION 1

1.1.1 Importance of Fine Sediments 1

1.1.2 Sediment and Pollutant Dynamics with Respect to Lakes and Estuaries 3

1.2 SEDIMENT TRANSPORT 4

1.2.1 Techniques to Assess Sediment Transport 6

1.2.2 Fine Cohesive Sediment Transport Processes 6

1.2.2.1 Erosion and Resuspension 6

1.2.2.1 Deposition - Settling Velocity and Flocculation 9

1.2.2.3 Consolidation 11

1.2.3 Discussion 12

1.3 SEDIMENT TRANSPORT IN LAKES AND ESTUARIES 12

1.3.1 Introduction 12

1.3.2 Lakes 13

1.3.3 Estuaries 15

1.3.4 Discussion 18

1.4 OBJECTIVES AND OUTLINE OF THE RESEARCH 19

CHAPTER 2 THE STUDY OF SEDIMENT DYNAMICS USING PARTCLE TRACER TECHNIQUES.

2.1 INTRODUCTION 21

3.2.4.1 Introduction 41

3.2.4.2 Measurements of Settling Velocity 43

3.2.4.3 Settling Velocity Studies 43

3.3 LABORATORY EXAMINATIONS OF ADSORBING FLUORESCENCE ON TO THE SEDIMENT SURFACE 46

3.3.1 Natural Fluorescent Organisms in Freshwater and Seawater 46

3.3.2 Fluorescent Dyes 47

3.3.3 Detection Equipment and Standardisation 47

3.3.4 Passive Adsorption of Dye 48

3.3.5 Active Adsorption using Natural Organics 50

3.3.6 Active Adsorption using a Synthesised Organic Compound 51

3.4 FLUORESCENT PAINTING OF SEDIMENT 54

3.5 DISCUSSION 55

CHAPTER 4 ARTIFICIAL FLUORESCENT SEDIMENT ANALOGUES: CHARACTERISTICS, DETECTION AND PRELIMINARY FIELDWORK.

4.1 INTRODUCTION 57

4.2 ANALYTICAL FLOW CYTOMETER (AFC) 57

4.2.1 Initial Investigations and Calibration of the AFC 57

4.2.2 Assessment of Artificial Fluorescent Particles 60

4.2.3 Analysis of the Artificial Fluorescent Particles on the AFC 63

4.2.4 Calibration of the AFC using the Artificial Fluorescent Particles 64

4.3 PHYSICAL CHARACTERISTICS OF THE FLUORESCENT PARTICLES 67

4.3.1 Stability 67
4.3.2 Size and Density 69
4.3.3 Surface Charge 69
4.3.4 Settling Velocity of Sediment and Fluorescent Particle Admixtures 70
4.3.5 Discussion 71

4.4 PRELIMINARY FIELDWORK EXPERIMENT 72

4.4.1 Introduction 72
4.4.2 Experimental Method 72
4.4.3 Sample Analysis Procedure 75
4.4.4 Results 76
4.4.5 Discussion 77

4.5 EVALUATION AND FUTURE APPLICATION OF THE TRACER PARTICLES 78

CHAPTER 5 A PARTICLE-TRACING EXPERIMENT IN A SMALL SHALLOW LAKE.

5.1 INTRODUCTION 79

5.2 LAKE HYDRODYNAMICS 79

5.2.1 Introduction 80
5.2.2 Wind Stress Induced Setup 80
5.2.3 Wind-wave Mechanics 81

5.3 SEDIMENT DEPOSITION MECHANISMS IN LAKES 84

5.4 STUDY SITE DESCRIPTION 86

5.4.1 Geological Formation and Catchment 86
5.4.2 Climate, Bathymetry and Hydrography 89
5.4.3 Past Studies 91
5.4.3.1 Sedimentation 91
5.4.3.2 Algal Blooms 94
5.4.3.3 Nutrient Levels 95
5.4.4 Overall Flow Regime 98

5.5 EXPERIMENTAL 99

5.5.1 Introduction 99
5.5.2 Experimental Procedure 99
5.5.3 Sampling Procedure 100
5.5.4 Additional Climatic Data and Results 100
5.5.5 Analysis 101
5.5.6 Tracer Results 104

5.6 TRACER DISPERSAL AND MODELLING 109

5.6.1 Wind-wave Model 109
5.6.2 Wind-water Current Model 116

5.7 SUMMARY 126

CHAPTER 6 A STUDY OF THE FINE SEDIMENT TRANSPORT DYNAMICS IN A MACRO-TIDAL ESTUARY: TAMAR ESTUARY, SW DEVON, UK

6.1 BACKGROUND TO THE TAMAR ESTUARY 131

6.1.1 Introduction 131
6.1.2 Site Description 133
6.1.2.1 Introduction 133
6.1.2.2 Geography and Hydrography 134
6.1.2.3 Tidal Regime 134
6.1.3 Previous Cohesive Sediment Studies 135
6.1.3.1 Turbidity Maximum 135
6.1.3.2 SPM Size Analysis 136
6.1.4 Areas Requiring Further Research 137
6.1.5 Background to this study 138

6.2 PRELIMINARY EXPERIMENTAL SURVEY 139

6.2.1 Introduction 139
6.2.2 Axial Surveys 139
6.2.3 Results 141
6.2.4 Summary 141

6.3 TRACING EXPERIMENT 149

6.3.1 Introduction 149
6.3.2 Field Equipment and Set-up 150
6.3.3 Field Sampling Methodology 154

6.4 RESULTS - INSTANTANEOUS SYNOPTIC DATA 157

6.4.1 Salinity 157
6.4.2 Current Velocity 159
6.4.3 SPM 162
6.4.4 Tracer Particles 165
6.4.5 Axial Survey 27 June 169
6.4.6 Axial Survey 3 July 169

6.4.7 Summary 169

6.5 DATA INTERPRETATION AND ANALYSIS 172

6.5.1 Introduction 172
6.5.2 Advection of Tracer with Salinity 172
6.5.2.1 Measured Against Predicted Advection Results 172
6.5.2.2 Dispersion and Diffusion Coefficients Equations 177
6.5.2.3 Results 178
6.5.3 Equilibrium of the Tracer with the Turbidity Maximum 180
6.5.4 Residual Transport Analysis of Current Velocity, SPM and Tracer Particles 184
6.5.4.1 Analysis Equations 184
6.5.4.2 Results 184
6.5.4.3 Current Velocity 186
6.5.4.4 Turbidity 186
6.5.4.5 Tracer Particles 188
6.5.4.6 Summary 191
6.5.5 Tracer Particle Residence Time 192
6.5.6 Sediment Particle Residence Time 194

6.6 SUMMARY 195

CHAPTER 7 CONCLUSIONS AND FURTHER RECOMENDATIONS

7.1 CONCLUSIONS 198

7.2 FUTURE RECOMENDATIONS 203

REFERENCES 205

LIST OF FIGURES

		Page
Figure 1.1	Schematic of a resuspension-transport-deposition cycle for sediment.	7
Figure 1.2	Schematic diagram of an estuary showing the turbidity maximum. (Adapted from Pethick, 1984).	16
Figure 2.1	Schematic diagram of the particle analysis and sorting of an AFC (adapted from Burkill, 1987a)	33

NOTE: Cells or other suspended particles are introduced at (A) in to the flow chamber (B) where they are hydrodynamically focused by sheath fluid. Monochromatic light from an Argon-ion laser (C) irradiates each particle as it passes singly through the beam. Particles scatter and may fluoresce light from the analysis point (D). A photodiode (E) quantifies the forward angle light scatter to measure particle size, while photomultiplier tubes (F) pick-up the 90° light scatter for particle refractive index, and two-colour, wavelength-selective fluorescence to measure biochemical properties of the particle. Signals from these sensors are processed electronically (G) and held in a computer file. The sample stream is vibrated by a piezoelectric transducer (H), producing uniform liquid droplets at 35,000 per second travelling at 10 m s^{-1}. Droplets containing particles exhibiting the pre-set scatter and fluorescence characteristics are electrostatically charged at the droplet formation break-off point. As these droplets pass charged plates (I), they are deflected into sort chambers (J,K). Particles not meeting the required sort criteria pass undeflected into waste (L). Particles may be analysed and sorted at up to 5000 s^{-1}, with collection purities of 98%.

Figure 3.1	Particle size spectra of estuarine sediment particles from the turbidity maximum of the Tamar estuary and the spectra of the fluorescent tracer particles used for the tracing studies.	37
Figure 3.2	Axial profile of the sediment bulk densities in the Tamar Estuary (Stephens *et al.*, 1992) with the tracer particle density plotted for comparison.	39
Figure 3.3	Electrophoretic mobility measurements for estuarine sediment, tracerparticles and aluminium hydroxide particles with different organic coatings (natural and P.M.A.) to assess particle surface charge and stability after washing through time. Results from other estuaries were taken from values given by Tipping *et al.*, (1981), Loder & Liss (1982) and Hunter (1983). See Section 4.3.3 for the tracer data.	42

Figure 3.4 Median settling velocity measurements of suspensions at different concentrations and salinities (0, 1 & 5) comprising (1) estuarine sediment (S), (2) estuarine sediment and tracer particles (S & T) and (3) tracer particles (T). 45

Figure 3.5 Time series of passive adsorption of fluorescent dyes on to natural estuarine sediment. 52

Figure 4.1 Calibration curve of Polyscience latex calibration beads measured on the AFC indicating calculated number of beads against observed number of beads. 59

Figure 4.2 Fluorescent excitation and emission spectra of particle suspensions and centrifuged supernatant of Yellow 7, Orange 6 and Polyscience Latex beads measured on a fluorescence spectrophotometer. 62

Figure 4.3 AFC plots of the Orange 6 tracer particles, Polyscience beads and Coulter Immunocheck beads. 65

NOTE: Particle Size is measured by Log Forward Angle Light Scatter (LFALS), fluorescence intensity is shown by logarithmic green fluorescence (LIGFL) and logarithmic particle volume as (LCVA). D indicates doublets.

Figure 4.4 Calibration curves of yellow and orange fluorescent tracer particles measured on the AFC indicating measured concentration against expected concentration. 66

Figure 4.5 Calibration curves of increasing orange tracer particles in a constant concentration of estuarine mud suspension, and increasing concentration of estuarine mud in a constant concentration of orange tracer particles. 68

Figure 4.6 Location map and fluorescent tracer particle contour dispersion plot of the study at Stokers Pit, Hemerdon, Southwest Devon. 74

Figure 5.1 Location of Loe Pool with the bathymetry (in metres), the fluorescent tracer particle injection site within the River Cober and the locations of the trisponder (a,b,c & d) shown. In addition cross sections 1 (X1) and 2 (X2), the river gauging station, Helston STW and RNAS Culdrose meteorological station are also shown.. 87

Figure 5.2 Mean monthly streamflow for the River Cober (1970-1979) and mean monthly rainfall within Loe Pool catchment (1941-1970). 90

Figure 5.3 Isopach map of the brown-clay surface sediment (in centimetres) of Loe Pool showing location of palaeolimnological cores on the lake bed. (Adapted from O'Sullivan *et al.*, 1982.). 93

Figure 5.4 Annual fluctuations in organophosphate concentrations from 1981-1990 measured above and below the Helston Sewage Treatment Works in the River Cober and in the outlet to the lake. 97

Figure 5.5 Daily mean stream inflow, rainfall and lake water level for Loe Pool during the study period 1st April 1990 to 25th May 1990. 102

Figure 5.6 Twelve hour averaged wind velocity vectors, one for each half-day period following injection for the duration of the experiment. Note that the first arrow to the southern end of the Pool denotes the first twelve hour period and the wind direction is towards the arrow head i.e. an easterly wind. 103

Figure 5.7 Measured tracer particle concentrations in the bed sediment of Loe Pool. The units are 10^5 particles per cm^2 of bed. A denotes the main area of accumulation. 105

Figure 5.8 Percentage of tracer within each concentration contour (regions A-L) providing a mass budget of the total tracer particle dispersal. Point X denotes the maximum of tracer concentration. 107

Figure 5.9 Tracer particle concentrations through cross-sections X1 and X2 from the fluorescent introduction point (Figure 5.1). 108

Figure 5.10 Tracer particle size distribution of the recovered bed sediment tracer (percentage weight in size bands 0-6, 6-10 and 10-20 μm) as a function of distance from the tracer injection point. 108

Figure 5.11 The significant wave height (H) and wave period (T) as a function of fetch from 200-1600 m at windspeeds of 10 and 20 m s^{-1}. 111

Figure 5.12 The wavelength (L) and wavespeed (C) as a function of fetch from 200-1600 m at windspeeds of 10 and 20m s^{-1}. 112

Figure 5.13 Wave orbital velocity (U_{π}) and bed shear stress (τ_{π}) as a function of water depth and fetch from 200-1600 m at a windspeed of 10 m s^{-1}. 114

Figure 5.14 Wave orbital velocity (U_{π}) and bed shear stress (τ_{π}) as a function of water depth and fetch from 200-1600 m at a windspeed of 20 m s^{-1}. 115

Figure 5.15 Bed shear stresses in Loe Pool for a 25 m s^{-1} south westerly wind indicating that at the point of high tracer concentration (A in Figure 5.7) the bed shear stress is approximately 0.25 Nm^{-2}. Units are in Nm^{-2}. 117

Figure 5.16 Bed shear stress at site A (see Figure 5.7) at a water depth of 1.5 m as a function of time during the first 20 days of the study (0-480 hours). Units are in Nm^{-2}. 118

Figure 5.17 Predicted wind driven lake setup for a 13 m s^{-1} easterly wind to indicate elevation during the first five days of the study period due to lake setup. Units are in millimetres. 121

Figure 5.18 Modelled depth-averaged, wind-driven water circulation within Loe Pool for a 5 m s^{-1} northerly wind (A) and a 13 m s^{-1} easterly wind (B). Note that west is vertically upwards on these diagrams. 122

Figure 5.19 Modelled depth-averaged, wind-driven water circulation within Loe Pool during the first (A) and second (B) half days after the tracer injection. Note that west is vertically upwards on these diagrams. 124

Figure 5.20 Modelled depth-averaged, wind-driven water circulation within Loe Pool during the third (A) and fourth(B) half days after the tracer injection. Note that west is vertically upwards on these diagrams. 125

Figure 6.1	Location map of the Tamar Estuary showing the freshwater weir and location and distance from the weir of the sampling Stations 1-6. The tracer injection point is also shown.	132
Figure 6.2	Axial survey of the Tamar Estuary on the 15th June HW-1 hr. 40 min.to HW+1 hr. 20 min.	142
Figure 6.3	Axial survey of the Tamar Estuary on the 15th June HW+1 hr. 45 min. to HW+ 2 hr. 45 min.	143
Figure 6.4	Axial survey of the Tamar Estuary on the 18th June HW-3 hr. to HW-1 hr. 30 min.	144
Figure 6.5	Axial survey of the Tamar Estuary on the 18th June HW-30 min. to HW.	145
Figure 6.6	Axial survey of the Tamar Estuary on the 22nd June HW-4 hr. to HW-1 hr. 45 min.	146
Figure 6.7	Axial survey of the Tamar Estuary on the 22nd June HW-1 hr. 45 min. to HW- 1 hr.	147
Figure 6.8	Instantaneous synoptic salinity data from Stations 4-6 on the 26th June.	158
Figure 6.9	Instantaneous synoptic current velocity data from Stations 1-6 on the 26th June.	161
Figure 6.10	Instantaneous synoptic turbidity data from Station 1-6 on the 26th June.	163
Figure 6.11	Instantaneous synoptic tracer concentration data from Stations 1-6 on the 26th June.	166
Figure 6.12	Axial survey of the Tamar Estuary on the 27th June.	170

Figure 6.13 Axial survey of the Tamar Estuary on the 3rd July. 171

Figure 6.14 The observed and calculated longitudinal tidal advection over the ebb and flood tidal cycle on the 26th June. 174

Figure 6.15 Longitudinal axial section, taken from the synoptic data, through Stations 1-6 showing salinity, tracer and turbidity on the ebb tide 11.00, 26th June. 182

Figure 6.16 Longitudinal axial section, taken from the synoptic data, through Stations 1-6 showing salinity, tracer and turbidity on the ebb tide 20.20, 26th June. 183

Figure 6.17 Depth-averaged ebb, flood and residual tracer mass component and mass gradients for the ebb and flood tide. 189

Figure 6.18 Estimate of the tracer particle residence time in the turbidity maximum based on the log of tidal events versus log tracer mass. 193

LIST OF PLATES

page

Plate 4.1 Photograph of the orange fluorescent particles used in the tracer study taken through a fluorescent microscope at x 100 magnification. 61

Plate 4.2 Preliminary fieldwork study at a China Clay mine showing tracer injection 73

Plate 5.1 Loe Pool, Cornwall looking south from the River Cober towards Loe Bar 88

Plate 6.1 The tracer particle sampling pump system used on the Tamar Estuary 152

Plate 6.2 Deployment of the bottom-mounted logging instrument package at Station 3 on the Tamar Estuary 153

Plate 6.3 The tracer particles being mixed on the Tamar prior to injection 155

Plate 6.4 The plume of tracer particles in the turbidity maximum of the Tamar Estuary immediately after injection 156

ACKNOWLEDGEMENTS

I would like to thank my supervisors Keith Dyer, Tony Bale and Geoff Millward for their help and encouragement during this project, especially Tony who willingly assisted me through all the daily problems during the early stages of the work. Thank you to the Hemerdon Estate, Roger Hamilton of the National Rivers Authority (Southwest) and to Nick Lawrence of the National Trust for access to the field sites. Thanks also to all the friends and colleagues whose technical and personal support has been invaluable.

Those at Plymouth Marine Laboratory, including the members of the estuarine group, especially Alan Morris, Reg Uncles, John Stephens and Mel Barton, and the boat crews of Norman Bowley and Fred Holt, as well as the flow cytometry staff, Peter Burkhill and Dave Robbins, deserve a special mention.

Thanks also to the field assistants Martin, John and Nick, and especially to Norman for repairing and replacing the equipment in the field during the surveys on Dartmoor and The Lizard.

Special thanks to all the people who assisted in the work on the Tamar Estuary, especially the co-organisers both at the Marine Laboratory and at the University, but who unfortunately are too numerous to mention. Thanks also to Paul Salmon and Heather Stephens without whom processing the samples and data collected from the Tamar would have seemed to be a very daunting task.

Finally, thanks to Pete, Meriel, Hamish, Paul, Chris, Andy and Kate who have helped over the years; and extra special thanks to Leesa, Josh, Hamish and Boris for putting up with the long hours.

J.K.M.

October 1994

AUTHOR'S DECLARATION

At no time during the registration for the degree of Doctor of Philosophy has the author been registered for any other University award.

This study was financed with the aid of a studentship from the Natural Environment Research Council, and carried out in collaboration with Plymouth Marine Laboratory.

Publications:

Marsh, J. K., Bale, A. J, Uncles, R. J. and Dyer, K. R. (1991). A tracer technique for the study of suspended sediment dynamics in aquatic environments. In: Proceedings of the International Association for Hydraulic Research, International Symposium on the Transport of Suspended Sediment and its Mathematical Modelling, Florence (Italy), 2-5 September 1991, pp. 665-682.

Uncles, R. J, Stephens, J. A., Marsh, J. K. and Bale, A. J. (1991b). Synoptic observations of fine-sediment concentrations and transport in the turbidity maximum region of an estuary. In: Proceedings of the International Association for Hydraulic Research, International Symposium on the Transport of Suspended Sediment and its Mathematical Modelling, Florence (Italy), 2-5 September 1991, pp. 389-404.

Marsh, J.K, Bale, A.J, Uncles, R.J. and Dyer, K.R. (1993). A particle- tracing experiment in a small, shallow lake: Loe Pool. In: Geomorphology and Sedimentology of Lakes and Reservoirs. (eds. J. McManus and R. W. Duck). John Wiley & Sons Ltd, Chap. 10, pp 139-153.

Signed .....

Date....28.12.95.....

CHAPTER 1

GENERAL INTRODUCTION

1.1 INTRODUCTION

The natural balance of many different environments has been altered as a result of increasing pressure from industrial and urban growth, deforestation, construction activity and the demand for land and resources. Some of the most marked changes have taken place in coastal regions where, for example, towns and ports have carried out expansion and land reclamation programmes in order to meet the need of increased growth and trade. Further changes to the environmental balance of coastal areas has resulted from urban expansion with its associated waste and effluent disposal and increased rate of runoff from rainfall carrying with it unintentional discharges, erodable sediment and topsoil, debris and waste. Industrialisation and urbanisation has led to a significant increase in the number of agricultural, industrial, nuclear, mineral and organic products in addition to sediments being introduced into rivers, estuaries and the marine environment in general. In many coastal areas, there are sharp conflicts of interest between the protection and management of the environment and the needs of industrial development, town-planning, fisheries, tourism and waste disposal.

1.1.1 Importance of Fine Sediments

Port expansion and maintenance, construction, coastal protection, land reclamation, dredging and beach rejuvenation often generate large quantities of sediment which require disposal or result in high suspended sediment concentrations in coastal waters. Mobile sediment or dumped sediment can have a considerable impact on the environment, causing increased siltation or water column turbidity leading to burial of benthic organisms, disrupting feeding and spawning grounds of fish, altering the sediment regime and preventing photosynthesis for organisms including coral, maerl and plankton. One large source of sediment released into

the coastal waters of the United Kingdom is dredged material from maintenance and capital dredging, which is estimated to be 50 million tonnes p.a. (Delo & Burt, 1991).

In addition to the physical alteration of the sediment balance, fine sediments (silts and clays) and the organic matter often associated with sediment have a high adsorptive capacity (Lamere Hennessee *et al.*, 1986). As a result, many of the allochthonous products introduced into rivers, estuaries and the marine environment, especially anthropogenic chemicals which are hydrophobic, enter the aquatic environment and are adsorbed onto fine suspended sediments.

It is therefore often more important, particularly from an environmental management viewpoint, to predict the movement of fine cohesive sediment rather than coarse sediment, even in low energy environments. For example, fine sediment undergoes repeated cycles of deposition and resuspension, often for months and years prior to final consolidation, continually recycling pollutants by resuspension and deposition of sediment (Morris *et al.*, 1982 a,b). In addition, activities by man and high energy events including flood erosion can cause a remobilisation of sediment-bound pollutants back into the water column. Sediments which have adsorbed pollutants can be recirculated and may cause a pollution hazard in the short term, or travel large distances before settling permanently, leading to a long term accumulation of pollutants to relatively high concentrations. Pollutants associated with sediment may then be gradually released into the water column, especially trace metals which cycle between dissolved and adsorbed phases (Duinker, 1980; Morris *et al* ., 1982a; Weirich, 1986). The sediments themselves are therefore both the physical location and the carrier mechanism for numerous pollutants and the fate of contaminants in waters is closely related to the fate of the suspended matter.

1.1.2 Sediment and Pollutant Dynamics with Respect to Lakes and Estuaries

Rivers, lakes, estuaries and coastal waters are both sinks and sources for sediment and pollutants associated with sediment, due to dispersal and redistribution of sediment by both natural and man-made processes (Turekian, 1977; Thompson & Eglinton, 1978; Wakeham *et al.*, 1980; Bale *et al.*, 1985; Ackroyd *et al* ., 1986; Luettich *et al.*, 1990; Delo & Burt, 1991). Pollutant and sediment discharges to rivers can be retained within the riverine system for long periods during low river flow conditions and be buried or immediately flushed out into a lake or estuary due to increased seasonal river flow (Carper & Bachmann, 1984; Bale *et al.*, 1985; O'Melia, 1985; Weirich, 1986).

Most pollutants enter a lake or estuary from river input, freshwater runoff, outfalls from within the catchment and from coastal waters on flood tides (Lake *et al.*, 1979; Buffle *et al.*, 1987). The pollutants are in dissolved, colloidal and particulate form, and are present both as a consequence of natural processes and anthropogenic activities (Lemmin & Imboden, 1987; Delo & Burt, 1991). Many studies have found an accumulation of pollutants within lakes and estuaries associated with bed sediment and high suspended sediment concentrations in the water column (Grieve & Fletcher, 1977; Readman *et al.*, 1982; Luettich *et al.*, 1990). The high turbidity areas, or turbidity maxima found in an estuary (Section 1.4.3) concentrate pollutants including polychlorobiphenyls (PCB), polyaromatic hydrocarbons (PAH) and trace metals during the months of low river runoff in the upper estuary where tidal oscillations maintain turbid waters (Readman *et al* ., 1982; Fresenius & Luederwald, 1984; Nuernberg, 1985; Morris *et al.*, 1986; Twilley & Ward, 1986, Abarnou *et al.*, 1987; Amos, 1987; Little *et al.*, 1987; Delo & Burt, 1991).

The importance of sediments and the cycling of sediments with adsorbed pollutants in all aquatic environments is clearly important both from an environmental and engineering viewpoint. A clear understanding of the processes which affect the movement, transport and accumulation of polluted and non-polluted sediment, in addition to the development of tools and techniques to enhance that understanding is required.

1.2 SEDIMENT TRANSPORT

1.2.1 Techniques to Assess Sediment Transport

In order to understand sediment dynamics in both lakes and estuaries, it is necessary to describe and discuss the techniques used for assessing sediment transport and the processes that affect the movement of sediment that are common to both environments, including erosion and deposition. The movement of sediment is a direct function of current velocity and the magnitude and direction of the residual current will dictate where the sediment is transported to, how quickly and whether the sediment will undergo a series of cycles of deposition, erosion and transportation before its final settling point.

It is important that techniques are developed to assess both the source and sink of sediment and to monitor the physical movement of sediment in order to establish any physical or chemical effects which might occur.

Several authors have concentrated on aspects of estuarine circulation and sedimentology in site specific case studies to confirm physical and chemical parameters, and features of estuaries (Allen *et al* ., 1980; Biggs *et al.*, 1983; Pejrup, 1986; Avoine & Larsonneur, 1987). In addition, other authors have investigated a specific feature of sediment movement or water circulation to emphasise and infer the general physical characteristics of the study area, sediment or water (Owen, 1970a,b; Eisma *et al.*, 1980; Burt, 1984; Kranck, 1984; Gibbs, 1985). To further advance the understanding of sediment movement new techniques have been developed (Bale *et al.*, 1987; Newman *et al.*, 1990a; Fennessy *et al.*, 1994).

Despite this knowledge of sediment movement in specific environments certain aspects of sediment transport remain difficult to predict (Uncles *et al.*, 1985; Dyer 1989), particularly in environments which are continually changing as a result of man's activities; for example maintenance dredging areas (Delo, 1988b). Delo claims that it is not possible to predict the behaviour of cohesive sediment directly from its physical and chemical properties alone and

1.2.2 Fine Cohesive Sediment Transport Processes

Fine cohesive sediment is continually transported in lakes and estuaries due to the dynamic conditions which exist as a result of natural phenomena including tides, waves, riverflow and wind (Nichols, 1984; Luettich *et al* ., 1990). The variability in the energy of these phenomena and a number of other important parameters (which have a greater or lesser significance depending on whether in a lake or estuarine environment) including water depth, fetch, water column stratification and chemical and mineralogical composition of the sediment affect the water column velocity and hence the degree of sediment transport (Hakanson & Jansson, 1983, Nichols, 1984). In high energy environments the current velocity may be sufficient to erode bed sediment into suspension where it will be advected with the residual current. Eventually, the current velocity decreases to a level at which the suspended sediment will settle out and be deposited on the bed once more. This cycle of sediment movement can be repeated several times before permanent deposition or flushing out of the lake or estuary occurs. Uncles *et al* ., (1989) and Luettich *et al*., (1990) have shown a continual cycling of sediment between the bed and the water column in an estuary and a lake, respectively. In addition to natural phenomena activities by man including construction, dredging and disposal leads to transport of sediment in lakes and estuaries and either removes or enhances the erosion stage of the cycle, thereby increasing the potential transport of the sediment. Figure 1.1 indicates schematically the sediment resuspension, transport and deposition cycle.

1.2.2.1 Erosion and Resuspension

Movement of sediment from the bed commences when the shear stress becomes sufficiently large to overcome the frictional and gravitational forces holding the sediment on the bed. This is known as the critical shear stress, and the velocity which determines the sediment movement is the critical shear velocity. Cohesive sediment on the bottom of a tidal estuary or lake comprises a complex sediment bed due to the variance in floc aggregate properties.

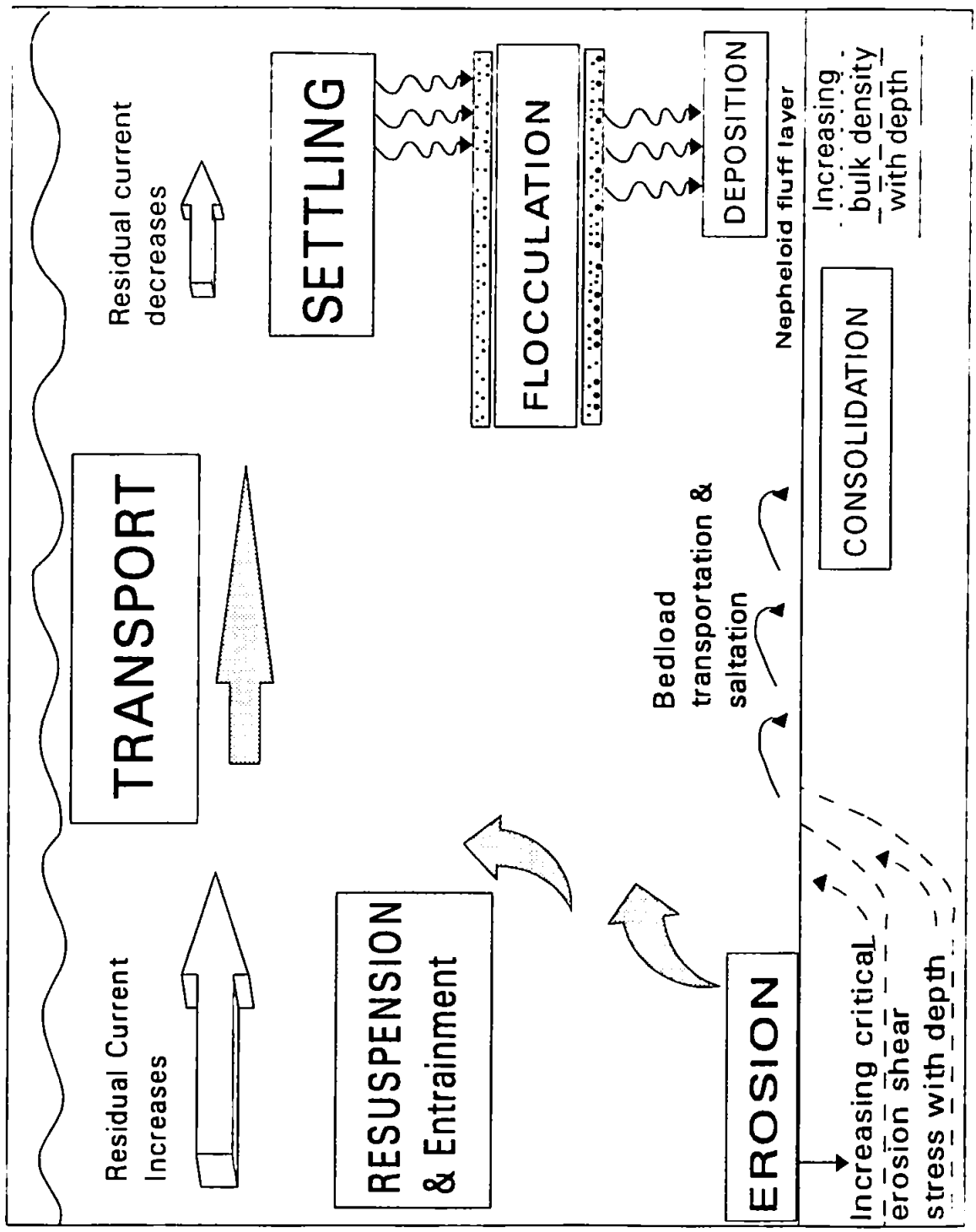

Figure 1.1 Schematic diagram of a resuspension-transport-deposition cycle for sediment.

The nature of the sediment bed varies spatially and with depth (Black, 1994).

For the purpose of this explanation and study of shallow marine and freshwater environments, the surface of the sediment bed has been simplified into two distinct layers, a consolidated bed over which a "fluff" or nepheloid layer lies (Nichols, 1984). The underlying, more compacted sediment may have a critical erosion shear stress of approximately 1 Nm^{-2}, and have a water content of between 50-70% (Dyer, 1986; Delo, 1988a). The overlying surface "fluff" layer is less compacted and comprises an interfacial sediment layer, which is composed of loosely held aggregated material with a water content between 85-100%, and which will erode at shear stresses of approximately 0.1 Nm^{-2} (Nichols, 1984; Newman *et al.*, 1990b). This "fluff" layer forms as a result of settling flocs in quiescent conditions during tidal slack water or during low flow conditions and represents a layer which is periodically resuspended. The erosion of this layer is often referred to as redispersion rather than resuspension and indicates the entrainment of sediment from a consolidating or settled mud bed. (Mehta *et al.*, 1982; Nichols, 1984).

The resuspension of a consolidated or settled bed often occurs as clumps of sediment, as a result of mass failure of the sediment surface during very high shear velocities and erosion shear stresses (Delo, 1988a). Increasingly larger shear stresses are required with depth through the sediment as shown in Figure 1.1. Movement of cohesive sediment therefore falls into two categories and is a function of the magnitude of the shear stress. Erosion of sub-surface sediment layers would usually occur during high riverflow conditions, waves or peak tidal flow. The term erosion is used here to define the initial movement of sediment off the bed and is directly related to the critical erosion shear stress and critical erosion shear velocity. Resuspension is defined as the entrainment of sediment once eroded into the water column and therefore is the mechanism of sediment movement.

The critical erosion shear stress of sediment is a function of numerous factors including salinity, microbiology, geochemistry and clay mineralogy. Some of the specific factors which affect critical shear stress include "glue" properties caused by pelletization of fine sediments

by tubificids (Fukuda & Lick, 1980), bacterially active compounds such as mucopolysaccharide films (Linley & Field, 1982), degree of consolidation (Section 1.2.2.3) (Stephens *et al.*, 1992), composition of the bed, biota and coverage of the bed (Montague, 1984), temperature and chemistry of the overlying water, and pore fluid and bioturbation (Lee *et al.*, 1981; Nichols, 1984; Parchure & Mehta, 1985). Nichols (1984) provides a comprehensive list of the factors affecting erosion and resuspension and Black (1994) reviews the level of understanding and processes of erosion of marine cohesive sediments to date. The range of variables which affect erosion makes it difficult to predict the critical erosion shear stress. However, Delo (1988a) proposes an empirical relationship between critical erosion shear stress and dry density; based on the complex interactions this is an over simplification (Stephens *et al.*, 1992).

Erosion of particles from the surface of a deposit by current or wave motion is the main process by which sediment is introduced back into the water column after primary deposition or as part of a continual cycle of resuspension and deposition. Once the sediment particles have been eroded and resuspended they can be advected and redistrubuted by the residual water currents. Transport and advection of suspended sediment in the prevailing water circulation occurs until the sediment begins to settle out when the bed shear stress equals the critical deposition shear stress. Dyer (1988) notes that in an estuary on the ebb and flood tide the current velocities can be the same, but the bed shear stress can be quite different due to bed roughness and stratification.

1.2.2.2 Deposition - Settling Velocity and Flocculation

Particulate material will remain in suspension whilst the turbulence and bed shear stress is sufficient to maintain the material in the water column (Dyer, 1988). When the shear stress and turbulence in the water column equals the critical depositional shear stress the particulate material begins to be deposited on the bed. Deposition of suspended particulate material (SPM) is controlled by two inter-related parameters; settling velocity and flocculation (Figure 1.1). The rate at which the particles settle, or settling velocity, is a function of the size and

density of the sediment particles and flocculation processes.

The basic parameter used in determining rates of deposition in either still or flowing water is the settling velocity of the flocculated sediment. Settling velocity is the rate at which a sediment grain settles out of suspension back to the bed. Settling velocity is dependent on the suspended sediment concentration; settling velocities increase with higher suspended concentrations since the frequency of inter-particle collision increases, leading to the formation of flocs (Krone, 1972; Stevenson & Burt 1985; Puls & Kuehl, 1986). Settling velocity is also a function of salinity, but this is considered to be of secondary importance to turbidity (Delo, 1988a). Flocculation increases with turbidity (Migniot, 1968; Kranck, 1981), and to a lesser degree with salinity (Kranck, 1975; Gibbs, 1983), leading to an increase in floc size and settling velocity up to a point when fluid shear, due to the particle falling through the water column, breaks up the inter-particle forces or when hindered settling takes place when the flocs are sufficiently close together that they impede each others settling and form an interface with the overlying water (Owen, 1970a; Dyer, 1988)

The process of flocculation and the size and type of floc is a function of a number of parameters, including organic-inorganic composition, grain size, density, pH, grain mineralogy, suspended particulate concentration, salinity, the number of inter-particle collisions and turbulence structure, internal shear and bed shear stress of the water column (Burt, 1984; Kranck, 1984; Eisma, 1986, Delo, 1988a; Weilenmann *et al.*, 1990). Flocculation depends on collision and cohesion (Krone, 1962); inter-particle collisions between suspended sediment due to local shear in the water column and cohesion causes them to adhere to each other and form aggregates of particles or flocs. Kranck (1984) and Eisma (1986) describe the importance of flocculation of suspended sediments and the different types of flocs. Eisma indicates that there are three types of suspended matter in estuaries and rivers; macroflocs which have a range in millimetres, microflocs which range up to 100+μm and mineral particles. Macroflocs often comprise microflocs loosely bound and individual mineral particles. Individual particles have densities of approximately 2.65 g cm^{-3}; whereas floc densities, because of the aggregation of water and minerals and flocs are in the

range 1.06 to 1.8 g cm^{-3} (Dyer 1986).

The varying densities of flocs inevitably means that some flocs will settle out before others and in conditions where bed shear stress and current velocity are critical, short-term fluctuations, such as changes from an ebb to flood tide around slack water in a tidal estuary, may lead to a separation between floc sizes (as seen by McCabe *et al.*, 1992). In the event of rapid settling to the bed due to flocculation, Dyer (1989) notes if the flux is high, water can become trapped between flocs creating a layer of homogeneous high concentration suspension or "fluid mud".

As a flocculated suspension settles, an interface forms near the surface separating the suspension from the clear water. This suspension/water interface falls with time as the sediment accumulates as a layer on the bottom. Therefore from an initial homogeneous suspension close to the bed the interface between suspension and water falls and meets the rising bed. The rate of fall is slower because of consolidation and the newly formed water/bed interface slowly reduces (Owen, 1970a; Been & Sills, 1981; Ginger, 1987; Dyer, 1988).

1.2.2.3 Consolidation

Continual settling of flocs on the sediment bed causes consolidation and squashing of the underlying flocs (Owen, 1970a; Partheniades, 1972). This consolidation causes an expulsion of water and an increase in the shear strength of the mud. Therefore, water content decreases with depth due to compaction, and the combination of low water content and high clay content causes increased shear strength in the sediment (Figure 1.1). Density and critical erosion shear stress increase almost exponentially with depth (Dyer, 1989). The degree of cohesion for fine-grained marine sediments controls erodibility and is not simply determined by grain size. Water content, mineralogy, cation exchange capacity, salinity of interstitial and eroding fluid, organic mucus content and Bingham yield strength are the parameters which affect consolidation (Owen, 1970b; Been & Sills, 1981; Burt & Parker, 1984; Ockenden & Delo, 1988).

1.2.3 Discussion

For the context of this study, there is quite clearly a size fraction of fine cohesive sediment which in a tidal estuarine or shallow lake environment undergoes repetitive erosion and advective transport followed by flocculation and deposition. In these environments the deposited sediment may only undergo partial consolidation before being eroded and the cyclic process is repeated. This may lead to long term retention of suspended particulates in environments, resulting in an accumulation of sediment and associated pollutants.

1.3 SEDIMENT TRANSPORT IN LAKES AND ESTUARIES

1.3.1 Introduction

As described in Section 1.1, an understanding of sediment particle dynamics is particularly important in shallow lakes and estuaries. There is a growing awareness of the role sediments play in pollutant dynamics, and in regulating the composition of water systems (Salomons *et al.*, 1987) due to the high adsorptive capacity of fine cohesive sediments for dissolved pollutants (Mehta, 1984; Lamere Hennessee *et al.*, 1986; Dyer 1989) and the repeated deposition and resuspension of sediment over long periods.

Although initially the objective of this research was to develop and test a particle tracing technique for the study of sediment dynamics in estuaries, it was considered essential to carry out preliminary field tests in less dynamic environments, and ideally without the variable of a tide. A shallow lake in West Cornwall offered an ideal test site for a sediment transport study. The lake study highlighted the need to describe the trial separately and evaluate several areas of interest which are specifically related to lake sediment dynamics and pollution.

1.3.2 Lakes

Lake research has invariably been carried out to investigate water quality and waste disposal (Gelencser *et al.*, 1982). This work has resulted in a better knowledge of lake circulation and an appreciation of the role sediments play in the movement and recycling of pollutants (Carper & Bachmann, 1984; Aalderlink *et al.*, 1985; O'Melia, 1985; Somlyody, 1986; Sigg *et al.*, 1987; Luettich *et al.*, 1990). It is recognised that lakes are efficient natural settling basins for inflowing sediment and particulate material due to extended hydraulic residence times which can range from months to years, (Weilenmann *et al.*, 1990). This allochthonous sediment which enters the lake acts as a carrier for many adsorbed nutrients and toxic substances that originate from around the lake catchment. Long residence times ensure these sediments remain in the lake causing nutrient and toxic build up over many years leading to an internal loading (Vollenweider, 1975; Ryding & Forsberg, 1980).

In circumstances where accumulations of pollutants occur over long periods, the lake's water quality and trophic state are altered, often irreversibly and the lake can remain affected due to a continual flux of pollutants from the bed sediment back into the water column during periods of bed sediment erosion and resuspension (Lemmin & Imboden, 1987; Luettich *et al.*, 1990) In many lakes, the breakdown and recycling of accumulated sediment and pollutants leads to eutrophication; defined as lakes which have high productivity and nutrient rich waters. Eutrophic lakes can be found world-wide, and even after the external loading of polluted inflowing water has ceased the eutrophic condition continues due to the internal loading (Michler *et al.*, 1980; Vass, 1980; Zullig, 1982; Buffle *et al.*, 1987).

The principal factors which influence water circulation, sediment remobilisation and hence water quality are interactive and include:

i) Wind - Water surface 'setup' occurs where the lake surface water establishes an elevation gradient opposing the wind stress. As part of the balance, lake surface currents are formed which generally circulate in the direction of the

wind with a compensatory bottom flow opposite to the wind direction. Wind also creates short period waves (Sobey, 1986) which, in shallow waters, can lead to significant bed shear stresses and sediment resuspension (Csanady, 1978; Hakanson & Jansson, 1983; Luettich *et al.*, 1990; Marsh *et al.*, 1993).

ii) Temperature - Density currents, as a result of a temperature gradient between river and lake water, largely control the rate of turbulent exchange between the two water masses, and therefore have a bearing on the fate and distribution of suspended and dissolved material (Hakanson & Jansson, 1983).

iii) Riverflow - The discharge of the inflow directly affects both the sedimentation processes by resuspension and deposition, and the residence time of the system (Weirich,1986). In lakes with short residence times the majority of sediment is washed straight through without releasing significant quantities of nutrients.

iv) Sediment mineralogy - Size and mineralogy of sediment particles directly affect the deposition and resuspension of the lake sediment, and the capacity for entrainment and binding of pollutants.

v) Organic matter - The level of organics and lake biota dictate the erosion, deposition and consolidation characteristics of the lake sediment (Buffle *et al.*, 1987).

vi) Global position - Coriolis forces and seasonal fluctuations in environmental conditions lead to characteristic sedimentation patterns and processes (Strum & Matter,1978; Pharo & Carmack, 1979; Smith 1979).

The most significant effect on lake water circulation and sediment remobilisation, particularly in shallow lakes (depth <5m as a function of fetch) is the formation of short-period waves, generated by wind (Sobey, 1986). These waves can lead to a resuspension of bed sediments releasing pollutants and nutrients back into the water column (Hakanson & Jansson, 1983). Nutrient levels and associated biogenic processes, i.e. algal blooms, in lakes with muddy beds have been found to correlate with episodic bottom sediment resuspension processes (Ryding & Forsberg, 1977; Gelencser *et al.*, 1982; Reynolds, 1984; Luettich *et al.*, 1990).

Ryding and Forsberg (1977) and Gelencser *et al.*, (1982) indicate that wind induced turbulence causes a release of phosphorus (perhaps the most detrimental nutrient to lake water quality) which was of a comparable magnitude to the average daily external supply to the studied lake. Luettich *et al.*, (1990) indicate that over 95% of the external supply of phosphorus may be retained in the bottom sediment and subsequent turbulent mixing can reload the water column. Therefore, turbulent mixing is the key regulating factor of nutrient transport from the sediment in shallow lakes by sediment resuspension.

1.3.3 Estuaries

A suspended particulate material (SPM or turbidity) maximum is a commonly observed feature in the low salinity reaches of many partially mixed and well-mixed estuaries (Allen *et al.*, 1980; Festa & Hansen, 1978; Officer & Nichols, 1980; Avoine *et al.*, 1981; Officer, 1981; Uncles *et al.*, 1991a,b) and is indicative of fine sediment transport in estuaries (Dyer, 1988). The turbidity maximum is generally located near the head of estuary within the freshwater-saltwater interface (Figure 1.2) and migrates up and down the upper estuary on the flood and ebb tide respectively. The range of migration, the physical position and the magnitude of SPM concentration varies with tidal amplitude (both tidal cycle and spring-neap cycle) and river flow (Buller & McManus, 1976; Allen *et al.*, 1980; Bale *et al.*, 1985; Avoine & Larsonneur, 1987; Vale & Sundby, 1987; Uncles & Stephens, 1989).

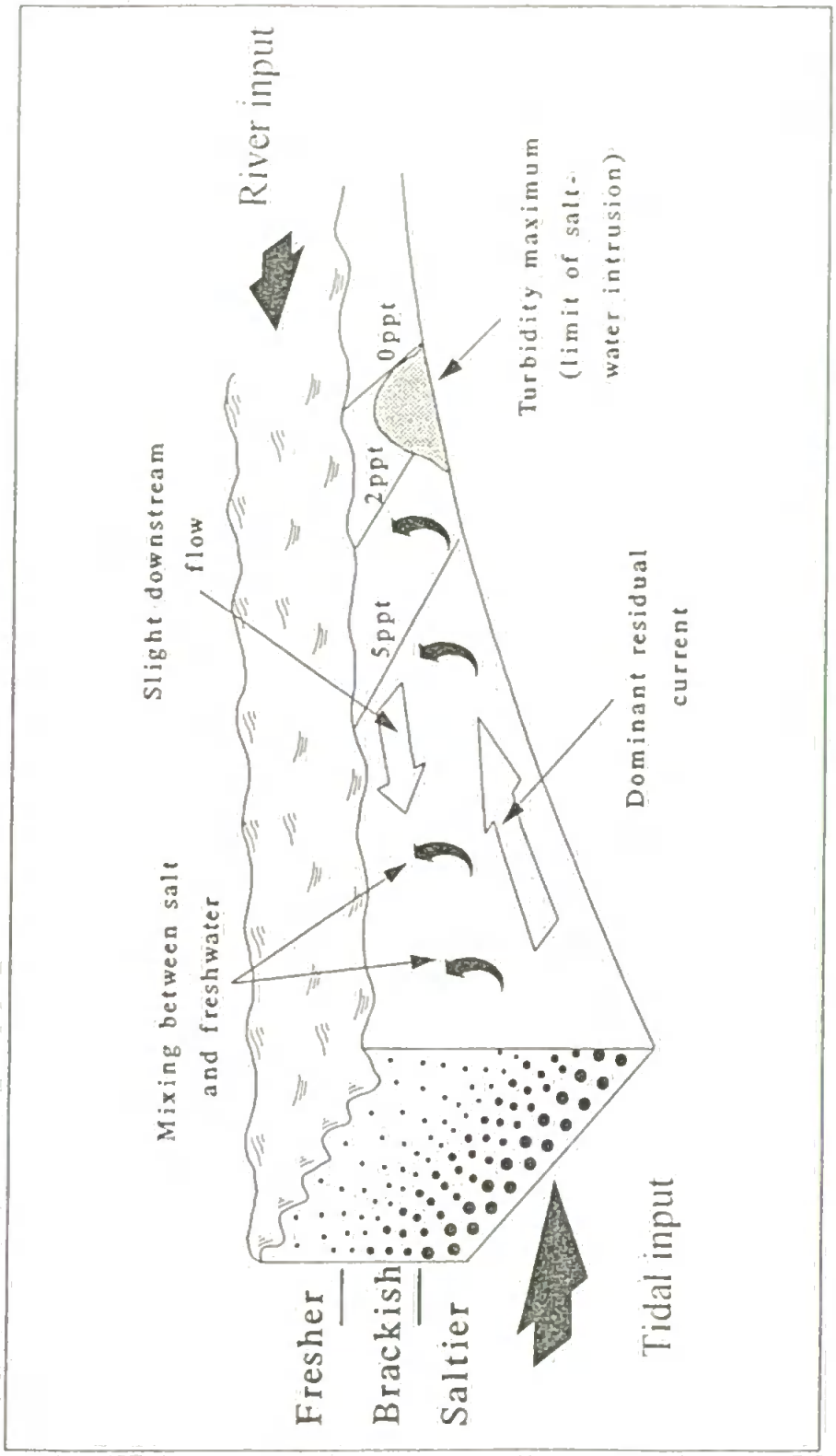

Figure 1.2 Schematic diagram of an estuary showing the turbidity maximum. (Adapted from Pethick, 1984).

The turbidity maximum is therefore a dynamic feature. The processes of formation are due to:

i) gravitational estuarine circulation, due to the mixing between the riverine inflow of less dense freshwater flowing down-estuary in the upper water column and the denser saline water flowing up-estuary in the lower water column (Dyer, 1973; Officer, 1976; Allen *et al.*, 1980; Morris *et al.*, 1982a; Bale *et al.*, 1985) (Figure 1.2). This circulation leads to an accumulation of riverine and coastal SPM at the freshwater-saltwater interface where a null point of residual velocity is found (Postma, 1967; Schubel, 1969; Festa & Hansen, 1978; Officer & Nichols, 1980; Dyer, 1988).

ii) tidal asymmetry, with flood currents exceeding ebb currents in the upper reaches of the estuary leading to increased erosion and resuspension of sediment and an up-estuarine tidal pumping and trapping of sediment (Allen *et al.*, 1980; Uncles *et al.*, 1984; 1985, 1991a; Uncles & Stephens, 1989). The sediment trapped in the upper estuary is deposited at high water levels due to prolonged slack high water and increased flocculation and settling induced by water laden with high suspended sediment concentrations (Section 1.2.2.2) close to the bed (Uncles *et al.*, 1991a)

iii) tidally induced shear forces causing local resuspension and deposition in the upper estuary (Allen *et al.*, 1980, Uncles *et al.*, 1984; 1985; 1991a,b).

Suspended sediments within an estuary, and in particular within the turbidity maximum, undergo successive cycles of erosion, transport and deposition prior to permanent deposition clearly affecting the cycling of adsorbed pollutants (Section 1.1). In addition, if sediment is trapped within the upper estuary and also actively pumped up-estuary, then any pollutants within the catchment may become incorporated with the sediment and retained within the turbidity maximum for long periods of time. This will lead to an accumulation of polluted sediment within the upper estuary, possibly for long periods until river flow increases and the turbidity maximum is displaced down estuary (Bale *et al.*, 1985).

Several studies have identified high levels of pollutants including PAHs (polyaromatic hydrocarbons), PCBs (polychlorobiphenyls) and trace metals associated with the turbidity maximum indicating an active process of pollutant cycling and retention (Choi & Chen, 1976; Grieve & Fletcher, 1977; Morris *et al.*, 1982b; Readman *et al*, 1982; Fresenius & Luederwald, 1984; Nuernberg, 1985; Ackroyd *et al.*, 1986; Morris *et al.*, 1986; Twilley & Ward, 1986, Abarnou *et al.*, 1987; Ackroyd *et al.*, 1986; Amos, 1987; Little *et al.*, 1987; Delo & Burt, 1991). Work by Ackroyd (1983) and Morris *et al.*, (1987) indicate a large removal of trace metals from solution in the turbidity maximum area of an estuary, and work by Morris (1986) indicates removal was due to uptake on to suspended sediment particles.

Actual determination of sediment transport pathways in estuaries is complex because there are many sinks and sources for the sediment, although intertidal mudflats around the high water mark are considered to provide a major sink (Dyer, 1989; Uncles *et al.*, 1991). Additionally, the complexity is increased due to tidal and seasonal fluctuations. Tidal variations can range from a single tidal cycle to a spring-neap cycle leading to a variation in tidal energy, turbulence and ultimately the degree of resuspension of sediment (Allen *et al.*, 1980; Bale *et al.*, 1985; Uncles *et al.*, 1985). Seasonal variations include river flow, solar irradiation and wind stress. The mechanisms involved in the net transport of sediment are difficult to quantify from short term measurements. Most sediment may be moved during short, high energy events rather than the intervening long, low energy periods. These high energy events are difficult to monitor. It is thought that major sediment exchanges occur between the turbidity maximum and the bed and intertidal areas, however, the magnitudes and frequencies of these exchanges are poorly known (Uncles *et al.*, 1985; Dyer, 1989)

1.3.4 Discussion

The preceding sections clearly indicate that an ability to examine the actual movement and dynamics of specific particles in riverine, estuarine and marine environments, in order to improve our understanding of sediment and pollutant transport pathways would be invaluable. To achieve this, a knowledge of the cyclical sediment processes including erosion,

transport, deposition and consolidation would be required, in addition to the development of tools and techniques to undertake the necessary research.

Some of the interactive processes for estuarine circulation and sedimentology are complex with certain areas poorly understood (Uncles *et al.*, 1985; Dyer, 1989; Bale 1988; Delo, 1988a), and there is a need to evaluate the parameters of cohesive sediment movement *in situ*. Delo (1988a) supports a laboratory based measurement *in situ* as opposed to field *in situ*, however he agrees the resultant data are of limited value when applied to the field situation. Additionally, the transport of sediments within a water column is not the same as the flow of water itself, due to settling, deposition and re-entrainment. Particle dispersal is not dictated by the same parameters as water flow and therefore it is imperative that the movement of particles and particle residence times be measured directly.

1.4 OBJECTIVES AND OUTLINE OF THE RESEARCH

The use of tracers as particle analogues is considered an extremely useful tool to better our understanding of sediment dynamics (Salomons & Mook, 1987; Dyer, 1989; Newman *et al*, 1990a; Spanhoff & Suijlen, 1990b). The aim of this research project was to develop a technique using tracers to provide a pragmatic approach for investigating mass and specific sediment movement in aquatic environments, specifically within an estuary.

It was hoped that by exploring the feasibility of such an approach, future investigations into sediment dynamics could employ the technique in parallel with other methodologies to provide a more complete picture of sediment movement and pollutant cycling, greatly assisting the management of aquatic environments.

CHAPTER 2

THE STUDY OF SEDIMENT DYNAMICS USING PARTICLE TRACER TECHNIQUES

2.1 INTRODUCTION

The dynamics of aquatic particles are important both in terms of the geochemical cycling of natural substances, and in the transport and fate of particle-reactive anthropogenic pollutants (Newman, 1990b). This is due to the high adsorptive capacity of fine suspended sediments for dissolved chemicals and pollutants (Mehta, 1984; Lamere Hennessee, 1986; Dyer, 1989). Two approaches in particular are commonly used to investigate the processes involved in pollutant cycling within aquatic environments and to determine sinks and sources of polluted cohesive sediments.

Firstly, changes in water chemistry can be used to provide information on the behaviour of trace constituents. Secondly, changes in suspended sediment composition can be monitored (Salomons & Mook, 1987). Fine sediments can travel large distances before permanent deposition and consolidation, resulting in accumulation of toxic chemicals and build up of sediment requiring dredging. To determine the impact of this accumulation, knowledge of the sediment source and the behaviour and processes involved during movement is indispensable. The sediment to be studied rarely has a sufficiently accurate fingerprint to allow precise tracing, and if no suitable natural tracers exist in the environment to be studied then artificial tracers provide an alternative.

Tracers have the ability to provide a more pragmatic approach to an engineering or environmental problem than synthesising instantaneous observations of sediment transport. The use of tracers for data acquisition yields information on the flow conditions and sediment transport mechanisms that occur after the introduction of the tracer. Tracers also enable observations to be carried out on the overall mass budget of sediment. In addition, tracers are

unique and extremely useful for studies of sediment movement during events which are too violent to allow sampling i.e. storms and floods. Therefore, the use of tracers enables the precise determination of whether a specific site acts as a sink or source for contaminants during short and long time-scales (Salomons & Mook, 1987).

2.2 SEDIMENT TRACING - A REVIEW

2.2.1 Introduction

Tracer techniques are used in a wide range of applications. In the marine aquatic environment, tracer experiments are employed for investigating water and particulate material residence times. To determine sediment movement, the particles themselves can be traced using natural or artificial tracers, or the water in which the sediment is being transported can be traced using fluorescent water dye.

Fluorescent dyes are frequently used for the study of surface water movement to provide information on the advection and mass budget of suspended sediment. Horizontal and vertical dispersion coefficients and flow patterns can also be determined by employing fluorescent water tracers.

2.2.2 Photoluminescence: Phosphorescence and Fluorescence

Luminescence is the process of emitting light unaccompanied by heat and is a property shared by most subtstances given appropriate circumstances. It is however, quite rare under normal conditions of daylight to have emissions of incident light wavelength, more commonly known as photoluminescence. There are also other types of luminescence including thermo- (heat), chemi- (chemical reaction), radio- (radioactive decay), electro- (electric current), bio- (organism activity), tribo- (frictional forces) and cathodo- (electron bombardment) with the initial source of energy defined by the prefix (Martindill, 1993).

Photoluminescence can be divided into two categories, phosphorescence and fluorescence. Phosphorescence is where the time between absorption and emission of photons is long enough to create an appreciable afterglow. Fluorescence is where the absorption/emission cycle is so fast as to appear instantaneous. The dividing line is generally accepted to be around 10^{-4} seconds. Absorption of a photon by a photoluminescence atom or molecule happens extremely quickly, in the order of 10 -15 seconds. The rest of the time is taken up converting the energy internally in a number of discrete stages before re-emission (Martindill, 1993).

All fluorescent organic compounds contain an extended series of conjugate double bonds, mostly in the form of benzene or heterocyclic rings, an electron acceptor and a donor group of atoms. The stimulus of light energy causes electrons to shift from the donor group to the benzene ring, which in turn gives up electrons to the acceptor group. A luminescing atom or molecule comprises one or more atomic nuclei surrounded by orbiting electrons, each with its own amount of energy. If the electron energy is increased or decreased it will change position, although there is a ground state which is the most stable. If energy in the form of a suitable incident photon is absorbed by an outer electron the electron will assume a higher energy level. The suitability of any photon for absorption will depend on its energy and whether this corresponds to the energy needed for the electron to jump to its next most stable state. Although reasonably stable, this excited condition is always less stable than the ground state, and almost immediately the energy may be ejected in the form of a new photon with exactly the same energy as the one absorbed. This is resonance radiation and is the most simple form of photoluminescence.

In most cases after the electron has assumed its higher energy level, but before the ground state is resumed, a small amount of energy is lost internally. Consequently when the new photon is finally emitted it has a lower energy than that absorbed. This is the general expression of Stokes Law, that emitting light will always have less energy, or a longer wavelength than absorbed light. The difference in wavelength of absorbed and emitted light is

referred to as the Stokes Shift. The energy lost internally, or non-radiative loss, is the major factor in determining the luminescent efficiency or quantum yield of the system (Martindill, 1993). The normal time for the electrons to return to their lower energy state is of the order 10^{-8} seconds or less.

2.2.3 Fluorescent Water Dyes

The most commonly used fluorescent water dye is rhodamine-B which is soluble in water and exhibits low toxicity (Jahnke & Michaelis, 1990). Rhodamine-B has been used extensively in studies investigating the advective transport and turbulent diffusion of conservative constituents in a water body (Jahnke & Michaelis, 1990; Kolb & Franz, 1990; Suijlen & Van Leussen, 1990). Detection of the fluorescent dye is by spectrofluorophotometer (sfpm) with detection limits of the order 10^{-11} kg m^{-3} using an *in situ* probe (Jahnke & Michaelis 1990). Suijlen and Michaelis (1990) describe detection by high pressure liquid chromatography (HPLC) with limits of the order 10^{-12} kg m^{-3} and with a capability of detecting a number of tracer materials simultaneously.

There are two significant disadvantages with fluorescent dye tracers and these are related to the stability and intensity of the fluorescent spectra. The fluorescent spectra, and therefore intensity of fluorescent dye, is affected by dye stability. External factors including pH, temperature, dye concentration, dimerization of the molecules and chemical interaction lead to a change in the fluorescence spectra. This prevents predetermined settings of sensitivity of an instrument throughout a monitoring study on a quantitative basis. One fluorescing molecule has only one photon of fluorescent light to emit. This prevents high detection limits being achieved, since many molecules are needed in a sample or close to a sensor head to enable the most sensitive detection systems to measure a fluorescence response.

However, the main disadvantage of the use of water dyes to determine sediment movement is that it assumes that suspended sediment behaves similarly to dissolved material, which is incorrect (Spanhoff & Suijlen, 1990a,b). Therefore, for a more accurate determination of

suspended sediment dynamics, particle tracers are more suitable.

2.3 PARTICLE TRACERS

2.3.1 Introduction

Fine sediments may travel large distances in estuarine and marine environments from their source to their final destination where they settle permanently and accumulate. The sources may be natural, erosion for instance, or anthropogenic, such as dumping. To determine the impact of a specific source it is always necessary to distinguish the source sediments or pollutants from background or other pollutant sources. The sediment to be studied rarely has a sufficiently distinct fingerprint to enable sourcing, which create a need for an artificial tracer (Spanhoff & Suijlen, 1990b).

A tracer particle is one which can be followed or monitored, above background through a system to enable some indication of how that particular system works. A tracer, for use in determining the sediment particle dynamics in freshwater and marine environments, has to fulfil certain requirements:

i) resemble the sediment closely, hydraulically and in terms of physico-chemical properties such as density, settling velocity, size and surface charge.

ii) have a conservative behaviour with time during transport and after deposition (Salomons & Mook 1987; Spanhoff & Suijlen, 1990b)

iii) be easy to detect rapidly and reliably, and be detectable above the background (Carey, 1989; Newman *et al.*, 1990a)

iv) cause no harm to the environment

Four basic categories of tracer can be used for particle tracing experiments in the field:

1) natural,
2) chemical,
3) radioactive and
4) fluorescent.

The latter is focussed on and discussed separately due to the particular relevance to this research project.

2.3.2 Natural Tracers

The use of natural tracers is advantageous over artificial and radioactive tracers due to the ease and frequency of sampling and the reduced cost, although the tracer must have a conservative behaviour during transport, with time and after deposition. Salomons and Mook (1987) applied the use of natural differences in composition between marine and fluvial sediments as a natural tracer, and were able to determine a mixing ratio between the two sediment types. Marine sediments were seen to be transported beyond the freshwater boundary in an estuary. However, the source of the natural tracer needs to be specific, and again the system has to be in equilibrium.

Differences in chemical, mineralogical and isotope composition of sediment have been used to interpret pollutant patterns in estuaries. However, problems have arisen due to the compositions varying with grain-size distribution. In addition, Salomons and Mook (1987) found that chemicals associated with sediment were reactive during transport within an aquatic environment, which in turn changed the sediment composition. For example, redox changes and physical processes such as differential flocculation and sedimentation changed the sediment composition. Wiley and Atkinson (1982) examined the possibility of using natural fluorescence, dissolved silica and salinity discharged by two different river types (piedmont and coastal plain) into the ocean as natural tracers. Natural fluorescence was

successfully used in the two study areas as a tracer for the examination of riverine-marine mixing processes.

2.3.3 Chemical Tracers

Although chemical tracers can be used which are both natural and added, Mahaut and Graf (1987), and Salomons and Mook (1987) consider the use of natural and artificial tracing methods to be complementary, each providing their own solutions to sediment transport problems. Added tracer particles enable the transport pathways in aquatic environments to be examined more closely, although the stability and residence time of the tracer determines over what time period this information is available.

Chemical tracers can be used for particulate tracing studies and these have been examined by Spanhoff and Suijlen (1990a). Generally these are man-made chemical compounds that enter the aquatic environment by deliberate legal or illegal introduction, industrial accidents, licensed emission or from more diffuse sources such as agriculture and atmospheric deposition, e.g. organophosphate pesticides, heavy metals (Spanhoff & Suijlen, 1990a). Many of these compounds are hydrophobic and are adsorbed on the suspended particulate material that transport them (Salomons & Mook, 1987). The distribution of the chemical can provide quantitative information on the paths and fate of the chemicals concerned and associated sediment.

Many chemicals are unreactive in the aquatic environment and can be used as a tracer including for example highly substituted cogeners of PCBs which have low solubility and bio-degradability. One problem with such chemicals is their strong affinity to the organic matter in sediments, resulting in different transport patterns to other components of the sediments (Spanhoff & Suijlen, 1990a). Another disadvantage is that chemicals are often difficult to measure on a routine basis. These chemicals, including PCBs and PAHs, are also lipophilic and as a result build up in the fatty tissues of organisms causing toxification of species high up the food chain. The chemicals which can be used as chemical tracers are therefore the

same nuisance chemicals which cause environmental problems and which require much greater monitoring and control of emission.

2.3.4 Radioactive Tracers

Deliberately released radioactive tracers cause much public concern (Spanhoff & Suijlen, 1990b), although they have been used to study particulate transport in many aquatic environments (Crickmore, 1976). Crickmore (1976) outlines techniques, developed and used by the Hydraulics Research Station during the 1960's and 1970's, using radioactive tracer particles to enable the interpretation of sediment transport in the engineering and dredge dispersal field. Several studies have involved the use of sand and silt sized radioactive particles with a half-life chosen to suit the experimental duration with *in situ* and continuous detection possible (Vukmirovic, 1963; Hubbell & Sayre, 1964). Bromine 82, a gamma-emitting isotope, which has a half-life of 36 hours, is especially useful for short-term dispersion studies. Other isotopes, such as Gold 198 (half-life 2.7 days) and Silver 110 (half-life 253 days), have been used for longer-duration studies. Moine *et al.*, (1985) studied sediment transport over a five year period using radioactive Scandium, examining the resuspension and drifting of sand particles.

Despite the regular use of natural radioactive tracers to measure particle residence time and sediment particle movement, success is limited due to difficulties in ensuring the tracer is in equilibrium with the sediment (Dyer, 1989). There are also other limitations to radioactive tracers, other than the obvious health risks and handling difficulties; they cannot be used in drying areas such as beaches, tidal flats etc. and as yet there is no successful labelling method for predominantly fine silt and clay deposits (Allen *et al.*, 1980).

Natural decay of elements provides a much more acceptable source of radioactive tracers which can be used for the study of long-distance particle transport, due to variations in their concentrations in the sediments. Natural radioactive tracers used during particle tracing experiments include many different elements, e.g. Carbon 14, Silicon 32, Lead 210 and

Thorium 234. Each environment must be tested specifically to find a natural tracer. Mahaut and Graf (1987) used natural radioactive isotopes to determine long-term and short-term sediment movements, although they concluded that it was necessary to use artificial tracers in order to observe the transport of specific particles.

2.4 FLUORESCENT TRACERS AND DETECTION

2.4.1 Fluorescent Tracer Particle Studies

Artificial fluorescent tracer particles are highly detectable above background fluorescence due to the specific fluorescence spectra of an added fluorescent element. Fluorescent tracers have a minimal health risk, and enable almost any aquatic environment to be studied, being able to examine specific processes and mechanisms involved in particle transport. Fluorescent tracers often require blind sampling, particularly if the tracer is evenly dispersed and remains within the study area. This can be overcome to a large extent with an accurate field survey of the study site and adequate sampling.

Several studies in recent years have used fluorescent particles for the determination of sand transport mechanisms and processes. Newman (1964) recognised the importance of fluorescent tracer particles in the understanding of sediment behaviour, and outlines the various chemicals and synthesis procedures required to manufacture a fluorescent block which can be crushed to a required size.

Ruck (1972) suggested that studying sediment movement could be undertaken using sediment petrography and marked tracer material. Ruck painted sand particles using "Wasserglas" (Na_2SiO_3) to act as a resin to allow the attachment of fluorescent paint to the particle surface. Hydraulic properties were unaltered after the washing and drying process, however detection proved difficult. Ruck (1977) avoided this detection problem by incoporating radioactive tracers enabling the initial location to be found more easily. Shrivastava (1975) outlined an approach to sand painting used in India, and provides a useful

breakdown of the available dyes, binders and painting techniques which can be used for field experiments.

However, the information on sediment particle transport using sand grains employed by Shrivastava (1975), Ruck (1977) and Mahaut and Graf (1987) had limited use due to the labour intensive detection (e.g. optical microscopy and ultra violet (UV) light under dark conditions), and poor resolution of the dispersed tracer particles. Fluorescent sand grains are now available commercially and have been used extensively in many beach and coastal applications worldwide (Farinato & Kraus, 1981; Kraus *et al.*, 1981; Burroughs, 1983; Ditmars *et al.*, 1986). Detection was still labour intensive using UV light employing manual counting or a spectrofluorophotometer and in some cases utilising precise selection of the specific resin and dye in question to be detected on the spectrofluorphotometer (Farinato & Kraus, 1981). This quantitative analysis provides an overall measure of fluorescence, not an accurate assessment of the number of particles.

These painting techniques cannot be used to manufacture cohesive sediment tracer particles, since they form hard blocks which cannot be broken up into their discrete grains with any degree of uniformity of the fluorescent coating (Section 3.4).

The need for a cohesive sediment tracer led to an examination of synthetic commercial particles which closely resembled natural silt particles (Draaijer *et al.*, 1984). Louisse *et al.*, (1986) found a fluorescent particle which had similar physical characteristics to cohesive sediment, which they called a 'Luminophore'. The fluorescent tracer particle comprised a highly fluorescent powder with small particle sizes which were detected by a fluorescence microscope. Spanhoff & Suijlen (1990a) describe the potential use of this fluorescent powder for the use in tracer studies examining large scale cohesive sediment transport. Newman *et al.*, (1990a,b) examined the possibilty of undertaking a particle transport study of a sewage plume using an identical fluorescent powder to Spanhoff and Suijlen manufactured by Day-Glo Color Corp. Extensive laboratory tests by Newman *et al.*, (1990a) suggested the powder was sufficiently analogous to fine cohesive sediment.

Newman *et al.*, (1990a) noted that if automated tracer particle counting was developed then fine particle tracers could be detected at lower concentrations. They showed analytical flow cytometry (Section 2.4.2) to be a viable method for detecting and sizing small fluorescent particles in laboratory suspensions. Extension of this technique to particle dynamics of a marine system, provided a valuable new tool for investigating the mechanisms underlying transport, deposition and erosion of natural aquatic particles.

Newman *et al.*, (1990b) introduced fluorescent particles into a coastal embayment system and after taking bottom sediment samples, particle concentrations in the top 2cm of bed sediment were counted using analytical flow cytometry. Some problems were encountered during this work i.e. the sampling grid was too coarse and particles were washed out of the system and so no information on the small scale variability was therefore obtainable. Newman *et al* (1990b) suggested that an evaluation be made prior to the experiment in order to determine the density and size distribution of the natural suspended sediment, the average depth of the water column and advective flushing rate of the site to prevent such problems; they concluded that with adequate experimental design the method was viable.

The use of a fluorescent dye within suitable resin material as a particle provides total stability from changing external factors, stabilising the fluorescent spectra, intensity and detection. In addition, the use of fluorescent dye in resin allows more fluorescent light photons within the particle, increasing the detection limits of the particles either in the field or in the laboratory.

2.4.2 Analytical Flow Cytometry

Analytical flow cytometry (AFC) is a novel technique for the rapid analysis (scanning more than 10^3 particles s^{-1}), and sorting of single cells based upon simultaneous, mutiple measurements of laser-induced particle fluorescence, light scatter and impedance (Burkill & Mantoura, 1990). AFC is a biomedical technique that is being increasingly applied in many other scientific fields, including oceanography (Holme-Hansen *et al*, 1984; Cucci *et al.*, 1986). This is due to its quantitative capability, versatility, sensitivity, speed, statistical

precision, and ability to identify cell subsets in, and sort them from, heterogeneous populations (Burkill & Mantoura, 1990). The technique used in this study has been reviewed recently by Shapiro (1988). The equipment used is the same as that reviewed by Burkill (1987a).

Particles within the flow chamber of the Analytical Flow Cytometer (Figure 2.1) are hydrodynamically focussed by a sheath stream. The laser light irradiates each particle as it passes individually through the beam. Each particle scatters the light and can fluoresce light which is recorded on a photodiode. Photomultiplier tubes measure the 90^{0} light scatter to give the particle refractive index, and measure the fluorescence properties of the particles in terms of red and green fluorescence. The signals are converted by sensors and held in a computer file. Detectors are mounted to measure forward-angle-light-scatter (FALS) which is then interpreted in terms of particle size by calibration, topographic and internal particle structure. Particle sorting is possible to a purity of greater than 98% using electrostatic charge generated by vibrations from a piezoelectric transducer in the sample stream. Filters optimise the fluorescence properties of particles in the flow cytometer allowing specific excitation and emission spectra to be examined. The lower the laser power the more precise the detection of particles, but the less defined the fluorescent peak. Therefore, adjustments in laser power can increase the fluorescent definition of particles but has the effect of lowering the detection of part of the particle population.

Although particle sizing can be carried out, albeit indirectly, Baier *et al.*, (1989) showed the sizing and electrostatic sorting of clay particles to be inaccurate; the particles were randomly orientated within the sample stream and therefore forward angle light scatter did not relate clearly to particle size. Despite the random orientation of the particles within the stream it is still possible to obtain a good representation of the particle size as found by Newman *et al.*, (1990a) and Marsh *et al.*, (1991).

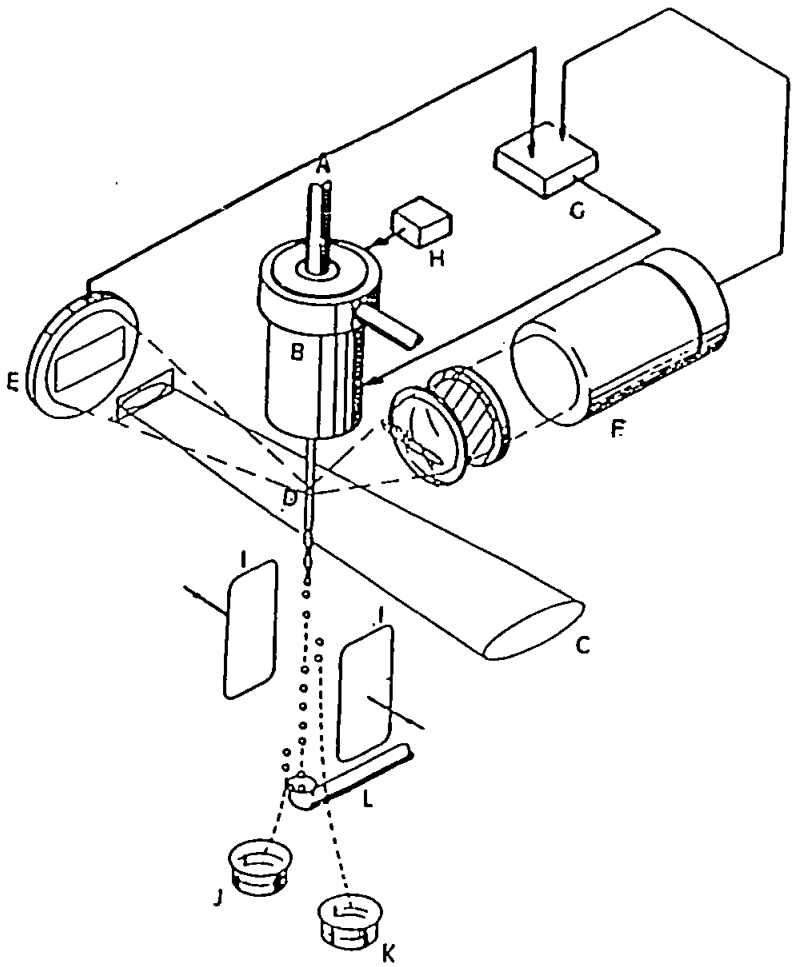

Figure 2.1 Schematic diagram of the particle analysis and sorting of an AFC (adapted from Burkill, 1987a)

NOTE: Cells or other suspended particles are introduced at (A) in to the flow chamber (B) where they are hydrodynamically focused by sheath fluid. Monochromatic light from an Argon-ion laser (C) irradiates each particle as it passes singly through the beam. Particles scatter and may fluoresce light from the analysis point (D). A photodiode (E) quantifies the forward angle light scatter to measure particle size, while photomultiplier tubes (F) pick-up the 90° light scatter for particle refractive index, and two-colour, wavelength-selective fluorescence to measure biochemical properties of the particle. Signals from these sensors are processed electronically (G) and held in a computer file. The sample stream is vibrated by a piezoelectric transducer (H), producing uniform liquid droplets at 35,000 per second travelling at 10 m s^{-1}. Droplets containing particles exhibiting the pre-set scatter and fluorescence characteristics are electrostatically charged at the droplet formation break-off point. As these droplets pass charged plates (I), they are deflected into sort chambers (J,K). Particles not meeting the required sort criteria pass undeflected into waste (L). Particles may be analysed and sorted at up to 5000 s^{-1}, with collection purities of 98%.

CHAPTER 3

SEDIMENT PARTICLE CHARACTERISATION AND THE EVALUATION OF ADSORBING FLUORESCENCE ONTO THE SEDIMENT SURFACE

3.1 INTRODUCTION

Outlined in Chapter 2 are the tracer techniques that have been developed for monitoring sediment dynamics. Although successful to a certain extent, suspended sediment movement has been inferred indirectly by the study of hydrodynamics, or traced directly by methods that have their disadvantages. Therefore, the development of a tracer particle technique for use in the monitoring of suspended sediment transport in freshwater and estuarine environments was undertaken. A tracer particle was required which was a good analogue of natural sediment and which would be accurately detectable.

In order to determine whether a tracer was a good sediment analogue, it was essential to firstly determine the physical characteristics of fine cohesive sediment. The physical properties of the sediment affect the erosion shear stress, the settling velocity and the transport dynamics in general. Having determined the physical properties it was then possible to assess the potential methods for labelling the sediment or creating a tracer.

Fine cohesive sediments are highly adsorptive of organic compounds, including pollutants (Lamere Hennessee *et al.*, 1986). By utilising this property it was considered possible to make natural sediment detectable for tracing by adsorbing an organic fluorescent dye or pigment onto the sediment surface or within the pores of the sediment itself.

3.2 PHYSICAL ASPECTS

3.2.1 Introduction

The size, density and concentration of sediment particles control their movements and settling behaviour within the water environment. The fundamental criterion of a sediment particle analogue is to have the same physical properties as the sediment to be studied. Therefore, these properties must be determined before a study of the particle dynamics within a system can be made using a tracer. In addition, if when a tracer is used, the sediment properties are altered, these changes must be quantified. The experiments described below were carried out to determine the physical properties of the natural suspended sediment from the turbidity maximum of the macro-tidal estuary of the River Tamar.

3.2.2 Size and Density

Bale & Morris (1987) and Fennessy *et al.*, (1994) discuss the relative advantages of the techniques available for measuring the size of particles. Aggregates are easily disrupted when samples are passed through a restricting orifice, e.g. in pipetting and sizing by Coulter Counter. Therefore, it was decided that the particle size of the sediment was to be measured with a Malvern Instruments Model 2200 laser diffraction particle sizer. The instrument comprises a light source which consists a 3mW laser, a spatial filter and beam expander and a detector which consists of a collecting lens, photodiode array and the electronic circuitry to interface with acomputer. Particle size distributions are derived from measurements of the near-forward, Fraunhofer diffraction spectrum that is produced by a particle population randomly distributed in the beam between the laser source and the detector array (Weiner, 1979).

In addition, in order to determine whether the suspended sediment characteristics in the turbidity maximum change during slack water, the size spectra changes during suspension of the sediment in a water column were assessed. Settled sediment samples were collected from

the bottom of a 0.5m column of suspended sediment which was allowed to settle for the set time periods of 5-15, 15-30, 30-60 and 60-120 minutes. The size spectrum of each subfraction collected was measured using the Malvern Particle Sizer.

Figure 3.1 shows the percentage of sediment particles in each size band (microns) of the fine cohesive suspended sediment from the turbidity maximum of the Tamar Estuary for the settling time of 30-60 minutes. The particle size ranged from less than 3 to greater than 30 microns with a median of 10.2 microns. These figures agreed with Bale (1987), who also determined the particle size of suspended sediment in the Tamar Estuary using settling experiments. Therefore, this size spectrum represents the sediment that had a settling velocity of less than 0.5m in 30 minutes, but faster than 0.5m in one hour. Unfortunately, the high concentration of sediment in the columns caused flocculation and high settling rates which altered the size spectra; this effect was not taken into account. During the settling period of 5-15 minutes, the suspended sediment spectra ranged markedly over a wide size band, from 50 to 200 microns. There was almost no difference between the size spectra of the sediment from the 15-30, 30-60 and 60-120 minute settling periods.

In addition to size spectra, the density of fine cohesive sediment needed to be determined. A density gradient column was tried, where calcium nitrate was hydrostatically balanced with distilled water in an attempt to obtain a density gradient in a glass tube. Unfortunately, this proved unsuccessful due to difficulties in creating a constant gradient. The density of an individual sediment particle is not an accurate measure of the settling characteristics of the particles, since flocs have settling rates which exceed that of constituent grains (Kranck, 1984; Delo, 1988a). The bulk density of sediment bed material is perhaps a more workable value when investigating the development of a fluorescent particle tracer technique. Thus, the bulk density of the Tamar Estuary was used and indicated an observed data range through the length of the estuary (0 to 30 km) as being 1.1-1.7 g cm^{-3} (Stephens *et al.*, 1992) and 1.1-1.4 g cm^{-3} within the region of tidal excursion for the turbidity maximum (which is a distance of 0-12 km from the weir on spring tides) as shown in Figure 3.2 (Stephens *et al.*, 1992). The density of flocs ranged from 1.1-1.4 gcm^{-3} (Dyer, 1979; Bale, 1987), agreeing closely with

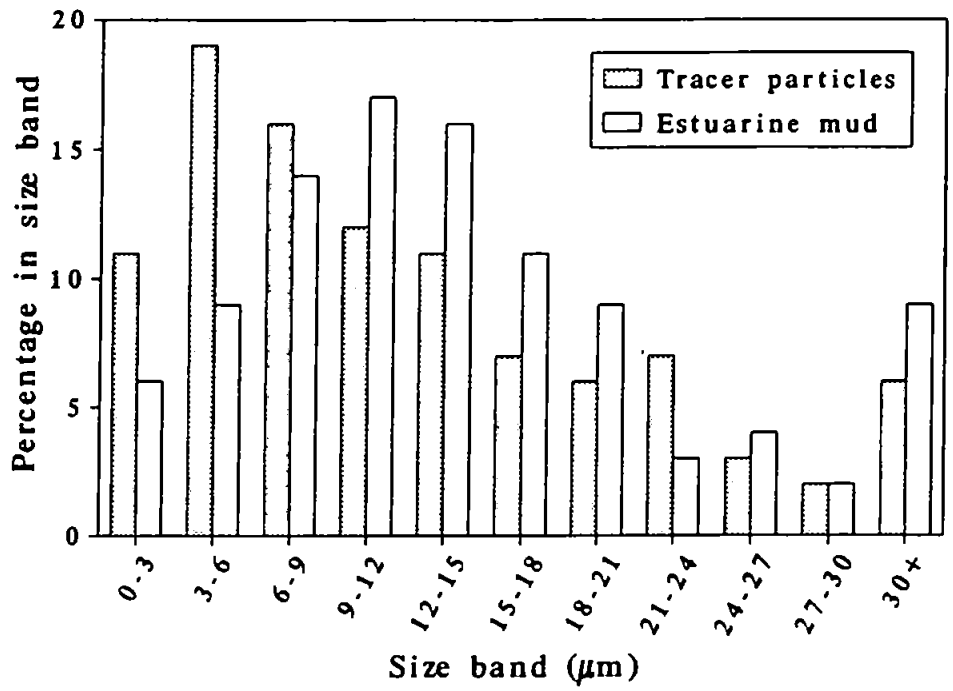

Figure 3.1 Particle size spectra of estuarine sediment particles from the turbidity maximum of the Tamar estuary and the spectra of the fluorescent tracer particles used for the studies.

the data shown in Figure 3.2.

To conclude, the results from the analysis of the size of the sediment particles and the density data of Stephens *et al.*, (1992) were used to assess the characteristics of potential tracers. This information was also used to determine the tolerances of changes to sediment properties which may occur as a result of fluorescent marking the sediment particles.

3.2.3 Surface Charge

3.2.3.1 Previous Studies

Natural organics or humics occur in all terrestrial and aquatic environments (Aiken *et al.*, 1985). Humics coat all natural surfaces and have important implications in all aspects of marine chemistry and physics, including flocculation (Sholkovitz, 1976), coagulation, sedimentation and adsorption of persistent organic chemicals within the environment (Choi & Chen, 1976; Stumm & Morgan, 1981) including PCBs and PAHs (McCarthy *et al.*, 1985).

The electrostatic attractive and repulsive forces which occur between suspended particles (surface charge) determines how they behave in terms of flocculation and settling. Determination of the surface charge of particles can be carried out using electrophoresis mobility measurements, which is the differential migration of charged particles through a given medium due to an imposed potential difference between immersed electrodes. Electrophoretic mobility (V_E in units $m^2 s^{-1} v^{-1}$) is the measured migration and denotes the charge of a particle.

The method commonly used for determining the electrophoretic mobility of a particle has been described by Davis (1982). Studies carried out by Hunter and Liss (1979) and Loder and Liss (1985) conclusively showed that by removing the organic coating from the surface of sediment particles, the electrophoretic mobility altered from negative with the coating, to positive without the coating. Natural organic coated particles used during the studies by

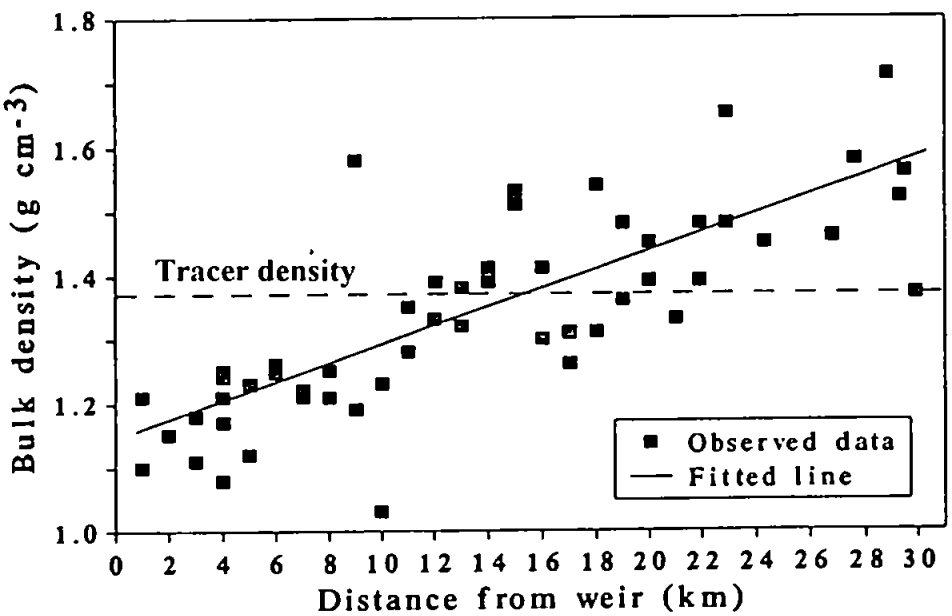

Figure 3.2 Axial profile of the sediment bulk densities in the Tamar Estuary (Stephens *et al.*, 1992) with the tracer particle density plotted for comparison.

Hunter, Loder and Liss recorded electrophoretic mobility which fell in the range -0.7 to -2.0 x 10^{-8} m^2 s^{-1} v^{-1}. These figures agreed with similar work carried out on both marine, estuarine and freshwater environments (Tipping *et al.*, 1981; Loder & Liss, 1982; Hunter, 1983).

3.2.3.2 Method and Results

The method used to measure electrophoretic mobility was similar to that outlined by Davis (1982). A charge was applied across a flat cell of known thickness and cross-sectional area (measured accurately using a micrometer and microscope which could be focussed both on the top and the bottom of the cell). Measurements were taken midway between the top and bottom of the cell. To remove organic material, all glassware was washed in chromic acid which was prepared by mixing 10g Na_2CrO_4 in 20ml of water and 100ml of sulphuric acid. Measurements were taken at a constant temperature of 25°C and the particles suspended in the cell were first measured whilst migrating under charge towards the positive electrode; repeat studies were then carried out whilst the sediment particles migrated to the negative electrode. Particles moved at varying speeds or mobilities depending on their amount of charge and whether positive or negative. The voltage remained constant and the polarity was reversed to monitor the particles travelling across the field of view in the opposite direction.

In addition to tests on estuarine material taken from the Tamar, further mobility studies were carried out using alumina (aluminium hydroxide). Aluminium hydroxide has a positive charge (Figure 3.3), but when mixed with natural organics (in this case river water) the charge becomes negative due to organic coatings. This supports the theory that surface charge changes take place when organic coatings are present.

The sediment analysed had a negative electrophoretic mobility based on more than 260 separate sample measurements. The results were similar to those found by Bale (1987), although the range of -3.4 to - 4.7 x 10^{-8} m^2 s^{-1} v^{-1} did not agree closely with the data from other estuarine studies (Tipping *et al.*, 1981; Loder & Liss, 1982; Hunter, 1983). The results are shown in Figure 3.3 indicating the spread of values for the estuarine sediment from the

Tamar, and the results from other estuarine studies. The sediment in the Tamar Estuary has an unusually high organic content (Stephens *et al.*, 1992) layer altering the surface charge which may explain the differences, although the technique is highly subjective, which is a more likely explanation, since the method of determining electrophoretic mobility involves measuring the mobility of an averageparticle whilst changing the voltage and direction of charge. The choice of average particle is not consistent particularly on different instruments and with different operators and this is made more difficult with irregular shaped, sized and charged particles as found in the Tamar Estuary. Hence, a large number of particles were sampled (i.e. 260 separate samples each analysed ten times for both positive and negative electrodes), in order to give a good average. However, the data displayed in Figure 3.3 provided a useful additional measurement of the physical properties of the fine cohesive sediment of the Tamar Estuary, despite differences with the sediment from other estuaries and coated aluminium hydroxide.

3.2.4 Settling Velocity

3.2.4.1 Introduction

The basic parameter used in determining rates of deposition in either still or flowing water is the settling velocity of the flocculated sediment. Settling velocity is dependent on the suspended sediment concentrations; settling velocities increase with higher suspended concentrations (Krone, 1972; Stevenson & Burt 1985; Puls & Kuehl, 1986). Settling velocity is also a function of salinity, but it is considered to have a secondary effect to turbidity (Delo, 1988a). As both turbidity and salinity increase, flocculation occurs leading to an increase in floc size and settling velocity up to the point of hindered settling, where the water moves through the pores between the particles, in contrast to the normal settling process of particles moving through the water (Owen, 1970a).

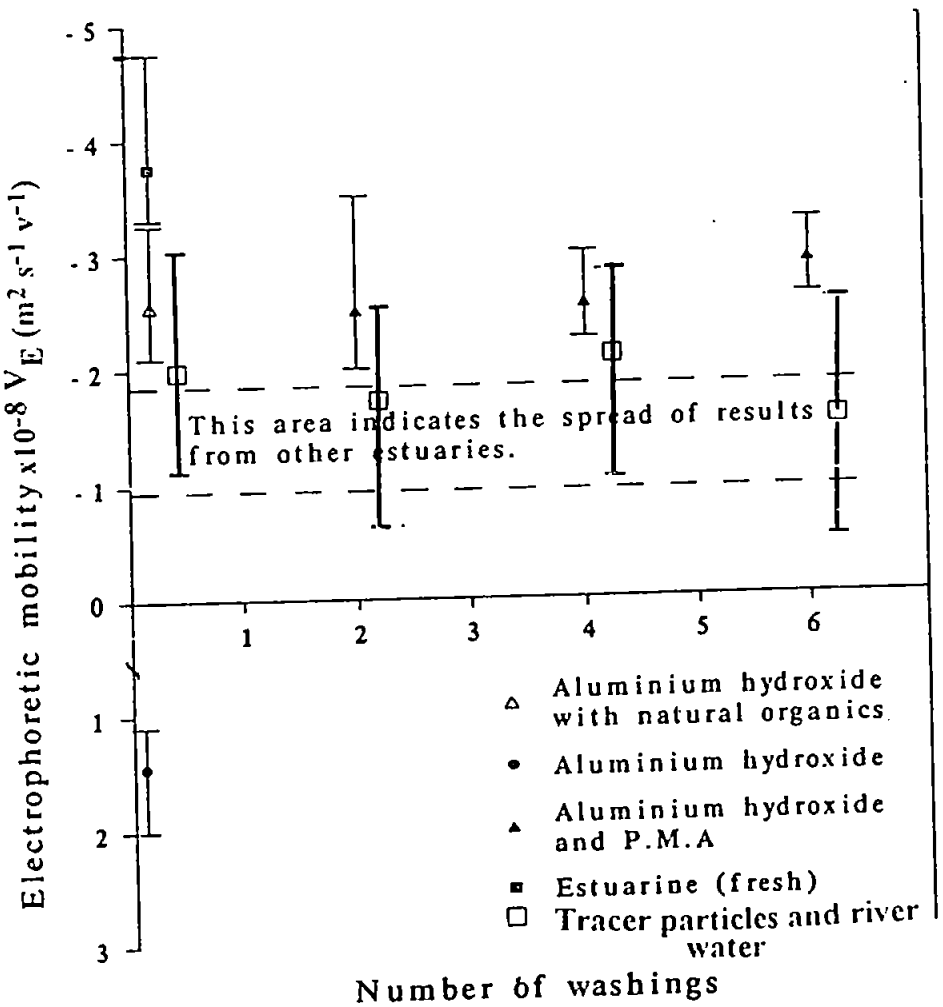

Figure 3.3 Electrophoretic mobility measurements for estuarine sediment, tracer particles and aluminium hydroxide particles with different organic coatings (natural and P.M.A.) to asess particle surface charge and stability after washing through time. Results from other estuaries were taken from values given by Tipping *et al.*, (1981), Loder & Liss (1982) and Hunter (1983). See Section 4.3.3 for the tracer data.

There is considerable variation in settling velocities for sediment from different estuaries (Delo, 1988a; Barton *et al.*, 1991), and therefore site-specific measurements are necessary for sediment dynamic studies.

3.2.4.2 Measurements of Settling Velocity

The settling velocity of flocculated sediment is usually represented by the median settling velocity W_{50}, which indicates that half the sediment by weight settles at a greater velocity than W_{50} (mm s^{-1}).

The most widely used technique for measuring settling velocity is the use of settling tubes, whereby a sediment of known concentration is allowed to settle over a precise distance with time (Owen, 1970a). Initially Owen used the technique in the laboratory followed by use as a field instrument (Owen, 1971; Barton *et al.*, 1989). Owen (1976), Delo (1988a) and Barton *et al.*, (1991) indicate that the laboratory measurements could be an order of magnitude lower than those measured in the field. This is because the suspension characteristics may be altered by the removal of the natural shear present in the flow, on isolation of the suspension within the quiescent conditions of the Owen tube. In addition, Delo (1988a) and Barton *et al.*, (1991) suggest salinity has an inconsistent effect in the field.

Burt (1984) and Fennessy *et al.*, (1994) describe the mode of operation for field studies and Van Leussen (1988) indicates the hydrodynamic and methodological limitations of the Owen Tube method.

3.2.4.3 Settling Velocity Studies

Barton *et al.*, (1991) described settling velocity studies in the laboratory using mud collected from the turbidity maximum of the Tamar Estuary and field measurements within the turbidity maximum itself. It was shown that the width and length of the tube did not significantly affect the magnitude of the settling velocity.

Studies were carried out to establish the physical settling characteristics of natural sediment particles using settling tubes similar to those described by Owen (1970a). The mud was collected at low tide from surface deposits in the middle of the upper Tamar Estuary and freshwater from the River Tamar was used to make up the varying turbidities.

The studies were carried out for various particle concentrations and salinities. Particle concentrations ranged from 0.1-10.0 g l^{-1} and salinities ranged between 0-5 ppt corresponding to the high turbidities and low salinities found within the turbidity maximum in the upper reaches of the Estuary.

The mud slurry was washed with freshwater from the River Tamar to remove salts, and the appropriate salinity was prepared using anhydrous sodium chloride. The sediment suspensions of different concentrations and salinities were left overnight to ensure that they equilibrated and that they would have the same characteristics as natural cohesive sediment. Particular care was taken over the suspended sediment concentration since this is the most influential factor affecting the flocculation processes, and thus settling velocity. Each settling velocity study was duplicated for each different salinity and turbidity to test for reproducability.

Figure 3.4 indicates that settling velocity is strongly dependent on suspended sediment concentration and that settling velocity increased with increased volumetric concentration. Figure 3.4 also indicates a decrease in settling velocity at increased concentrations of particles for a salinity of 5 ppt. This may be due to hindered settling, but the effect is not evident at the salinity of 1 ppt. Salinity appears to have limited effect other than at particle concentrations lower than 0.3g l^{-1}.

The results in Figure 3.4 also indicate that the median settling velocity increases with concentration up to a value at which a further increase in concentration hinders settling. This agrees with the work by Owen (1970a), Krone (1972), Kranck (1984) and Barton *et al.*, (1991). The results also show that the effects of salinity are secondary to those of

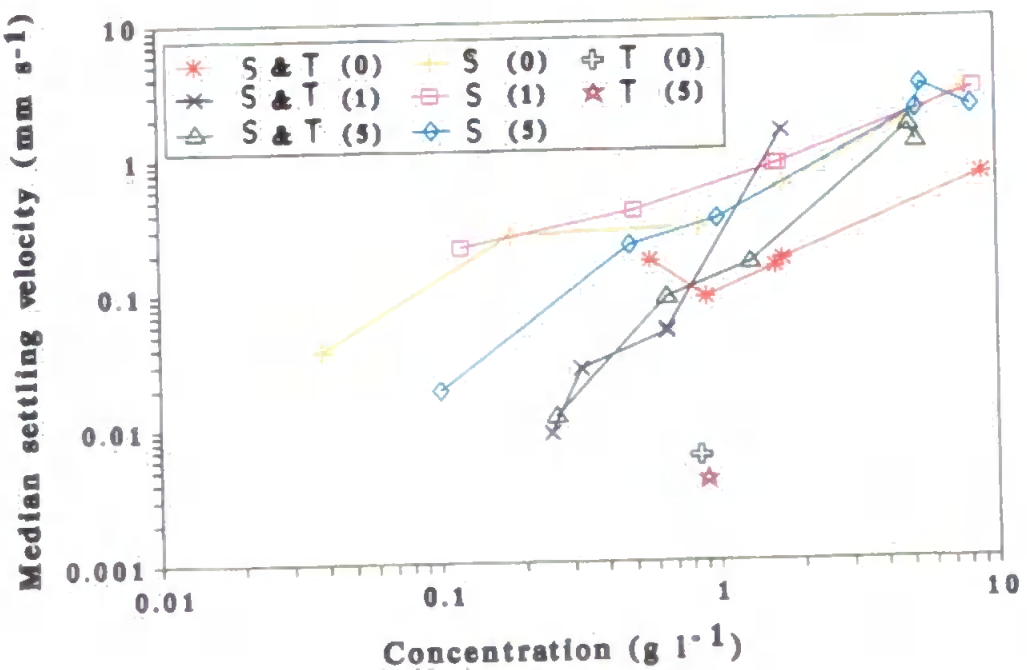

Figure 3.4 Median settling velocity measurements of suspensions at different concentrations and salinities (0, 1 & 5) comprising (1) estuarine sediment (S), (2) estuarine sediment and tracer particles (S & T) and (3) tracer particles (T).

concentration, which agrees with the work performed by Owen (1970a), Delo (1988a) and Barton *et al.*, (1991). The laboratory results of settling velocity using mud from the Tamar Estuary turbidity maximum agree closely with those given by Barton *et al.*, (1991).

3.3 LABORATORY EXAMINATION OF ADSORBING FLUORESCENCE ONTO THE SEDIMENT SURFACE

3.3.1 Natural Fluorescent Aquatic Organisms

The movement of contaminants can only be understood through a knowledge of the movement of particles (Dyer, 1989). Therefore, when considering a tracer it is important to chose one that closely resembles the sediment particles under study. The complexity and range of the physical properties of natural estuarine sediment, as described in Section 3.2, highlights the difficulty in creating a non-sediment based analogue. The ideal approach is to fluorescently mark natural sediment ensuring that the fluorescence is sufficiently different to naturally occurring fluorescence particles including algae and phytoplankton.

Seawater absorbs large quantities of ultraviolet light, between 200 and 300nm with lower absorption at 300 to 400nm, and large quantities of infrared light (720-1000nm), while marine organisms absorb light within the visible spectrum. For example, green algae absorb light and fluoresce between 350 and 450nm when excited, with a peak absorbency at 410-420nm. Green algae also absorb visible light at a peak of 700-720nm. The size of phytoplankton and zooplankton is variable and ranges from a few microns to several millimetres. Therefore, there are many organisms which naturally occur in the water environment with a similar size range to suspended sediment and which are fluorescent.

Within the visible spectrum, between the wavelengths of 450 and 700nm, there are fewer fluorescent organisms. Some species of diatoms, fucoids and dinoflagellates fluoresce within this range, but with a medium level of absorbency (Meadows & Campbell, 1988).

3.3.2 Fluorescent Dyes

The optimum fluorescence spectra of dye (between 450-700 nm) which could be used to mark sediment needed to be different to naturally fluorescent particles in both freshwater or seawater. A soluble pink rhodamine based dye, 'Soluble Intermediate Pink', was purchased from SWADA, London, which had a 550nm excitation spectra and 570-580nm emission spectra.

A Perkin-Elmer Model 3000 Fluorescence Spectrophotometer (FSPM) was used to measure the fluorescence spectra of the dye and determine the dye's stability. Five samples of the fluorescent dye at concentrations ranging from 4.1 to 14.9 $\mu g\ l^{-1}$ were tested immediately after preparation and one month later. Measurements were made using two clear quartz cuvettes, one containing distilled water as a blank control and the other containing the pink dye solution. The fluorescence excitation and emission spectra were consistent between serial dilutions, and remained constant after one month.

Once it was confirmed that the FSPM was capable of detecting the dye, it was necessary to test whether fluorescent particles could be detected without light scatter problems. A dilution of fluorescent latex calibration spheres was prepared, the latex suspension was successively washed in clean water and centrifuged to assess whether leaching of the fluorescence occurred into the supernatant liquor. The results indicated that if particles are fluorescent and do not leach colour into the supernatant then the FSPM can detect the fluorescence. For a dyed sediment to be successful as a tracer there must be no leaching of the dye.

3.3.3 Detection Equipment and Standardisation

The FSPM detected significant levels of diffraction and reflection of light with different sediment suspensions; for example a mud suspension was measured to have the same relative fluorescent units as a concentrated solution of fluorescent dye.Therefore, to assess whether the fluorescent dye was passively adsorbed onto the sediment it was necessary to determine

the background fluorescence intensity of the sediment suspension without dye. The light transmission levels of suspended sediment samples were measured using the Malvern Particle Sizer, and then the relative fluorescence of the suspensions was measured using the FSPM. The results are shown in Table 3.1.

Light transmission	Fluorescence $\mu g\ l^{-1}$
100%	0.05
60%	12.0
50%	23.3
40%	38.5
30%	60.0
20%	76.5
10%	97.0

Table 3.1: Fluorescent intensity as a function of light transmission for different concentrations of sediment suspensions.

These results enabled an estimation of the degree of fluorescence expected for a sediment suspension that produced the above light transmissions. In order to compare the results of investigations on the adsorption of fluorescent dye, the sample sediment suspensions to be tested were all made up to have a light transmission of 30%.

3.3.4 Passive Adsorption of Dye

The method for creating a fluorescent marked natural sediment particle was approached step-by step. Firstly, an attempt was made to dye the surface of the sediment. Due to the adsorptive nature of fine cohesive sediments to organic compounds it was considered possible to adsorb an organic fluorescent dye or pigment onto the surface or within the pores of the sediment itself. If this proved successful it would enable the sediment to be detected and its

movements traced.

Sediment (collected by settling between 15-30 minutes; size 1-30 microns; Section 3.2.2) was mixed with the dye to assess any passive adsorption onto the sediment. The fluorescence of the sediment and the supernatant liquor were measured after centrifugation. The suspension was centrifuged, the decanted supernatant fluorescent intensity was measured and then clean water was added to the remaining sediment. The suspension was then mixed, followed by measurement of the fluorescent intensity; the process was repeated. The sediment and dye suspension was washed 7 times in total. The results are shown in Table 3.2.

No. of washings	Fluorescence in µg/l	
	Suspension	Supernatant
1	68	96
2	64	81
3	60	69
4	75	60
5	75	68
6	62	52
7	68	49
Sediment only (average)	64	12

Table 3.2: The fluorescence of sediment suspensions and supernatant after successive washes

The results indicate that no fluorescent dye was passively adsorbed on to the sediment since the fluorescence intensity of the sediment did not remain higher than the background level of 63 after successive washes.

A study was carried out to assess whether the previous studies had not allowed sufficient time for the dye to adsorb, particularly if the adsorption process required a number of hours. Figure 3.5 indicates the fluorescent intensity (mg l^{-1} of dye) of sediment having been added to a known dye concentration of 23 mg l^{-1} over a period of time in order to measure the uptake of dye over a longer period. The stirred fluorescent dye solution was measured on the FSPM to provide initial fluorescence intensity. Discrete samples of sediment and dye suspension were tested for fluorescent intensity as was the supernatant after centrifugation. The results indicate an initial adsorption of approximately 2.0 mg l^{-1} of dye onto the sediment when corrected for dilution of the solution with sediment. The fluorescence intensity measured on the FSPM shows decreasing levels during the subsequent hours. The dye concentration at the end of 8 hours was significantly less than the fluorescence level at the start of the test. The fluorescence intensity of the sediment alone at a similar concentration was between 18-20 mg l^{-1}.

Duplicate studies were undertaken to establish whether it was possible to force dye adsorption by increasing and decreasing the concentration of dye. It was concluded from these studies that passive adsorption was not stable and therefore direct adsorption needed to be investigated. Various techniques for physically attaching the fluorescent dye to sediment were tried by trapping the dye within natural or synthesised organic compounds.

3.3.5 Active Adsorption using Natural Organics

The surface organics were removed from some estuarine sediment in order to determine whether dye could be adsorbed into the mineralogical structure of the sediment, and the organics then re-adsorbed, hence trapping the dye within the sediment particle structure. The organic layer from the sediment was removed by dissolving the organics with potassium hydroxide (KOH) and heating the sediment in an oven at 180°C to breakdown and disassociate the organic material. Several studies were carried out to adsorb dye onto the sediment surface or in to the sediment structure with little or no success. One example involved the following methodology.

A 1 litre solution of dye at a concentration of 17.55 mg l^{-1} was added to 1 g of ashed inorganic sediment and stirred for 4 hours using a magnetic stirrer. The liqiud was split into two 500 ml aliquots. One of the 500 ml aliquots was analysed for passive adsorption; the sediment was successively washed four times and the sediment and supernatant measured for fluorescence using the FSPM, as described above. The other 500 ml was mixed with 500 ml of river water with a high organic content and stirred thoroughly. The sediment received four successive washes and centrifugations, and the fluorescence of the sediment and supernatant was measured using the FSPM The FSPM did not detect any adsorption of the dye onto the sediment.

3.3.6 Active Adsorption using a Synthesised Organic Compound

Humic and fulvic substances in soils and aquatic environments provide an organic layer which creates a medium to support animal and plant life. This is particularly important when rejuvenating soils from mining waste piles or slag heaps and in aquatic environments after pollution spills. Anderson and Russell (1976) describe the synthesis of a good analogue of natural humic substances called poly-maleic acid (PMA), which they used to rejuvenate soils and improve soil substance and structure.

The recipe for synthesis was obtained and PMA synthesised in the laboratory. It was suggested by Dr. H.A. Anderson (pers. comm.) that fluorescent dyes could possibly be mixed during the initial stage of synthesis of the molaic acid or possibly to the final compound of PMA prior to the dialysis.

It was considered that the synthesis of PMA, with a fluorescent dye may allow active adsorption of fluorescence onto the sediment surface and therefore further synthesis with the pink dye was carried out. There was no alteration in fluorescent spectra of the dye during PMA synthesis which was checked by using the FSPM. The synthesised PMA with dye was then attached to the surface of natural sediment and to sediment that had been ashed so that it was inorganic. However, the measured fluorescence of the sediment particles did not

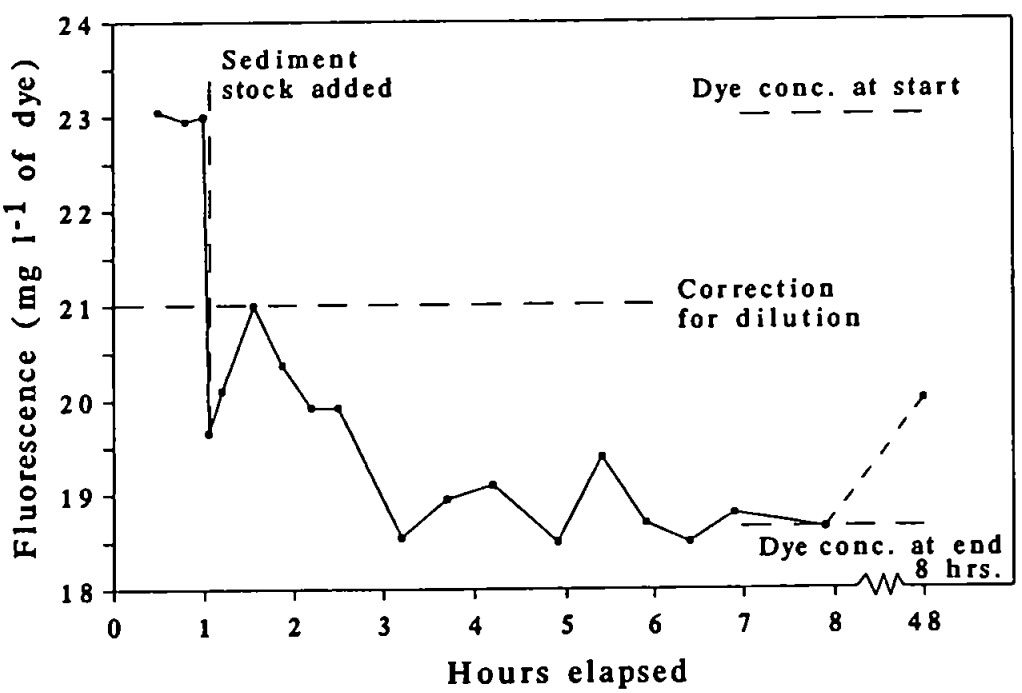

Figure 3.5 Time series of passive adsorption of fluorescent dyes on to natural estuarine sediment.

indicate additional fluorescence above that of the background fluorescence; the FSPM did not detect adsorption of the dye.

A further series of tests were carried out also using the pink dye. The dye was mixed with 1) natural estuarine particles, 2) inorganic ashed estuarine particles, 3) estuarine particles with PMA, 4) inorganic ashed estuarine particles with PMA, 5) alumina and 6) alumina with PMA. The adsorption of PMA on to sediment and alumina was tested using electrophoretic mobility tests as described in Section 3.2.3. As can be seen from Figure 3.3 the attachment of PMA to alumina had the same result as attaching natural river organics to the alumina, with the alumina changing from a positive surface charge to negative as a result of adsorbing organic or simulated synthesised organics in the form of PMA.

This effectively showed the PMA readily adsorbed onto the sediment surface within a few minutes, and remained adsorbed after a series of washings (using the technique described in Section 3.3.3), which supported the technique for investigating the adsorption of dye. However, the pink dye when synthesised with the PMA could not be detected above the background fluorescence. If a detectable dye could be successfully synthesised with the PMA, and PMA was adsorbed onto the alumina it was possible that PMA and dye could be adsorbed on to natural or ashed sediment.

Further dyes were obtained from different manufacturers to ensure that the behaviour of the Soluble Intermediate Pink dye described previously was not anomalous. A total of eight dyes were mixed during synthesis or dialysis of the PMA with no success. It was noted at this point that the PMA not only had a brown visible colouration, but also had a fluorescent spectra which may have caused slight masking of some dyes used. The eight dyes used, including Soluble Intermediate Pink are listed below with the respective excitation (Ex.) and emission (Em.) characteristics and sources.

i) D-275, Molecular Probes Inc., Oregon USA - a cationic lipophilic dye with a carbocyanine and strong absorbtion properties. (Ex. 484, Em. 507nm)

ii) D282, dye as above, but slightly different fluorescence spectra. (Ex. 547, Em. 571nm)

iii) Invisible Pink, SWADA, London (Ex. 555, Em. 575nm)

iv) Insoluble 1 - Invisible Yellow, SWADA, London (Ex. 420, Em. 515nm)

v) Acidine Yellow - Townley, Warrington (Ex. 457, Em. 497nm)

vi) Acrylon Pink - Townley, Warrington (Ex. 551, Em. 578nm)

vii) Acidine Rhodamine - Townley, Warrington (Ex. 567, Em. 582nm)

viii) Soluble Intermediate Pink, SWADA, London (Ex. 550, Em. 580nm)

To ensure comparability between tests, each suspension of sediment was made up to the standard 30% light transmission, then the fluorescence was measured of both the suspension and supernatant (as described in Section 3.3.3).

All the dyes were tested with sediment (natural and ashed) and alumina both with and without PMA. The tests proved unsuccessful with no measurable adsorption of any dye detectable using the FSPM.

3. 4 FLUORESCENT PAINTING OF SEDIMENT

At the same time as trying the additional fluorescent dyes, enquiries were made into the use of commercially manufactured fluorescent sands using fluorescent paint, and whether the technology could be applied to fine cohesive sediments also. British Industrial Sands at Kings Lynn, East Anglia were approached to produce a small quanitity of fluorescent silt, although the smallest size fraction they manufactured was 60μm with a red or blue fluorescent lacquer.

In order to attempt to fluorescently mark natural fine sediment it was necessary to freeze dry a mud sample in order to paint the mud with a fluorescent lacquer whilst dry.

The result was a hard cement-like structure which would not disaggregate, grind or break-up very easily. The structure and properties of the natural sediment had obviously been changed. This possibility was not pursued further.

3.5 DISCUSSION

The physical properties of sediment collected from the turbidity maximum of the Tamar Estuary were investigated. The results provided data which could be used to assess any alterations in the physical characteristics of sediment dyed to enable tracing, or used to assess potential sediment analogues that could be traced.

In order for a particle to be detectable by measuring fluorescence, it must be fully coated with fluorescent material or be fluorescent itself. The complexity and dynamics of a system to which a fluorescent sediment or tracer may be added could be extremely vigorous, dispersive and dilutive, particularly in highly turbid waters, and therefore it is essential that there is a very high chance of being detected in any samples collected if present.

The FSPM, when standardised, could be used to determine the fluorescence of particles and not just dyes. However, these studies showed that permanent passive adsorption of fluorescent dyes did not occur and de-adsorption was prompt. Active adsorption of dyes was attempted by removing the organic layer that coats sediment and then fluorescently marking the surface of the sediment and then re-coating the sediment with an organic layer. This also proved unsuccessful. Nevertheless, the removal of the organic layers or the addition of organic layers with fluorescent dyes may be possible in the future if there is a better understanding of the surface structure of the sediment and areas of adsorption.

Due to the inability to permanently dye the surface of the sediment it was decided that further research be carried out to develop an artificial sediment analogue that could be traced in natural aquatic environments.

CHAPTER 4

ARTIFICIAL FLUORESCENT SEDIMENT ANALOGUES: CHARACTERISTICS, DETECTION AND PRELIMINARY FIELDWORK.

4.1 INTRODUCTION

In the previous chapter the investigations into the physical characteristics of natural sediment from the Tamar Estuary are described. The unsuccessful attempts to label natural sediment with fluorescent dye led to the following investigation into the use of fluorescent sediment analogues as tracers. In order to assess the physical properties of a potential fluorescent analogue it was necessary to establish a method of detection. The experimental procedure and the detection limits are described below. The physical properties of the potential analogue were then measured and compared with those of natural sediment.

Once it was established that the fluorescent analogue was satisfactorily similar to natural sediment a preliminary field study was undertaken to test the experimental procedure developed.

4.2 ANALYTICAL FLOW CYTOMETER (AFC)

4.2.1 Initial Investigations and Calibration of the AFC

The analytical flow cytometer and its uses have been described in Section 2.4.2. Analytical flow cytometry uses laser light energy to excite the electrons within a particle which then emit light of a specific wavelength which is recorded.

To assess the viability and accuracy of the AFC for the determination of fluorescent particles, a calibration study was carried out. A precise serial dilution of calibration beads was prepared

in order to compare the measured against expected number of beads and create a calibration curve. Polyscience latex calibration beads were used for the dilution, since these beads when tested on the FSPM appeared to have a clear fluorescence peak with no leaching taking place (Section 3.3).

Suspensions of known concentrations of the beads were prepared by serial dilution. Four samples of each concentration were then analysed on the AFC to measure the number of beads. A sample of beads was also analysed using the Malvern Laser Diffraction Particle Sizer. The resulting size spectra had a mean of 21.5 μm with a standard deviation of 1.4 μm. This result was comparable with the manufacturers specification of 21.1 μm. The measured number of beads was then compared with the known number of beads per ml, determined using the manufacturers specifications and formula. The results of the calibration curve are shown in Figure 4.1 and the correlation coefficient was 0.95. Thus, the technique appeared satisfactory, with the observed deviation possibly caused by errors in the manufacturers specifications, inaccuracies in pipetting, non-uniform mixing of the calibration beads and analysis by the AFC at an inconsistent uptake rate.

Using the calibration curve data it was possible to estimate the number of latex beads or fluorescent particles that would be required to study the movement of sediment in an estuary and for detection at low concentrations. Assuming a 10 km long section of estuary which has a width of 25 m and depth 2 m then the volume of the estuary would be 5×10^8 l. If it is also assumed that the average turbidity in the estuary is 100 mg l^{-1} then there would be a total of 5×10^4 kg of suspended particulate material. Assuming the minimum detectability of 10 latex bead particles in 50,000 sediment particles (from Figure 4.1) then this represents 0.02% of 5×10^4 kg which equals 10 kg of latex beads. The use of latex beads would thus be prohibitively expensive (in the region of millions of pounds) and therefore cheaper material was required.

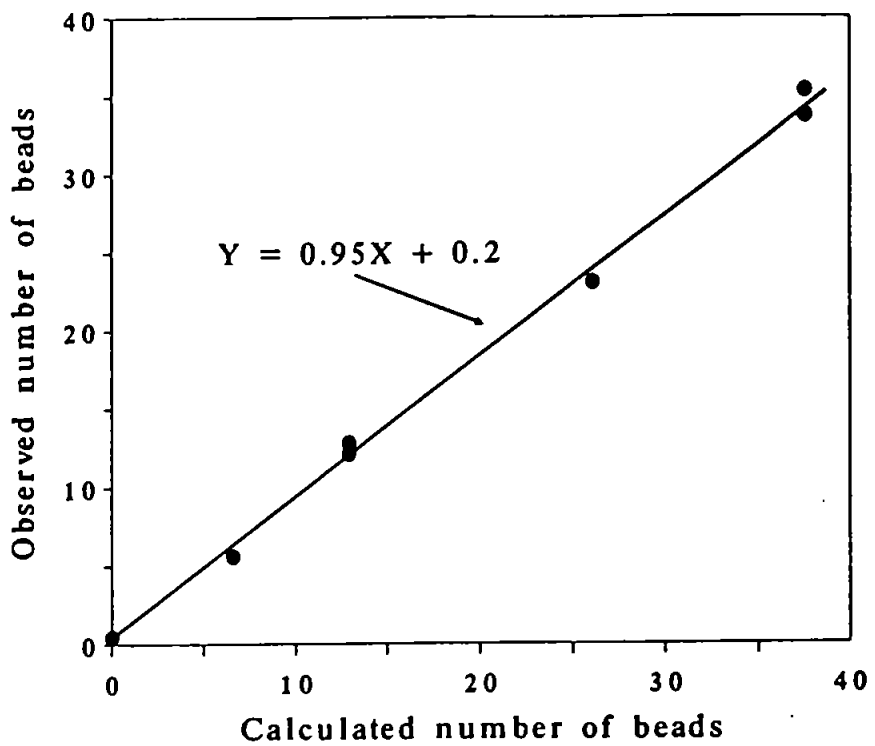

Figure 4.1 Calibration curve of Polyscience latex calibration beads measured on the AFC indicating calculated number of beads against observed number of beads

4.2.2 Assessment of Artificial Fluorescent Particles

The fluorescent soluble dye used in Chapter 3 was supplied by SWADA who also manufacture an insoluble powder material which comprises a highly fluorescent inert formaldehyde resin particle with a size range of 0.1-20 μm, mode 3-6 μm, and a density of 1.37 g cm^{-3} (manufacturers specifications). Investigation of the particles using fluorescent microscopy indicated that they had an irregular non-spherical structure and a modal volume of approximately 10-15 μm^3 (Plate 4.1). The characteristics of the resin indicated that it was harmless to the environment and that it had many similarities to natural sediment. Further tests were carried out to determine whether the particles could be detected and to assess the degree of similarity with natural sediment. SWADA could also supply the resin in different fluorescent colours, densities, and size of particles, and therefore it was anticipated that the right combination of characteristics of the material could be obtained and provide an analogue of natural sediment.

Fluorescent particles with different fluorescent spectra were obtained from SWADA . These included; Red 12, with an excitation (Ex) and emission (Em) peak of 555 nm and 600 nm respectively, Yellow 7 Ex 425 nm, Em 530 nm, and Orange 6 Ex 475 nm, Em 530 nm.

Red 12 was not used further due to the excitation and emission spectra being incompatible with the 488 nm Argon ion laser in the AFC.

Particles of Orange 6, and Yellow 7 were further investigated using the procedures described in Section 3.2. The excitation and emission spectra measured are shown in Figure 4.2. The results indicate that no fluorescence leached out of the particles into the supernatant after centrifugation, suggesting that the particles had stable and detectable fluorescence characteristics.

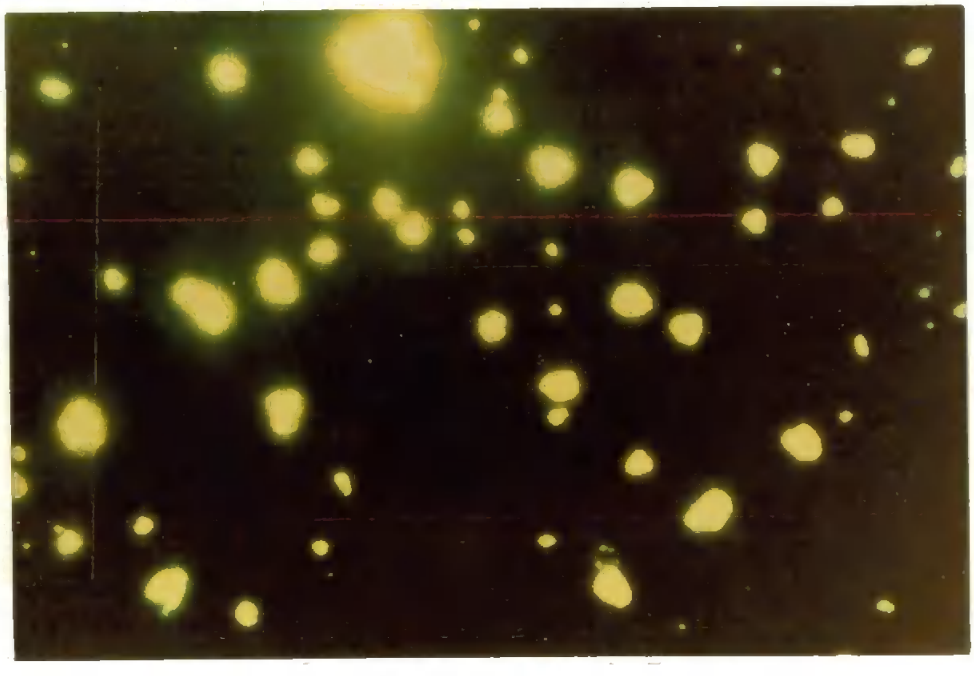

Plate 4.1 Photograph of the orange fluorescent particles used in the tracer study taken through a fluorescent microscope at x 100 magnification.

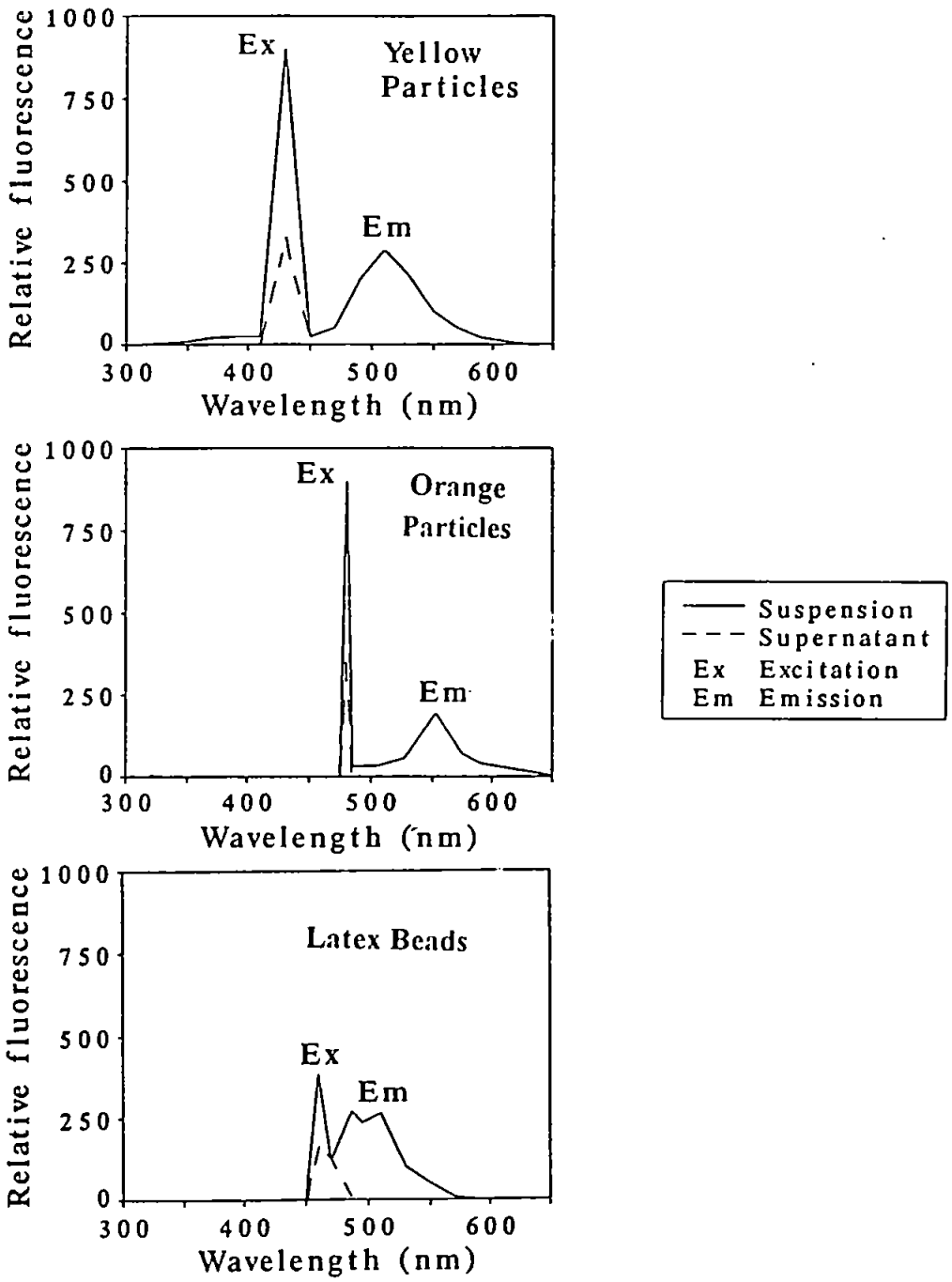

Figure 4.2 Fluorescent excitation and emission spectra of particle suspensions and centrifuged supernatant of Yellow 7, Orange 6 and Polyscience Latex beads measured on a fluorescence spectrophotometer.

Figure 4.2 also shows graphically the differences between the two fluorescent materials. The yellow particles have a higher luminescence i.e. a relative fluorescence for emissions of approximately 300 units, compared with the orange particles with a relative fluorescence for emissions of approximately 200 units. The excitation peaks are in different locations; the excitation wavelengths for the yellow and orange particles are 420-450 nm and 470-480 nm respectively. The excitation fluorescence spectra of the yellow particles is wider than that of the orange which had a very defined excitation fluorescence spectra since the material comprises fewer components and is essentially rhodamine based. The orange particles were found to have an excitation wavelength closest to the optimum wavelegth for the AFC laser of 488 nm, making them possibly more detectable on the AFC than the yellow particles.

4.2.3 Analysis of the Artificial Fluorescent Particles on the AFC

The next stage in the laboratory tests of the fluorescent particles was to analyse the particles on the AFC, and compare the detection to the calibration curve of Figure 4.1. Two types of calibration beads were used to enable comparison with the irregular artificial fluorescent particles, including the Polyscience latex beads (21.1 μm size) and Coulter Electronics Immunocheck latex beads (6 μm size). The latter calibration beads were used because they varied less in size and had a narrower band of fluorescence.

The data are displayed in Figure 4.3, with the green fluorescence on a log scale (LIGFL), the particle volume on a log scale (LCVA) and the forward angle light scatter or particle size on a log scale (LFALS). The results for the Immunocheck beads indicated a very precise particle volume, size and fluorescence intensity, shown by a narrow band of fluorescence and volume or size. Doublets (D) were detected where two beads were stuck together, shown by an increased size and fluorescence. The percentage of doublets was particularly small, less than 3% by volume. The small variation of the Immunocheck beads was clear and was expected since they are used for calibration of the AFC, and it suggested that the beads could be used for calibrating the size axis and fluorescent intensity of other particles with a high degree of accuracy.

The Polyscience bead analysis indicated a more variable fluorescence intensity and volume. The dark central region denoted the modal size by volume, but the deviation from the mode was large as shown by the hatched area.

Orange 6 fluorescent particles were also run and were significantly more variable with large differences in the fluorescence intensity and particle volume. The dark area at the top of the LIGFL scale represents highly fluorescent material which is too fluorescent to fit on the scale, and therefore accumulated in the last channel. The variation of fluorescent intensity is likely to be due to uneven spread of the fluorescent pigment within the resin itself or on the surface and the angular shape of the particles (Plate 4.1). A variation on size is also indicated in Figure 4.3 for the orange particles. The fluorescent particles are clearly detectable and sufficiently fluorescent with a specific spectra that they are unlikely to interfere with natural fluorescence from inorganic and organic compounds, including clay minerals etc., and natural organisms in the water environment.

4.2.4 Calibration of the AFC using the Artificial Fluorescent Particles

Since the orange and yellow fluorescent particles were readily detectable on the AFC the detection limits upon dilution were assessed. The fluorescent particles were serial diluted initially and the numbers of particles counted when mixed with varying numbers of natural estuarine particles.

Figure 4.4 shows the calibration curves for the orange and yellow particles, with the measured concentration of particles plotted against that expected. The plots show a similar trend to that in Figure 4.1 for the Polyscience beads. The correlation coefficients are 0.93 (+/- 6.2%) for the orange and 0.88 (+/- 8.6%) for the yellow particles, which indicate a good correlation. The measured concentrations were obtained from analysis on the AFC and the expected concentration was produced by adding a precise pipetted volume of a stock suspension. The exact numbers are not known since the particle size range is large and the density is not sufficiently precise to quantify the numbers accurately. The concentrations

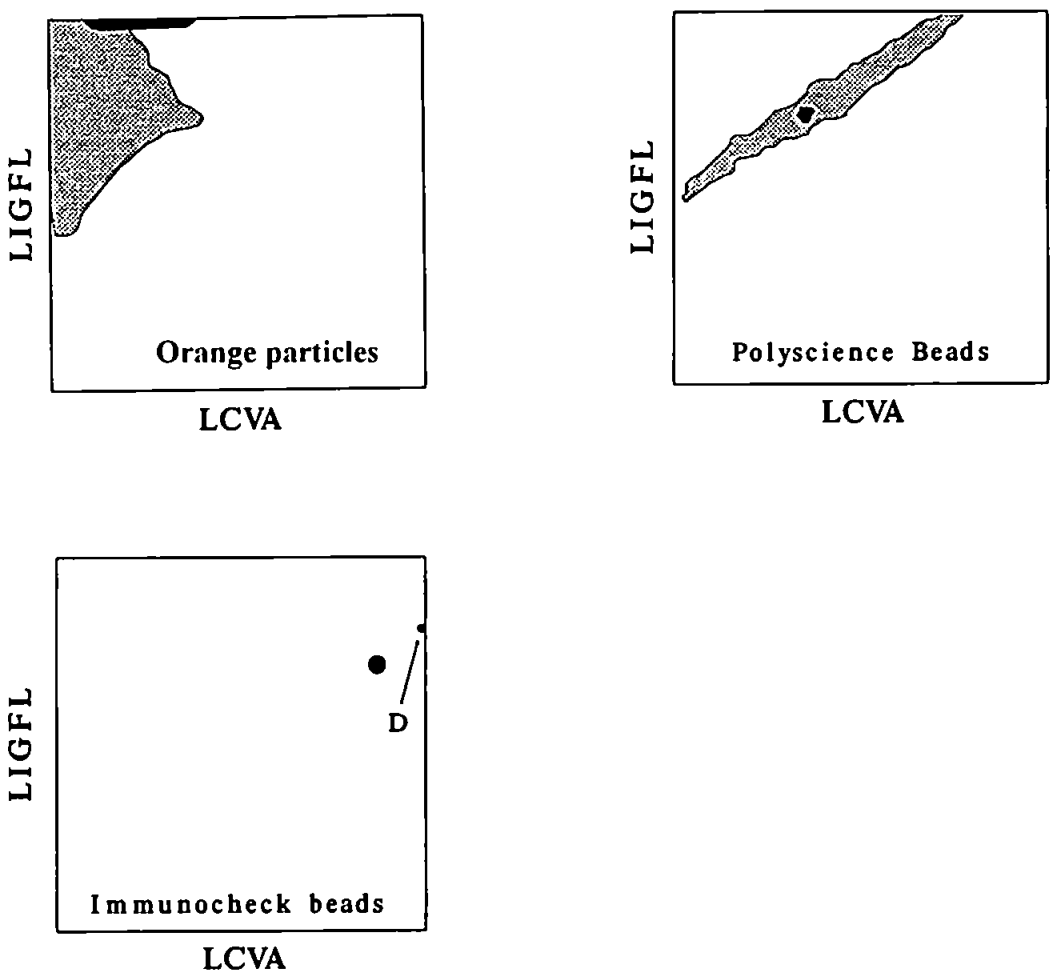

Figure 4.3 AFC plots of fluorescence intensity (shown by logarithimic green fluorescence - LIGFL) versus logarithmic particle volume (LCVA) for Orange 6 tracer particles, Polyscience beads and Coulter Immunocheck beads. The graphs indicate the variance in fluorescence and size/volume of each particle population. The density or number of particles in each band are denoted by the colour with a higher density coloured black and fewer particles shaded grey. The Immunocheck beads clearly have a tight fluorescent spectrum and uniform size, whereas the Orange 6 particles have a wide range of size and fluorescence with a high population with intense fluorescence. D denotes doublets, two particles stuck together.

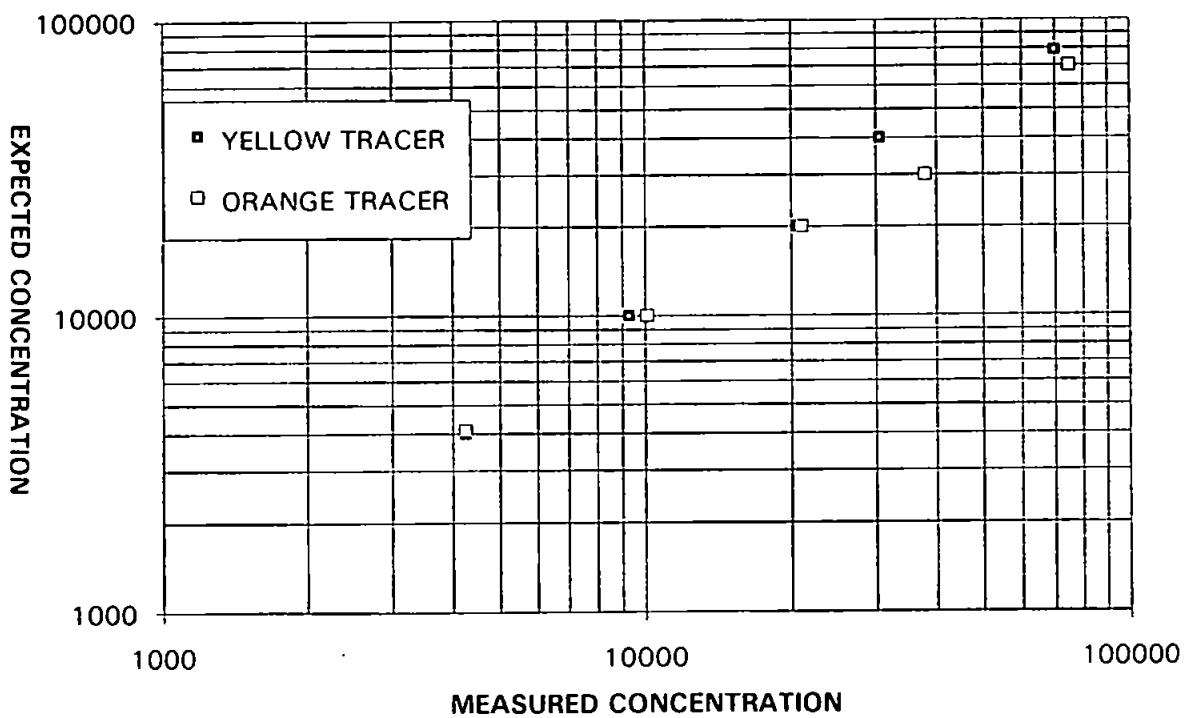

Figure 4.4 Calibration curves of yellow and orange fluorescent tracer particles measured on the AFC indicating measured concentration against expected concentration.

therefore represent the expected and measured changes in concentration

In order to assess the ability of the AFC to distinguish between natural sediment and the fluorescent particles, orange particles were added in increasing amounts to a constant concentration of estuarine mud. The mud contained a wide range of particles sizes with some natural inorganic and organic materials which were partially fluorescent. The resulting correlation shown in Figure 4.5 was reasonably good, despite a background fluorescence and indicates that the AFC is capable of distinguishing between the sediment and the fluorescent particles, and that the inclusion of sediment does not have a marked effect on the fluorescent detection of the orange particles.

Figure 4.5 also shows a plot of constant orange particle concentration with increasing mud, providing an assessment of the lower detection limits of the orange particles in turbid conditions. The increase in mud concentration provided a turbidity range from approximately 0.1 to 2.1g l^{-1}, at which levels the fluorescent particles were still detected on the AFC. The cost of the orange particles was such that if used as a tracer in a study of sediment movement in the Tamar Estuary, as described in Section 4.2.1, it would be relatively inexpensive at a cost of the order of several hundred pounds.

4.3 PHYSICAL CHARACTERISTICS OF THE FLUORESCENT PARTICLES

4.3.1 Stability

Once it was established that the fluorescent particles were detectable by the AFC and could potentially be used as a tracer, physical characteristics of the orange fluorescent particles were examined in order to assess their viability as a sediment analogue. The orange particles were chosen since they were considered to be the most detectable on the AFC with the highest correlation coefficient. In order to examine the physical properties of the fluorescent particles, first it was necessary to establish that the particles were stable in water, and determine the optimum method for dispersion.

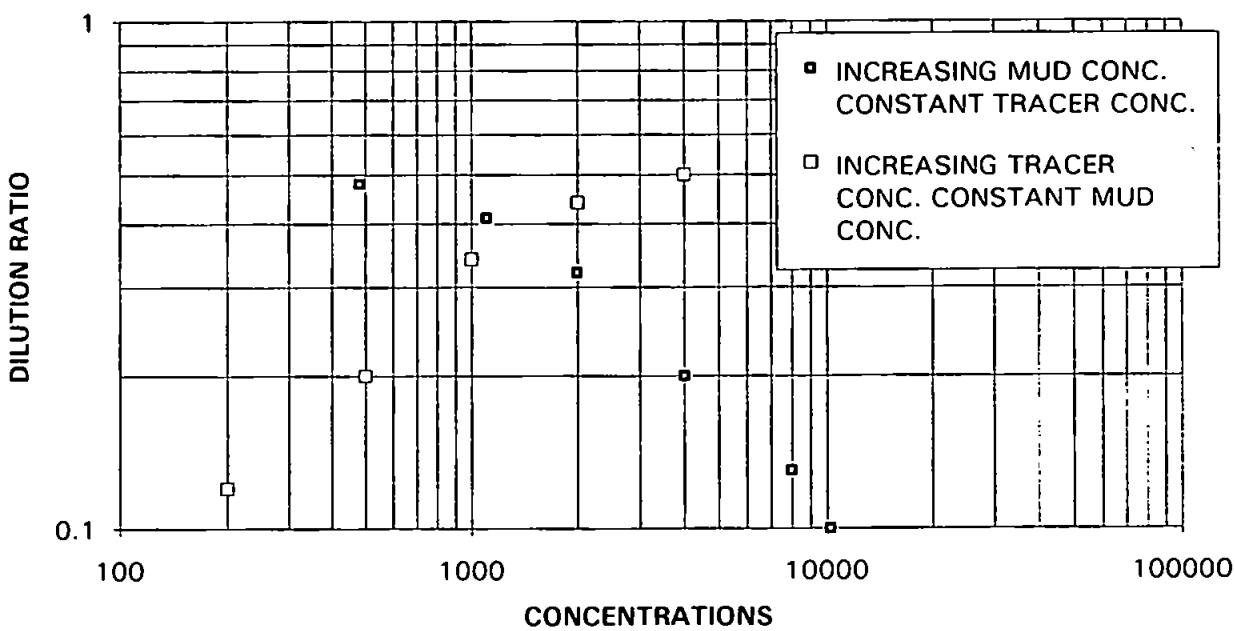

Figure 4.5 Calibration curves of increasing orange tracer particles in a constant concentration of estuarine mud suspension, and increasing concentration of estuarine mud in a constant concentration of orange tracer particles.

The fluorescent particles were supplied in a dry powder form which had to be mixed into an aqueous suspension. Tests indicated that the minimum surfactant levels was 0.2% aqueous solution for 1g of particles. Decon 90 was used as a surfactant and was a phosphate free, non-toxic, biodegradable 2% aqueous solution with a pH of 10.7. In order to detect any size spectra changes, suspensions of the orange particles were prepared with different solutes, including potassium chloride (3.5 ppt), tap water, deionised water, riverwater and seawater. Mixing was repeated, and the suspensions of different waters and orange particles were left to stand for 18 hours. There were no detectable differences in the particle size spectra before or after standing in any of the solutes.

4.3.2 Size and Density

Having established that the fluorescent particles were stable in water, the size and density of the particles were examined to ensure that these parameters were comparable to the natural sediment of the Tamar Estuary. A suspension of fluorescent particles was prepared to a similar concentration or turbidity as the estuarine sediment suspensions described 3.2.2 (tested by percentage light transmission described in 3.3.3) in order to mimic as closely as possible the same flocculation and settling rates for the fluorescent particles as the sediment. A size determination by settling was carried out on the fluorescent particle suspension for the time period 30-60 minutes with size spectra measured on the Malvern Particle Sizer. The results are shown in Figure 3.1 which indicates the percentage of particles in each size band. The results compare very closely with the sediment size spectra for the sediment over the same time period. The density of the fluorescent material, 1.37 g cm^{-3} (manufacturers data) was comparable with the density of flocs and bulk density of sediment collected from the turbidity maximum area and the middle estuary region of the Tamar Estuary (i.e. 10-22 km) as shown in Figure 3.2.

4.3.3 Surface Charge

The surface charge was measured by electrophoretic mobility as described in Section 3.2.3.2. The fluorescent particles had a positive electrophoretic mobility when mixed in a de-ionised

water suspension. However, when mixed with freshwater organics collected from a river which flows into the lower Tamar Estuary, the fluorescent particles became negative within a few seconds, indicating the particles were coated with organic material. This agreed closely with the tests carried out on alumina.

The results are shown in Figure 3.3. Subsequent washing of the fluorescent particle suspension followed by centrifugation did not indicate a significant change to the surface charge characteristics. The electrophoretic mobility for the organic coated fluorescent particles ranged from - 0.5 to -2.8 x 10^{-8} m^2 s^{-1} v^{-1} which falls within the range for estuarine sediment measured from other estuaries, but not for the estuarine sediment from the Tamar. Due to the nature of the equipment and subjective approach of analysis this variance was not considered significant. In addition, as noted in Section 3.2.2, the sediment in the upper Tamar Estuary has a relatively high particulate organic content (POC) of 8%, hence increasing surface charge, due to high levels of silt and clay content with associated organic material as compared with 2% for the lower estuary (Stephens *et al.*, 1992). The studies were repeated with other water types and the results indicated that the mobility was a function of different organic coatings and variation in charge. The results for the different waters ranged from -0.5 to -3.7 x 10^{-8} $m^2 v^{-1} s^{-1}$ suggesting a reasonable comparability with the estuarine sediment measurements

4.3.4 Settling Velocity of Sediment and Fluorescent Particle Admixtures

Settling velocity tests were carried out for sediment and fluorescent particle admixtures in the same way as those described in Section 3.2.4. Particular attention was given to the concentration of sediment and fluorescent particles to ensure the results of the sediment and sediment-fluorescent particle admixtures were comparable.

Figure 3.4 indicates that at any concentration, the addition of fluorescent particles caused a slight decrease in the settling velocity, at both high and low salinities and high and low concentrations. This slower settling rate suggests that the floc size and density formed may not have been as large, possibly due to variations in charge between the fluorescent particles

and sediment particles. At salinity 5 ppt, the mud suspension of concentration 5.6 g l^{-1} had a fall velocity of 3.2 mm s^{-1} whereas, the mud suspension containing fluorescent particles at a similar concentration of 5.5 g l^{-1} had a reduced settling velocity of 1.25 mm s^{-1}. The settling velocity of the fluorescent particle suspensions was also reduced as salinity increased.

The slightly lower median settling velocity of the fluorescent particle/sediment suspensions (S&T) indicated that the particles were not behaving exactly like the cohesive estuarine particles (S). An explanation for this slower settling velocity is given by Kranck (1984) who found, when studying estuarine cohesive mud, that a slower velocity was indicative of single grain settling in some instances. The settling velocity of the sediment and tracer suspensions (S&T) may therefore be lower than the sediment suspensions (S) because the data reflects a median range of settling velocities comprising single grain settling of fluorescent particles and flocs with varying fluorescent particle concentrations incorporated within them. The median settling velocity for the fluorescent particles suspensions (T) indicate a considerably lower velocity also due to single grain settling and the fact that the fluorescent particles were not mixed with estuarine sediment and therefore had a different surface organic charge and flocculation characteristic.

4.3.5 Discussion

The fluorescent particles were sufficiently similar in size, density, surface charge and settling velocity to estuarine particles to consider them suitable as possible tracers. The addition of tracer to the sediment suspensions caused a reduction in the median fall velocity at all salinities. This reduction was most pronounced at low concentrations of salinity. As salinity increased from 0 to 5 ppt the variance between fall velocities of suspensions with and without fluorescent particles at all concentrations declines, so it can be presumed that with increasing salinity the effects will be further reduced. Therefore, at high turbidity or suspended solids concentrations and salinities of greater than 5 ppt, the fluorescent particles behave in a similar way to the natural estuarine particles. Thus, the fluorescent particles could be used as sediment tracers for estuarine particles in an estuarine turbidity maximum.

4.4 PRELIMINARY FIELDWORK EXPERIMENT

4.4.1 Introduction

After examination of the physical characteristics of the orange fluorescent particles it was decided that the particles were a close analogue of cohesive sediment, and should be tested as a tracer. The overall objective was to undertake a pilot study of the tracing method to ensure that the experimental procedure, analysis and detection limits using the AFC were suitable in a field study. Permission was obtained from Hemerdon Estate, c/o English China Clays PLC, to undertake a dispersion study in a 150m by 100m pool called Stokers Pit, Lee Moor, situated in a disused china clay quarry located on Dartmoor, Southwest Devon (Plate 4.2). The site was chosen because it was relatively small and easily accessible for a pilot study.

4.4.2 Experimental Method

A preliminary survey of the experimental site was carried out. Echosoundings were made using a small portable echosounder. The soundings indicated a very irregular base with particularly steep sides where the china clay had been dug out. Buoys were deployed in an approximately rectangular grid of dimension 100m by 50m marking the sample sites as seen from Figure 4.6. The pit had no obvious stream inputs or outputs and was no deeper than 18m.

At the centre of the buoyed grid (Figure 4.6), 500g of orange tracer particles were introduced (approximately 10^{13} by number) in a detergent/water slurry onto the water surface. After the introduction of the particles the system was left for 24 hours for the particles to disperse and settle. The prevailing wind direction was southwesterly.

Plate 4.2 Preliminary fieldwork study at a China Clay mine showing tracer injection.

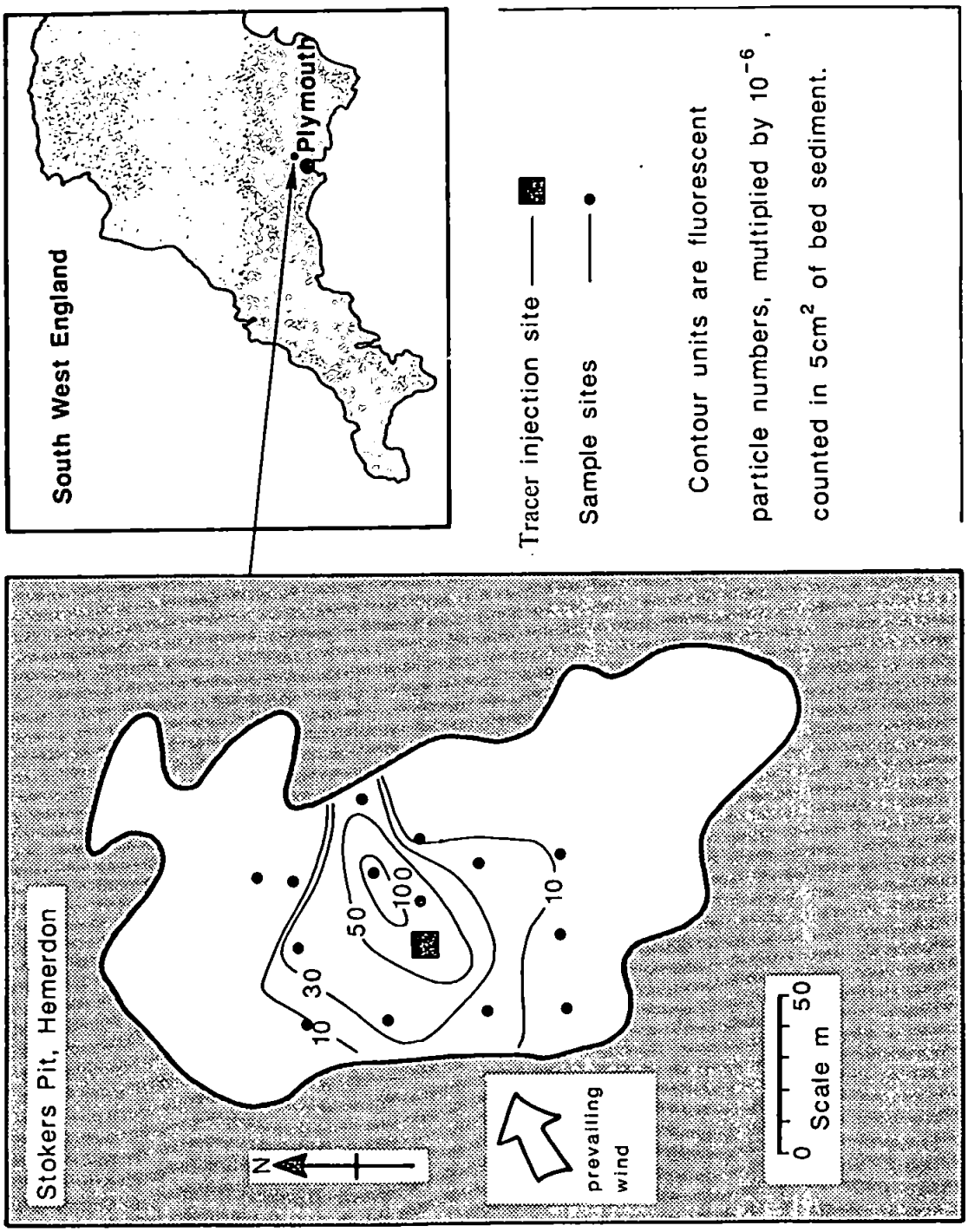

Figure 4.6 Location map and fluorescent tracer particle contour dispersion plot of the study at Stokers Pit, Hemerdon, Southwest Devon.

4.4.3 Sample Analysis Procedure

A gravity corer was used to remove a 5 cm^2 core from the bed at each sample point of the study site; the core comprised the sediment, the fluorescent tracer particle horizon and at least 10ml of overlying water. The top 2cm of each core was removed and placed in a sample pot. The volume of each sample varied and therefore the volume (W in ml) was measured. The volume of each sample taken (i.e. the volume in the storage pot) was assumed to contain 100% of the fluorescent tracer particles over the 5 cm^2 area and it was assumed that the particles settled as a thin uniform horizon on the sediment surface.

After vigourous stirring, and being placed in an ultrasonic bath, 1ml of each sample was removed and added to 50 ml of deionised filtered water to give volume X. This diluted sample was then placed in an ultrasonic bath and 1ml was removed and placed in a vial to which 10µl of Coulter Electronics Immunocheck latex beads were added giving a total volume of 1010µl (Volume Y). A Coulter Counter Multisizer was used to measure the number of latex beads per ml of sample (F). The Coulter latex beads were added to each sample in order to count the precise number of latex beads in each sample. This is made possible by the specificity of the beads in terms of size and fluorescence allowing a region to be drawn around the beads on the AFC and determining the precise number of beads within the total particle count. It was assumed that the fluorescent particles, latex beads and natural sediment were homogeneously mixed in the sample and therefore if a certain number of beads were detected during analysis in each sample as a proportion of the number originally added an indication of the volume scanned was possible.

Each sample was then scanned on the AFC to a total count of 65,000 particles which comprised the number of latex beads (S), fluorescent particles (N) and natural sediment [65,000 - (S + N)]. The volume V of the scanned sample was determined using

$$V = S/F \qquad (4.1)$$

Therefore the total number of fluorescent particles in the pot and the $5cm^2$ core is given by:

Total no. particles = N.Y.X.W/V (4.2)

where Y = 1010 µl and X = 51ml.

This simple calculation enables the data to be displayed as numbers of particles cm^{-2} of sediment bed. Replicate analyses of samples and sampling were carried out to determine the inaccuracies in the analysis on the AFC and on the production of each sample. Errors in analysis ranged from 0-7%.

4.4.4 Results

The ratio between fluorescent and non-flourescent natural sediment in each sample core was determined. These results have been plotted on Figure 4.6 and visually contoured to show the dispersion pattern. The same samples were re-analysed after 3 months in the dark at $4^{\circ}C$ to assess alteration of the fluorescent particles. The results are shown in Table 4.1.

The repeat analyses indicated a good repeatability in sample preparation and analysis on the AFC with any variability possibly due to pipetting such small volumes of latex beads and the samples not being homogeneously mixed. The difference between the two sets of results for samples analysed immediately after sampling in the field, and 3 months later after the samples had been stored indicates that there was no detectable breakdown or disassociation of the tracer particles. Indeed, there appeared in most samples to be an increase in tracer concentrations. This is most likely to have resulted from the need to increase the laser power of the AFC (from 250 mW initially, to 300 mW after the 3 month storage period). The laser power was adjusted to increase the definition between the fluorescent tracer particles and the china clay mud which like all sediment gave a background measure of fluorescence (see Section 3.3.3). Increased definition was required because some of the particles had a reduced fluorescence, possibly diminished in some way by the organic coatings on the surface of the particles.

Sample site	Fluorescent particles cm^{-2} x 10^6	
	Original	3 months
Centre	10	34
A	13	1 (SD 0.87*), 2 (SD 0.34**)
B	2	5
C	79	21
1	1	4 (SD 0.24*), 5 (SD 0.06**)
2	0.5	25
3	2	6
4	5	8
5	77	22 (SD 1.6*), 28 (SD 0.8**)
6	7	2
7	21	31
8	1	19
9	7	43
10	2	

Table 4.1: The total fluorescent particle numbers in the bed sediment samples. The samples were analysed immediately after the study and re-analysed after 3 months storage. In addition, 10 repeat samples were also prepared and analysed shown as * and 10 repeat analyses were carried out on the same sample shown as **. (Sample 10 had leaked and was not analysed).

4.4.5 Discussion

This preliminary study was carried out in order to investigate the use of the fluorescent particles, the behaviour and dispersion of the particles and subsequent detection of the fluorescent particles in a field situation. As a result sampling was limited to only a few sites. With the distance between sample points being large, small scale variations in dispersal were

lost, as noted by Newman *et al.*, (1988a). From the results displayed in Figure 4.6 there is an indication that lateral spreading occurred, decreasing towards the edges of the sampling area. Lateral dispersion was greatest in the deepest (central) region of the pool where the particles remained in suspension in the water column for longer. Higher tracer concentrations were found immediately around the injection site as would be expected. The high counts found in the north-east and south-west of the area could be explained by the prevailing wind pattern producing a north-easterly travelling surface water flow and a sub-surface south-westerly travelling counter flow. This preliminary study demonstrates the effective use of the fluorescent particles as a tracer, and the detection of the tracer particles by the AFC at low dilutions using a standard procedure. A lowest detection limit of 5-10 fluorescent particles in 65,000 total particles was concluded from the study based on analysis and sampling repeatability.

4.5 EVALUATION AND FUTURE APPLICATION OF THE TRACER PARTICLES

Fluorescent orange and yellow resin particles were found to be closely analogous to natural sediment from the Tamar Estuary, and readily detectable using an analytical flow cytometer. Calibration of the AFC enabled the number of fluorescent particles in a sample to be measured. An analysis procedure was then developed for diluted samples containing natural sediment and the fluorescent particles.

A preliminary field experiment in a relatively simple system was carried out to assess the suitability of the fluorescent particles to trace natural sediment movement. It was found that the analysis technique developed to determine the number of tracer particles in diluted samples taken in the field was successful.

Thus, it appeared that the fluorescent particles were a suitable tracer for detecting sediment movement in natural aquatic environments. It was decided that further field experiments would enable further testing of the procedures developed for detecting the tracer, and additionally provide information on the sediment dynamics of the sites studied.

CHAPTER 5

A PARTICLE-TRACING EXPERIMENT IN A SMALL SHALLOW LAKE

5.1 INTRODUCTION

Sediments play an important role in pollutant transport dynamics and eutrophication within lakes (Michler *et al.*, 1980; Vass, 1980; Zullig, 1982; Buffle *et al.*, 1987; Lemmin & Imboden, 1987; Salomons *et al.*, 1987). The ability to predict cohesive sediment transport within lacustrine waters has great importance, both economically and ecologically in providing sound management and development plans for lakes. The physical processes involved in cohesive sediment transport include erosion, flocculation, deposition and consolidation, and have been described in Section 1.2.

An understanding of these physical processes is essential in order to examine the particle dynamics of a lake system, but must be combined with a specific knowledge of lake hydrodynamics and the relationship between water movement and cohesive sediment transport. Lake hydrodynamics and physical controls or mechanisms of sediment transport in lakes are therefore described.

After confirmation of the suitability of the fluorescent resin particles to be used as a sediment tracer (described in the preceding chapter), and the method of detection was proven to be accurate, the technique was applied in a study of a small shallow lake, Loe Pool, Cornwall. The resulting distribution of the tracer was interpreted using a depth-averaged hydrodynamic model of the wind-driven circulation within the lake which enabled an assessment of the tracer dispersion and the natural sediment dynamics.

5.2 LAKE HYDRODYNAMICS

5.2.1 Introduction

The effects of wind on a water surface and the resulting wave formation have been well documented (Sverdrup & Munk, 1947; Rattray & Hansen, 1962; Bowden, 1983; Sobey, 1986). When wind blows over a water surface it generates both low-frequency water motions (currents) and surface wind waves. Many aspects of the resulting bottom currents have been investigated for both oceanic continental shelf and estuarine environments, but few studies have taken place in lacustrine environments (Lemmin & Imboden, 1987).

Wind stress drives water circulation within a lake depending on the magnitude and direction of the stress, the shoreline shape and topography, and the lake bathymetry. The near-surface waters, and the whole water column in shallower areas, tend to move in the direction of the wind stress with a reverse compensating flow being present in the near-bed waters, especially in deeper areas. In shallow lakes, such as Loe Pool, wind-driven waves can also create residual currents (drift through the water column) although in small lakes with limited effective fetch this is not significant because friction and eddy viscosity limit the depth at which a return flow is possible. Thus, in shallow lakes, there is limited vertical circulation and most water movement is fairly uniform with depth, with any compensating flow being in the horizontal. The principal force for water currents and circulation is therefore wind-induced lake setup.

5.2.2 Wind Stress Induced Setup

The effect of wind shear on the water surface results in upwelling, setup (the piling up at one end of a basin in the form of a temporarily inclined water mass) (Csanady, 1978) and seiching (the oscillation of the setup when the wind stress is removed, generally insignificant in smaller lakes) (Sly, 1978). Wind-wave action and wind-water currents, due to setup, drive

lake hydrodynamics.

5.2.3 Wind-wave Mechanics

Wind-wave action primarily causes erosion at the bed in shallow water, but some energy is transferred to Stokes Drift creating residual water circulation. Surface wind-waves produce an oscillatory motion in the water. The water circulation follows circular paths or orbits in deep water. In shallower water (at water depths where $L/2 > h > L/20$; where L is the wavelength and h is the water depth), where the wave begins to feel friction from the bottom and the vertical component of the orbit is restricted, the motion becomes more of an elliptical path. The orbital motion becomes narrower with depth until it becomes a to-and-fro horizontal motion with a smaller amplitude than that at the surface (Komar & Miller, 1973; Dyer, 1986). If the horizontal motion level is at the lake bed (only in shallow lakes) then the motion will lead to disturbance of the bed sediment. Erosion is then initiated if the motion is sufficient to exceed the critical erosion shear stress, and the sediment is then transported by drift due to a dominant residual flow in one direction.

The critical depth, or wave base depth (i.e. the depth at which the to-and- fro horizontal motion becomes negligible) separates areas of transportation and deposition in a lake There is a direct relationship between the wave base motion and the maximum grain size that can be moved by that motion.

The amplitude of water motion at the bed (d_o) as a result of wind-wave action is given by:

$$d_o = H/\sinh(2\pi h/L) \qquad (5.1)$$

where H is the significant wave height.

The maximum wave orbital velocity (U_m) associated with this amplitude is given by:

$$U_m = \pi d_o / T \qquad (5.2)$$

where T is the wave period.

In fetch-limited conditions, surface waves have short periods (Section. 5.6) limiting turbulence. Under such viscous conditions, a laminar flow boundary layer develops due to bottom drag, within which sediment movement will occur. The limiting effect of the waves prevents the boundary layer from growing to a thickness of more than a few millimetres. U_m and d_o are the values at the top of this boundary layer with a velocity gradient existing within the layer.

Stratification plays a significant role in determining the bottom boundary layer thickness and resuspension of sediment due to wave action. Wave action increases turbidity which in turn causes the boundary layer to be more defined (Madsen & Grant, 1986).

As the velocity of the to-and-fro oscillating wave motion increases there is a point when the water movement exerts a combined drag and lift stress sufficient to move the bed sediment particles. At this point, erosion and transportation begin. Komar and Miller (1973) calculated this critical velocity for non-cohesive sand grains; this can be given in terms of a shear stress. This critical velocity can be adapted for use in cohesive sediment transport composed primarily silt and clay deposits. There have been several studies of peak bed shear stress (τ_w) calculations in unidirectional flows, but work on oscillatory water-wave motion is complex, due to varying current accelerations.

Dyer (1986), Delo (1988a) and Luettich *et al.* (1990) provide an interpretation of erosion and transportation of cohesive sediment under different shear stresses and further examine the τ_w for these sediments; peak bed shear stress is given by:

$$\tau_w = 0.5 f_w \rho (U_m)^2 \qquad (5.3)$$

where ρ is bed sediment density. In fetch-limited conditions, such as those found in Loe Pool, where a viscous laminar flow exists the wave friction factor (f_w) is given by;

$$f_w = 2 (Re_w)^{-0.5} \quad (5.4)$$

and

$$Re_w = U_m d_o / \nu \quad (5.5)$$

where ν is the molecular viscosity = 1×10^{-6} $m^2 s^{-1}$. NOTE: The wave Reynolds number (Re_w) is $< 10^6$ for Loe Pool for windspeeds up to Force 10, suggesting laminar flow is predominant.

The erosion threshold for non-cohesive sediments is often reached before the transition from laminar to turbulent flow occurs (Komar & Miller, 1973). The erosion threshold itself is a function of the wave period and since short period surface waves are most common, then fine cohesive sediment movement must occur under laminar flow conditions. Luettich *et al.*, (1990) found this to be the case whilst carrying out a study of the dynamic behaviour of suspended sediment concentrations on Lake Balaton, Hungary. They found a significant increase in the suspended sediment concentrations during an episodic wind event. Concentrations rose from a background of 15 mg l^{-1} to in excess of 150 mg l^{-1}. Similar results have been measured by Lesht *et al.*, (1980) and Carper and Bachmann (1984).

Luettich *et al.*, (1990) used a single mass transfer equation generated from measured data, and found that vertical fluxes were significantly more important than horizontal advection (Stokes Drift) for suspended sediment concentrations. The study by Luettich *et al.*, (1990) was simplified due to the shallow nature of Lake Balaton (mean depth 3.2m) with no vertical gradients. The model was based on depth averaged conditions, with wave-induced bottom stress being the principal forcing factor for resuspension.

Luettich *et al.*, (1990) found their empirical model suggested the bed was behaving very similarly to a non-cohesive unconsolidated turbid suspension, positioned immediately above the bed, and which was possibly kept mobile by mean current shear and bioturbation. The

sediment character suggests that the bed was cohesive. Other studies have found similar occurrences (Drake & Cacchione, 1986).

5.3 SEDIMENT DEPOSITION MECHANISMS IN LAKES

Lake sedimentation mechanisms are all controlled by winds, riverflow, atmospheric heating and the catchment charactersitics. Initially allochthonous sediment on entering a lake under riverine flow is transported by turbulent mixing from river inflow as a result of horizontal and vertical shearing. The degree of mixing is dependent on the relative density difference between the two water masses, although the river inflow can maintain and amplify lake circulation.

The initial distribution of allochthonous sediment entering by river is either dominated by river plume (a function of discharge and velocity) and distributed as a delta or river plume, or by wind-wave action where no deltaic distribution pattern is visible (predominantly in low river discharges). Seasonal changes, particularly in temperate zones can lead to seasonality in the distribution of sediment; high river flow resulting in deltaic distribution and sedimentation and low river flow results in a general spread of sediment with lake circulation dominant in distribution as opposed to riverine plume.

Most lakes have a border region of bed sediment between sediment distributed by river action, in the form of a delta, and sediment distributed by wind-wave action. The presence and location of this border is a function of the river discharge. A river discharge has similarities to the expansion of a submerged jet with zones of reverse flow (Jopling, 1960).

The bed and suspended sediment load of an inflowing river often gives rise to a fan-shaped delta; as the river water slows down the suspended load settles out. Lakes with low river discharge (as in the case of this study) tend to have limited river dispersion, and seasonal variations cause changes in sedimentation patterns, especially in winter months when there is high river flow. Flocculation (a function of aggregation) is enhanced in river mouth areas due

to the drop in turbulence and the high inorganic and organic sediment suspensions. Flocculation is affected by suspended sediment concentrations, and leads to an increase in particle size and therefore particlesettling velocities, accelerating particle removal and decreasing particle concentrations in the water column..

Sedimentation and deposition, in lake areas dominated by river action, generally decrease logarithmically with distance from the river mouth. In shallow high energy zones there is often zero deposition or erosion taking place. With high river flow, the deeper low energy zones are dominated by flocculated particles (Downing & Rath, 1988) with an $Re < 0.5$. The horizontal component of the laminar flow around the particle is much larger than the vertical component and therefore the particle will travel relatively long distances. Pollutants are commonly associated with these areas of high accumulation (Hakanson & Jansson,1983).

Secondary transport deposition processes, initiated by wind-wave action causing resuspension, mixing and transport does occur in lakes. Sediments are not uniformly distributed in lakes, although many studies demonstrate sediment accumulation with depth (Lehman, 1975; Likens & Davis, 1975; Sly, 1977; Davis & Ford, 1982; O'Sullivan *et al.*, 1982). Sediment accumulation results primarily from the resuspension of sediments by wind-wave action in addition to several other less dominant parameters summarised by Downing and Rath (1988). They found highly variable sedimentation within small uniform sampling sites possibly resulting from animal activity, sediment transport by bottom currents and small scale variations in the bottom profile.

The morphology of a lake, its orientation and climatic conditions influence the transport of sediment. Water movements are a function of the wind and are therefore temporally changing creating spatially non-uniform water motions which transport suspended sediment and which can erode surface bed sediment.

The effects of limited fetch and duration of the wind produce low energy short period wind-wave events causing a partial and selective transport mechanism of the suspended and

bedload sediment. However, there are a great many problems in making a clear association between wave energy and the sediment response (Hakanson & Jansson, 1983).

5.4 STUDY SITE DESCRIPTION

5.4.1 Geological Formation and Catchment

Loe Pool is a shallow (mean depth 3.3m) eutrophic, freshwater shoreline lake (Figure 5.1 and Plate 5.1), situated near Helston, Cornwall, U.K. (50°4'N, 5°17'W).

During the Pleistocene, South-west England was subjected to intense periglaciation, forming tors on the granite moors and high alluvium deposition over the rest of the landscape. Fall in sea-level, up to 100m, caused rivers to excavate into the earth leaving deep valleys. At the beginning of the Holocene, sea levels rose, flooding the valleys and causing infill with marine deposits (O'Sullivan *et al.*, 1989).

Some valleys remained as brackish estuaries, such as the Fal and Tamar, whereas others such as Slapton Ley, (Devon) and Loe Pool formed shoreline lakes as a result of bar production by longshore currents. Loe Pool was probably formed in medieval times by the shingle bar (Coard, 1987).

The geology of the catchment comprises granite (58% by area) including gravel and fine grained alluvium beds and killas (42% by area) or baked slates formed by the granite intrusion. The catchment is drained by 3 main rivers, of which the River Cober (Figure 5.1) drains 73% and provides 93% of the water entering the lake with an average annual flow of 1.0 cumecs.

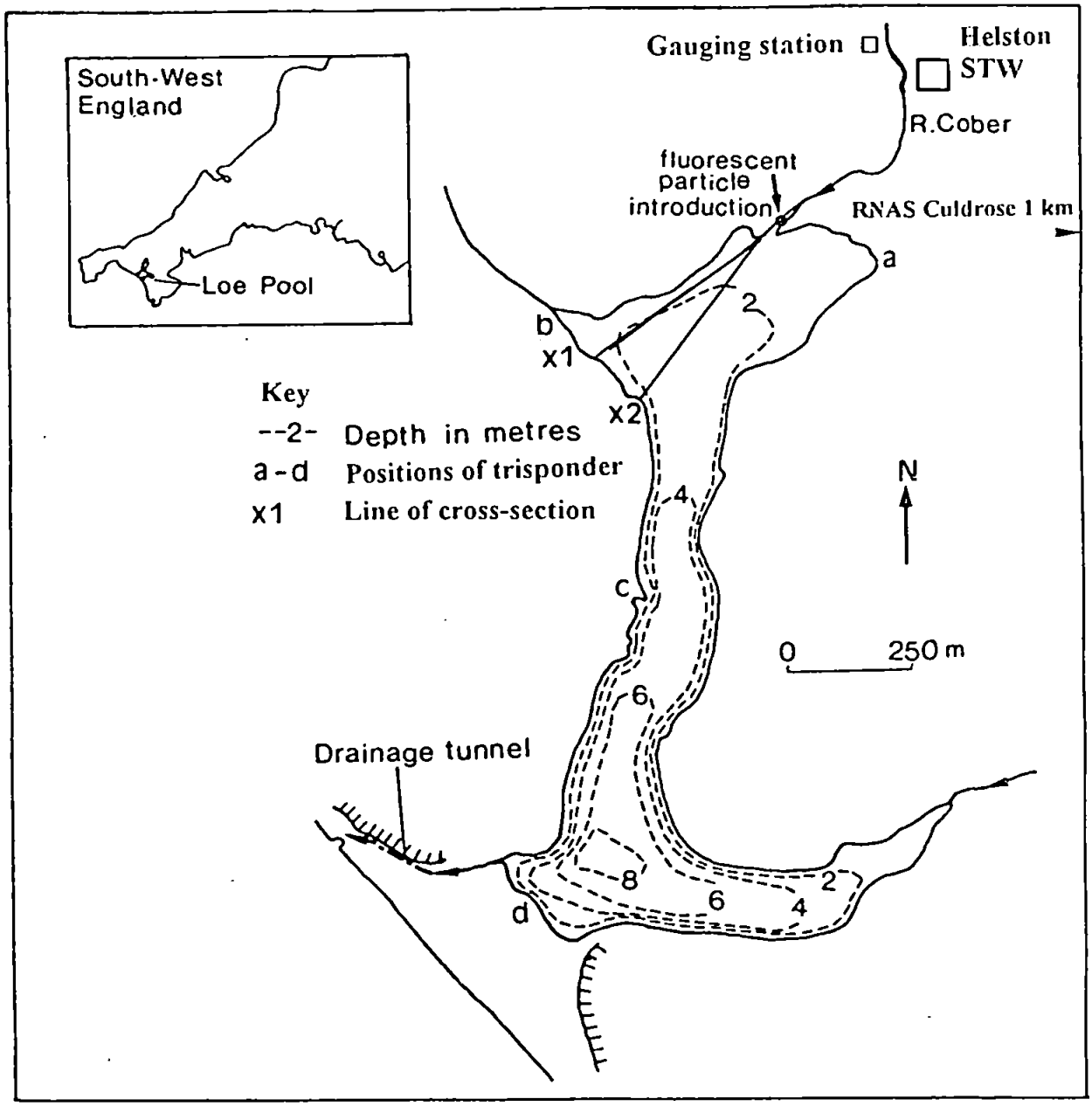

Figure 5.1 Location of Loe Pool with the bathymetry (in metres), the fluorescent tracer particle injection site within the River Cober and the locations of the trisponder (a,b,c &d) shown. In addition cross sections 1 (X1) and 2 (X2), the river gauging station, Helston STW and RNAS Culdrose meterological station are also shown.

Plate 5.1 Loe Pool, Cornwall looking south from the river Cober towards Loe Bar.

5.4.2 Climate, Bathymetry and Hydrography

Loe Pool experiences a temperate maritime climate with prevailing winds from the south-west. Seasonal average temperatures vary between 5°C in February and 16°C in August (Simola *et al.*, 1981). Rainfall shows monthly variations with maxima during October to February and minima during April to August (Figure. 5.2). Lake volume (average 2.07x 10^6 m^3) varies seasonally as a result of fluctuating water levels and river discharge. This fluctuation has been minimised recently due to the construction of a drainage tunnel built by South West Water Authority (SWWA, now South West Water Services Ltd) during the 1980s. The rainfall and controlled water level affect the residence time of the lake, which can vary from 8-11 days during the winter months up to 150 days during dry summers (based on mean monthly gauged flow during 1972-1988; source SWWA).

Figure 5.1 indicates that Loe Pool is a shallow gradual sloping lake. The contours surrounding the Pool are steep, in places rising to 60-70m. This would suggest that Loe Pool originally was a deep lake with steep sides and has infilled with both marine and fluvial sediments. The upper basin has a small riverine deltaic deposition and around the neck of the Pool there is an irregular feature of shallow water possibly formed by the existence of a wind-driven gyre. Generally there is an increase in depth with distance from the river mouth to the deepest point of 10m.

The erosive and transportation powers of the River Cober are limited. The shallowness of the lake prevents prolonged thermal stratification. Wind induced mixing is effective in maintaining homogeneity. The oceanic climate prevents large differences between air-water, and lake-river water temperatures. Thus turbulent exchange and circulation resulting from small temperature gradients and low river input are limited. These factors have a strong bearing on the fate and distribution of suspended and dissolved material and sedimentation processes. It is the intention of this study to examine the effect the wind and river input have on the overall circulation in the lake and the subsequent particle dynamics.

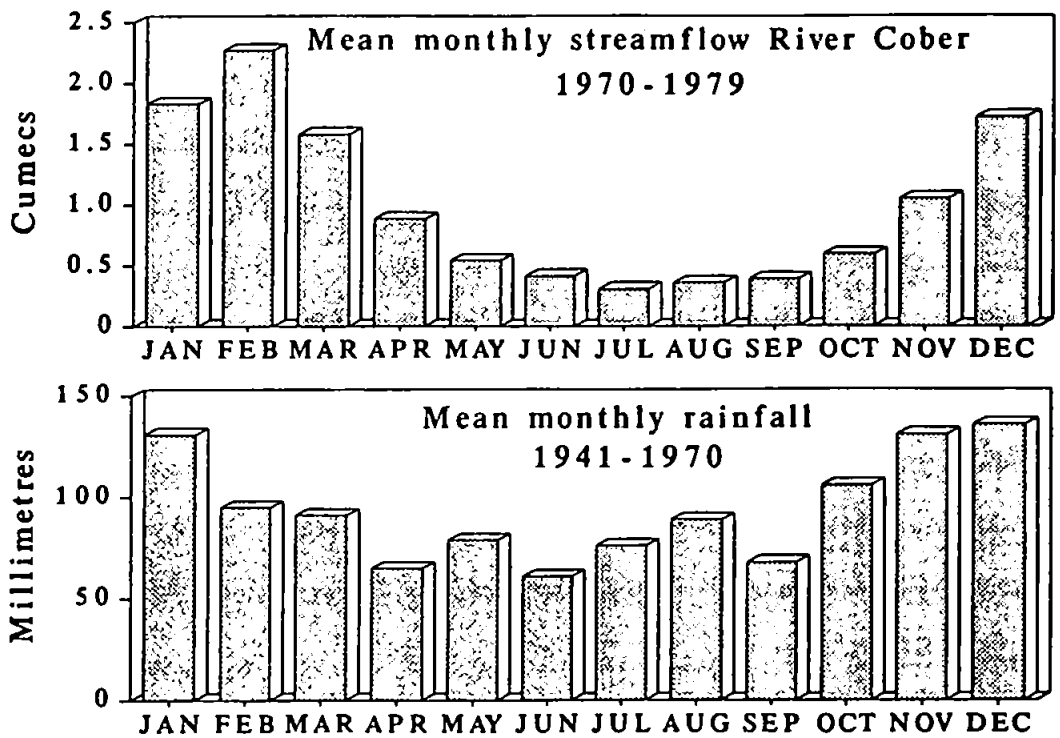

Figure 5.2 Mean monthly streamflow for the river Cober (1970-1979) and mean monthly rainfall within the Loe Pool catchment (1941-1970).

5.4.3 Past Studies

5.4.3.1 Sedimentation

Palaeolimnological studies allow the reconstruction of past lacustrine environments and communities. Loe Pool largely remained unaffected by anthropogenic influences until tin mining spread into the area during the latter part of the 19th century (Coard, 1987). The mine wastes, resulting from the mining activity, contributed huge influxes of allochthonous sediment into the River Cober. The shoreline of Loe Pool has undergone a remarkable change in terms of shape and position, along with colonisation by vegetation. This has caused a 17% reduction in the lake's area between 1910 and 1980 (Coard, 1987). This significant infill affected the physical and chemical composition of the lake's sediment, and also caused a decrease in the lake volume and residence time. This would have had the effect of reducing the nutrient loading, and caused the lake to be more susceptible to wind-induced mixing.

This infilling peaked in the early part of the 20th century when historical records show the Pool was red on several occassions due to mining (Coard, 1987). The end of mining in 1938, when the mines were purchased and closed by the estate owners, the Rogers family, provides an excellent boundary in the sediment stratigraphy for dating, although subsequent flushing of surface mine deposits could extend the boundary date beyond 1938.

Cores removed during the palaeolimnological studies show 3 distinct types or zones of sedimentation occurring during the last 200 years. The following descriptions are taken from Pickering (1987) and Coard (1987):

"Zone A provides the base sediment in the core which is largely uninfluenced by man. It comprises a layer >140 cm in thickness of regular laminated black/brown sediment with no bioturbation. It has a density of 1.36 g/cm^{3} and a water content of 52-60%. Estimates suggest a sedimentation rate of 2.0 g cm^{-2}yr^{-1}."

"Zone B has a thickness of 30-140 cm of finely laminated red and grey clays mixed with dark layers. There is limited bioturbation. The density is 1.7 gcm^{3} maximum with a water content of 37.6% minimum. The sedimentation rate is 26.3 g cm^{2}yr^{-1}. Immediately surrounding the Cober inlet there is limited clay content due to sand and coarse silts transported down river being deposited on the delta."

"Zone C is the surface layer and comprises a 20-60 cm layer of unconsolidated brown, intermittently laminated highly bioturbated sediment. It is a highly organic gyttja, with the light and dark brown laminations just below the surface (top 0-5 cm). The density is 1.1-1.2 g cm^{3} with a water content of 80-90% due to its unconsolidated nature. The sedimentation rate is 0.1 g cm^{2}yr^{-1}."

The red clay/brown gyttja boundary, between Zone B and C, marks the boundary for the cessation of tin mining and therefore can be used to determine long term sedimentation patterns (Pickering, 1987). Figure 5.3 shows contours (in cm) of the thickness of Zone C taken from 36 cores. There is a clear deltaic deposition effect around the inflow of the River Cober and in the bay of Penrose Stream (O'Sullivan *et al.*, 1982). There is an unexpected increase in sediment deposition at the north end of the Loe, where the lake narrows, suggesting the existence of a gyre in this area. Throughout the Loe, sediment deposition is relatively low, with an overall focussing in the deep low energy zone at the southern end, with sedimentation proceeding in a southerly direction from the main stream inputs.

Clearly, in the area surrounding the River Cober inlet, river-dominated sedimentation is mainly deltaic with a general logarithmic decrease with distance from the river mouth. Figure 5.3 shows the non-uniform distribution of sediment in Loe Pool with this variation possibly explained by those parameters described by Downing and Rath (1988) (Section 5.3).

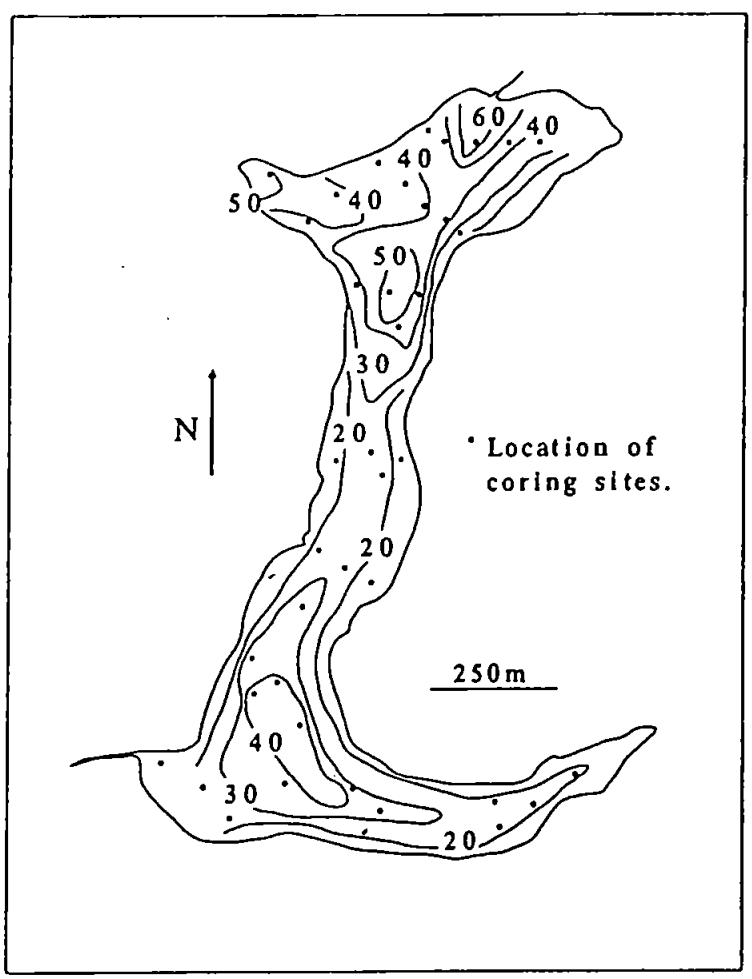

Figure 5.3 Isopach map of the brown-clay surface sediment (in centimetres) of Loe Pool showing location of palaeoliminological cores on the lake bed. (Adapted from O'Sullivan et al., 1982.)

5.4.3.2 Algal Blooms

Loe Pool has been of considerable interest throughout history because of its specific flora and fauna and the geological background of its formation and continuing existence behind the shingle bar (Coard, 1987). The ecological importance was recognised when the bar and wetland, surrounding the River Cober inlet, was listed as a Site of Special Scientific Interest (SSSI).

The frequent and obtrusive occurrence of algal blooms during summer months instigated palaeolimnological studies on the Pool. Coard *et al.*, (1983) notes that in summer months, total chlorophyll *a* levels in the water column could exceed 500 mg l^{-1} in more sheltered areas of the lake.

The National Trust (owners of Loe Pool), and the National Rivers Authority are particularly interested in the causes and long-term effects of the blooms. Several studies have taken place in recent years in an attempt to provide valuable information and data regarding this obvious eutrophication of Loe Pool (Pickering, 1987; Coard,1987). These palaeolimnological studies have provided an empirical basis for the reconstruction of past lacustrine environments and communities, recording trophic changes within the sediment.

Loe Pool undergoes a seasonal variation between well mixed, oxygenated conditions throughout winter months, to periods of oxygen stress at the bed during summer months. This indirectly causes laminated sediments to occur due to processes such as changes within the lake ecosystem, and variation in the intensity of erosion and transport of allochthonous material (Simola *et al.*, 1981).

Analysis of lake sediment has indicated that the Pool has become increasingly eutrophic throughout the 20th century from anthropogenic enrichment with nutrients. Evidence which supports this was obtained from the analysis of sedimentary organic matter, chlorophyll degradation products, total phosphorus, sterols and diatom and cladoceran remains in

sediment. Coard (1987) suggests that the majority of the sterols, were C_{29} sterols, indicating a considerable allochthonous input of organic matter into the system.

O'Sullivan (1990) summarises from previous studies that the palaeochemistry analysis on the lake sediments confirms the Pool began to change to a more eutrophic state in the 1930s, coinciding with the commissioning of Helston Sewage Treatment Works (STW). In recent years it has been increasingly evident that the Pool has been undergoing nutrient enrichment resulting in blooms of Cyanobacteria (blue-green algae) (O'Sullivan *et al.*, 1989). It is noted that blooms have occurred in most years since 1968 (O'Sullivan *et al.*, 1989), most of which are preceded by low levels of dissolved inorganic nitrate and high levels of dissolved inorganic phosphates. Maximum nutrient levels have been measured between June and August in the lake waters (Coard, 1987), at times of hot, dry sunny weather, typical of the summer months. The bloom itself causes a reduction in the available oxygen which results in the death of large numbers of fish. Reynolds (1979) also suggests there may be a period of windy weather, preceding the calm phase, altering the algal buoyancy resulting in an increase of algae near the surface.

5.4.3.3 Nutrient Levels

Nitrogen (N) and phosphorus (P) within lake sediments can originate from both point and diffuse sources in the catchment. Sewage and waste water discharge from human settlements, mainly Helston and RNAS Culdrose (total approximately 15,000 residents; seasonal variations due to tourism do occur) and nutrient rich runoff from agricultural use of fertilisers comprise the majority of these sources (Coard, 1987). Helston STW discharges into the River Cober influencing the nutrient supply to the Pool. RNAS Culdrose discharges both into the the Pool, via Carminowe Creek, and directly into the sea. SWWA (now South West Water), the managers of the Works, appear to accept no responsibilty for the phosphate enrichment and eutrophication of the Pool (O'Sullivan, 1989). They state that "Helston STW is nothing to do with the problem". The Environmental Science Department at Plymouth

Polytechnic carried out a survey which found "polluted water algae" dominant in and around the River Cober inlet caused by organic matter entering the system (Coard, 1987).

Monitoring for nutrients in the River Cober has been carried out, originally by SWWA and then by the National Rivers Authority, with data beginning in 1976. The data suggests that 19.8 T yr^{-1} of P (Figure 5.4) enter Loe Pool with an average concentration downstream of the STW of 0.635 mg l^{-1}; 92% of which is from Helston STW. Approximately 26% of this influx leaves the system, mainly occurring when the flushing time is very short during the winter months. The data suggests the Pool is approaching saturation since in the early 1980s 10% of P added left the Pool, whereas by the late 1980s this figure had risen to one quarter of that added. Data has not been taken at regular intervals over the years, which prevents any close examination of the daily and monthly fluxes.

The data also shows an input of 195 T yr^{-1} N entering Loe Pool with an average concentration of 6.25 mg l^{-1}; 29% from Helston STW. The remainder originates from agricultural runoff in the catchment area. Approximately 58.4% leaves the system suggesting Loe Pool is close to complete saturation in N, although N is less damaging in terms of altering the trophic state of the lake.

The conclusion from this large amount of work is that Loe Pool has undergone a major change and is now eutrophic due to severe loading from agricultural and sewage waste (O'Sullivan, 1990). The only long term solution is to further treat sewage to remove P (Wankowski, 1979) or to stop sewage effluent discharge into the lake altogether.

Phophorus is in a permanent state of flux between the water column, where it is available to algae, and the sediment. Turbulent mixing is a key factor in the remobilization of P from the sediment. Therefore, the sediment dynamics within a system, such as Loe Pool, play a significant role in determining the water quality.

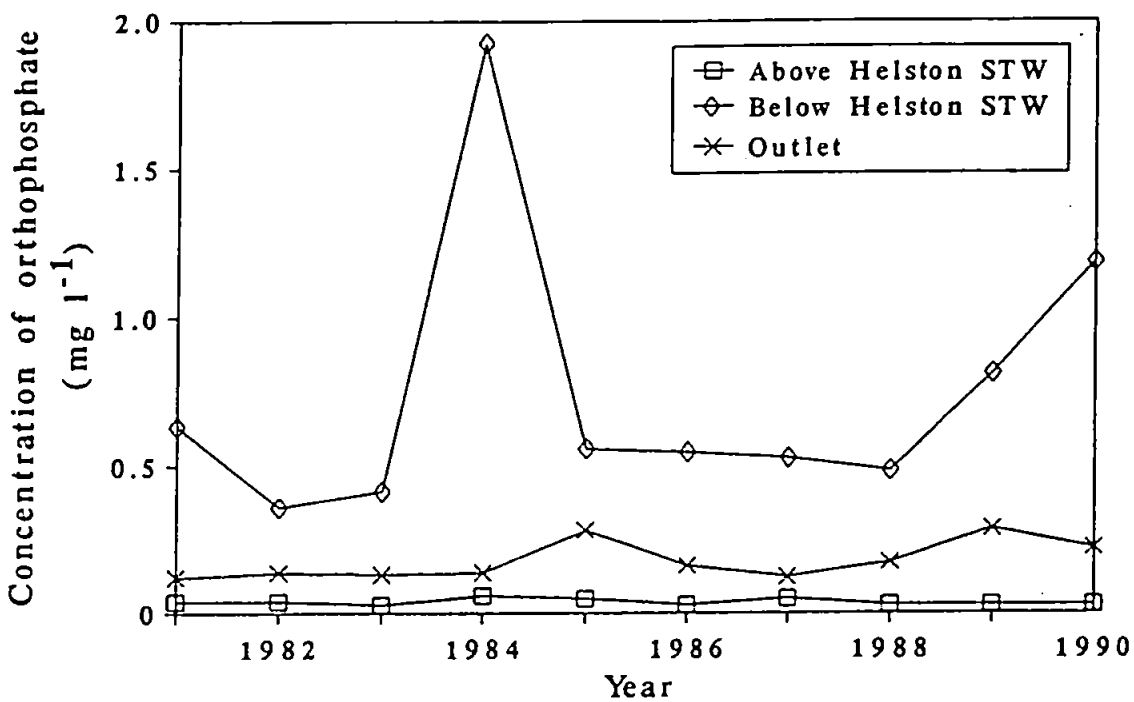

Figure 5.4 Annual fluctuations in organophosphate concentrations from 1981-1990 measured above and below the Helston Sewage Treatment Works in the River Cober and in the outlet to the lake.

5.4.4 Overall Flow Regime

Loe Pool appears to have a limited riverine circulation, with mainly deltaic sedimentation localised around the entrance to the river Cober in the most northerly basin. Resuspension and transport after this initial deposition must be due to wind-wave currents and bottom current action, caused by wind set-up.

The overall flow hydrodynamics is governed by the wind speed and direction, modified by the topography of the surrounding areas and the shore (Figure 5.1). Any wind, except that from the southwest, would experience some interference. The windfield over such small lakes is normally rather uneven, due to the influence of lee effects. The observed wind flow, if measured above the lake surface, would be a growing boundary layer rather than a fully developed turbulent flow. This would also have a similar effect in the water column. Hansen (1979) suggests that a lee effect would be experienced over a length 6 times the height of the sheltering feature, and over a further distance of 7 times the height it will grow to at its fully developed value. In front of the lee giving feature the corresponding length would be 2 times the height.

This lee effect tends to reduce the fetch and is described as the effective fetch (Hakanson & Jansson, 1983). The effective fetch for Loe Pool is difficult to determine due to funnelling effects from the valley, however values were calculated to assist in the interpretation of the particle dynamics data (Section 5.6).

5.5 EXPERIMENTAL

5.5.1 Introduction

The orange fluorescent particles described in Chapter 3 were considered to be a satisfactory sediment analogue and tracer, and were released into Loe Pool as part of a tracer particle experiment. A depth-averaged hydrodynamic model of the wind circulation of the lake was used to interpret the observed distribution of the tracer particles.

5.5.2 Experimental Procedure

On arrival at Loe Pool, a visual survey was carried out, and four sites were found to position the transmitters of a trisponder navigational system used to obtain positional data. The transmitting slaves were installed alternately, as needed,at key locations (sites a-d) around the perimeter of the Pool to enable the precise determination of sampling sites (Figure 5.1). Using a small inflatable boat, a preliminary survey of the Pool was undertaken which included bathymetry, and current velocities of inputs and outlets.

Comparisons were made between the bathymetry recorded in previous studies (Pickering, 1987) and those measured in this study. Volume and lake residence times were calculated to allow an estimation of the dispersion and transport of the fluorescent tracer. The tracer particles are negatively buoyant with a still water settling time within the lake of several hours. Based on all this information, and the measured main inflow, a sampling frequency was decided. The residence time during the study period was over 100 days and therefore it was decided to sample in the area immediately surrounding the River Cober inlet, and along the uppermost stretch of the Pool with a greater frequency of 1 sample per 25 m^2. Fewer samples were to be taken in and around the outlet and Carminowe Creek at a frequency of 1 sample per 35-40 m^2.

5.5.3 Sampling Procedure

Background samples were taken to determine any fluorescence of the water and bottom sediment. On 28 April 1990 at 20.00 hours, 5kg of tracer particles (mixed thoroughly with a laboratory surfactant, and then diluted with water from Loe Pool) were injected beneath the water surface at the mouth of the River Cober (Figure 5.1). The tracer was added on a windless evening, with no visual water disturbance other than the inflowing river.

The system was left for 3 days before the surface layer of the bed sediment (approximately the top 2cm) was systematically cored using a gravity corer. Water samples were collected from around the Pool during the 3 day stabilising period and were analysed using a fluorescence microscope in the field. Fluorescent tracer particles were found to have travelled throughout the Pool, although no quantitative interpretation was possible using these results. A total of 756 samples were collected during the following 20 day study period, and returned to the laboratory for analysis on the flow cytometer.

5.5.4 Additional Climatic Data and Results

Data on rainfall, river flow, lake water level and nutrient levels were obtained from the NRA Southwest, during the study period (Figure 5.5), in addition to long term data where available. The meteorological office at RNAS Culdrose (situated 1km due East of Loe Pool, Figure 5.1) measured windspeed and direction hourly and provided valuable wind and rainfall data. This data was obtained to help interpret mixing and dispersion patterns.

The river flow gauging station was originally situated at Helston Park Gauging Station (Figure 5.1), but was replaced by one at Trenear, higher up the River Cober. An overlap of the data from January 1988 to May 1989 allowed a linear regression for the 2 sites to be carried out enabling the extrapolation of river flow entering Loe Pool during the study period. Measured daily lake water levels and river flow allowed the calculation of residence

time and a correction factor for the lake volume.The river flow and water level decreased steadily during the study period from the 20th April onwards, however despite the reduction in volume, the decrease in river flow caused the residence time to rise over 100 days. The estimated river flow at Helston fell steadily from a high point of 0.52 cumecs, at the beginning of the study period, to 0.19 cumecs at the end.

Rainfall data during the study period (Figure 5.5) shows a slight correlation between precipitation and changes in river flow. The annual pattern for monthly rainfall shows a similar pattern to river runoff (Figure 5.2).

The wind data, measured at c.100m above sea level, can only provide a guide as to the prevailing wind at Loe Pool, with no consideration for local effects. Figure 5.6 shows half-daily wind vectors for each day of the study period starting at the same time as the tracer injection; for hours with identical directions the vectors are overlayed (NOTE: the wind is from the end of the line towards the arrow, i.e. for days 2-5 the wind is predominantly from the ENE). These vector lines indicate the wind was acting with considerable strength (up to 15 m s^{-1}) from an easterly direction for the first few days after introduction of the tracer. This wind pattern will have had a marked effect on the initial dispersion and advection of the tracer particles.

5.5.5 Analysis

The bed sediment core samples (756 in total) were stored at 4°C in the dark and were analysed on the Analytical Flow Cytometer as described in Section 4.4. The gravity corer removed a 5cm^2 core comprising the sediment, the fluorescent tracer particle horizon and at least 10 ml of overlying water. The volume of core and surface water varied between samples, so this needed to be measured for each sample.

The simple calculation described in Section 4.4 enables the data to be displayed as numbers of tracer particles cm^{-2} of lake bed over the whole area of Loe Pool.

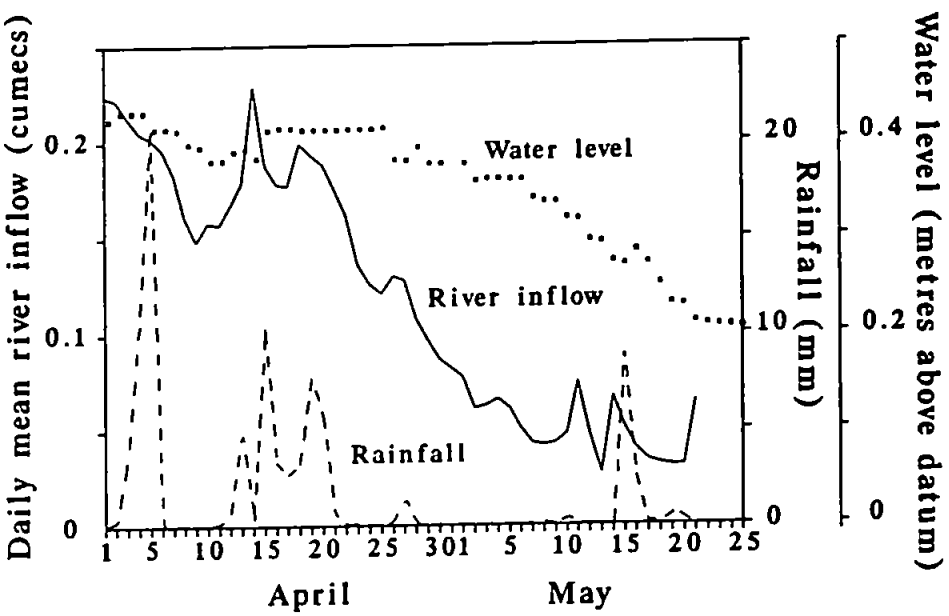

Figure 5.5 Daily mean stream inflow, rainfall and lake water level for Loe Pool during the study period 1st April 1990 to 25th May 1990.

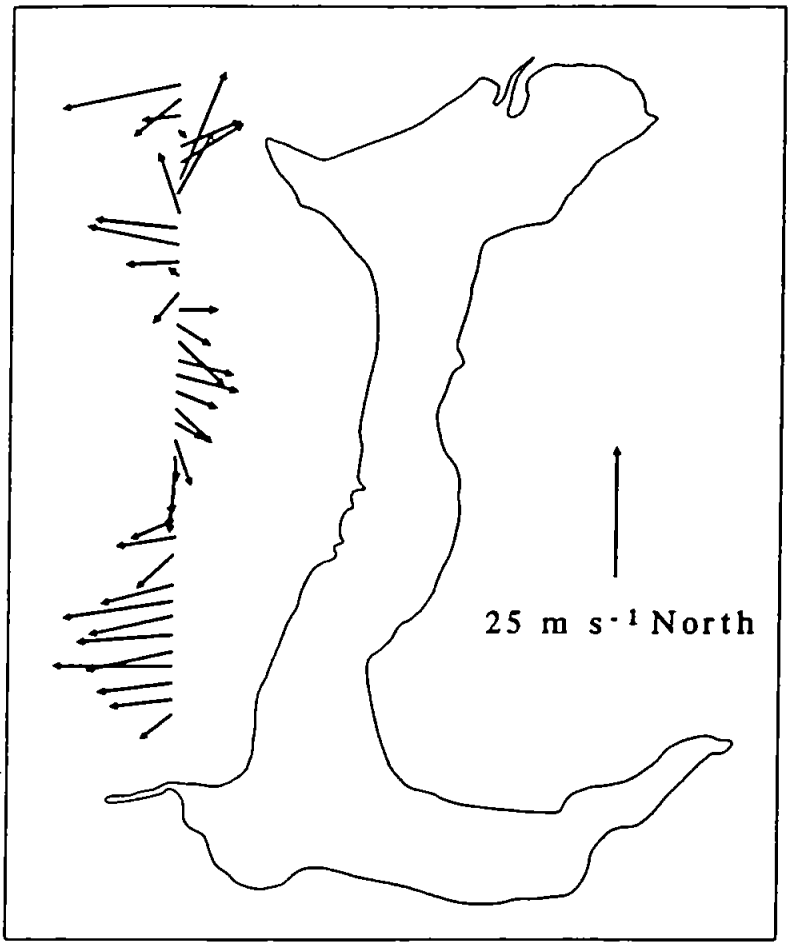

Figure 5.6 Twelve hour averaged wid velocity vectors, one for each half-day period following injection for the duration of the experiment. Note that the first arrow to the southern end of the Pool denotes the first twelve hour period and the wind direction is towards the arrow head i.e. an easterly wind.

Analysis of the water and sediment samples collected from Loe Pool prior to the tracer study gave no evidence of background fluorescent particles within the system. In addition, replicate core samples and analysis were carried out. Core samples were taken at a moored buoy to within 1m of each other, to provide data on variability with distance from a core taken, with limited success. Five duplications were carried out with the first three cores having a variance of 18-32%. However the error increased dramatically with the last seven replicate cores to between 147-270%. Disruption of the bed, caused by the impact from the corer and irregular sedimentation (Downing & Rath, 1988) are the main causes for this discrepancy. In addition, handling the boat's position, especially in deeper water prevented precision in the coring positions.

5.5.6 Tracer Results

Figure 5.7 shows the concentration contours of the number of tracer particles cm^{-2}. There is an obvious high concentration of tracer in the North basin, with concentrations in excess of 10×10^5 tracer particles cm^{-2}. The particles were spread over a large area with considerable dispersion and advection having taken place. These results are discussed in much greater detail in Section 5.6. The distribution data from the area of lake bed around Carminowe Creek and Loe Bar was in places patchy, and as a result only limited interpretation has been possible.

The distribution of the brown clay sediment of Loe Pool (previously described in Section 5.4.3.1) shows similarities to the tracer contour data. One must remember that the latter is an instant injection rather than an accumulation over more than 40years. The existence of predominantly deltaic sedimentation in and around the River Cober inlet which spreads down approximately one quarter of Loe Pool agrees closely. In this respect, an instantaneous injection of fluorescent tracer particles would closely mimic the entering of sediment, undergoing a similar radial spreading and deposition often associated with alluvial fans. There was also a noticeable accumulation in the deeper part of the Pool, possibly due to remobilisation and redistribution of the sediment by wind-wave action.

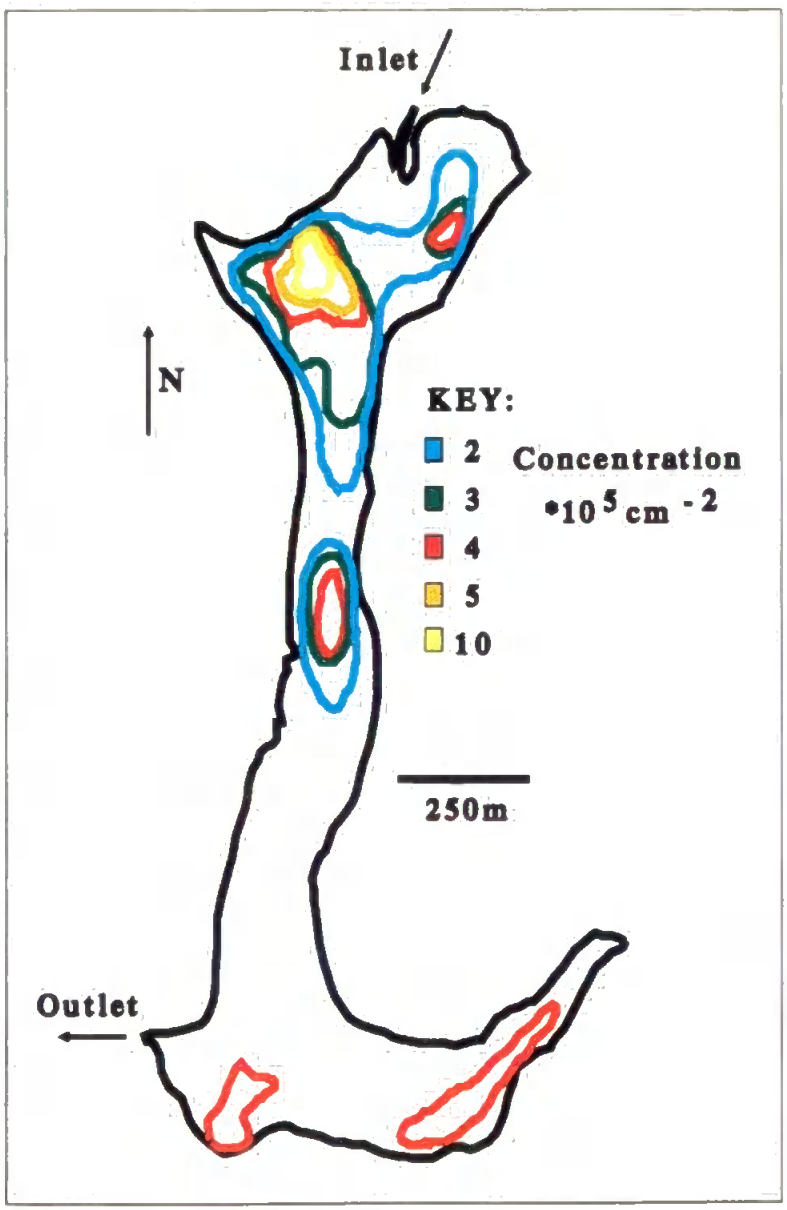

Figure 5.7 Measured tracer particle concentrations in the bed sediment of Loe Pool. The units are 10^5 particles cm^{-2} of bed.

The area of Loe Pool has been calculated (from this study) as 577,000 m^2 with an average depth of 3.3 m at Ordanance Datum (O.D.). During this study the water level was averaged at 0.284 m above O.D. giving a volume of 2.07 x 10^6 m^3. Each tracer concentration contour is split into labelled areas (A-L) of tracer particles numbers cm^{-2}, with a total of 70.9% of the tracer particles found in the large area to the North (F-L), with the areas (C-E) containing a further 19.4% (Figure 5.8). Core sampling was repeated (in zones A & L) at the very beginning and at the end of the sampling period to provide quantitative information on the degree of remobilisation. The profiles however, once plotted, were infact 15-20 m apart, and although the data suggests that some redistribution took place, the evidence is not conclusive.

Therefore, 90% of the tracer is deposited and retained within the northern area of Loe Pool over the duration of the survey. Assuming the tracer particles are analogous to natural suspended sediment then 90% of sediment and any associated pollutants entering Loe Pool will also remain in this area over the same timescales.

The sum of the particles integrated spatially for areas A to L was 3.81 x 10^{14} particles. Initially 5.326 kg of tracer particles were added. Microscopy and AFC indicate the main particle population comprised particles smaller than the manufacturers specified size of 4-6 μm. The measurements made during this study suggests that large numbers fell into the size range of 2-4 μm with an angular "platey" structure. Analysis of several samples using the above techniques indicated an average size of 3.25 μm long and a volume of 10-15 μm^3. Manufacturers density is 1.37 g cm^{-3}, therefore in 5.326 kg of tracer particles (where one particle weighs 1.8 x 10^{-11}g) there are a total of 2.99 x 10^{14} particles. Thus, there is agreement between the amounts injected and that detected, within acceptable margins of error.

Figure 5.9 shows two cross-sections (X1 and X2) taken through area X in different places (see Figure 5.1) showing the high concentration of tracer particles found in this area relative to the surrounding area. The cross-sections suggest the majority of particles were advected between 150-225 m from the injection site.

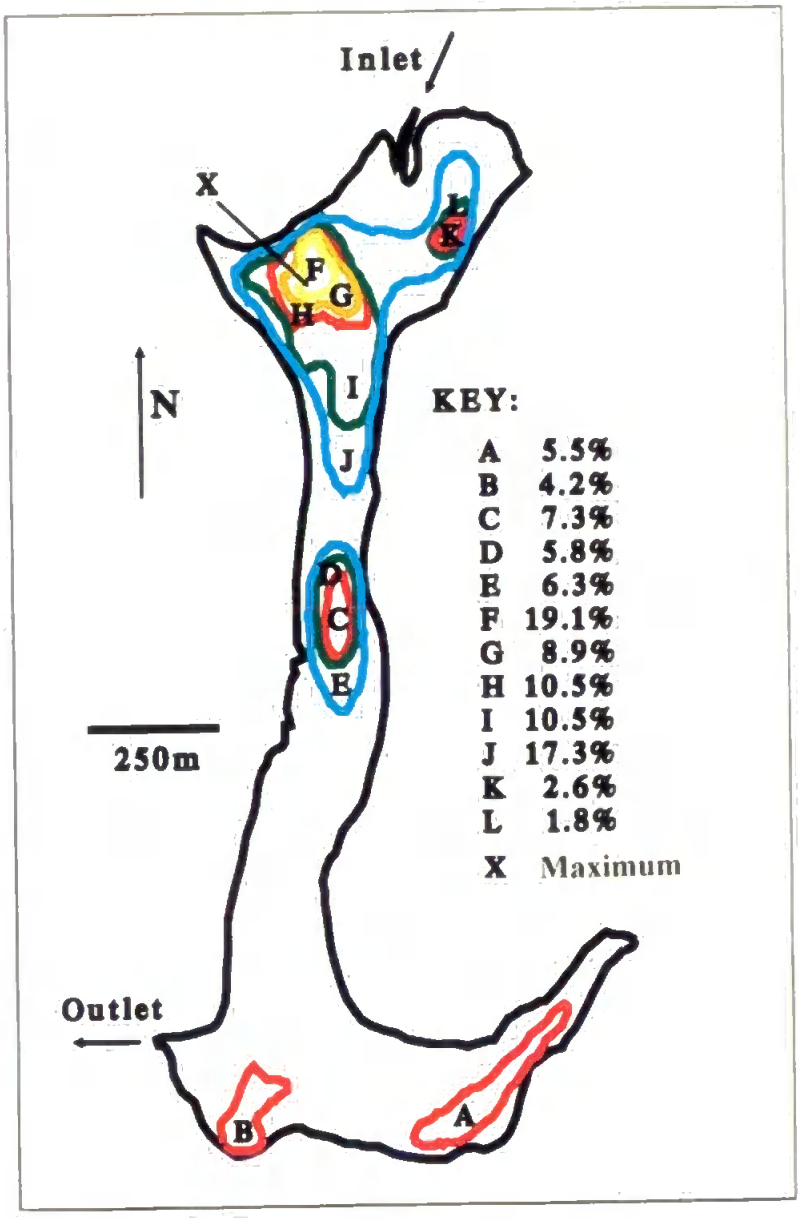

Figure 5.8 Percentage of tracer within each concentration contour (regions A-L) providing a mass budget of the total tracer particle dispersal. Point X denotes the maximum of tracer concentration.

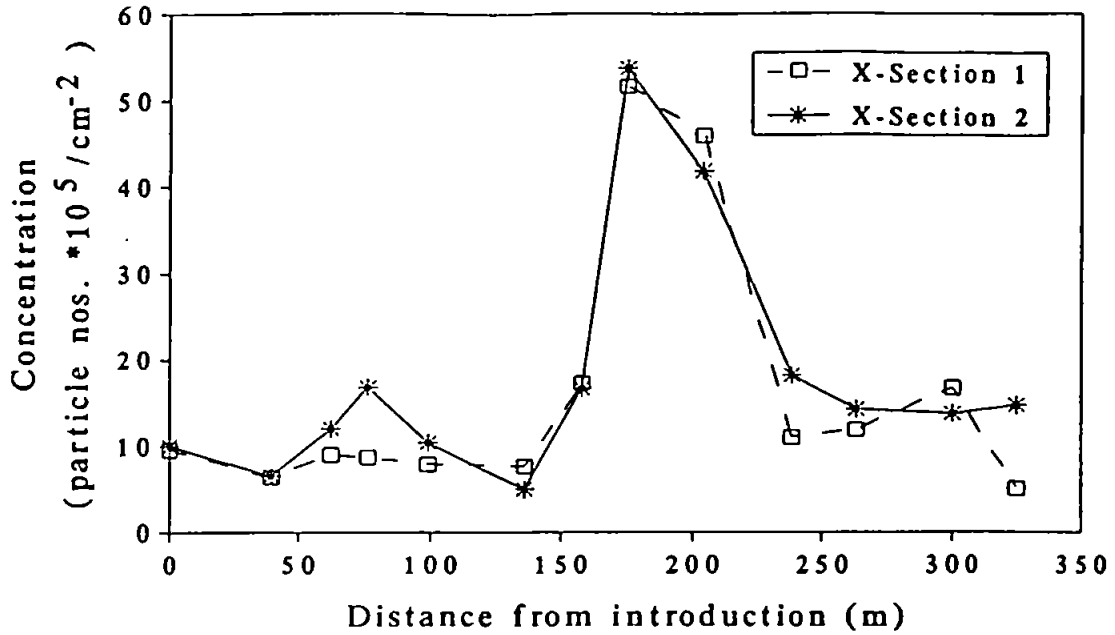

Figure 5.9 Tracer particle concentrations through cross-sections X1 and X2 from the fluorescent introduction point (Figure 5.1).

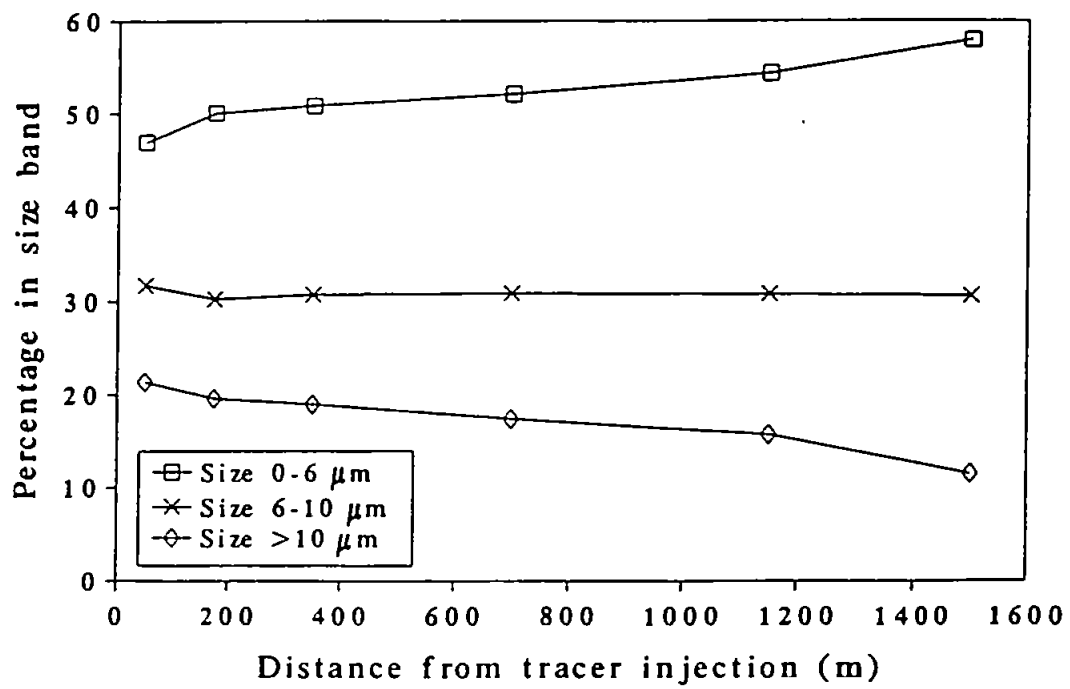

Figure 5.10 Tracer particle size distrubution of the recovered bed sediment tracer (percentage weight in size bands 0-6, 6-10 and 10-20μm) as a function of distance from the tracer injection point.

From the AFC analysis particle size can be measured (Section 4.2.3) and Figure 5.10 shows how the tracer particle size varied with distance from the point of injection. Despite the mean size (4-6 μm) being small, there was sufficient variation in the particles (0-20 μm) to detect distribution patterns. The percentage in the smallest size band increased by 11% over 1600 m distance from the tracer injection site with an 11% decrease in the percentage in the largest size band. Thus, a greater proportion of the smallest particles travelled furthest from the introduction site.

5.6 TRACER DISPERSAL AND MODELLING

5.6.1 Wind-wave Model

A model was developed which would explain and predict the movement of the tracer particles and cohesive sediment within Loe Pool using information from previous studies (see Section 5.2). The model assumed a spatially uniform windspeed due to the unknown local effects described in Section 5.3. It was based on a classical dimensional analysis, originally used by Sverdrup and Munk (1947) to represent the effect of wind and fetch where

$$H, C = f(F,t,W,g,h) \qquad (5.6)$$

where H is the significant wave height, C is the wave phase speed, F is the fetch, t is the time, W the windspeed, h is the water depth and g is the acceleration due to gravity.

The prediction model used two equations relating wave height (H), period (T), windspeed and fetch as given by:

$$gH/W^2 = 0.0026\,[g.F/W^2]^{0.47} \qquad (5.7)$$

$$gT/W = 0.46\,[g.F/W^2]^{0.25} \qquad (5.8)$$

(Smith & Sinclair, 1972). Thus allowing the fetch-limited conditions to be calculated.

For all sine and cosine waves C = L/T where L is the wavelength, and

$$C = [(gL/2\pi)\tanh(2\pi h/L)]^{0.5} \qquad (5.9)$$

(Pond & Pickard, 1983; Dyer, 1986). This allows the phase speed (C) and the wavelength (L) to be iterated.

Knowing the water depth, wave height and the wavelength, the horizontal displacement (d_o) at the bed due to the elliptical orbital motion of a wave at the surface can be calculated (Komar & Miller, 1973)(Section 5.2). The maximum horizontal velocity (U_m) can be calculated followed by the peak bed shear stress (τ_w) due to the wave. Several publications are available, having used this method to investigate sediment erosion, resuspension and transport studies (Sleath, 1984; Dyer, 1986; Soulsby & Smallman, 1986; Delo, 1988a; Luettich *et al.*, 1990).

Running this model under varying wind speeds and fetch at a fixed water depth of 2m enabled maximum wave orbital velocity and associated bed shear stress to be determined. Figures 5.11 and 5.12 clearly shows the rapid increase in wave height, period and wavelength with increasing fetch and windspeed. The wavespeed, however, reaches saturation at 2.1 m s^{-1}. The maximum effective

fetch of Loe Pool is approximately 600m, assuming the parameters outlined by Hakanson and Jansson (1983) and Hansen (1979). Therefore at 20 m s^{-1} wind speed the maximum significant wave height is 0.6m, the maximum wave period is 2.4 seconds and the maximum wavelength is 5m. Fetches plotted above 600m are shown for reference only.

The significant wave height doubles with increasing windspeed and fetch to a maximum in very strong winds of 0.4 m. The increase with both wind and fetch show that the wave height has a strong function with windspeed.

Figure 5.13 indicates that wave orbital velocity and associated shear stress would be impacted down to a water depth of 2.5 m in Loe Pool under a windspeed of 10 m s^{-1}. The minimum orbital velocity in the area around the Cober delta, with a depth of between 0.5-2.0 m is 0.04 m s^{-1} which provides a shear stress of 0.05 Nm^{-2}. Erosion of the surface unconsolidated sediment occurs at 0.1 Nm^{-2} (Dyer, 1986) and therefore under these conditions erosion would occur at depths of 0-1.5 m.

The most common winds experienced in this area of England are southwesterly between 5-15 m s^{-1} as an annual average (source RNAS Met. Lab.). Under these conditions a sediment bed of 80-90% water content, such as that found at the bed surface in Loe Pool (Coard, 1987), gives a dry density of approximately 100-230 kg m^{-3} (Delo, 1988a). This sediment has a critical bed shear strength of 0.3-0.8 Nm^{-2} (Delo, 1988a). Therefore, the maximum water depth at which the highest water content sediment bed would be eroded would be down to 1.5 m and under fetch conditions of 1600 m. During the study period the fetch was predominantly <600 m and the wind rarely exceeded 10 m s^{-1}, and therefore we would expect minimal remobilisation of the sediment after primary deposition.

Figure 5.14 indicates that higher windspeeds increase the maximum orbital velocity down to several metres depth with the resulting shear stress causing resuspension to a depth of 2 m with a 20 m s^{-1} wind from the southwest. The inclusion of larger fetches is intended to show how a slight increase in these parameters could alter the erosion conditions within the Pool.

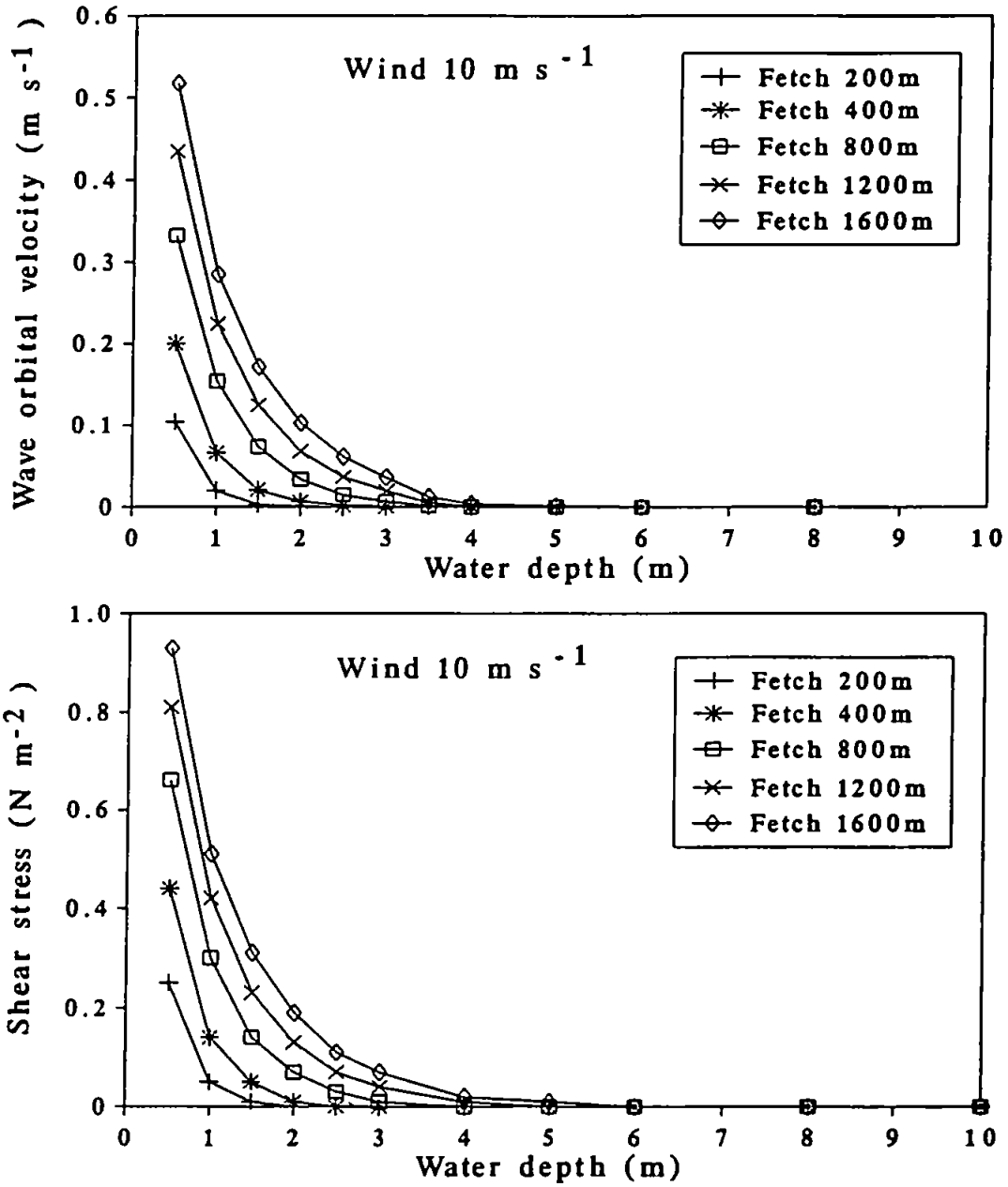

Figure 5.13 Wave orbital velocity (U_m) and bed shear stress (τ_w) as a function of water depth and fetch from 200-1600 n at a windspeed of 10 m s^{-1}.

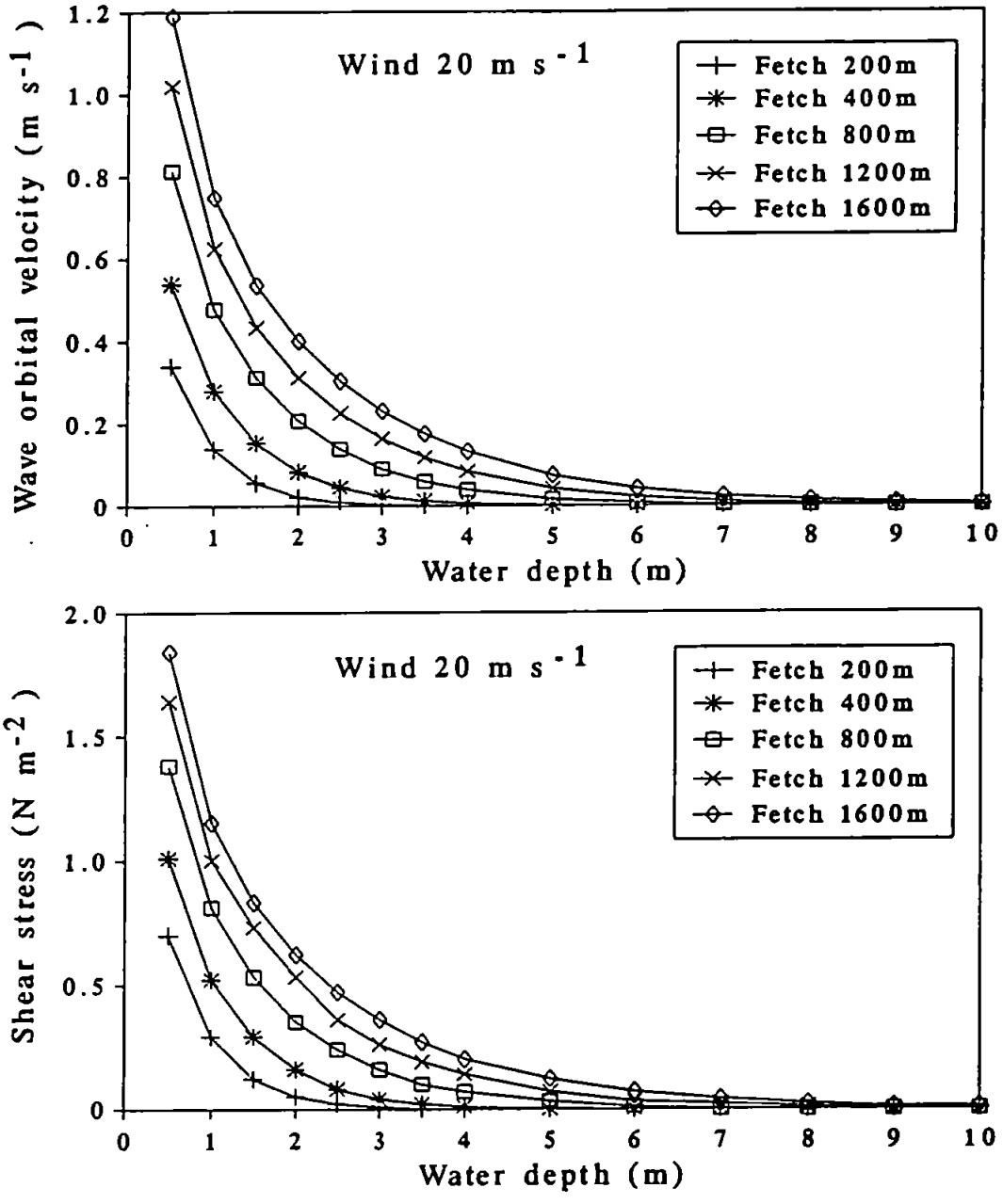

Figure 5.14 Wave orbital velocity (U_m) and bed shear stress (τ_w) as a function of water depth and fetch from 200-1600 n at a windspeed of 20 m s^{-1}.

Although there was limited remobilisation of the bed sediment during the study period, it is important to note that under southerly wind conditions a significant proportion of the upper area of the Pool, around the river mouth, where approximately 90% of the sediment and pollutants are deposited, is eroded. This remobilisation of the sediment causes a large internal re-loading of the water column possibly initiating algal blooms (Section 5.4.3). Due to the long hydraulic residence times of lakes, such areas act as efficient natural settling basins for particles and pollutants which on re-erosion suddenly release heavy metals and synthetic organic compounds back into the water column (Weilenmann *et al.*, 1990).

The sinking tracer particles will deposit on the bed of the lake if the bed shear stresses are sufficiently weak. Bed shear stresses for a 25 m s^{-1} south westerly wind are contoured in Figure 5.15. A comparison with Figure 5.8 shows that the tracer particle maxima occur in areas where the stresses are less than 0.5 Nm^{-2}. Stresses in very shallow water (less than 0.5m) tend to be much higher and can be of the order of 1 Nm^{-2}. The wave-induced stresses at location X (Figure 5.8) during the study are shown in Figure 5.16 and never exceed 0.2 Nm^{-2} during the study even towards the end of the study period when there were strong south westerly winds.

5.6.2 Wind-water Current Model

In addition to oscillatory wave motion, the wind also produces a steady movement of the surface layer of water in the same general direction as the wind. This movement is communicated to the layers below by internal shear stresses. Below the surface, the velocity of the wind-induced current varies with depth, usually decreasing in speed and rotating in direction due to Coriolis Forces. However in small shallow lakes the earths rotation is negligible with the principal driving force for bottom currents being wind setup (Lemmin & Imboden, 1987).

Bowden (1983) suggests a general rule of thumb for the current velocity to be approximately 3% of the windspeed. The wind driven current has 2 components; a Eulerian drift generated

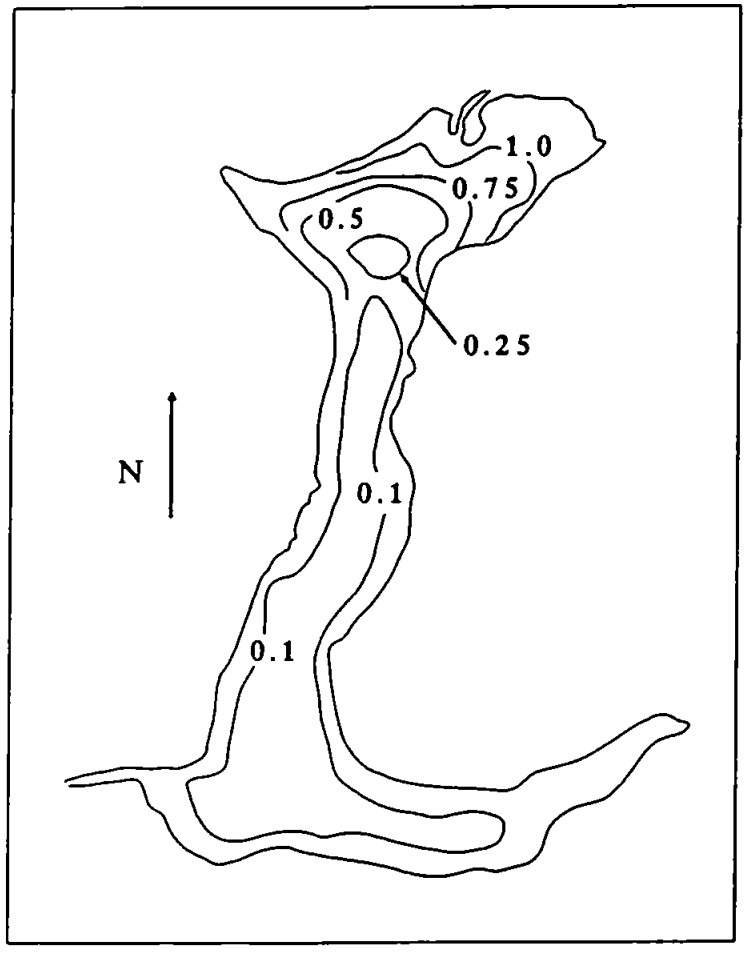

Figure 5.15 Bed shear stresses in Loe Pool for 25 m s^{-1} south westerly wind indicating that at the point of high tracer concentration (X in Figure 5.7) the bed shear stress is approximately 0.25 Nm^{-2}. Units are in Nm^{-2}.

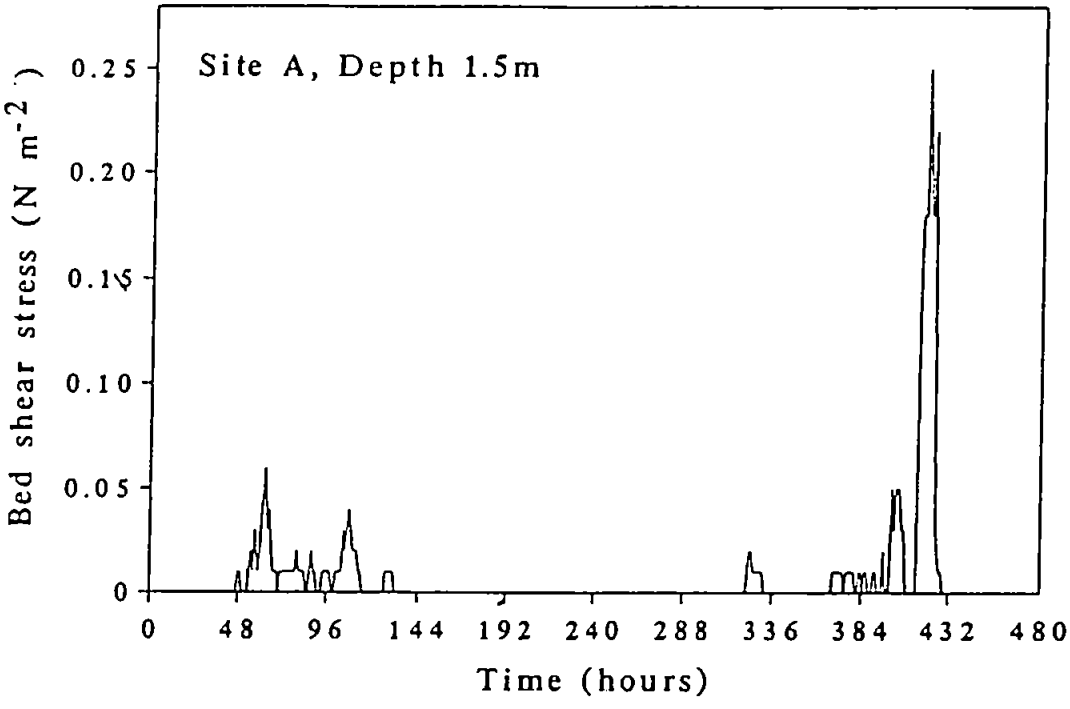

Figure 5.16 Bed shear stresse at site A (Figure 5.7) at a water depth of 1.5 m as a function of time during the first 20 days of the study (0-480 hours). Units are in Nm^{-2}.

by the wind stress on the sea surface, and a Lagrangian drift due to wave motion, known as the Stokes Drift. Stokes Drift occurs because the orbits of the water particles are not closed, with the result that after the passage of each wave there is a net movement in the forward direction. The wind-driven current decreases rapidly with water depth falling from 0.9 to 0.75% wind speed at 3 m depth.

In deeper waters, with stratification, a transverse setup can occur with the surface current running one way, and the current close to the bed running in the opposite direction (Luettich *et al.*, 1990). This wind-driven current causes a setup to occur, with the elevated water surface at the far end of the lake, and reduced water level where the wind is strongest pushing down on the lake's surface. This forms a gradient which in turn produces an overall current balancing the opposite flow.

The outline and depth contours of Loe Pool were digitized using facilities based at Polytechnic Southwest under the guidance of the NERC Computer Staff. This co-ordinate data was incorporated into a depth averaged model, initially described by Uncles (1982), by Dr. R.J. Uncles of the Plymouth Marine Laboratory and myself. The model was used to evaluate the residual currents by examining the horizontal pressure gradients which form as a result of the wind setup. A 53 x 43 array of points with spacing of 33 x 33m approximately covers the region G.R. S.W. 64-66W and 24-26N.

The depth averaged equations of continuity and momentum are, respectively:

$$\delta\xi/\delta t = - \nabla (h\mathbf{v}) \qquad (5.11)$$

and

$$\delta\mathbf{v}/\delta t = - (\mathbf{v} \nabla) \mathbf{v} - g \nabla\xi - \mathbf{f} \times \mathbf{v} + \tau_w - D \mathbf{v} |\mathbf{v}| /h \qquad (5.12)$$

where t is time, g is the acceleration due to gravity, ξ is the surface elevation, h the total depth, $\mathbf{v}$ is the depth averaged velocity, $\mathbf{f}$ is the Coriolis parameter (1×10^{-4} s^{-1}), D the bottom drag coefficient (2.5×10^{-3}), $\mathbf{W}$ the wind velocity and τ_w the surface wind stress where:

$$\tau_w = \rho_a C_D W |W| \qquad (5.13)$$

with ρ_a the density of air and $C_D = 3 \times 10^{-3}$ +/- 50% (Uncles *et al.*, 1986)

The terms represent the residual current acceleration (equal to zero in steady state conditions), which is equal to the inertial acceleration, the acceleration due to the surface slope forcing, Coriolis acceleration, the acceleration due to wind stress and the retardation due to the quadratic frictional drag at the bed.

Figure 5.17 is the surface elevation at each point in the Pool at the time of the tracer introduction and is a reflection of the wind blowing on the surface causing a setup. The model balances a gradient of elevation and a force due to the wind stress by generating a residual current flow around the lake, which can be seen in Figure 5.18 for a northerly wind of magnitude 15 m s^{-1} (A) and an easterly wind of 13 m s^{-1} (B) different wind directions. The resulting circulation pattern describes the modelled hydrodynamics of the Pool.

The limited discharge of the river inflow assists only partially in the overall advection of the tracer particles. If we assume that the tracer particles enter the lake in a turbulent jet (Jopling, 1960), with a longitudinal velocity which decays as the reciprocal of the distance travelled from the site of introduction, then the average velocity of the particles would be approximately 0.008 m s^{-1}; this is the maximum velocity for a turbulent jet entering an infinite body of water. In reality, current speeds will be reduced due to the effects of bottom friction on the inflowing river. The momentum from the river therefore does cause the tracer particles to remain suspended in the water column, until the wind-water currents begin to take effect.

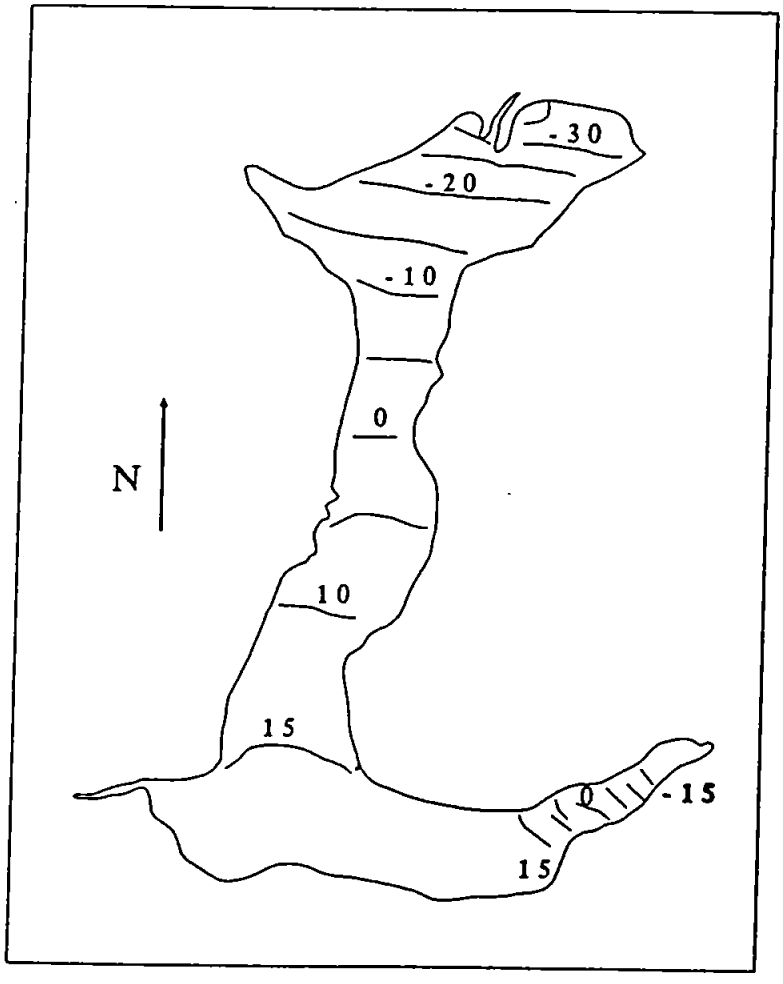

Figure 5.17 Predicted wind driven lake setup for a 13 m s^{-1} easterly wind to indicate elevation during the first five days of the study period due to lake stup. Units are in millimetres.

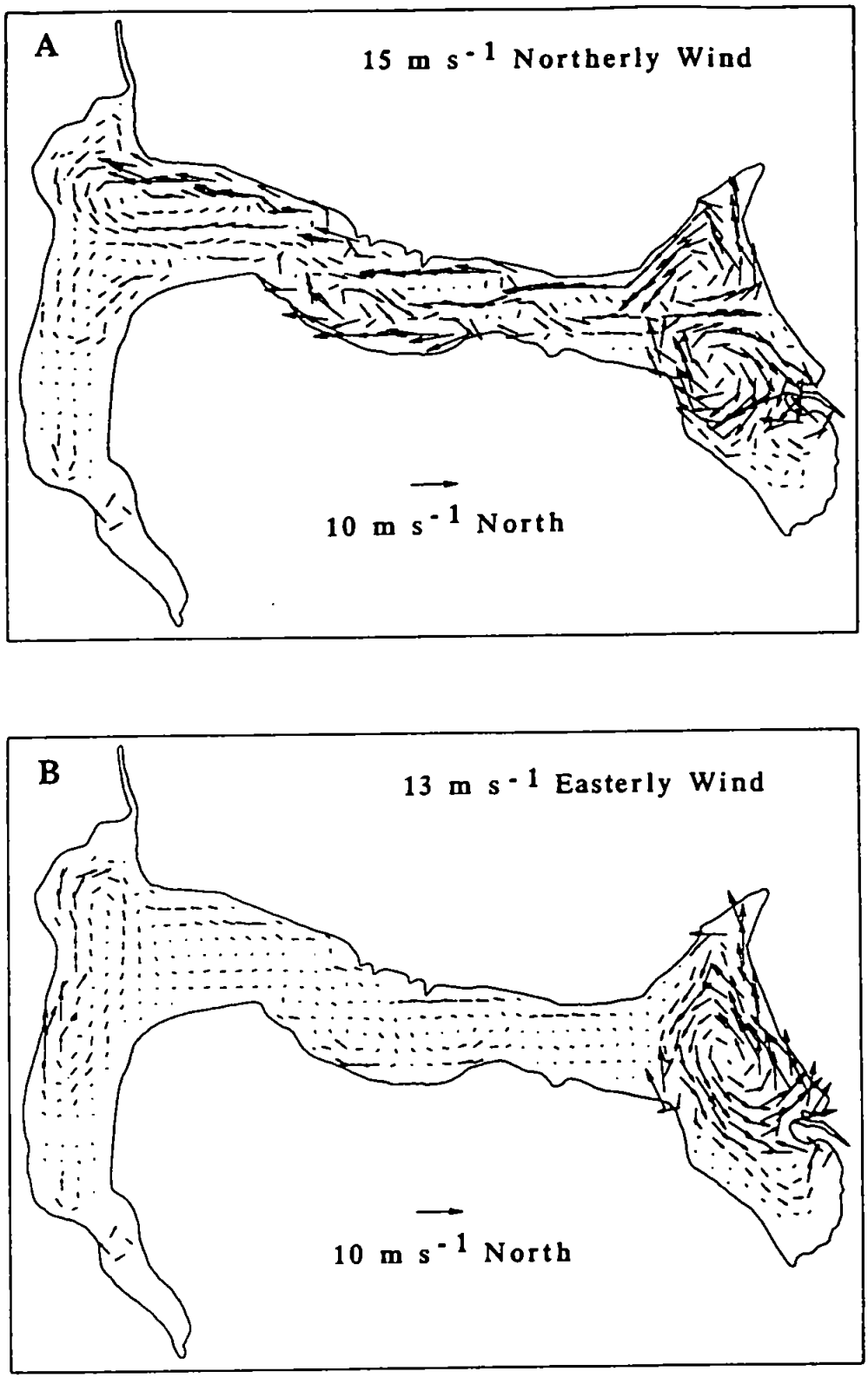

Figure 5.18 Modelled depth-averaged, wind-driven water circulation within Loe Pool for a 15 m s^{-1} northerly wind (A) and a 13 m s^{-1} easterly wind (B). Note that west is vertically upwards on these diagrams.

Figures 5.19 and 5.20 show the wind-water circulation patterns which existed for the first four half-days (12-hourly averaged readings) after the tracer introduction. The most noticeable feature is the very dominant gyre, in the upper region of Loe Pool, close to the river outlet. The gyre remained in approximately the same position, even as the windspeed varied. The highly concentrated region X (Figure 5.8) approximates very closely with the centre of the gyre. Over successive half-day periods the centre migrated slightly, causing wider spreading of the settling particles. Applying Stokes settling velocity for the tracer particles, the particles had a settling time of approximately 7-12 hours in this water depth, but with increased turbulence this settling time would have increased and therefore the tracer particles would have continued to be influenced for several days. Two secondary gyres existed, directly east of the river outlet, which would have continued to recirculate any tracer particles. Their positions varied slightly during the first two days although there was a similarity to the tracer contours of regions K and L.

Further gyres were also evident along the Loe causing the spreading of the tracer, clearly seen in regions C-E. South of this point the gyres were slightly more confused and less pronounced under the north-easterly winds which were experienced for the first 7-9 days of the study period. Figure 5.18 shows the water circulation patterns for the lake under a moderate northerly and easterly wind. Current velocities rarely exceed 0.1 m s^{-1} which provide sufficient turbulent mixing to maintain fine silts and clays in suspension, but not allow resuspension. Under northerly wind conditions the main gyre split into two and caused tracer concentrations to be centred around these two points. Water circulation patterns for southerly and westerly wind flow are the exact opposite since the equations of continuity and momentum are reversed.

During the study period the wind was predominantly from the NE-ENE (Figure 5.6) causing the tracer particles to be distributed as already described above. The wind-wave action for the first few days was minimal, due to the limited effective fetch. Bed sediment would only be resuspended immediately surrounding the shoreline (i.e. <50cm.). However, towards the end of the study period the wind was from the southwest, and had a velocity of 10-15 m s^{-1}

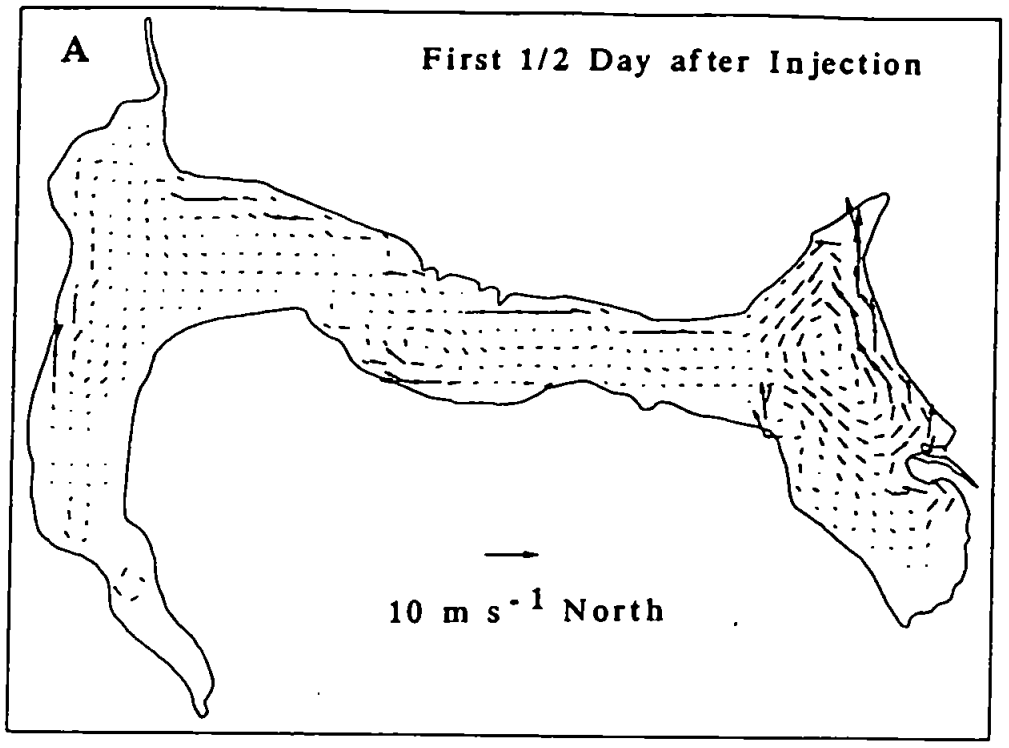

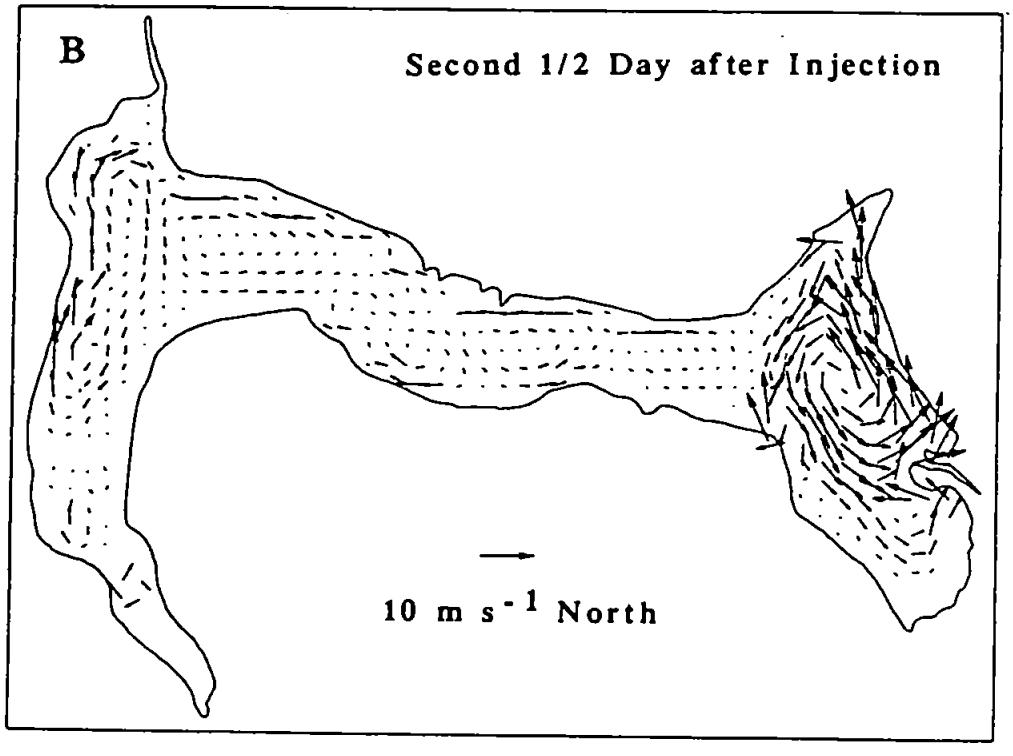

Figure 5.19 Modelled depth-averaged, wind driven water circulation within Loe Pool during the first (A) and second (B) half days after the tracer injection. Note that west is vertically upwards on these diagrams.

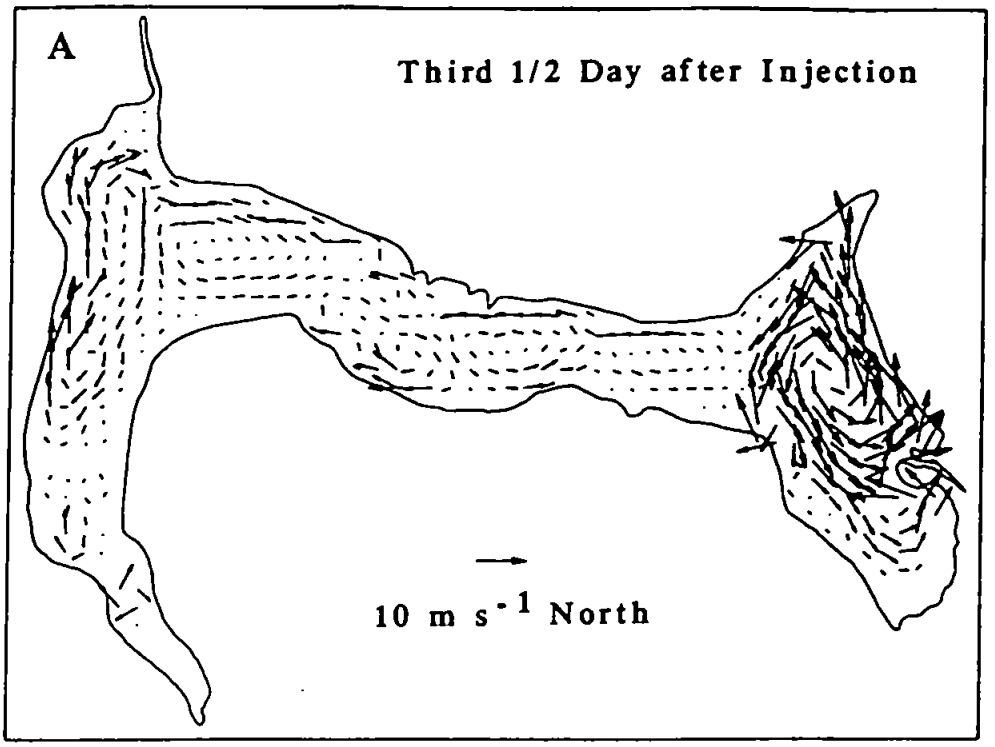

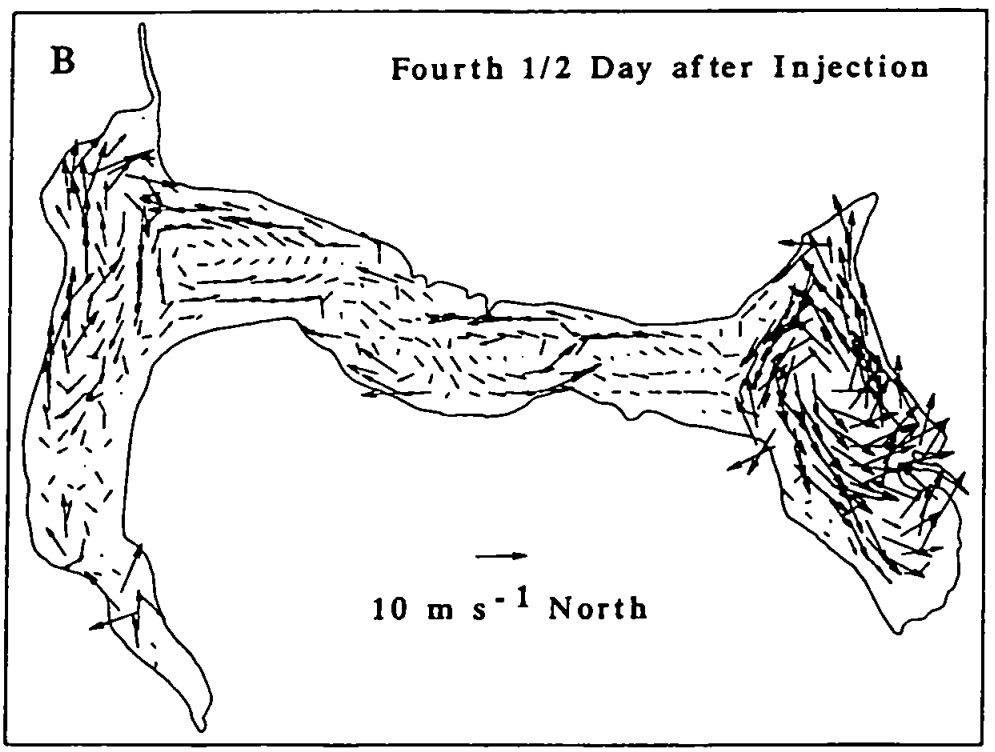

Figure 5.19 Modelled depth-averaged, wind driven water circulation within Loe Pool during the third (A) and fourth (B) half days after the tracer injection. Note that west is verticilly upwards on these diagrams.

resulting in the main gyre having a reversed flow but in the same position. The effective fetch was 600 m and sediment resuspension would have occurred to a depth of 1.25-1.5 m.

The models and data suggest that the tracer particles would have circulated in the upper region around the main gyre until settling out in a radial pattern from the centre of the gyre. Limited wind conditions prevented the tracer from being redistributed, and therefore the tracer concentration contours seen in Figure 5.7 represent primary deposition.

5.7 SUMMARY

Loe Pool is a shallow eutrophic shoreline lake influenced by a temperate maritime climate. River flow, lake residence time, stratification and circulation reflect climatic seasonality. Sedimentation in the lake is predominantly fine cohesive clays and silts originating from the allochthonous influx of the catchment and the river discharge.

Several studies have shown that the sediment acts as an effective sink for nutrients and pollutants. Turbulent mixing is the key regulating factor in the release and reloading of a water column. Some authors have found up to 100% of the external supply is released after a storm event. This has serious implications for shallow lakes with post-depositional migration both vertically and horizontally being important.

Loe Pool has an overall flow regime regulated by wind-wave and wind-current action, since river discharge is minimal. The sedimentation is generally not uniformly distributed, with 17% of the lakes surface area disappearing in the last 70 years. River action sedimentation does occur, as seen in Figure 5.3, in the form of a delta which extends into the lake for the first 100m. The remainder of the lake is covered with a highly flocculated sediment with specific accumulation in the deeper areas. During the winter months, when river discharge is generally higher, river action sedimentation is dominant.

Consolidation of the sediment is minimal due to the small influx of allochthonous material. However, during the mining period higher sedimentation is reflected in the water content of this sediment layer (minimum 37.6%). Erosion only occurs under conditions of large fetch and strong winds.

The shape and morphology of Loe Pool, and climatic conditions strongly influence the transport of sediment within the lake system. Loe Pool is eutrophic, with frequent algal blooms which began around the time of the commissioning of the Helston Sewage Treatment Works. Severe loading of the Pool with nutrients and pollutants originating from sewage, and pollutant point and diffuse sources. Data from SWWA suggests 19.8 T a^{-1} P of which 92% originates from the STW and 195 T a^{-1} N mainly from agricultural sources; 26% and 58% leave the system, respectively. The Hydrological Relevant Load (HRL, i.e. the amount of nutrient available for growth in spring, plus that which enters during the growth season) must therefore be in excess of 33% and 50% suggested by Vollenweider (1975) and Jorgensen (1980), and Ryding and Forsberg (1980), respectively. The sediments act as a huge sink to the nutrients and pollutants.

Accuracy of analysis on the AFC was good ranging from 0-7%, with sample preparation ranging from 2.6-14.7%, allowing for an average AFC variability of 4.75%. Errors for the repeat cores were good initially, but bed distortion, non-uniform sediment distribution and inaccurate coring possibly explain the large inconsistences.

High concentrations of tracer particles occurred in the northern region with two well-defined maxima. The natural, brown-clay sediment of Loe Pool shows some similarities to the tracer particle concentrations, in particular an accumulation in the northern region, although many differences do exist. However, much of the natural sediment entering the lake will do so during spate conditions when water circulation patterns may be different from those during this experiment. There is an accumulation of natural sediment in the deeper part of the lake which is not a feature of the tracer particle data. This accumulation is possibly due to remobilisation and redistribution of sediment deposited in the northern area by wind-wave

action during extreme weather conditions.

The majority of tracer particles were deposited between 150-225 m from the injection site. There was significant spatial variation for the size range between 0-20 μm. The percentage by weight in the smallest size band increased by 11% over the 1600 m distance from the tracer injection site, with a corresponding 11% decrease in the percentage in the largest size band. A greater proportion of the smallest particles travelled furthest from the injection site.

A budget of recovered tracer particles shows that approximately 90% by weight were found in the northern area. The estimated number of 'recovered' particles was 3.8×10^{14}. The estimated number of injected tracer particles was 2.9×10^{14} particles. The difference between these estimates is possibly the result of sampling variability and errors in the analysis technique.

Assuming the tracer particles to be analogous to natural suspended sediment, then the results imply that approximately 90% of the sediments entering Loe Pool will, in the short-term, remain in this northern area, and that any sediment-borne anthropogenic pollutants will accumulate within the deposited sediment there.

The winds were predominantly from the east and north during the first few days after injection of the tracer particles. A numerical model of the circulation shows that the depth-averaged, wind-driven circulation in the lake is typically of the order of 0.1 m s^{-1} and that the shallow, northern part of the lake has a particularly strong circulation. In the case of a northerly wind, the circulation within the northern area consists of two strong, opposing gyres. For an easterly wind, there is one strong and one weak gyre.

The model was run for the duration of the experiment using actual runoff and wind-stress data. During the first two half-days following injection of the tracer particles, when the wind was mainly easterly, a large gyre existed to the south and west of the river mouth. The centre of this gyre corresponded with the location of the tracer particle maximum in the bed

sediment. The secondary tracer particle maximum in the northern area corresponded to a region of very slack currents to the south and east of the river mouth. In addition, any steering of the wind field by topography will introduce a northerly component to the wind-stress which would have emphasized the tendency for particles to be accumulated to the south and east of the river mouth, as well as in the main gyre region to the south and west.

The circulation patterns remained similar, but stronger during the first few days after injection, so that the tracer particles experienced a fairly stable flow-field for a much longer period than the Stokes settling time as they sank to the bed. Bed shear stresses for the first and second half-days following injection indicate that the tracer particle maxima occurred in areas where the stresses were less than 0.1 Nm^{-2}.

These wave-induced stresses increased with wind speed during the following few days, but never exceeded 0.2 Nm^{-2} in the area of maximum concentration, or 0.4 Nm^{-2} in the area of secondary maximum concentration. Moreover, if resuspension had occurred, the wind-driven flow patterns would have tended to maintain tracer particles in the northern region.

Maximum wave-induced bed shear stresses occurred near the end of the sampling period when a 25 m s^{-1} wind blew from the southwest and the fetch was a maximum. Stresses reached 0.4 Nm^{-2} in the area of maximum concentration and 0.8 Nm^{-2} in the area of secondary maximum concentration.

The surface sediments within Loe Pool have, typically, 80-90% water content. The corresponding dry density is approximately 100-230 kg m^{-3} and the critical bed shear-strength for erosion is estimated to be 0.3-0.8 Nm^{-2}. Therefore, one would expect minimal remobilisation of the deposited sediment for a considerable period following the initial deposition, although some resuspension may have occurred near the end of the sampling period.

CHAPTER 6

A STUDY OF THE FINE-SEDIMENT TRANSPORT DYNAMICS IN A MACRO-TIDAL ESTUARY: TAMAR ESTUARY, SW DEVON, UK

6.1 BACKGROUND TO THE TAMAR ESTUARY

6.1.1 Introduction

Partially stratified to well mixed estuaries usually exhibit a zone of high turbidity within the upper estuary where concentrations of suspended solids can reach several orders of magnitude greater than those carried by the inflowing freshwater and marine sources (Dyer, 1988; see Section 1.3.3). Postma (1967), Schubel (1969) and Allen *et al.*, (1980) have described these features and discussed the combination of hydrodynamic factors which leads to their formation and maintenance. The maximum turbidity zone acts as a particle trap which retains selected fractions of influxing materials either in suspension or cycling between suspended and deposited states (Festa & Hansen, 1978; Officer, 1980; Allen *et al.*, 1980, Morris *et al.*, 1982b; Bale *et al.*, 1985, Uncles *et al.*,1985, Morris *et al.*, 1987).

The Tamar Estuary, (Figure 6.1) has a pronounced turbidity maximum in the low salinity region (Bale, 1987; Uncles & Stephens, 1989). The formation, enhancement, migration and chemical cycling characteristics of the turbidity maximum of the Tamar Estuary have been studied extensively in order to better understand the mechanism of formation of turbidity maxima in general from both an environmental and engineering viewpoint.
Spatial variability and chemical cycling of many different parameters have been studied including trace metals (Knox *et al.*, 1981; Loring *et al.*, 1983; Morris *et al.*, 1982a; Ackroyd *et al.*, 1986), persistent chemicals (Readman *et al.*, 1982) and water quality parameters (Morris *et al.*, 1981, 1982b).

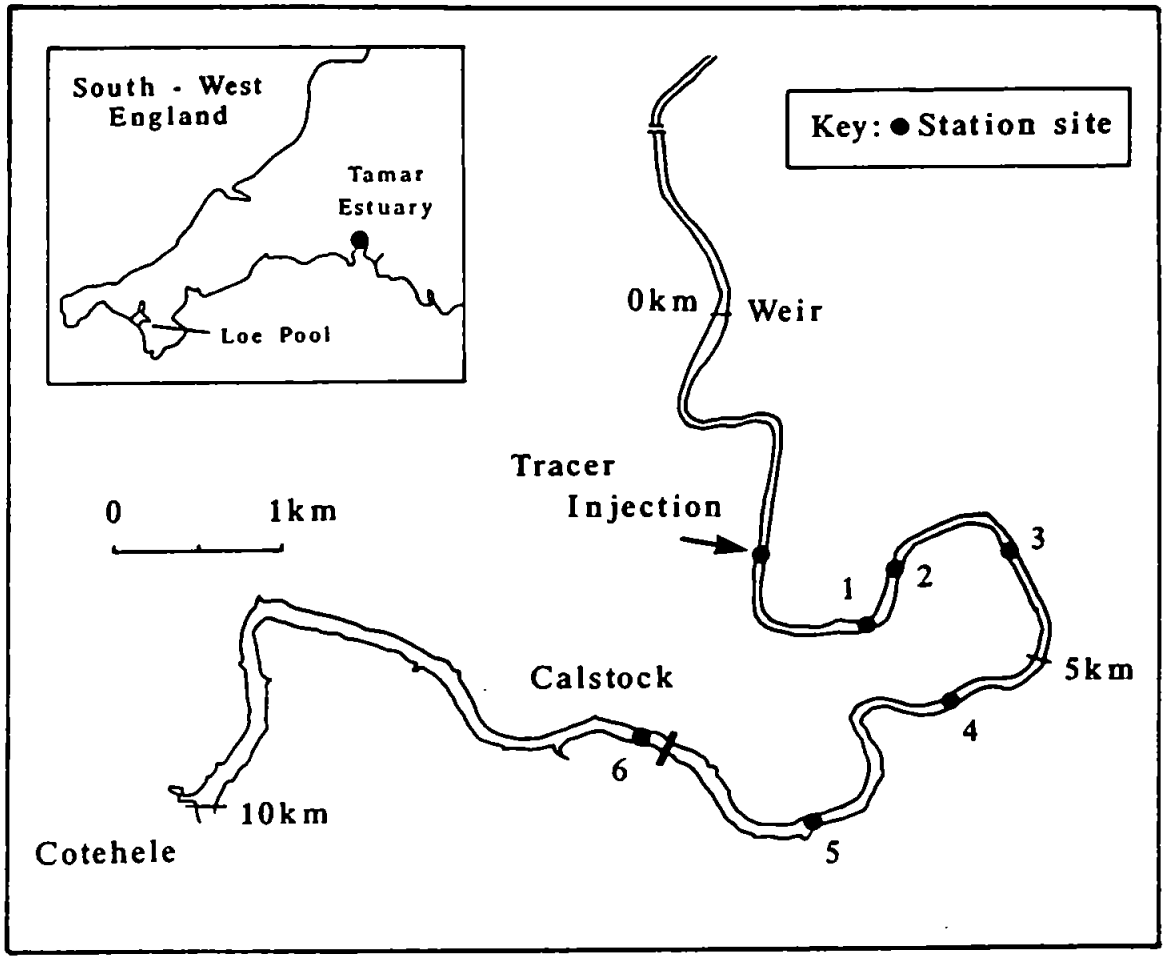

Figure 6.1 Location map of the Tamar Estuary showing the freshwater weir and location and distance from the weir of the sampling Stations 1-6. The tracer injection point is also shown.

Physical data on tidal regime (George, 1975), internal waves (Sturley, 1990) and determination of size spectra, settling velocity and floc density (Bale *et al.*, 1987; Bale & Morris, 1987; Fennessy *et al.*, 1994) have all enhanced the understanding of estuarine processes, sediment mobility and pollutant transport. Modelling of empirical data by Harris *et al.*, (1984) to establish dispersion of toxins and Uncles *et al.*, (1985, 1987) assessing dispersion of salt and suspended sediment with respect to contaminant transport, has enabled an overview of studies carried out.

6.1.2 Site Description

6.1.2.1 Introduction

The Tamar Estuary is a good example of a partially mixed macro-tidal estuary (Bale *et al.*, 1985; Uncles *et al.*, 1988) and presents an ideal site for the study of fine sediment dynamics and the application of the tracing technique in a macro-tidal estuary. Bale (1987) outlines the reasons for the suitability of the Tamar Estuary as a natural environment 'testing laboratory'. In summary, it is typical of a large number of macro-tidal estuaries in temperate regions, it is relatively 'clean' in that it has no major industrial or fluvial discharges into it. The Tamar is navigable to the limit of its tidal influence, and therefore the whole of the salinity gradient can be surveyed. Topographically, the estuary for the most part is uncomplicated with only two major tributaries, both near the mouth, and it has an uncomplicated 'U' shaped cross-section channel (George, 1975) which simplifies interpretation.

The Estuary has been actively studied for many years by many organisations including the Institute for Marine Environmental Research (now Plymouth Marine Laboratory) a component body of the Natural Environment Research Council, Plymouth Polytechnic (now the University of Plymouth) and the University of Birmingham. These studies have produced an extensive amount of information on the circulation, sedimentology and pollution chemistry of the water column and sediments (Morris *et al.*, 1982 a, b; Bale *et al.*, 1985; Uncles *et al.*, 1985, Barton *et al.*, 1991; Loring *et al.*, 1983).

6.1.2.2 Geography and Hydrography

The Tamar Estuary extends 31 km from a weir at Gunnislake, the head of the estuary, to Plymouth Sound (Figure 6.1); Bale (1987) provides a full description of the estuary. The Estuary has two major tributaries; the Rivers Lynher and Tavy located in the lower estuary at 7km and 9.8km from the Estuary mouth, respectively. Approximately 50% of the freshwater flow into the Tamar Estuary is from the River Tamar over Gunnislake weir (Uncles *et al.*, 1983). Typical monthly mean river flows at Gunnislake range from 3.3 $m^3 s^{-1}$ in May to 70.1 $m^3 s^{-1}$ in November, although after periods of heavy localised rainfall, spates can produce flows as high as 140 $m^3 s^{-1}$

The flushing time of the estuary, (defined as the time required for up-estuary freshwater inputs to replace the up-estuary volume of freshwater) varies with location and is dependent on river flow. For example, at the mouth the flushing time is of the order of three weeks, whilst upstream at 15 km from the weir it is typically one week or less. The mean flushing time for the whole of the Estuary is typically one week. However, in extreme conditions, such as low runoff during spring tides, it can be as long as three weeks (Uncles *et al.*, 1983).

Salinity distributions in the Tamar Estuary vary with the state of the tide and with river runoff. The Estuary experiences a wide range of salinity distribution, from well mixed to highly stratified with pronounced salinity gradients of up to 20 ppt (Uncles *et al.*, 1983).

6.1.2.3 Tidal regime

George (1975) detailed the tidal regime of the Tamar Estuary and indicated the asymmetry in the tidal curve at the Estuary mouth at Devonport with flood tides having a shorter duration than ebb tides which results in stronger current speeds on the flood tide. This asymmetry becomes more pronounced in the upper Estuary (Uncles *et al.*, 1989). High water at the head of the Estuary is approximately 1 hour after high water at Devonport. At the head of the

Estuary the ebb tide runs for approximately 7.5 hours and the flood for 4.5 hours.

Uncles *et a.,l* .(1989) described a rapid acceleration from maximum ebb to maximum flood currents with only a brief period of slack water. At high water however, there is an extended period of slack water which begins at high water and continues well into the ebb tide period. This asymmetry leads to tidal pumping as described in Section 1.3.3.

6.1.3 Previous cohesive sediment studies

6.1.3.1 Turbidity maximum

A turbidity maximum is a phenomenon which is frequently observed in the low salinity reaches of the Tamar Estuary (Bale, 1987; Uncles *et al.*, 1991a,b). The location of the turbidity maximum varies during the tidal cycle, the spring-neap cycle, with tidal range and river flow (Bale *et al.*, 1985; Uncles *et al.*, 1985). In the Tamar Estuary the maximum migrates up-estuary during low freshwater discharge, and down-estuary during high freshwater discharge (Bale *et al.*, 1985). The migration of the turbidity maximum down estuary in winter months during periods of high river runoff (and hence high turbidity) leads to a deposition of suspended sediment in the mid-estuary region below 10 km. This mid-estuarine deposit supplies source material for subsequent up-estuarine transport and entrainment during the subsequent summer months of low river runoff (Bale *et al.*, 1985) and due to the high silt/clay content and unconsolidated nature the upper estuarine sediment is eroded and entrained within the turbidity maximum during the tidal cycle.

Tidally induced resuspension is an essential mechanism for generating a strong, spring-tide turbidity maximum, and the location and magnitude of the maximum is largely dependent on the flood tide transport of suspended sediment (Uncles *et al.*, 1985) and to a lesser degree on gravitational circulation and local upper estuary resuspension of sediments (Uncles & Stephens, 1989). Bed sediment is resuspended and incorporated into the turbidity maximum during spring tides and largely deposited and returned to the bed during neap tides (Stephens

et al., 1992). Stephens *et al.*, (1992) showed that the degree of consolidation increased down-estuary from the head of the Tamar Estuary, and was caused by an increased bed shear stresses due to tidal currents and the limited period for consolidation following deposition during slack-water periods.

This continual cycling of sediment within the turbidity maximum region 'feeds' the maximum particularly during spring tidal conditions with greater contributions taking place during flood tides. This effect is further enhanced by vertical stability and stratification of ebb tides diminishing vertical turbulent mixing (Darbyshire & West, 1991) enabling larger flocs to form and settle to the bed and remain in the upper estuary as observed by McCabe *et al.*, (1993). Observations by Uncles *et al.* (1989) and Barton (1992) provide current data and settling velocities of flocs and explain the settling, deposition and resuspension that occurs. Uncles *et al.*, (1991b) notes that intratidal variations in water column SPM and salinity stratification, and therefore stability and vertical mixing, also play a role in fine sediment transport and turbidity maximum formation.

6.1.3.2 SPM size analysis

Bale & Morris (1987) determined floc size spectra in the turbidity maximum using *in situ* laser diffraction technology. They indicated that the bulk of particles measured *in situ* ranged from 37.6 to 188 μm (predominantly large flocs) and above, whereas size analysis of discrete samples from the turbidity maximum taken simultaneously by pump sample ranged from 25-70 μm. Analysis of grains after treatment to remove organic coatings indicated a size range from 6-10 μm with 30% below 1.9 μm (predominantly individual grains and microflocs). Further size analysis by McCabe *et al.*, (1993) indicated that the size spectra measured *in situ* varied between ebb and flood tide and spring and neap tidal conditions. Two predomimant modes in the floc distribution were measured comprising 5.8 μm and 100 μm and larger. The spring flood turbidity maximum consisted almost entirely of particles less than 6 μm in diameter, whereas the neap flood turbidity maximum consisted of large flocs centred around 200 μm (McCabe *et al.*, 1993).

6.1.4 Areas requiring further research

Despite the enormous volume of work undertaken on the Tamar Estuary several significant areas of research remain inconclusive. These include:

i) The establishment that tidal pumping of suspended sediment is directed up-estuary at spring tides and contributes to the formation of the turbidity maximum (Uncles *et al.*, 1985).

ii) The understanding of how the sediment balance and water and salt budgets are maintained (Uncles *et al.*, 1985).

iii) The precise source of sediment which incorporates within the turbidity maximum during low river runoff summer months. Bale *et al.*, (1985) suggests that migration of the turbidity maximum during high river runoff conditions allows deposits of sediment to form in the middle estuary. When the turbidity maximum migrates upstream during lower runoff conditions, tidal pumping provides the mechanism and the deposits provide the source for an enhanced turbidity maximum during the summer months.

iv) The particle residence time of the turbidity maximum and rates of cycling within the estuary. Bale *et al.*, (1985) and Dyer (1989) highlight the uncertainty of particle retention and the location of the sinks of sediment which leaves the turbidity maximum during both high and low river runoff conditions. The residence time, cycling and accumulation of dissolved and particulate contaminants within the turbidity maximum, and the estuary as a whole, can not be accurately predicted without a clearer understanding of this aspect (Readman *et al.*, 1982; Uncles *et al.*, 1987).

v) The dispersion coefficients of suspended particulate within the turbidity maixmum region relative to the dispersion coefficient of salinity (Uncles *et al.*, 1985).

vi) The degree of settling and resuspension during a tidal cycle (Dyer, 1989).

vii) Evidence that a parcel of water laden with suspended particles which moves up and down the estuary close to the bed has a tendency to deposit particles at its high water position rather than its low water position indicating the degree of entrapment on tidal mudflats in the upper reaches of an estuary (Uncles *et al.*, 1991).

viii) The assessment of the proportional effects of neap and spring tides for the formation and maintenance of the turbidity maximum (Bale *et al.*, 1985; Uncles *et al.*, 1985; Stephens *et al.*,1992) .

The importance of these points in advancing the knowledge of sediment and pollutant dynamics are clear, and invariably involve interdisciplinary work to evaluate each component simultaneously.

6.1.5 Background to this study

This study was designed to use the developed technique (described in Chapter 4) to answer more specifically some of the above aspects and to validate the technique for future work.

The aim of this study was to investigate sediment transport in the upper reaches of the Tamar Estuary within the turbidity maximum, to establish the particle residence time of the maximum, and investigate entrapment, dispersion coefficients of particulates in comparison to salinity, and establish the degree of settling and resuspension during the ebb and flood tides. In addition an estimate of the proportional influence of spring and neap tides was to be made. The experiment was also designed to assist our understanding of the mechanisms that control the chemical cycling of contaminants in the turbidity maximum.

6.2 PRELIMINARY EXPERIMENTAL SURVEY

6.2.1 Introduction

The aim of the tracer experiment was to investigate sediment transport within the turbidity maximum during low summer freshwater discharge and spring tidal conditions. An assessment of ebb and flood variability over a complete tidal cycle was also planned. In order to meet all these requirements the study was set for the 26th June 1990 which was a spring tide with an early morning high water enabling the tracer to be released at slack high water in the upper Estuary prior to commencement of the ebb tide. The times of high and low water allowed full use of the daylight hours to complete the study. The high and low water times for the tide and tidal range at Devonport on the 26th June were 0815 - 5.1 m, 1415 - 1.1 m and 20.28 - 5.4 m.

In order to design the tracer experiment and determine methodology and equipment requirements it was necessary to undertake a series of axial surveys on the Tamar Estuary in advance on the 26th June. Numerous axial surveys of the Tamar Estuary have been undertaken and the results discussed and modelled (Morris *et al.*, 1982a; 1987; Uncles *et al.*, 1985; 1987; Uncles & Stephens, 1989). The results highlight a dominant turbidity maximum in the upper estuary between 0-10 km from the weir associated with the limit of saline intrusion, although as Uncles & Stephens (1989) note the turbidity maximum can occassionally be upstream of the freshwater-saline interface and therefore can not be affected by gravitational circulation. Generally higher concentration of SPM is also noted during spring tides as opposed to neaps, and with flood tides as opposed to ebb.

6.2.2 Axial Surveys

Prior to the tracer study, three longitudinal axial surveys of the Tamar Estuary were undertaken on 15th, 18th and 22nd June. The surveys were carried out using 'Tamaris' a 12 m flat bottomed Rotork sea-truck, and involved continuous logging of salinity, temperature and

suspended solids in the upper 1 m surface waters of the Estuary using the same technique as described by Morris et al., (1982b). In addition, the daily mean freshwater flow into the Estuary across the weir at Gunnislake was obtained from the NRA.

The objectives of the surveys were to:

i) Determine the magnitude and position of the turbidity maximum relative to tidal state

ii) Determine the probable range of excursion of the turbidity maximum

iii) Quantify the suspended particulate loading of the turbidity maximum

iv) Obtain a salinity and temperature profile of the Estuary

v) Assess suitable sampling sites for the tracer study

The axial surveys were carried out on both flood and ebb tides under the following conditions:

15th June

HW - 1hr 40min to HW +1hr 20 min at HW Slack from 31-1.2km
HW + 1hr 45min to HW + 2hr 45min at Ebb tide from 1.2-10.5km

18th June

HW - 3hr to HW - 1hr 30 min at Flood tide from 17.2-1.2km
HW - 30 min to HW at HW Slack from 6.3-1.2km

22nd June

HW - 4hr to HW -1hr 45 min at Flood tide from 13.3-1.9km

HW - 1hr 45min to HW-1 at Flood tide from 1.9-8.9km

6.2.3. Results

The results from the axial surveys on the 15th, 18th and 22nd are shown in Figures 6.2 to 6.7 respectively. The salinity results show a gradient from 32 ppt in the lower estuary to 0 ppt in the upper estuary. The steepest salinity gradient was in the middle estuary between 6 and 18 km with a migration of the freshwater-saline interface during the tidal cycle. The upper saline limit is situated at 4 km during neap slack water on the 15th and 18th and moves down-estuary on the ebb tide to 6 km approximately 2 hours after slack water. The data from the 22nd indicated the saline limit was positioned a large distance down the Estuary even close to high water slack. This was due to the high river discharge on the day of the survey leading to displacement of the turbidity maximum down-estuary (Bale *et al.*, 1985) and dilution of the salinity gradient.

6.2.4 Summary

The axial profiles clearly indicated the existence of a turbidity maximum in the upper reaches of the Estuary with maximum concentration on the neap tides (15th,18th) between 180-420 mg l^{-1} and maximum concentration on the spring tide (22nd) between 450-800 mg l^{-1}. The turbidity maximum on the 15th was clearly associated with the limit of saline intrusion between 0-4 km at slack water, and as the ebb tide commenced the turbidity maximum concentration increased slightly from 375 to 425 mg l^{-1}. This may be due to an increase in current flow and erosion of bed sediment and entrainment into the surface waters. However work by Barton (1992) and Uncles & Stephens (1989) suggests that stratification is significantly enhanced during the commencement of the ebb tide, and that increase in turbidity lags the increase in velocity by approximately one hour. Therefore, due to an

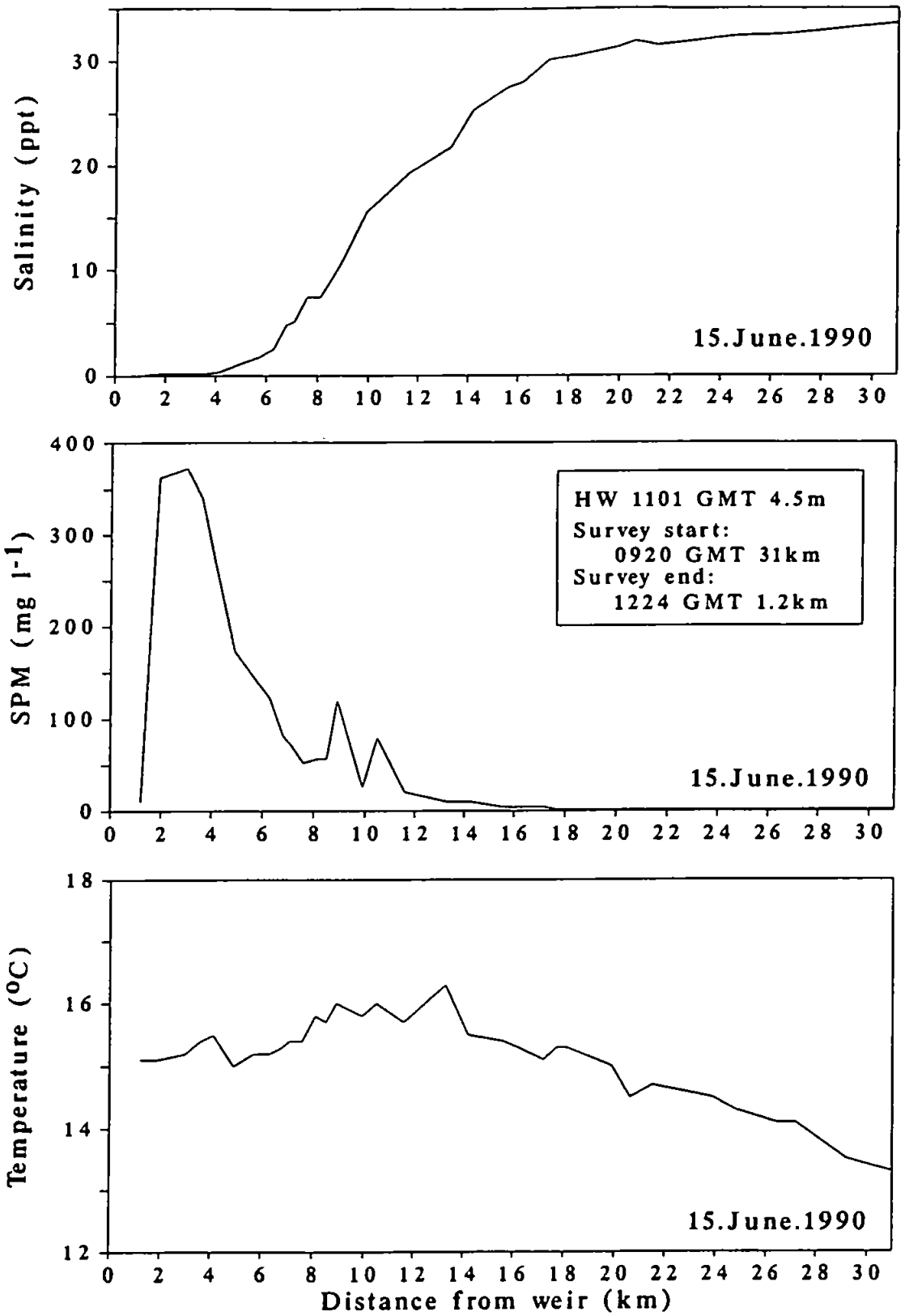

Figure 6.2 Axial survey of the Tamar Estuary on the 15th June HW-1 hr. 40 min. to HW+1 hr. 20 min.

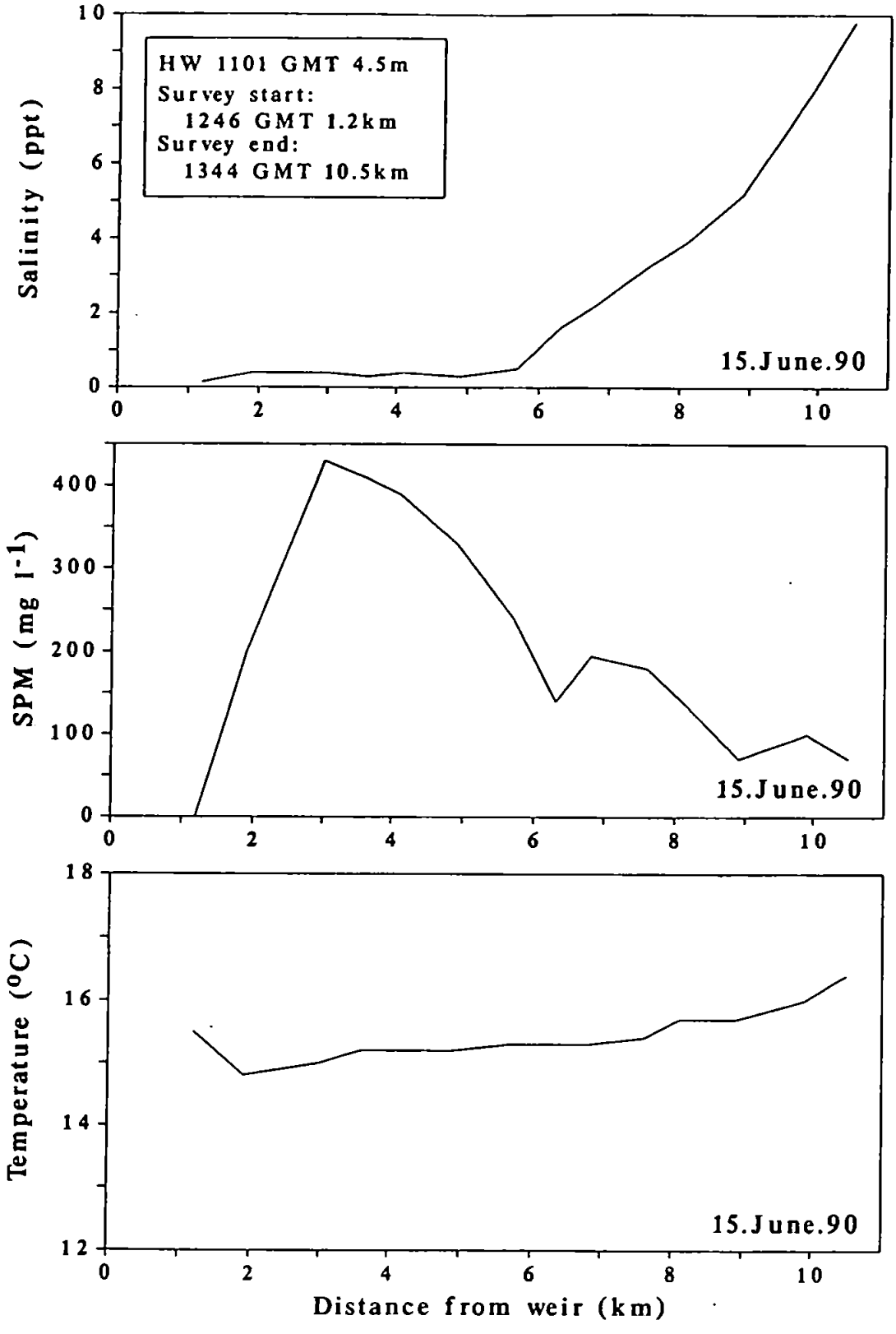

Figure 6.3 Axial survey of the Tamar Estuary on the 15th June HW+1 hr. 45 min. to HW+2 hr. 45 min..

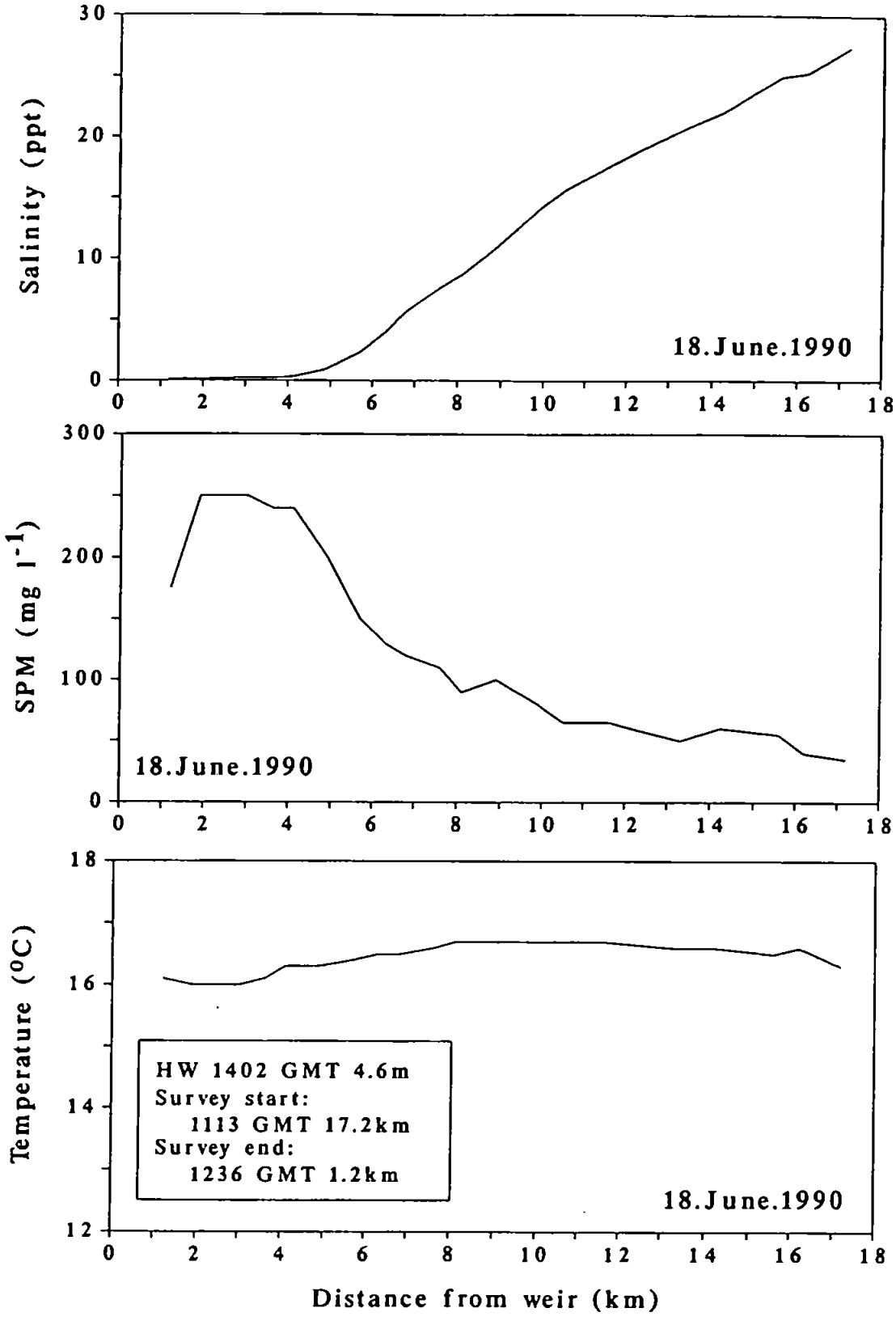

Figure 6.4 Axial survey of the Tamar Estuary on the 18th June HW-3 hr. to HW-1 hr. 30 min..

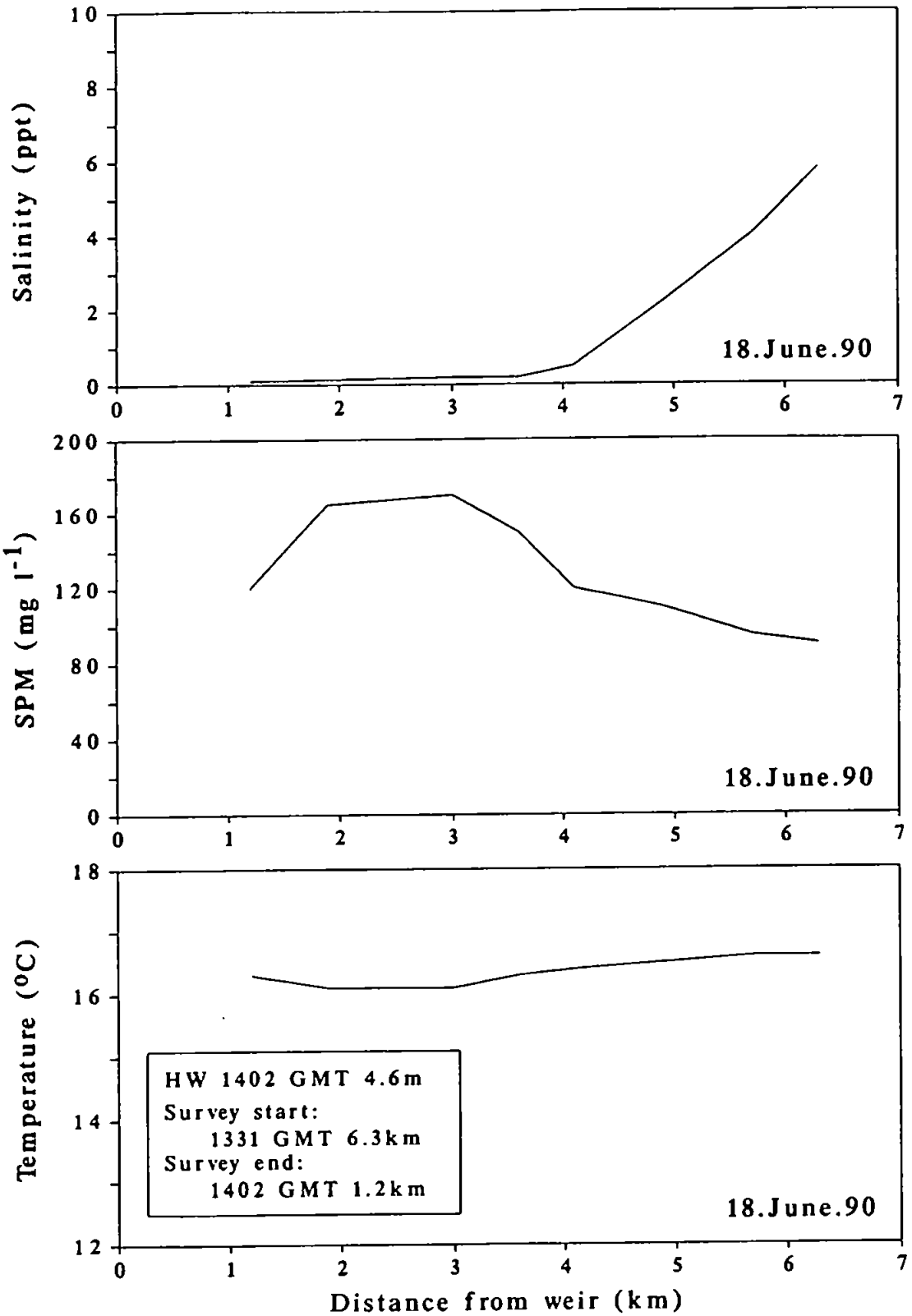

Figure 6.5 Axial survey of the Tamar Estuary on the 18th June HW-30 min. to HW.

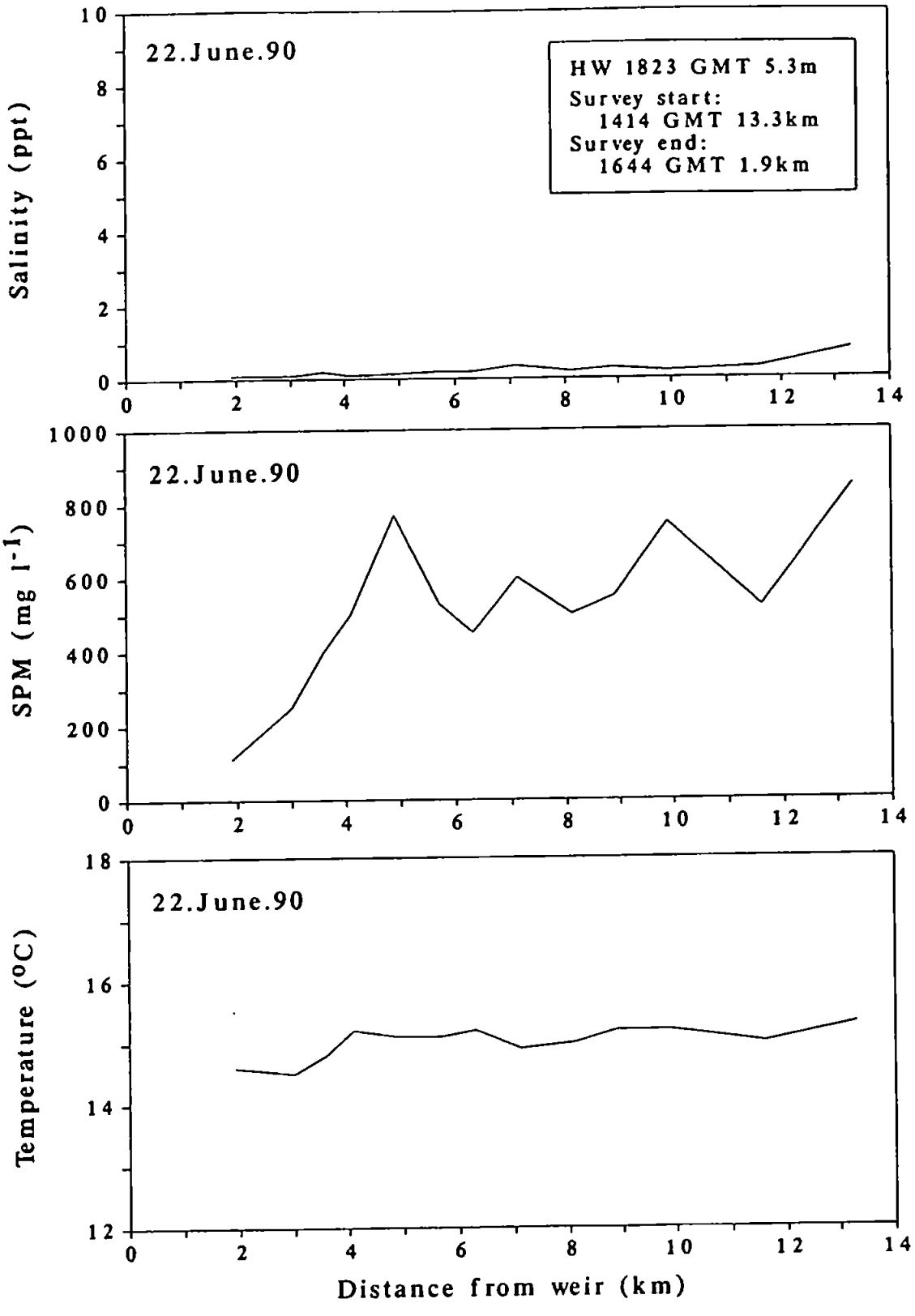

Figure 6.6 Axial survey of the Tamar Estuary on the 22nd June HW-4 hr. to HW-1 hr. 45 min..

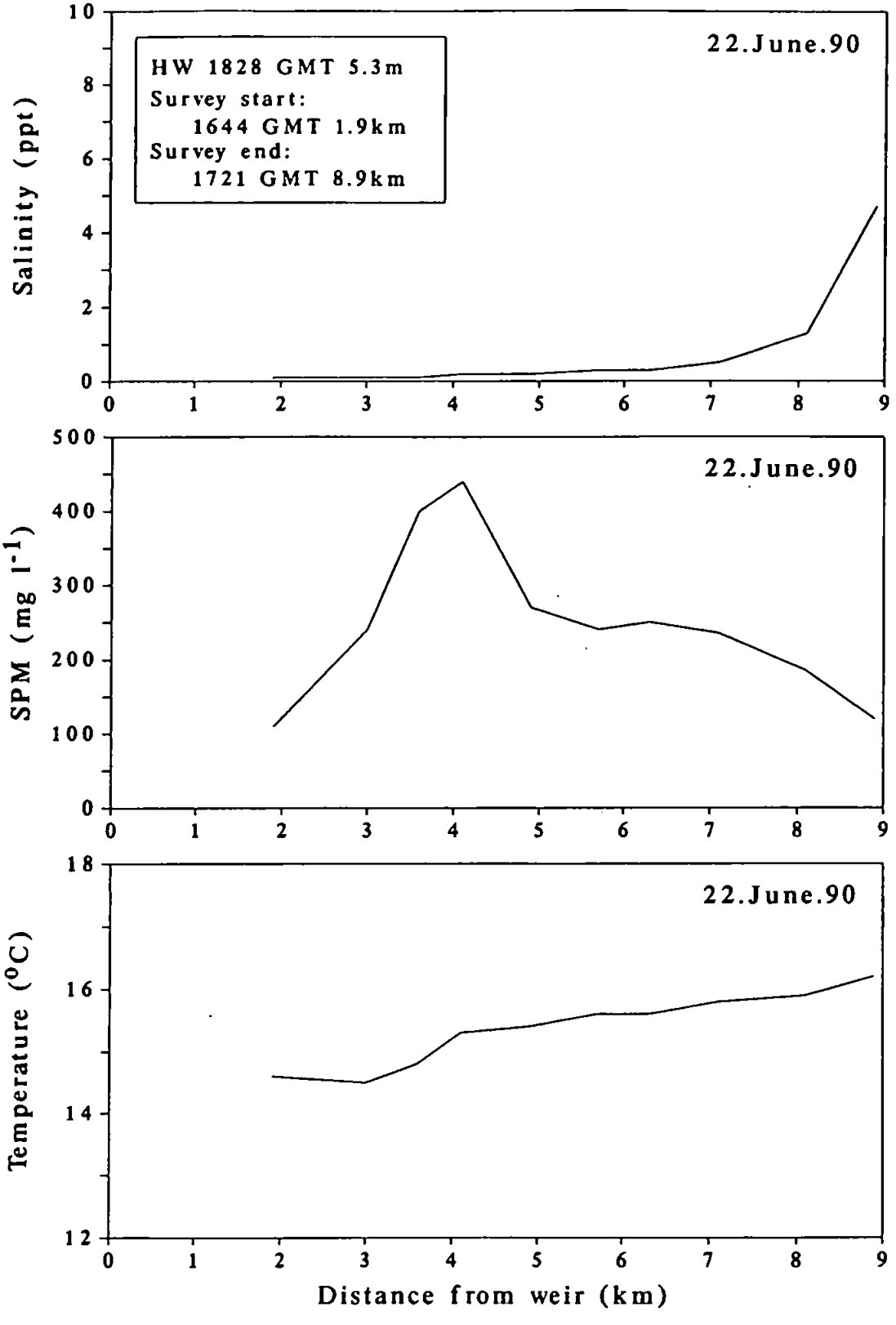

Figure 6.7 Axial survey of the Tamar Estuary on the 22nd June HW-1 hr. 45 min. to HW-1 hr.

extended period of slack water at ebb tide this variation may be due to variability across the width of the Estuary, and indicate that minimal settling occurred of the suspended sediment.

The peak concentration of the turbidity maximum on the 18th, the lowest neap tide and lowest tidal energy, at slack water was 180 mg l^{-1} and was comparatively lower than the 15th. In addition, the freshwater river discharge was the lowest for the month of June for the 2 days prior to the 18th decreasing the level of riverine suspended material in the upper estuary. The opposite was the case for the axial survey on the 22nd since the freshwater discharge from the river on the day of the survey was 6 times higher than the 15th and 18th and was the highest recorded discharge for June. The 22nd was close to the top of the spring tidal conditions, and the survey, carried out during flood tide, indicated high SPM concentrations due to increased erosion of the bed sediment. The SPM concentration decreased slightly towards slack water due to settling of suspended sediment in the upper estuary as noted by Uncles *et al.*, (1991a)

From the axial surveys the turbidity maximum SPM concentration was estimated to range from approximately 250-450 mg l^{-1} dependent on prevailing weather conditions and the freshwater discharge. The position of the turbidity maximum over a full tidal cycle was estimated to be between 2-10 km during the spring tidal conditions with the range of excursion being from a peak SPM concentration at high water slack between 2-4 km to peak SPM concentration at low water slack between 8-10 km. This agreed with previous studies carried out in the Tamar Estuary by Morris *et al.*, (1982b) and Uncles *et al.*,(1985). The salinity profiles indicated that there was little fluctuation within the upper 5-6 km of the Estuary, and there was little fluctuation in temperature within the upper estuary region.

The axial profiles enabled the position of the sampling sites and the equipment needed for the different sites to be determined. Six vessels were anchored within the range of migration of the turbidity maximum, and the positions were chosen on straight reaches of the estuary to enable detection of the longitudinal migration and minimsing cross-estuary variation whilst remaining logistically accessible and out of the main navigational channel for other vessels. The sites (Station 1-6) for the vessels are shown in Figure 6.1, positioned from 3.0 km to

8.5 km. The axial profile salinity data indicated that there was no need to have salinity equipment on the boats above Station 4 since there was no fluctuation in salinity. Temperature equipment was also not required since the axial profile data indicated a temperature fluctuation of 15.5 to 16°C between the upper and middle estuary (0-18 km from the weir).

The sampling frequency was based on the axial profiles and velocity data from previous hydrodynamic studies in the estuary. Park & James (1990) discuss a hydrodynamic survey in a partially stratified estuary to assess mass flux and mass transport mechanisms of salt and water, and suggest that a standard sampling rate is typically once every hour, but only a few studies have been conducted with sufficient spatial resolution to estimate longitudinal mass fluxes precisely. Since one of the main objectives of the tracing experiment was to establish the mass flux of tracer it was considered essential to have good spatial synoptic data with samples every 20 minutes.

6.3 TRACING EXPERIMENT

6.3.1 Introduction

The aim of the tracer experiment was to investigate sediment transport within the turbidity maximum during low summer freshwater discharge and spring tidal conditions in order to establish the particle retention within the maximum, excursion rate and investigate deposition, entrapment and erosion process. The study involved the injection of the fluorescent tracer, with similar properties to the suspended particulate material found in the turbidity maximum, and monitoring its advection and dispersion over an ebb-flood tidal cycle and subsequent spring-neap cycle. Measurements were carried out at six sample sites, between 3 and 8.5 km from the upper tidal limit (Figure 6.1).

6.3.2 Field Equipment and Setup

The main experimental fieldwork of the Tamar Estuary took place on the 26th June 1990. Six boats were moored in the positions predetermined by the axial studies (Figure 6.1) and each site was chosen to be on a straight section of the Estuary to minimise cross-sectional variation in circulation. The six moored vessels were supplemented with an additional boat, the Rotork Sea Truck, which traversed the Estuary in a supply and assistance capacity. This vessel undertook the tracer release at the location shown in Figure 6.1.

Each of the stationary sampling vessels were supplied with equipment to measure water depth, current velocities and salinity and a simple pump system to collect water samples for tracer and SPM (Plate 6.1). Supplementary to this, four of the boats had the added capacity of temperature measurement. Suspended sediment concentrations were measured later by gravimetric analysis, in the laboratory, of the water samples collected. The tracer particles were detected and counted per unit volume using AFC as described in Section 4.4.

The sampling equipment comprised a large flat disk weight attached to a rope with a current meter impeller 30 cm above. Immediately above the impeller was an inlet pipe for a small centrifugal bilge pump used to take water samples, and a T-S bridge (where appropriate). The sampling equipment was positioned so that the current meter was orientated approximately in the direction of main flow. The pump needed to be primed at all times.

The equipment used during the day varied due to availability and the limitation of space and water depth, particularly at stations 1 and 2. The equipment used on each vessel is outlined in Table 6.1.

Station No.	Position	Equipment Deployed
1	3.0 km	Pump, Braystoke current meter and impeller
2	3.7 km	Pump, Brystoke current meter and impeller
3	4.6 km	Pump, Braystoke current meter and impeller, MC-5 T/S Bridge
4	5.6 km	Pump, Braystoke current meter and impeller, MC-5 T/S Bridge
5	7.0 km	Pump, MC-5 T/S Bridge, NBA DNC-3 current meter
6	8.5 km	Pump, MC-5 T/S Bridge, NBA DNC-3 current meter
Tamaris		Axial Survey Pump, Partech SPM, MC-5 T/S Bridge & Tracer Release

Table 6.1: Equipment used on the 26th June 1990.

Additional data was also collected at Stations 3 and 5 using a logging instrument package similar to that described by Uncles *et al.*, (1989). The package comprised bottom-mounted sensors which monitored current, SPM concentration, salinity, conductivity, temperature and pressure (water depth) as functions of time at 0.25 m above the bed (Plate 6.2). The package was developed to study advective effects along the axis of the Estuary on a tidal cycle, and the spring-neap and seasonal variability, and was used during this study to provide additional data to correlate with the vertical profile and synoptic data from the fixed stations. The package was deployed to provide data over a spring-neap tide period to enable extrapolation of the detailed synoptic data. The sampling frequency was every 5 minutes and the sensors logged data for 5 days prior to the tracing study and for a subsequent 7 days after the study.

Plate 6.1 The tracer particle sampling pump system used on the Tamar Estuary.

Plate 6.2 Deployment of the bottom-mounted logging instrument package at Station 3 on the Tamar Estuary.

6.3.3 Field sampling methodology

The sampling procedure commenced at 10.20 BST and finished at 20.40 enabling synoptic data collection over approximately a 10.5 hour period during peak ebb and flood tides. The sampling frequency was 20 minutes at each sampling station. Sampling and measurement took place at three depths (when water depth allowed) by raising and lowering the sampling equipment on the rope using depth graduations every 20 cm. The bottom sample was taken 35 cm above the sediment bed by lowering the weight to the bed sediment and then raising it 5 cm. This was to ensure that uniform sampling took place even with different operators and that the weight did not sink into the sediment bed causing variations in readings and high turbidities. Water depth, salinity, direction of current flow and velocity averaged over 1 minute at each depth were measured during the sampling period. Current velocity data was not measured at Stations 1-4 at low water due to the shallow water depth, and also for this reason only one water sample was collected. The suspended solids and tracer concentration data was determined later in the laboratory.

The injection of tracer particles took place within the turbidity maximum region between approximately 09.45 and 10.00 during high-water slack of the spring tide. The time of high water at the head of the Estuary was approximately 09.30. The tracer release point was determined by a surface water axial profile, as described in section 6.3.2, from 5 km to 1 km from the freshwater weir in order to establish the location of the turbidity maximum (Figure 6.1). The maximum was located between 1.9-2.3 km from the weir.

The fluorescent tracer particles were mixed with estuarine water over a 30 minute period to enable equilibration of temperature, salinity and therefore density, in addition to surface charge (Plate 6.3). The mass of tracer injected comprised 44.5 kg mixed in a 1300 l estuarine mud, water and tracer slurry; approximately 6.3×10^{15} tracer particles were added creating a visible orange plume (Plate 6.4). The tracer injection boat was thoroughly washed within the tracer release area to remove any tracer contamination before returning down the estuary.

Plate 6.3 The tracer particles being mixed on the Tamar prior to injection.

Plate 6.4 The Plume of tracer in the turbidity maximum of the Tamar Estuary immediately after injection.

On the day following the main experimental fieldwork (27/06/90) and one week later (03/07/90) axial surveys of the surface waters were carried out to collect discrete water samples along the Estuary in order to determine the distribution of tracer concentration relative to the location of the saline intrusion and the turbidity maximum. The sensor system and parameters measured were the same as for the axial surveys conducted on the 15th, 18th and 22nd.

The freshwater daily mean flow river discharge for the period 1st June to 20th June ranged between 1.85-3.15 $m^3 s^{-1}$, but rainfall on the 21st and 22nd June led to an increase in discharge on the 22nd to 10.3 $m^3 s^{-1}$ which then decreased to 3.85 $m^3 s^{-1}$ on the 26th and 27th of June which was normal for the month (Bale *et al.*, 1985).

6.4 RESULTS - INSTANTANEOUS SYNOPTIC DATA

6.4.1 Salinity

Salinity data, shown in Figure 6.8, was not measured at Stations 1-3 since the preliminary surveys indicated no fluctuation in salinity in this section of the estuary. Station 4 showed only minimal variation from 0.5-1.4 ppt through the tidal cycle with no stratification measured between surface and bottom suggesting that the shallow water depth, which rose to a maximum at high water of 4.5m, was well mixed. At Station 5 a higher level of vertical stratification was measured during high water with a salinity range from 1.5 to 5.5 ppt from surface to bottom respectively. A similar stratification pattern was observed at Station 6 with surface to bottom salinities ranging from 5.5 to 12 ppt. The stratification is present at high water at both Station 5 and 6, but commences to breakdown after 11.00, approximately 1.5 hours after high water and the stratification has completely decayed by 12.00. These observations agree very closely with data presented by Barton (1992).

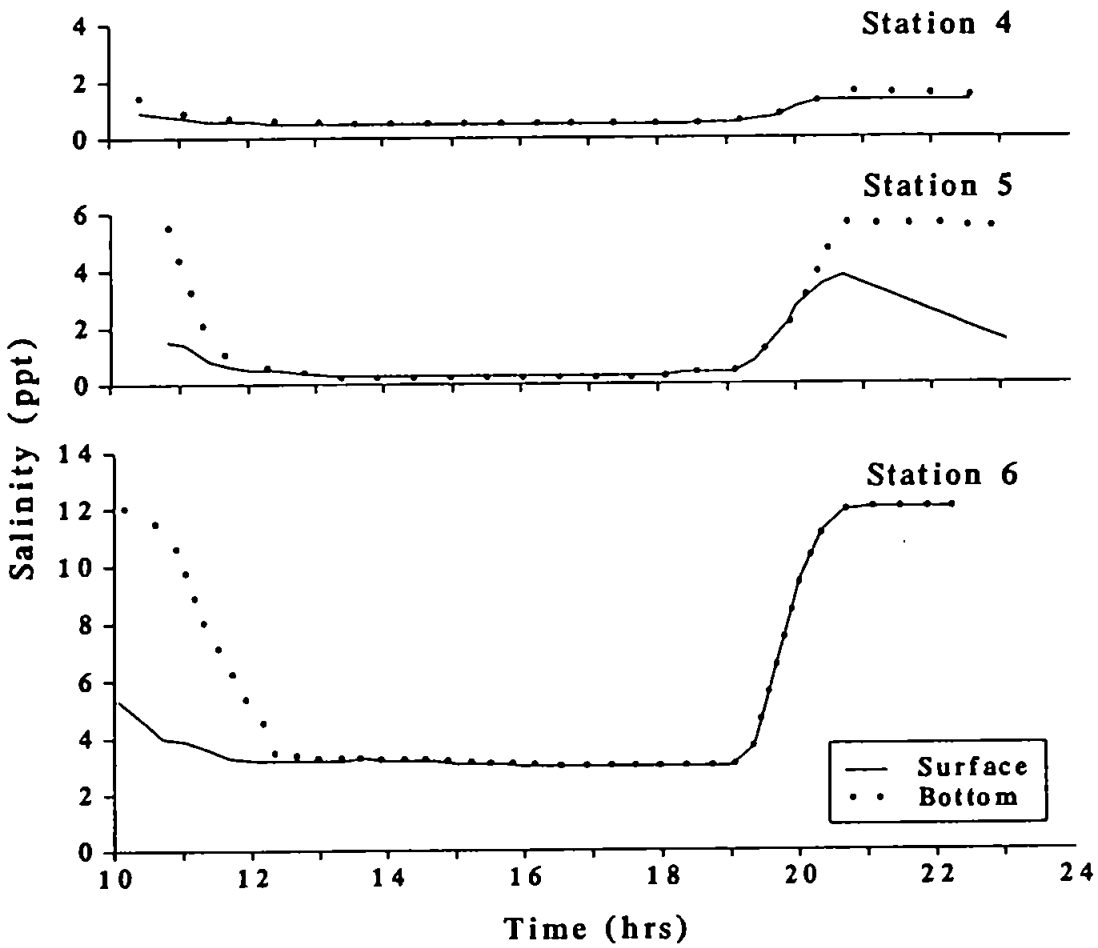

Figure 6.8 Instantaneous synoptic salinity data from Stations 4-6 on the 26th June.

On the flood tide there was no stratification observed at Station 4 and 6 as expected due to the vertically well-mixed nature of flood tides (Darbyshire & West, 1991; Barton, 1992) however at Station 5 during the first two hours after low water a well-mixed water column becomes stratified and remains so for the remainder of the flood tide with surface salinity decreasing to less than 2 ppt. This was possibly due to the reversal of the flood tide in the surface waters. The current direction does show variation of between 20-30° during this period indicating that any reversal is localised. The well-mixed water column seen at Station 4 and 6 maintained well into the slack high water period with stratification forming from high water.

6.4.2 Current Velocity

The synoptic current velocity data is shown in Figure 6.9. There are two clear maxima of current velocity for the ebb and flood tides. Surface current velocities were generally higher than bottom current velocities at all stations due to riverine water close to the surface enhancing the surface current velocity, and sediment bed frictional effects reducing bottom currents. Ebb current velocities were consistently lower than the flood current velocities with peaks of 0.8 m s^{-1} on the ebb tide and between 1.0-1.2 m s^{-1} on the flood tide.

The ebb tide commenced approximately 1 hour after high water, however relatively low ebb velocities were measured for the first two hours with a small maximum at 11.00 at all Stations followed by a decrease in velocity until 12.00. This observation coincides with the salinity stratification breakdown described in Section 6.4.1 and was due to a density-driven up-estuary current close to the sediment bed which opposed the ebbing tide and which formed as a result of very strong vertical salinity stratification during the early ebb tide (Barton, 1992) and the effects of tidal asymmetry. The existence of an up-estuary flow may have also enhanced the current velocities at the bed.

The current velocity begins to increase dramatically after the complete decay of stratification at 12.00 and increases at all Stations to a second and larger maximum occurring between 13.00-14.00 at HW+4-5. Station 4 exhibits a further maximum due to the position of the boat being out of the mainstream channel during the ebb tide (pers. comm boat Skipper) and indicating that the channel cross-secton at that station was decreasing significantly in response to the slow fall in water level as low-water slack approached. This further supports the significance of the up-estuary current proposed by Barton (1992) and the breakdown of the salt intrusion (McCabe *et al.*, 1992) on the current velocity and observations by both that the ebb tide current velocities decrease for a short period followed by a rapid acceleration after stratification breakdown. This rapid increase is enhanced by the up-estuary, density driven flow disappearing with the salinity breakdown.. During low tide conditions the shallow water depth enabled only one flow reading at Stations 1 to 3 which indicate a reasonably constant riverine flow from 15.00 onward.

Low water was particularly brief as shown by the decrease in ebb currents and the subsequent rapid increase in flood current velocity at Stations 5 and 6. The frequency of sampling however, every 20 minutes, did not pick up the tidal change in direction and velocity at all Stations, most notably Station 3. The commencement of the flood tide, at 15.20 approximately 8 hours after high water, indicates that the water column was vertically well-mixed as noted by Uncles *et al.*, (1991) and Darbyshire & West (1991) although surface current velocities are slightly higher at most Stations indicating some stratification however, as Barton (1992) suggests that single-point measurement can be influenced by vertical stratification whereas depth-mean values can indicate a different result. The main tidal surge occurred between 17.20 at Station 6 to 18.20 at Station 1, which is a distance of 5.5 km indicating an average tidal propogation velocity of 1.53 m s^{-1}. The peak flood velocities occur approximately 40-60 minutes after the flood tide change. The depth-averaged instantaneous current velocity data is described by Uncles *et al.*, (1991b) in more detail.

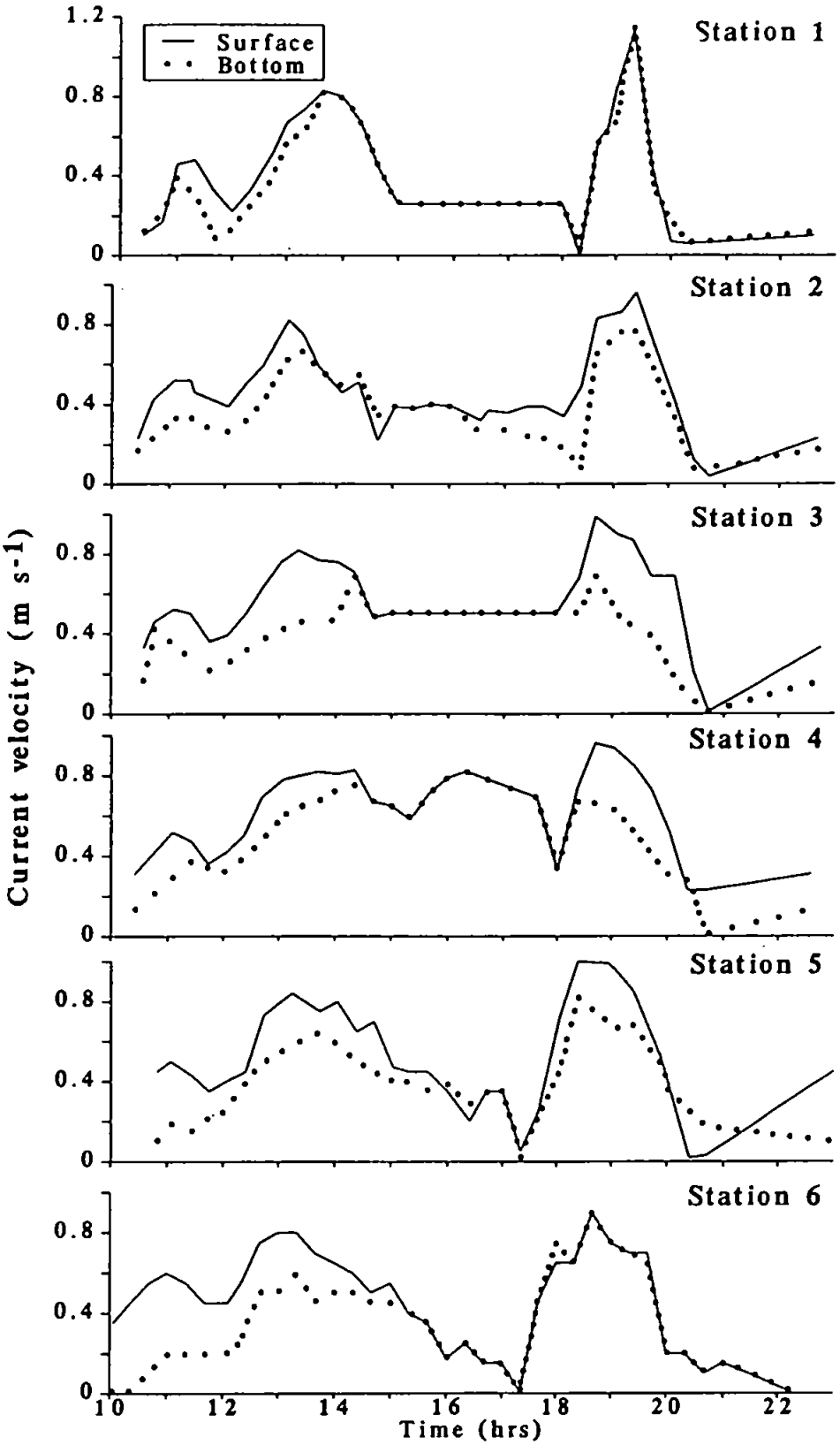

Figure 6.9 Instantaneous synoptic current velocity data from Stations 1-6 on the 26th June.

6.4.3 SPM

The synoptic turbidity data is shown in Figure 6.10. The turbidities on the flood tide were generally higher than the ebb, and higher at the bottom of the water column than at the surface. The data indicated a poor correlation between ebb current and suspended load for Stations 1-3 possibly due to prolonged slack conditions at high water which led to settling and consolidation of the SPM. There was a good correlation for Stations 5 and 6 with an observed lag of between 1.5 to 3 hours before an increase or maxima in current velocity led to an increase or maxima in turbidity. The lag on the flood tide was generally shorter with a range of 1.5 to 2.5 hours. This was due to higher flood velocities leading to a higher critical erosion shear stress and the existence of a mobile stock of sediment deposited during the short period of slack water which led to an availability of fine sediment for resuspension.

The maxima of turbidity on the ebb tide ranged from 9 g l^{-1} at Station 3 to 1.5 g l^{-1} at Station 6. The maxima at Stations 1 to 3 around 15.00 were due to the shallow water during low tidal conditions and the dominant riverine flow. The maxima of turbidity on the flood tide ranged from 26 g l^{-1} at Station 3, categorised as fluid mud, to 1.5 g l^{-1} at Station 6 on the flood tide. Clearly high levels of resuspension took place during the flood tide, but since the peak turbidities did not correlate at adjacent stations as the flood tide develops this suggests that the resuspension of mud only occurred within the local environs of each station. The measured high concentrations were therefore a result of localised shear stress in response to local current velocities. This agrees with measurements made by McCabe *et al.*, (1992) where flood tides resuspend any large flocs which settled out during the ebb and during spring tides primary particles were eroded from the bed to form the bulk of flocs.

These measurements would appear to suggest that localised resuspension is a significant process in the formation and magnitude of a turbidity maximum relative to tidal pumping of sediment. A net up-estuary migration of sediment may take place, but this data would suggest that the process may well be lengthy and possibly only occurring during spring flood tidal activity (Uncles & Stephens 1989, Barton *et al.*, 1991 and Uncles *et al.*, 1991b).

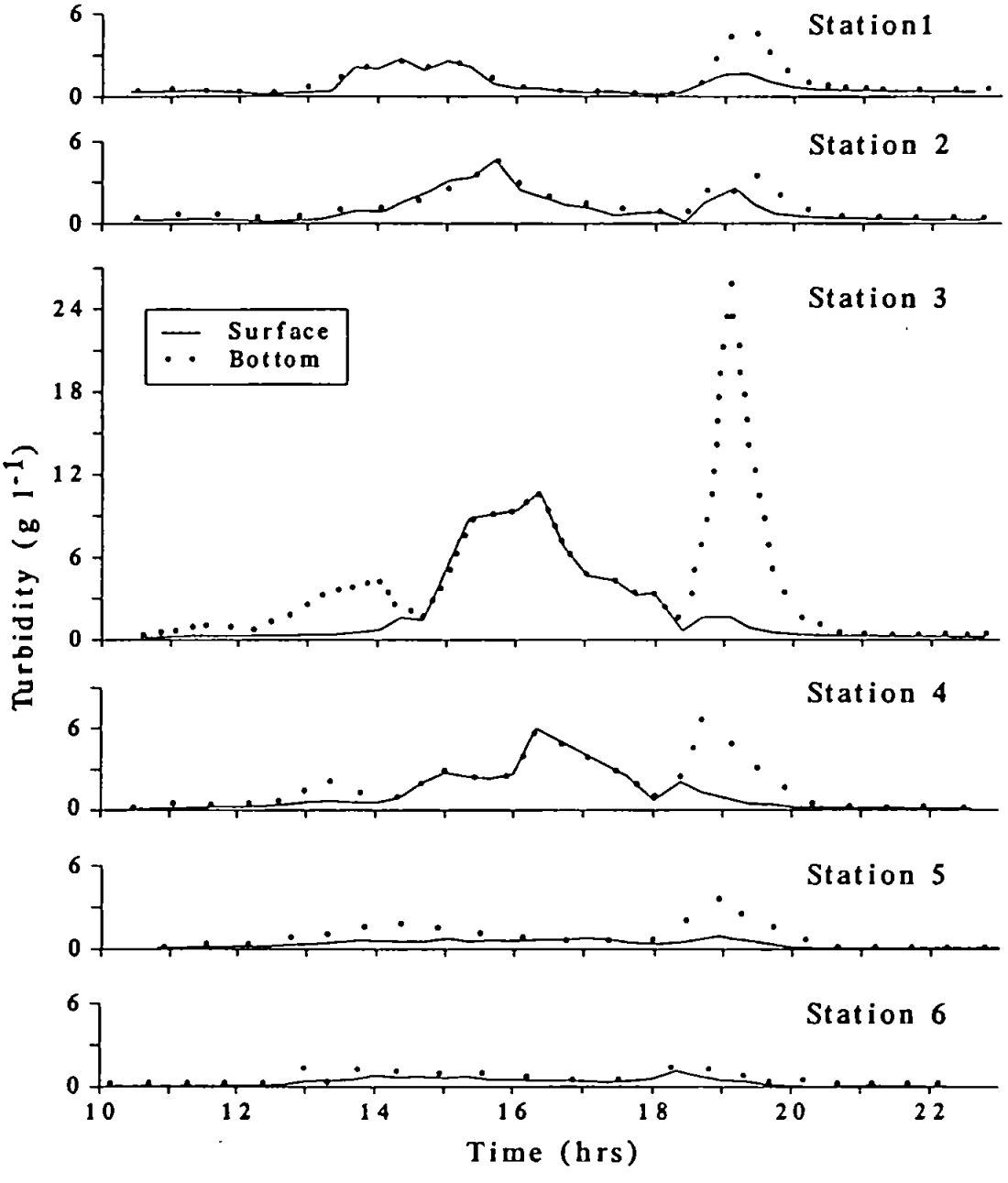

Figure 6.10 Instantaneous synoptic data from Stations 1-6 on the 26th June.

McCabe *et al.*, (1992) indicated that two size populations of flocs occurred in the turbidity maximum even in energetic spring tide conditions with small flocs transported up and down the estuary on the tide and larger flocs which were deposited and hence undergo a more localised resuspension-deposition cycle with small scale transport. The high SPM measurements caused by local resuspension activity during this study may therefore mask any transport of small flocs which occurred with the advection of the saline intrusion and the migration of the turbidity maximum.

The data indicate that some settling of suspended sediment does take place during slack water with SPM concentrations decreasing to between 0.3-0.6 g l^{-1} during low water and between 0.05-0.4 g l^{-1} during high water. Uncles *et al.*, (1991b) notes that flood currents decelerated slowly after maximum speed, and an extended period of slow currents begins around high water leading to a tendency for water laden with suspended particulate to deposit particles on the sediment bed at the high water position. The concentration of suspended sediment remaining in the water column at slack water confirms the existence of two size populations, one which does not settle out, and a population which does settle out when the velocities decrease below approximately 0.2 m s^{-1} although the size spectra and settling velocity will be dynamic dependant on tidal state.

The SPM measurements indicated a difference between surface and bottom concentration and between stations. The data showed a surface turbidity maximum migrated down-estuary with the ebb tide and back up-estuary with the flood tide which agreed with the axial profiles and a bottom maxima of turbidity behaved quite differently. The surface turbidity maximum was often associated with the freshwater-saline interface, whereas the bottom turbidity maximum remained within the centre of the surface turbidity location around Station 3 which further supports the existence of a dual floc population.

The bottom turbidity maximum, within the central section of the upper estuary, may be fed during the ebb tide by upper estuary resuspension and density driven up-estuary currents due

to vertical stratification. As the ebb tide current velocities decrease close to low water the suspended sediment settles out leading to net sedimentation in the region. During the flood tide the recently settled sediment is resuspended, and the high concentration is therefore due to localised tidal resuspension with no significant net transport due to a resultant increase in flocculation and settling of the suspended sediment back to the bed. This agrees with the schematic representation of resuspendable sediment mobility described by Morris *et al.*, (1986), although the summer accumulating shoal shown is spread over a larger area (10 km) than this data would suggest. This data shows that during this study the central region around Station 3 was the main, even if temporary, storage area for the mobile stock of fine sediment associated with the surface turbidity maximum.

Uncles *et al.*, (1991a) provide detailed interpretation of the depth averaged instantaneous SPM data. Uncles *et al.*, note that the near-bed sensor instrumentation deployed prior to the tracing experiment confirmed the synoptic data measured at the six Stations. Peak flood conditions for current and SPM exceeded peak ebb conditions. The sensor package also detected a double-peak for flood SPM levels; the first peak was associated with the maximum flood current speed surging up-estuary and the second with the passage of the freshwater-saline interface. High SPM levels in the mid upper estuary which agreed with the synoptic data supported the accumulation of stock sediment in the vicinity of Station 3.

6.4.4 Tracer Particles

Figure 6.11 shows the tracer concentrations at surface and bottom as a time-series for the ebb-flood tidal cycle. The tracer particle/estuarine water slurry was introduced at the start of the ebb tide at approximately 10.00. The tracer particles were advected down-estuary on the ebb tide as a very pronounced peak through each of the stations. Generally on the ebb tide the tracer was measured at the surface before the bottom samples, but the bottom samples, particularly at Stations 1, 3, 5 and 6 had higher tracer concentrations than at the surface. This suggests that the surface currents were flowing faster than the bottom and that tracer particles settled out during the overall transport down-estuary, agreeing with observations by

Uncles et al., (1987) and Stephens et al., (1992).

At Station 1 the tracer was detected at the surface (time 10.40) before the bottom (time 11.00) indicating higher surface than bed level current velocities and the existence of horizontal stratification in the upper estuary at this stage of the ebb tide. The peak of tracer was detected at Station 1 at 11.20 . This coincided with a peak in current velocity, which was followed by a decrease in velocity until 12.00. This may have led to a rapid decline in the tracer concentration due to settling on the bed. At Station 2 the tracer also arrived at the surface (time 11.20) before the bottom (time 11.40). Stations 3-6 indicate the tracer arrived at the surface and bottom at the same time, so far as the frequency of sampling indicates, highlighting the breakdown of stratification and a well mixed water column. The low tracer concentrations at Station 4 indicated the sampling vessel was out of the mainstream flow and highlighted cross-estuarine variability.

The leading edge of the tracer particles arrived at Station 6 at approximately 14.00 when the current velocity was 0.6 m s^{-1} and the trailing edge passed at 16.00 when the current velocity was 0.2 m s^{-1}. Based on the current velocities measured at Station 6 the advection of tracer particles would have continued for approximately 3.6 km beyond Station 6. The mobile vessel detected high concentrations of tracer 3.1 km down-estuary of Station 6 (a total migration of 11.1 km from the release site) immediately after slack water. Slack low water occurred at approximately 15.20 at Station 6 and tracer particles were measured within 20 minutes after slack water with a tracer concentration peak in less than 1 hour suggesting that tracer must have settled out on the sediment bed down-estuary of Station 6 approaching slack low water.

The tracer peaks returned up-estuary on the flood tide to the vicinity of the original injection site although the peaks were less pronounced. At Stations 1,3,4 and 5 the bottom samples measured higher tracer concentration. This was due to the erosion of tracer deposited on the sediment bed during the ebb tide or slack water. This was confirmed by the tracer particles measured at Station 1 and 6 where tracer particles were detected before the anticipated

return of the advected tracer peak since at Station 6 tracer advected down-estuary long before slack low water, but tracer was measured immediately the tide turned. At Station 1 tracer was detected at 17.40, only 20 minutes after the commencement of the flood tide at Station 6 indicating immediate resuspension of tracer from the sediment bed. Tracer arrived at Station 3 and 2 at 1900 and 19.40, respectively.

Figure 6.11 also shows the spread of tracer at each Station between the leading and trailing edges of the plume. The results show that the spread was generally lower during the ebb tide than the flood tide and the spread increased from Station 1 to 6 on the ebb tide and from Station 6 to 1 on the flood tide. The spread on the flood tide became large at Stations 2 to 4 and spanned approximately 3.5 hours and the spread at Station 1 spanned over 5 hours. However, despite deposition and subsequent erosion of tracer from the bed the concentration of tracer at Station 1 remained low (less than 1000 particles per ml) until 19.00 indicating a continuous erosion of bed sediment and tracer for 80 minutes.

At the start of the flood tide there was a strong correlation between the increase in turbidity and tracer concentration measured. At Station 6 the turbidity concentration increased simultaneously with the tracer resuspension at 18.20 which coincided with the start of the flood tide suggesting that the tracer was part of a stock which had been recently deposited during slack high water and was eroded by the flood tide. Figure 6.10 indicated that SPM concentrations were dominated by localised resuspension at Stations whereas Figure 6.11 indicated that the movement of tracer was dominated by tidal advection implying that the tracer did not behave similarly to SPM. However as discussed in Section 6.4.3 the high SPM concentrations measured may well have masked the tidal advection of a small floc size population on the ebb and flood tide. The tracer concentration measured visibly decreased over time from Station 1 to 6 on the ebb tide and then on the flood tide from Station 6 to 1. This suggested that large quantities of tracer was deposited on the bed possibly indicating the tracer was both behaving like the larger flocs and undergoing deposition and erosion primarily in the upper estuary and a secondary size fraction was tidally advected.

6.4.5 Axial survey 27th June

An axial survey of the surface water, as described in Section 6.4.3, was carried out the following day (27/06/91). The results, given in Figure 6.12, indicated a large peak of tracer particles situated 5 km downstream of the weir at a salinity of approximately 0.5 ppt and slightly down-estuary of the turbidity maximum. The tracer having undergone 2 tidal cycles, had formed a more stable association with the natural suspended fine sediment. The tracer particles had also travelled further up-estuary than the original release site. This indicated that an up-estuary residual transport of tracer particles had occurred.

6.4.6 Axial survey 3rd July

A further axial survey was carried out one week later (03/07/91). The surface waters were again sampled, this time during neap tidal conditions. The tidal range was only 2.3 m and because of the slower tidal currents the turbidity maximum SPM concentrations increased to 270 mg l^{-1} (Figure 6.13) as compared with 700 mg l^{-1} on the 27th June. The tracer particles were closely associated with the turbidity maximum and had a well-defined peak in the same position as the SPM peak. Both peaks were clearly associated with the head of the saline intrusion at approximately 4 km downstream of the weir. Uncles *et al.* (1991), notes that the residual transport of suspended sediment at neap tides is generally directed down-estuary and decreases in magnitude away from the head. Therefore sediment derived from the freshwater input was being deposited within the estuary.

6.4.7 Summary of the synoptic tracer data

Tracer particles were found to advect with the tidal currents and remained in the upper estuary primarily associated with the saline intrusion. Some particles were deposited on the inter-tidal mudflats in the upper reaches during the ebb tide and in the lower reaches at slack water with resuspension taking place on the flood tide. The freshwater residence time of the

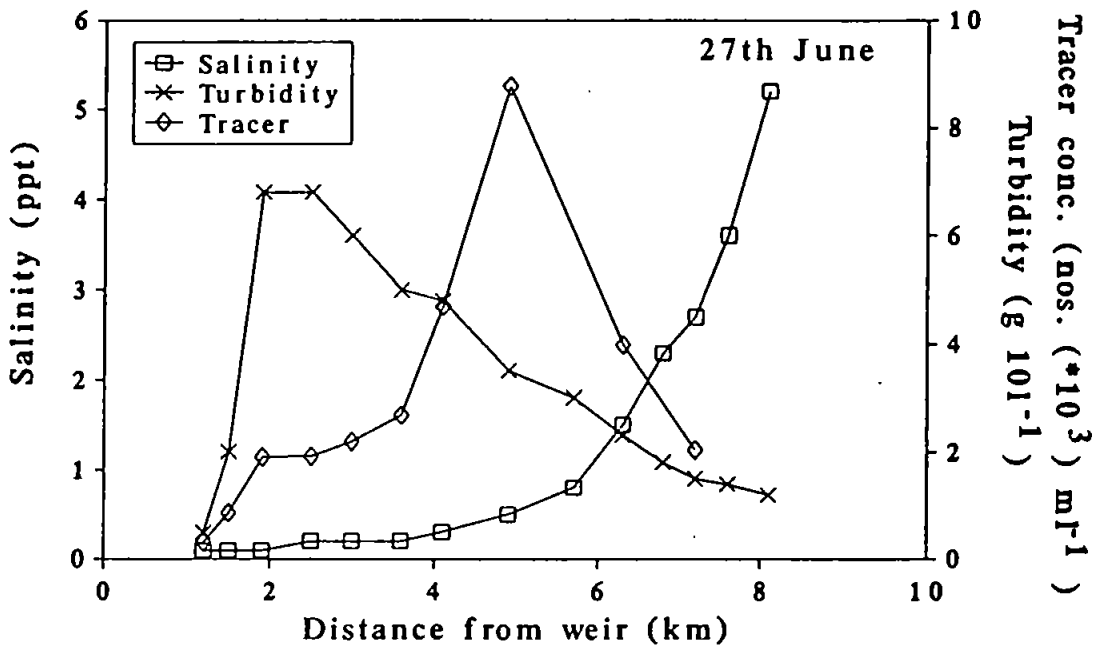

Figure 6.12 Axial survey of the Tamar Estuary on the 27th June.

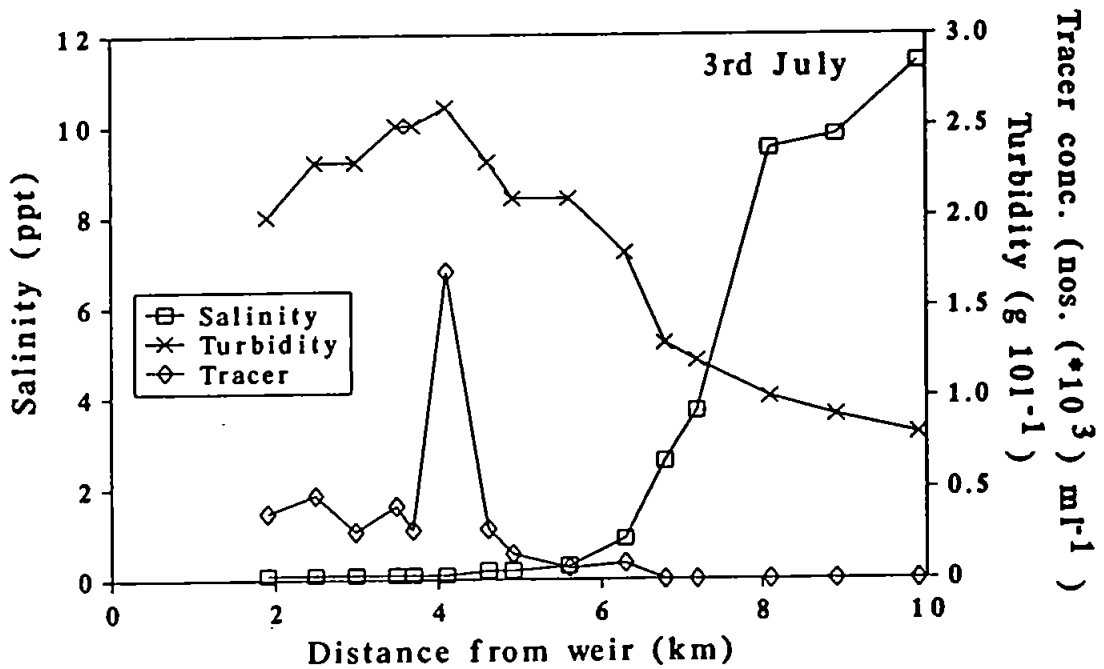

Figure 6.13 Axial survey of the Tamar Estuary on the 3rd July.

upper estuary and the turbidity maximum is approximately between 1-3 weeks during low runoff river conditions (Uncles *et al.*, 1983). The tracer was detectable during the neap tide one week after the initial injection when, despite low rates of resuspension of bed sediment. This data indicated that the tracer particles had possibly become associated with the turbidity maximum and therefore the residence time could be substantially longer ranging from weeks to years (Bale *et al.*, 1985; Dyer, 1989).

6.5 DATA INTERPRETATION AND ANALYSIS

6.5.1 Introduction

In order to evaluate the instantaneous synoptic data to determine whether tracer did behave in a similar way to SPM and to establish the source of sediment, the cycle of deposition and resuspension and particle residence time within the turbidity maximum it was necessary to interpret and analyse the data. Depth-averaged and tidally averaged data is presented in order to assess the residual movement of the tracer and sediment both spatially and temporally. There are two possible processes for the movement of the tracer which are tidal advection with the migration of the saline intrusion or deposition-resuspension on a more localised scale. The data presented in Section 6.4 indicated that the tracer was advected down estuary and did undergo localised deposition on the ebb tide and resuspension on the flood tide. It is therefore necessary to quantify the magnitude of each process.

6.5.2 Advection of tracer with salinity

6.5.2.1 Measured against predicted advection results

Figure 6.14 provides a visual interpretation of the depth-averaged observed arrival and leaving time of the tracer at each station, referred to as leading and trailing edge respectively, over the tidal cycle. The predicted times are also shown which were calculated from the depth averaged current velocity and averaged between two stations and weighted for the

proximity to each station. No calculated data is available for Station 1 on the ebb tide and Station 6 on the flood tide due to the lack of current velocity data immediately preceding each station.

In all cases on the ebb tide the observed time span of the pulse (ie from the leading to the trailing edge) was longer than the predicted measurement from the current velocity due to extension of the trailing edge since the observed leading edge agreed closely with the predicted. The pulse span increased from approximately 1hr 40 minutes at Station 1 to 2 hours at Station 6 due to turbulent mixing. At all Stations on the ebb tide, excluding Station 3, the leading edge for the observed was generally very close to the predicted. At Station 3 the tracer was measured significantly in front of the calculated by approximately 30 minutes.

This observed speeding up was due to the current velocity measurements indicating a decrease (Figure 6.9) to a minimum, occurring at 12.00, when the tracer actually arrived at Station 3. This suggests that the tracer in suspension continued to be advected at the same rate and the current velocity point measurements were not indicative of the mean velocity. This may be because of secondary flows around the bends in the estuary between Station 2 and 3 (Figure 6.1) with the current velocity speeding up around the bends on the outside advecting the tracer much more quickly. The predicted data was based on the current velocities measured at Station 2 and 3 which are both in a straight section of the estuary where secondary flows would be less dominant due to the estuary being relatively well-mixed compared with the waters around a bend. In addition if settling of tracer took place at the leading edge of the pulse between Station 1 and 2, possibly because of the mid-estuary island, obstacles, disused boat quays, decreasing current velocity all setting up secondary flows and creating turbulent mixing, this would lead to a delayed arrival of tracer at Station 2 which would in turn lead to a predicted delay in the arrival of tracer at Station 3. If the mean current velocity was maintained and a decrease was in fact localised then this would further enhance the difference between the predicted and observed tracer arrival at Station 3.

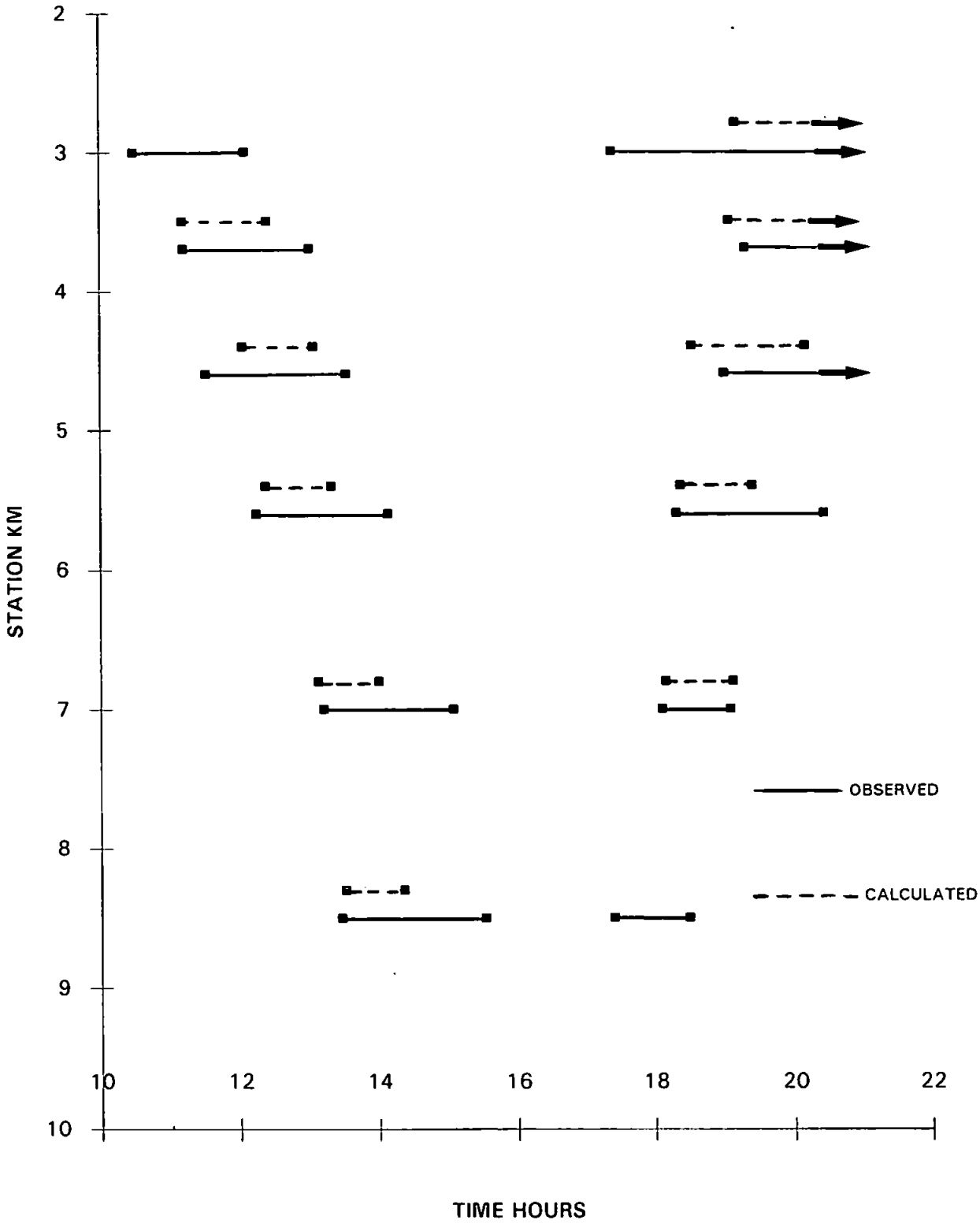

Figure 6.14 The observed and calculated longitudinal tidal advection over the ebb and flood tidal cycle on the 26th June.

The indication of the tracer being observed to arrive at each Station as predicted indicated that the transport processes were advective with a good correlation between current velocity and transport of tracer. The delay in the trailing edge and the extension of the pulse span indicated either that diffusion of the tracer took place or that settling and resuspension of the tracer occurred during the flux of tracer material due to secondary processes where localised horizontal and vertical variations in current velocity, turbulence, flocculation and shear stress led to differences in the actual movement of the tracer.

The good correlation between the leading edge for the observed and predicted indicated that the current velocity measurements taken were a good indicator for the actual tracer advection. The extension of the trailing edge would be due to tracer in the leading edge or front of the pulse being affected by secondary flows including eddies, variations across a channel with speeding up around a bend on the outer edge and slowing on the inner edge and tracer being trapped in the lee of obstacles. As a result of this secondary flow the tracer may have settled out and been resuspended then re-joining the main flow once more. In addition turbulent mixing would cause a widening of the plume, with time, as the tracer pulse advected down the estuary.

At the commencement of the flood tide the observed pulse is substantially shorter at Station 6 than at the end of the ebb with an overall length of approximately 1 hour. This is due to the increased flow velocities during the flood tide resuspending material deposited around slack low water confirmed by the good correlation between turbidity and tracer concentration. The predicted against observed data indicates a close correlation at Station 5 for both the leading and trailing edge, but above Station 5 there is considerable variation. The observed against calculated data indicates a substantial extension of the pulse towards the trailing edge at Station 4. This was possibly due to tracer undergoing a series of deposition and resuspension cycles primarily due to a decreasing of the current velocity as the flood tide progresses and indicating that vertical and horizontal fluctuations in current velocity occurred enhanced by the position of Station 4 out of the mainstream.

The span of pulse decreases slightly for Station 2 and 3 due to the decreasing current velocity; interestingly the observed data places the pulse ahead of the observed at both Stations. This again is due to the fluctuations in secodnary flows and the instantaneous current velocity data measurements. The observed trailing edge of tracer was never detected at Stations 1 to 3 due to the rapid decrease in current velocity and subsequent settling of tracer.

At Station 1 the leading edge was clearly ahead of the calculated advected tracer plume by approximately 1 hour and 40 minutes. This indicated erosion of tracer from the sediment bed due to increased current velocity associated with the tidal wave propogation which travelled up the estuary at the turn of the flood tide. The tracer was deposited during slack high water. The tide was estimated to have turned at Station 1 between 18.20 and 18.40 although the shallow water prevented a current direction being taken until 18.40, however tracer was detected at 17.40 indicating erosion during the very end of what would be considered to be the ebb tide.

The resuspension must therefore be a result of the advancing flood tide which actually commenced before measurement could take place or due to a change in turbulence and bed shear stress from the down-estuary riverine flow immediately prior to the flood tide starting. This data supports the idea that instantaneous current velocities are not very representative as discussed by Barton (1992). An additional consideration is an observation by Stephens *et al.*, (1992) that the critical erosion shear stress of bed sediments increases progressing down-estuary possibly indicating that this region of the estuary is more susceptible to erosion.

The data discussed indicates that the residual depth-averaged tracer was advected down and up-estuary with close correlation to the tidal cycle in the estuary and the saline intrusion. It is useful therefore to establish how close a correlation the tracer has to salinity by evaluating the dispersion coefficients for salinity and the diffusion coefficient of the tracer.

6.5.2.2 Dispersion and diffusion coefficient equations

Dyer (1973) provides an explanation and formula for the dispersion of salinity and dye in an estuary and notes that in one-dimensional estuaries, where the distribution of parameters are in the x direction only, it is possible to determine the longitudinal advection of salt. However this does not allow for lateral or vertical variations in the mean flow. In a homogeneous estuary, dispersion can occur due to velocity shear caused by friction from the sediment bed leading to greater longitudinal advection at the surface than at the bottom and vertical eddy-diffusion causing mixing throughout the water column. The equation for the coefficient of longitudinal dispersion K_x for salinity in well mixed and homogeneous estuaries is as follows:

$$K_x = R.\overline{S} / A\ \overline{\delta S}/\delta x \qquad (6.1a)$$

where K_x can be calculated for any position in an estuary if the river flow (R), cross-sectional area (A) and the mean salinity ($\overline{S}$) and salinity gradient with distance $\overline{\delta S}/\delta x$ are known.
The coefficient of longitudinal dispersion K_x for tracer can be given by:

$$K_x = R.\overline{T} / A\ \overline{\delta T}/\delta x \qquad (6.1b)$$

where the mean tracer is $\overline{T}$ and $\overline{\delta T}/\delta x$ is the tracer gradient with distance.

The formula for dispersion of dye in a trapezoidal channel is also given in Dyer (1973) as:

$$K_x = 5.93\ h\ U_* \qquad (6.2)$$

where h is the depth of flow and U_* is the friction velocity. For a drag coefficient of 0.002, K_x is given as:

$$K_x = 0.26\ \overline{U}.h \qquad (6.3)$$

where $\overline{U}$ is the depth mean velocity.

Equations 5.1 and 5.3 were used to determine the dispersion coefficients of salinity in the upper estuary. The diffusion coefficient K_x for the tracer is given by:

$$K_x = \sigma_x^2 / 2t \qquad (6.4)$$

where σ_x is the width of tracer peak at half-height, taken from Figure 6.11, and t is the time interval.

6.5.2.3 Results

The results are shown in Table 6.2. No agreement is seen for any of the axial profiles due to lack of data points during an axial profile and in the upper reaches due to the variation in salinity as a result of each survey being undertaken during a different tidal state and range. In the upper saline limit of the estuary Equation 6.1a is not very suitable due to the small variations in salinity at high water which makes the salinity gradient term (δs) tend to zero making the term invalid.

The salinity dispersed at an average dispersion coefficient of 1.42 $m^2 s^{-1}$ (SD 0.89) over the ebb and flood tide for Equation 6.3 with ebb and flood components of 1.08 $m^2 s^{-1}$ (SD 0.35) and 1.76 $m^2 s^{-1}$ (SD 1.12).

The tracer diffused at an average coefficient of 0.41 $m^2 s^{-1}$ (SD 0.21) over the tidal cycle for Equation 6.4 with ebb and flood components of 0.37 $m^2 s^{-1}$ (SD 0.15) and 0.45 $m^2 s^{-1}$ (SD 0.25).

The tracer also diffused at an average coefficient of 0.19 $m^2 s^{-1}$ (SD 0.23) over the tidal cycle for Equation 6.1b with ebb and flood components of 0.31 $m^2 s^{-1}$ (SD 0.28) and 0.07 $m^2 s^{-1}$ (SD 0.03).

Date	15/6	18/6	22/6	26/6	26/6	26/6	27/6	3/7	26/6	26/6	26/6	26/6
Tidal Profile	axial	axial	axial	flood	ebb	axial	axial	axial	flood	ebb	flood	ebb
Equation	6.1a	6.1a	6.1a	6.3	6.3	6.1a	6.1a	6.1a	6.1b	6.1b	6.4	6.4
1				1.11	0.21							
	1.26								0.05	0.06	0.06	0.25
2				0.96	1.15							
		0.43	3.15				0.75	2.85	0.05	0.31	0.39	0.23
3				1.05	1.86							
	0.39	0.25	6.84				0.42	5.71	0.09	0.14	0.62	0.63
4				1.47	2.24							
	0.12	0.20	2.62			0.51	0.13	0.19	0.11	0.18	0.39	0.31
5				1.46	3.83							
	0.07	0.02	0.22			1.1		0.06	0.04	0.85	0.80	0.42
6				0.41	1.29							

Table 6.2: Results for the dispersion coefficient (K_x in $m^2 s^{-1}$) for salinity (averaged) during the preliminary and post axial profiles and the main study for tracer and salinity indicates which equation has been used for the calculation. Dispersion coefficients based on a gradient between two stations are shown between Station No. positions (1-6). No data was available at certain stations due to zero values or the survey ceasing before a station.

Clearly the data for salinity is not statistically good with large fluctuations in the data and considerable variations with the values quoted in Dyer (1973). The reasons why there may have been variation both in the actual values compared with other authors and the variance in these data possibly include not using the tidal mean salinity in equation 6.1a which seemed a reasonable assumption since the error should be slight over the period of data collection whether synoptic or axial survey. In addition the differences may be due to the cross-sectional area term not being carefully determined for each data point (on the axial survey) or at each of the Stations. There was also no salinity data at Stations 1-3 due to no salinity gradient being detected and therefore this reduces the ability to apply a gradient from the upper to lower estuary effectively. Lack of the salinity data at these Stations makes it impossible to compare the dispersion and diffusion of salinity and tracer respectively with one another during the initial stages of the tracer release.

Further anomalies in the salinity data between the axial surveys and the main study are that the axial surveys are surface only whereas the main study data is depth-averaged. The wide variety in coefficients is due to the estuary not conforming with the assumptions made in the equations with the estuary comprising an irregular topography with large bends and variations in the channel cross-section causing secondary circulation.

No conclusions can be drawn from this data other than the formula for dispersion and diffusion of salinity and tracer particles did not provide comparable data. The tracer clearly was advected with the saline intrusion, but the data presented here does not provide an accurate prediction of the tracer movement.

6.5.3 Equilibrium of the tracer with the turbidity maximum

Figures 6.15 and 6.16 show a longitudinal axial section from the synoptic surface water data collected at each Station at two specific time intervals of 11.00 at the commencement of the ebb tide and at 20.20 towards the end of the flood tide. The data on the ebb tide indicated the saline intrusion limit was within the upper estuary upstream of Station 4, but due to having

no data salinity data from above Station 4 it was impossible to indicate the location of the upper limit. The turbidity maximum rose to a concentration of approximately 400 mg l^{-1} at Station 1. The tracer was detected at the surface only at Station 1 at 11.00 am and therefore was just starting to be advected down estuary on the ebb tide. The data indicated that the tracer was released into the surface water turbidity maximum in the upper reaches of the estuary. Previous data indicated that the tracer was advected down estuary whereas SPM behaves differently with more lcoalised deposition and resuspension processes being more important. The tracer became disassociated with the surface turbidity maximum during the period of the tidal cycle.

Figure 6.16 indicated that the tracer maximum was associated with the surface turbidity maximum once more on the flood tide with peak tracer concentrations at Station 1 and peak turbidity at Station 1 rising to approximately 500 mg l^{-1} . This data suggests that even if disassociation occurred between tracer and the surface turbidity maximum either side of low water and during the peak ebb and flood tides the tracer becomes re-associated with the turbidity maximum at the end of the flood tide. What this data does not indicate however is that the bottom turbidity maximum section is quite different with the peak turbidity occurring at Station 3 and decreasing towards Station 6 and Station 1 even though the decrease to Station is less significant. The bottom peak at Station 3 was 886 mg l^{-1} whereas at Station 1 it was 660 mg l^{-1}. This indicates the problems of using surface profiles to establish the precise location of the actual turbidity maximum within an estuary.

The depth of the sensing equipment used for a profile clearly dictates the turbidity maximum data obtained. The river flow and tidal conditions would also have an effect with the tidal range causing varying turbidity within the water column and spatially and temporally within the estuary. It is therefore difficult to determine whether dissassociation occurs for dissolved and soild phase pollutants.

With respect to Figures 6.12 and 6.13, the fact that one was carried out on a spring tide (27/6) and the other on a neap tide (3/7) would lead to a significant difference in erosion and

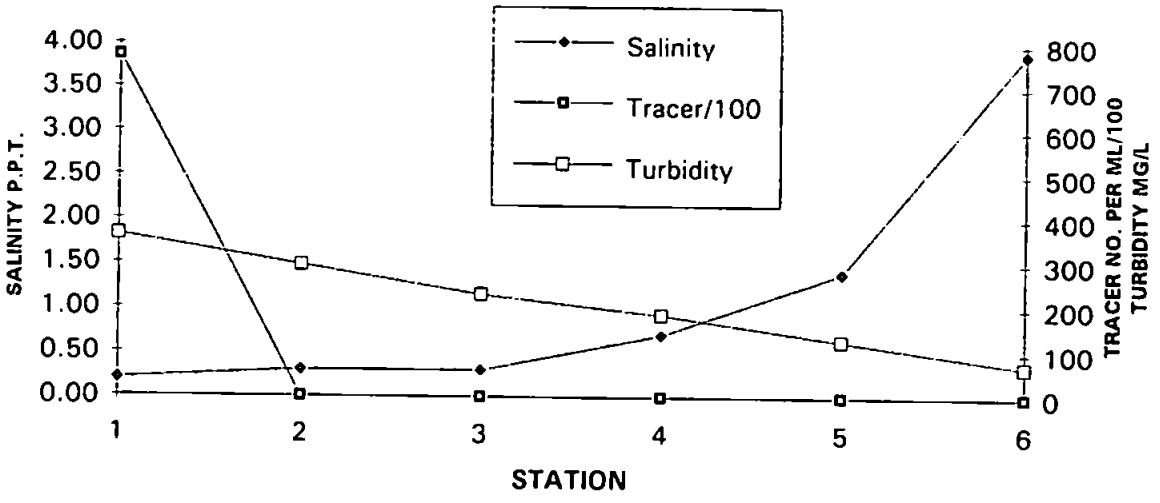

Figure 6.15 Longitudinal axial section, taken from the synoptic data, through Stations 1-6 showing salinity, tracer and turbidity on the ebb tide 11.00, 26th June. NOTE: Salinity data for Stations 1-3 were estimated tending to 0 ppt and freshwater.

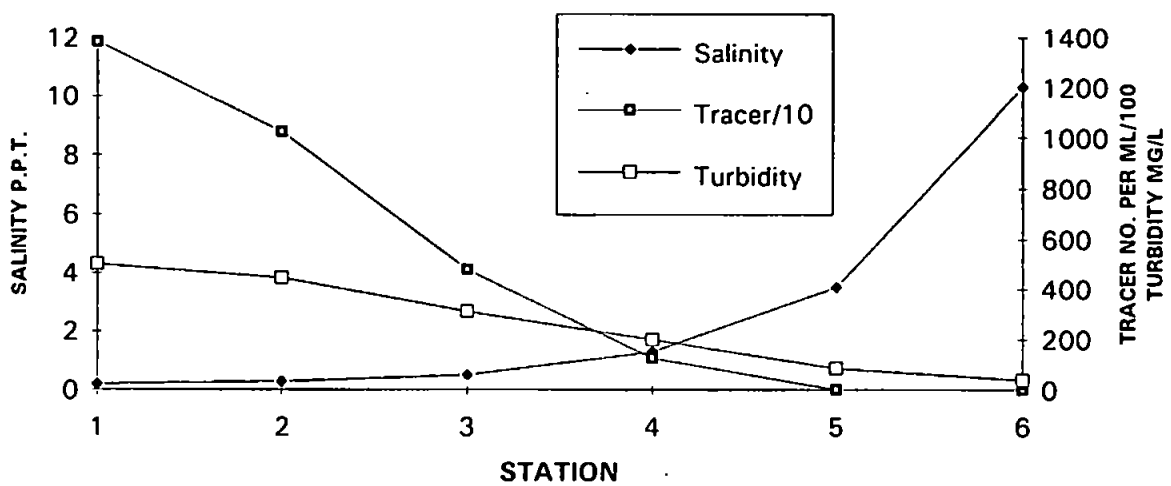

Figure 6.16 Longitudinal axial section, taken from the synoptic data, through Stations 1-6 showing salinity, tracer and turbidity on the ebb tide 20.20, 26th June.

transport of sediment and tracer, as shown by the decrease in concentration of both on the neap tide. This makes the prediction of particle residence times in the turbidity maximum and the deposition-resuspension cycle of particles very difficult. It is not possible to conclude whether the tracer was in equilibrium with the turbidity maximum after 12 hours or 7 days from this data and additional data would be required in order to provide a definitive answer.

Clearly the depth averaged residual tracer provides a more accurate picture of the tracer transport, its association with the turbidity maximum and the overall migration vertically, spatially and temporally. The depth averaged data does not provide information on the vertical variance which may occur in the water column however. The reduced tidal range and current velocity on the neap tide led to a lower neap SPM concentrations (Figure 6.13) which may have allowed the small floc distribution, of the two populations, described by McCabe *et al.*, (1993) to be detected whereas during the spring tide this is not the case. A percentage of the tracer may have been in equilibrium with the small floc population immediately after the tracer release, but spring conditions on the day masked this.

Dyer (1989) notes that due to the long timescales involved in the response of the sediment to the changing current pattern, it is unlikely that the turbidity maximum will reach a steady state distribution within the estuary as does salinity. In order to establish whether there was a dual population of tracer and that tracer was both advected with the saline intrusion and undergoing localised deposition and resuspension it is necessary to carry out further analysis of the data.

6.5.4 Residual Transport Analysis of Current velocity, SPM and Tracer particles.

6.5.4.1 Analysis equations

A tidally averaged evaluation of the suspended sediment concentration data was carried out; it is described in more detail in Uncles *et al.*, (1991b). In addition the mass budget of the tracer particles through each section of the Estuary was determined by Marsh *et al.*, (1991).

$$T_{FG} = (\delta T_{FM}/\delta x) \qquad (6.9)$$

The residual tidally averaged rate of water transport per unit width is given by:

$$\langle Q \rangle = \langle HU \rangle = \langle H \rangle.(\langle U \rangle + U_s) = \langle H \rangle U_L \qquad (6.10)$$

where

$$U_s = \langle HU \rangle / \langle H \rangle \qquad (6.11)$$

with U_L denoting the up-estuary water transport current and with the tilde (~) defining a temporal deviation from the tidal average where:

$$\tilde{U} = U - \langle U \rangle \text{ and } \quad \tilde{H} = H - \langle H \rangle \qquad (6.12)$$

The instantaneous transport of suspended sediment per unit width is given by:

$$Q_P = \overline{HUP} \qquad (6.13)$$

where P is SPM concentration and the residual transport per unit width, per unit tidally-averaged depth is:

$$G = \langle Q_P \rangle / \langle H \rangle = \langle HUP \rangle / \langle H \rangle = G_L + G_{TP} G_V \qquad (6.14)$$

The synoptic data is presented in Table 6.3; negative denotes up-estuary transport and positive is down-estuary transport.

6.5.4.2 Current velocity

The depth averaged (overbar) and residual (tidally-averaged, < >) currents are $\langle\bar{U}\rangle$. The residual current comprises an up-estuary water transport 'pumped' by a tidal wave, denoted as $\bar{U}_s$, of magnitude approximately 0.1 m s^{-1} and a down-estuary water transport of fresh, riverine water in steady, laterally homogeneous conditions, denoted as $\bar{U}_L$, also of magnitude approximately 0.1 m s^{-1}. However, at Station 6 the current is up-stream which may have been due to up-estuary density-driven currents (Uncles *et al.*, 1985). The summation of the component currents to give the residual which is depth and tidally averaged ($\langle U\rangle$) are typically down-estuary of magnitude 0.2 m s^{-1} at the four upper Stations and decreased at the lower Stations.

6.5.4.4.Turbidity

The SPM flux G is divided into three components G_V, G_{TP} and G_L comprising vertical shear transport G_V which is down-estuary and negligible except for Station 3 and 4 where localised resuspension, as described previously, had a significant effect. The tidal pumping of SPM given by G_{TP}, was directed up-estuary at all stations with a peak at Station 3, counterbalanced by down-estuary transport advection by the residual water transport component $\bar{U}_L$ given by G_L. The total residual flux term, G, for SPM is directed up-estuary at all stations excluding Station 4. This indicates that the dominant tidal pumping and transport of SPM up-estuary was driven by tidal asymmetry. However there is a clear indication that high SPM due to tidal pumping creates localised resuspension and deposition indicated by the high SPM remaining within the vicinity of each Station. This is certainly the case for Station 3 where despite a high up-estuary tidal wave water transport ($\bar{U}_s$) the high SPM value at Station 3 is not seen at Station 2. The anomaly at Station 4 may have been due to the location of the sampling vessel situated on the edge of the main channel, possibly experiencing return flows on the outer edge of the Estuary and influenced by circulation due to a large bend in the Estuary.

Station No. (km)	$\langle\bar{U}\rangle$ ms^{-1}	U_s ms^{-1}	U_L ms^{-1}	G_V $ppmms^{-1}$	G_L $ppmms^{-1}$	G_{TP} $ppmms^{-1}$	G $ppmms^{-1}$	T_{EM}	T_{FM}	T_{RM}	T_{EG}	T_{FG}
										Tracer particle numbers x 10^{14}		
1 (3.0)	0.14	-0.08	0.06	3.7	90.3	-143.3	-49.3	47.9	-3.6	44.3		
											56.3	-3.2
2 (3.7)	0.16	-0.06	0.10	0.5	115.7	-125.9	-9.7	8.5	-5.9	2.6		
											-3.9	-1.9
3 (4.6)	0.21	-0.09	0.12	69.8	358.1	-443.8	-15.9	12.0	-7.7	4.4		
											4.3	-0.8
4 (5.6)	0.29	-0.13	0.15	19.0	225.6	-137.0	107.6	7.7	-8.5	-0.8		
											-6.2	-6.0
5 (7.0)	0.10	-0.06	0.05	2.8	26.6	-92.2	-62.8	16.4	-16.9	-0.5		
											7.4	-8.3
6 (8.5)	0.04	-0.06	-0.02	-0.6	-8.3	-16.2	-25.2	5.3	-4.5	0.9		

Table 6.3: Tidal average (<>) synthesis of longitudinal velocity (U), SPM (G) flux and tracer particle mass data (T) at Stations 1-6. See text for an explanation of the symbols. Up-estuary is negative. Stations are listed as 1-6 followed by their distance from the weir (X in km) and their tidally averaged depths (<H>, m).

The tidally averaged data provides a clear summary of the components of current velocity and SPM. The data confirms that despite the residual currents being down-estuary the total residual flux of SPM, G, was directed up-estuary, which implies continuing transport of mud to the upper reaches. The residual flux was of the order of 1-2% of the maximum instantaneous fluxes. The anomaly at Station 4 indicates that there is cross-sectional variation across the estuary.

6.5.4.4 Tracer Particles

The fluorescent tracer particle mass transport, defined as the total number of particles passing through a Station, are presented for the ebb tide (T_{EM}) and flood tide (T_{FM}) components and the residual tracer mass (T_{RM}) in addition to the mass gradients between Stations 1 to 6 and 6 to 1 respectively for the ebb (T_{EG}) and flood tide (T_{FG}). Figure 6.17 indicates the results of the tracer mass and gradients. The total number of tracer particles added intially was 6.3×10^{15} and at Station 1, 4.8×10^{15} were measured indicating a loss between the release point and Station 1, a distance of approximately 1km, that 25% of the tracer remained in the upper estuary. The low current velocity conditions at slack high water, and high SPM concentrations would create conditions where significant flocculation and settling out could occur. There is also a significant loss between Stations 1 and 2, of approximately 78% of the value at Station 1. Higher mass measurements at Stations 3 and 5 suggest that the sampling frequency was insufficient and that the peak of tracer was missed. The ebb masses for Stations 2 to 6 average approximately 1.0×10^{15} which is 20% of the value measured at Station 1 and 15% of the total tracer particles added.

On the flood tide the tracer mass values (T_{FM}) range from 0.8 -16.9 $\times 10^{14}$, with an average of 7.8×10^{14} which indicates minimal loss between the ebb and flood tide at the lower Stations. Station 5 records the highest tracer mass for the ebb (excluding Station 1) and flood tides indicating that the sampling point was central to the main flow and that the estuary was well mixed at this point with little cross-sectional variation or stratification. At other Stations, particularly Station 4 the position of the sampling point was clearly offset from the mainflow.

A substantial loss between Station 1and 2 highlighted by the ebb mass gradient figures (Table 6.3) suggests that a large proportion of the tracer settled out to the bed. This reinforces the observation of tracer particles eroding and being detected at Station 1 with entrapment on the mudflats at high water (Uncles *et al.*, 1991b). The breakdown of up-estuary density driven currents and a decrease in current velocity between the tracer peak arriving at Station 1 and 2 may have created conditions for settling with continued up-estuary transport close to the bed around Station 1. The rising flood tide rapidly submerged the mudflats and caused resuspension and up-estuary transport of the tracer particles although there is not a noticeable increase in the flood-tide mass budget at Station 1. The average mass remained fairly constant between Station 2 to 6 which suggests that the majority of material that was in suspension at Station 2 remained in suspension for the ebb tide and subsequent flood tide. This may support observations by McCabe *et al.*, (1993) that a dual size population exists the largest of which undergoes continual recycling from bed to suspension and back and the remainder which stays in continuous suspension.

The mass gradient T_{EG} loss between Station 5 and 6 may be due to a decrease in current velocities approaching low water slack and as a result of high localised SPM large amounts of tracer settled out. On the commencement of the flood tide a mirror image is almost created indicating that all the material that settled out during the ebb tide was remobilised on the flood tide. The mirror image can clearly be seen by the close proximity of the ebb and flood mass gradient values between Stations 4 and 5.

The high tracer mass at Station 5 on the flood supports the initial high mass measured on the ebb tide further indicating the errors associated with Stations 2 to 4 on the ebb tide. The mass for the ebb and flood at Station 5 are 16.4×10^{14} down-estuary on the ebb tide and 16.9×10^{14} on the flood tide. This indicates there was no loss between these Stations or downstream of Station 6 despite the significant migration of approximately 3.5 km beyond Station 6. Exchange obviously did occur, but the high flood current velocities led to a complete resuspension of material. Despite erosion of tracer at Station 1 prior to the arrival of the main advected pulse the tracer mass at Station 1 remained low. This was partially due

to the rapid decrease in the flow close to high water slack and the possibility of large amounts of tracer being deposited on the mudflats resuspension was slow and around the high water mark. Mixing in the shallower waters on the mudflats may have been insufficient to ensure tracer detection in the centre of the estuary at that point.

A net loss to the bed clearly took place up-estuary and in close proximity to Station 1. The weak current velocities associated with high-water slack do not appear to have been sufficient to erode the material from the bed back into suspension. Approximately 75% of the tracer added reached Station 1 and a maximum of 25% reached Station 2 and beyond. The mass of tracer that returned to Station 1, including material clearly eroded from the bed prior to the arrival of the advected pulse, was approximately 6%. Therefore a loss of 20% took place between Station 5 and 1 on the flood tide primarily due to decreasing tidal currents and high SPM leading to flocculation and settling. A steady decrease in mass from Station 4 to 1 on the flood would suggest a gradual deposition of material along the length of the upper estuary.

6.5.4.5 Summary

Relative to the ebb transport of particles at Station 1 the tidal sum at each of the lower Stations was very small, implying that most of the particles remained in the upper estuary. The fact that the ebb numbers did not decrease monotonically indicated the existence of sampling errors. The residual flux of SPM, G, was generally up-estuary, implying continued transport of fine sediment to the upper reaches whereas the residual numbers of tracer particles passing a Station cross-section were relatively small compared with the total tracer particles released.

In contrast to the residual SPM flux up-estuary, the residual transport of tracer was down estuary for one tidal cycle, and therefore the SPM and tracer responded in a different way to the tidal processes of erosion, transport and deposition. The significant loss of tracer between Station 1 and 2 on the ebb tide indicates a substantial deposition of tracer to the sediment bed

implying most of the tracer remained in the upper estuary. In addition, the fact that the ebb tracer concentrations did not decrease monotonically indicated that the frequency of sampling led to errors in the measurement of tracer; for example the tracer concentration at Station 5 was higher than Station 2,3 and 4 suggesting that the peak of the tracer was missed at these latter stations or the estuary at these points was not cross-sectionally uniform.

The residual tracer mass data (T_{RM}) indicates on the whole a significant down-estuary flux between Station 1 and 2.

6.5.5 Tracer particle residence time

Figure 6.18 provides an estimate of the particle resistence time of the added fluorescent particles shown by the log of tidal events versus log of tracer concentration. The particle resistence time is defined as the number of particles inside the volume divided by the number leaving per unit time. The time for the added tracer mass to reduce to 1/e of the original value is a measure of particle retention time and is known as the e-folding time. The e-folding time for these data is approximately 16-18 hours, i.e during the subsequent ebb tide immediately after the study.

If it is assumed that the tracer mass measured on the ebb tide represents 100% of the fluorescent particles added then after the flood tide 45% was detected. On the following day, 27thJune, 7% was detected and 1 week later on the 3rd July, 0.05% was detected.

This estimated decay does not agree closely with observations by (Readman *et al.*, 1982; Bale *et al.*, 1985; Dyer, 1989) that some particles will be retained for long periods estimated to be months to years. However, from previous data presented the particles were clearly retained within the upper estuary and it appears that only a small proportion were detected even on the first ebb tide with approximately 35% of the material added being detected on the ebb tide. A large proportion of the tracer particles were retained within the upper estuary possibly for an indefinite period particularly if there was insufficient bed shear stress to erode

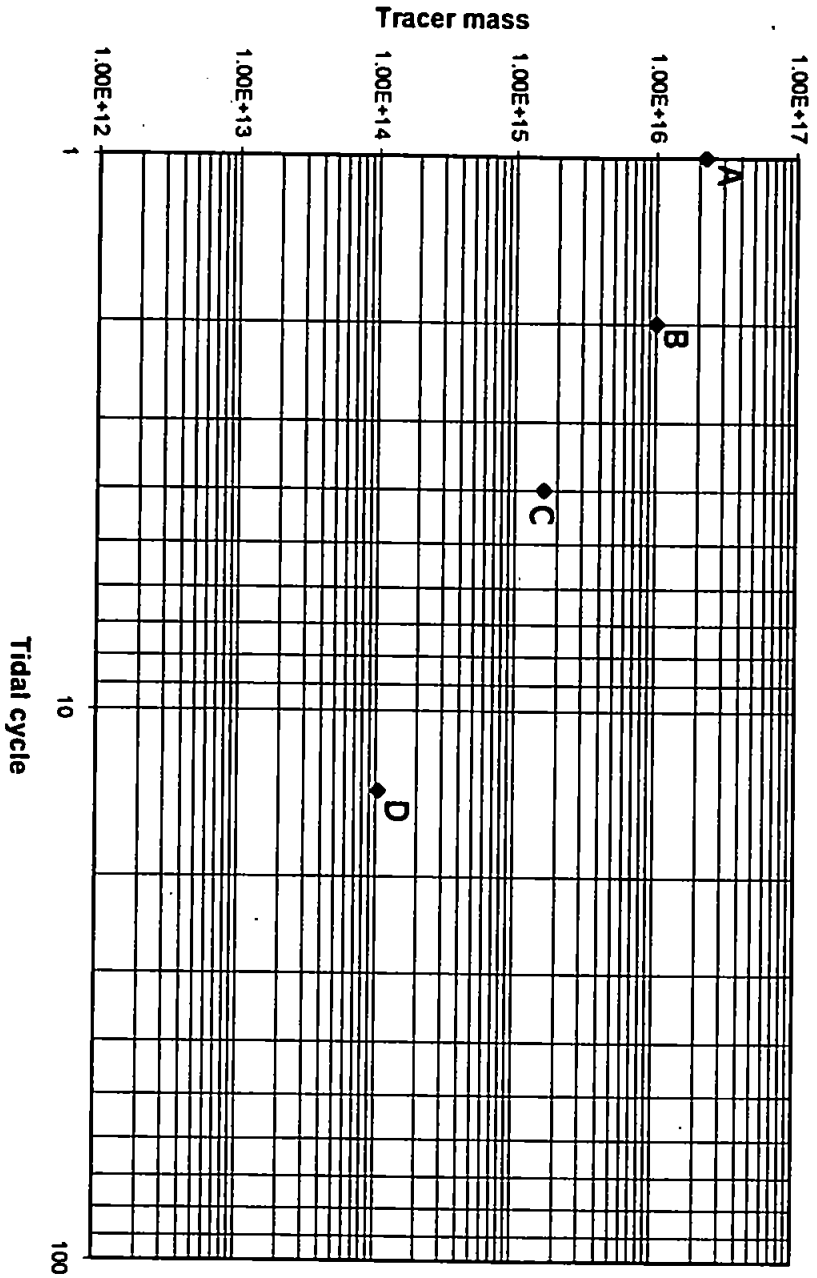

Figure 6.18 Estimate of the tracer particle residence time in the turbidity maximum based on the number of tidal cycles elapsed from the first ebb tide when the tracer was released on the 26th June versus tracer mass (total number of tracer particles). **A, B, C** and **D** denote the first (26th June ebb) second (26th June flood) fourth (27th June) and fourteenth (3rd July) tidal cycles respectively.

the particles. The material that remained in suspension and advected with the tide however, appears on the whole to have returned. Deposition resuspension cycles in addition to sampling frequency and methodology (particulary during axial profiles), may account for a significant proportion of the loss.

The axial profile on the 3rd July indicates lower SPM and tracer particle concentration associated with neap tide conditions. This suggests that insufficient resuspension of tracer and entrainment into surface waters led to a lower concentration being measured. This data does not therefore indicate that there was a loss of tracer down-estuary, but lack of data does not allow an accurate prediction of particle retention.

It is possible to summarise that a significant proportion of tracer particles remained close to the introduction site in the upper estuary indefinitely or until increased river flow, possibly in the winter months, scoured and eroded the material off the bed. This material may then be relocated in the middle estuary followed by gradual up-estuary tidal transport due to tidal pumping. The smaller fine particle fraction which was advected with the saline limit during the study appears to have remained in suspension during spring tide conditions, but not neap. There is no indication that tracer was flushed out of the estuary since between stations 2 to 6 on the ebb and 6 to 2 on the flood there was almost a mirror image implying minimal losses. The tracer particle residence time could therefore indeed be months.

6.5.6 Sediment Particle Residence Time

The tracer particle data indicates substantial retention of material in the upper estuary. In the case of sediment it appears that if introduced at a point in the upper estuary it will remain there and be deposited on the bed. Sediment entering the estuary from the river or similar fluvial input will be deposited on the bed when the turbulence and shear stress are such that settling and deposition takes place. Sediment already in the upper estuary will be eroded, resuspended and transported in two ways; either by bulk transport and saltation in high energy activity and usually associated with the larger particles and flocs or by localised

resuspension of the finer material. the former tends to be localised even with relatively fine grains whereas the latter may be over a distance of several kilometres

Clearly the overall indication is that sediment is advected up-estuary by tidal pumping and that redistrubution of upper estuary sediments takes place to create a mobile stock of SPM. The retention of sediment in the upper estuary is indicated and several mechanisms act to maintain these maxima of turbidity whether at surface water or bed sediment level.

Sediment on the whole, and specifically fine cohesive sediment, is retained in the upper estuary. What is not clear however is for how long, although it appears to be more than 1 week and is therefore longer than the freshwater residence time.

6.6 SUMMARY

Fluorescent particles introduced into the upper reaches of the Tamar Estuary were seen to be advected down and back up estuary on the ebb and flood time through established sampling stations. There was a strong correlation of this advection with the migration of the saline limit.

The Tamar Estuary has a flood dominant tidal regime which leads to a residual up-estuary transport of sediment, however the data indicates a more localised maximum associated with the bed sediments and formation of a mobile stock.

Stratification of the water column at the commencement of the ebb tide minimised mixing of the released tracer particles with an up-estuarine bed level current and down-estuarine surface water current. This was maintained long after the extended period of slack high water and well into the ebb tide. As the ebb tide commenced, the water column became more homgeneous and peaks in current velocity were followed by peaks in SPM concentration 1-1.5 hours later. Slack low water was extremely short (less than 30 minutes), followed by a rapid increase in curent velocity and SPM concentration.

Approximately 65% of the released tracer remained close to the release point and deposition took place close to the high water mark. Significant deposition also took place close to the high water mark. Significant deposition also took place in between the two uppermost sampling stations and on commencement of the flood tide this was re-eroded and measured in the water column..

Two tracer particles populations exised during the study; one which remained permanently in suspension and advected with the saline intrusion and the other which settled out and remained deposited. High bed sediment SPM concentrations in localised areas masked the ability to assess whether the tracer and sediment in suspension were associated with salinity. The tracer particles clearly become associated with the suspended particulate material after a few days however the data also indicates that this took place within a few hours during the main study.

The tracer particles deposited on the bed are estimated to have an indefinite residence time since increase shear stress from high seasonal river flow would be the prime mechanism for erosion. The tracer particles which remained in suspension during the main study appeared to have settled out on a neap tide. Up-estuarine tidal pumping of sediment, particularly on spring tides, and the existence of localised maxima of turbidity at bed sediment level woud indicate a substantial retention of sediment, particularly fine cohesive sediment, and associated pollutants. Over a long period this would lead to a net accumulation over a period of low river flow which may disrupt these processes.

The residence time of sediment in the upper estuary is estimated to be between weeks to months if not substantially longer. The SPM in the upper estuary is therefore not necessarily associated with a single turbidity maximum which migrates with the saline intrusion, but rather a series of maxima temporally and spatially dependant on tidal range, and comprising of varying particle populations.

7.0 CONCLUSIONS AND FURTHER RECOMMENDATIONS

7.1 CONCLUSIONS

An understanding of fine cohesive sediment transport is important in all aquatic environments in order to predict changes in the sediment balance and fate of adsorbed pollutants. In many aquatic environments, including a tidal estuary and shallow lake, there is often a size fraction of fine cohesive sediment which undergoes repetitive erosion and advection transport by flocculation and deposition.

The study of fine cohesive sediment transport has been carried out on several occasions using both natural, chemical and water soluble dye tracers in order to determine water circulation and predict the movement of this sediment which predominantly remains in suspension for long periods. The development and field testing of a fine cohesive sediment particle tracing technique is described which enables the actual measurement of particle dynamics. Particle transport is not a function of the same processes as water circulation and therefore it is imperative that the movement of particles and particle residence time be measured directly.

The use of particle tracers provides a pragmatic approach to evaluating the flow conditions and sediment transport mechanisms that occur after the introduction of the tracer in addition to mass budget calculations. The particle tracers also enable the precise determination of whether a specific site acts as a sink or source for contaminants and over what timescales.

In order to develop an analogue of fine sediment it was necessary to establish the physical properties of the sediment. The size, surface charge, density and settling properties of the natural sediment from the upper reaches of the Tamar Estuary was determined with close correlation to observations from previous studies and authors. The natural sediment analysed was collected from the banks of the estuary and was assumed to represent material periodically resuspended on the flood tide and deposited on the ebb tide. The size ranged from 3 to 30 μm with a mean of 10.2 μm, the density was between 1.1-1.4 g cm^{-3} and surface

charge from -3.4 to -4.7 x 10^{-8} m^2 s^{-1} v^{-1}. The settling velocity at 1 g l^{-1} concentrations and at salinity of 1 ppt was 0.5 mm s^{-1}.

Studies were carried out to passively and actively adsorb a range of fluorescent dyes to the surface of the natural sediment with little or no success and as a result artificial fluorescent particles were examined. An artificial particle was found with similar size spectrum and density although the range of surface charge was slightly lower. When mixed with natural sediment the settling velocity of the floc decreased to 0.3 mm s-1 at 1 g l-1 concentration and salinity of 1 ppt.

An analytical flow cytometer (AFC) was used to assess the detectability of the artificial particles initially in water and subsequently in varying concentrations of estuarine sediment. A calibration curve of measured versus expected (determined from particle counter instument) particle counts was determined indicating a close correlation and a high detectability of approximately 1 artificial particle to 5000 sediment particles. The AFC was fine tuned to the optimum fluorescent wavelength and from a range of different coloured artificial particles orange was chosen as the most suitable for detection, cost and proximity to the peak spectra of AFC laser source.

A preliminary study using the orange artificial particles was carried out in a disused china clay pit. Analysis of the samples indicated dispersal of the particles over a wide area. The samples were analysed again after 3 months to check for stability. The results indicated that the tracer was stable and the sample storage method preserved the sample.

The fluorescent particles were considered to be analogues of the natural sediment particles analysed and it was decided that further field experiments would rigourously test the procedures developed for detecting the tracer and enable the sediment dynamics to be determined at the study sites.

Although initially the objective of this research was to develop and test a particle tracing technique for the study of sediment dynamics in estuaries, it was considered essential to carry out a preliminary field test in a less dynamic environment, and ideally without the variability of a tide.

A preliminary study was carried out in a eutrophic shallow lake, Loe Pool. Loe Pool has a significant allochthonous influx of sediment and several previous studies have indicated the sediments act as an effective sink for nutrients and pollutants with turbulent mixing regulating release back into the water column. The water circulation in the lake is predominantly wind-wave and wind-current induced since river discharge is minimal. Internal loading of the lake with nutrients and pollutants mainly originates from Helston Sewage Treatment Works where 92% of the total phosphorous is sourced, with only 26% of the total inflowing phosporous actually leaving the lake.

Artificial fluorescent particles were released in to the inflowing river in order to assess the transport of the suspended particulate material of the river. Bed sediment samples were taken for analysis. High concentrations of tracer particles occured within 150-225 m from the injection site. There was a significant spatial variation for the size range of particles with the smallest particles travelling the furthest distance from the injection site. A budget of recovered tracer particles showed that approximately 90% by weight were found in the northern area and therefore if the particles are considered to be analogous to natural suspended sediment then 90% of the inflowing sediment will also be deposited in this area. If this sediment has pollutants and nutrients adsorbed on to the surface then this area will inevitably become internally loaded.

The diffusion and transport of tracer from the input point was evaluated using a depth-averaged numerical model to predict wind-driven circulation. During a northerly wind the circulation in the area of maximum tracer concentration measured comprises a single circulatory gyre. The wind during the initial period immediately after the tracer release was from the east and the tracer maxima were closely associated with the centres of the two

gyres, suggesting that the lake hydrodynamics controlled the transport and deposition of the tracer particles. The wind-wave action in this region, despite the water depth being generally less than 2 m, was negligible even during maximum fetch conditions of a south westerly wind.

The bed shear stress created by the wind-driven circulation or waves was not sufficiently large to cause erosion and secondary redistrubution of the tracer. Therefore suspended sediments entering the shallow northern region, under low river flow conditions, would tend to enter into the main wind-driven gyre to be recirculated in either a clockwise or an anti-clockwise direction (depending on the wind direction), until settling out. Limited entrainment occurs into the smaller, most secondary gyres, but the data shows that almost 75% of the tracer particles would have remained there until buried or consolidated by overlying sediment, or resuspended under wave activity form strong southwesterly winds. The circulation model suggests that the majority of resuspended sediment particles will remain in the shallower norther region.

With every subsequent storm event mainly from the southwest, the water column would be consistently reloaded by the polluted sediment. This would cause a considerable increase in the nutrient levels after a wind event, leading to an algal bloom and increase nutrient concentrations.

With the increased confidence gained from the lake study tracer was released into the upper reaches of the Tamar Estuary at the commencement of an ebb tide and slack high water. Six stationary sampling points were moored axially along the estuary and synoptic current velocity, salinity and water depth were measured in addition to water samples for SPM and tracer (both determined in the laboratory).

Tracer particles were advected down-estuary on the ebb tide, after the initial stratification of flow had broken down and were advected up-estuary on the flood tide. There was a strong correlation between this advection and the migration of the saline limit. The increase in SPM

lagged the increase in current velocity by 1-2 hours. There was a clear flood dominance in the estuary with the highest current velocity and SPM concentrations occuring on the flood tide.

The residual transport of SPM was up-estuary, a function of tidal-pumping, however the data indicates a more localised maxima associated with the bed sediment and formation of a mobile stock. The residual transport of tracer was down-estuary however, this was due to the available synoptic data indicating a net loss between Stations 1 and 2 to the sediment bed. Approximately 65% of the tracer particles added never arrived at Station 1 and therefore must have been deposited during the high slack water period. Below Station 2 there was negligible loss between the ebb and flood tide indicating the tracer deposition was a function of the residual transport between Stations 1 and 2.

In addition, the proportion of trace material advected with the saline intrusion migration was small relative to the initial quantity added and possibly represented the fine particle size range. A dual population of size therefore appears to exist in the upper estuary. The small size flocs, advected with the saline limit, underwent a certain degree of deposition and resuspension due to variations in secondary flow, turbulent mixing and shear stress, but a large number remained in suspension. The larger flocs were deposited and remained on the bed for sustained periods and eroded only during high energy activity including peak spring flood tides and high river flow conditions. This leads to a more localised deposition-resuspension cycle as seen at Station 3.

The tracer particles in suspension clearly underwent cycles of resuspension and deposition due to secondary flow and did not appear to behave similarly to the saline limit in this respect. The dispersion and diffusion coefficients for salt and tracer particles respectively did not appear to have a close correlation. The tracer particles did become associated with the SPM in the estuary and were retained within the upper reaches of the estuary with virtually no loss below Station 6 during slack low water. The tracer particles remained in the upper reaches for a minimum of 1 week and SPM concentrations were substantially less. This

indicates that the particles were retained within the turbidity maximum significantly longer than the fresh water residence time.

It is clear from this study that a substantial influx of sediment particulate into the upper estuary is retained within the upper estuary and if this sediment has a high pollutant content associated with it accumulation will take place. A proportion of the particulate will be deposited on the sediment bed and remain there for long periods with periodic resuspension during high energy activity. The remainder will be advected down and up estuary indefinitely undergoing repetitive cycles of deposition and resuspension both spatially and temporally. This will lead to an overall accumulation of sediment and pollutants into a sediment bed level maximum or maxima maintained by tidally induced resuspension, gravitational circulation and tidal asymmetry.

The particle residence time, based on this data could therefore range from weeks to months given the cyclic nature of the spring-neap cycles. Unfortunately insufficient sampling was carried out of successive tidal cycles and hence the data was not available to determine this more accurately. The data does demonstrate the dynamic and complex nature of the estuary.

Clearly the technique presented here offered for the first time an ability to accurately trace fine cohesive sediment transport for material which is permanently in suspension or in a constant flux of deposition and resuspension. The rapid detection system offered by the AFC, the detectability of the tracer particles and the ease of use ensure that this technique can offer a great deal to enhance the understanding of the sediment balance, pollutant transport and sediment dynamics in many aquatic environments.

7.2 FUTURE RECOMMENDATIONS

This research provides data on the initial feasibility of using artificial fluorescent resin particles for fine cohesive sediment transport studies. A great deal has been learned from this research and despite advances in the technique and initial use in field environments several

areas require further research.

(i) A more detailed evaluation of the tracer particles and the physical properties of both the tracer and natural sediment particles in different aquatic environments.

(ii) An examination of the surface chemistry, charge and structural properties of natural sediment particles in order to assess how the passive or active adsorption of fluorescent dyes may be improved. The requirement for high surface coverage, for detection, may make this difficult to achieve however.

(iii) To develop an in-situ detection system which will enable synoptic real-time data to be collected particularly in dynamic environments including estuaries.

(iv) A more detailed study of wind-driven circulation, wave erosion or tidal resuspension of bed sediment in shallow waters in order to assess precisely when, or under which conditions, the release of bed sediment or associated pollutants take place.

(v) With respect to estuarine study in order to address the areas of research requiring further examination (section 6.1.4), it is necessary to increase the frequency of sampling from 20 to 5 minutes, particulary at peak current velocities. In addition, an increase in the cross-channel sampling and sampling over a greater range of distance and time over a period of weeks to months after the release of both the surface and bottom water column and bed sediment would be very informative. The availability of an in-situ detector could however assist in the spatial and temporal data acquisition.

REFERENCES

AALDERLINK R.H., LIJKLEMA L., BREUKELMAN J., VAN RAAPHORST W., BRINKMAN A.G. (1985). Quantification of wind induced resuspension in a shallow lake. Water Sci. Technol. 17:943-954.

ABARNOU A., AVOINE J., DUPONT M.P., LAFITE R., SIMON S., (1987). Role of sediments on the distribution of PCB in the Seine Estuary (France).In: Dynamics of turbid coastal environments. (EBSA 16th Annual Symposium)., (ed. Uncles, R.J.) Cont. Shelf. Res., Vol. 7, No. 11-12, 1345-1350.

ACKROYD D.R. (1983). The removal and remobilisation of heavy metals during estuarine mixing. Ph.D. Thesis, Plymouth Polytechnic. pp 228.

ACKROYD D.R., BALE.A.J., HOWLAND.R.J.M., KNOX.S., MILLWARD G.E., and MORRIS.A.W. (1986). Distribution and behaviour of dissolved Cu, Zn, and Mn in the Tamar Estuary. Estuarine Coastal Shelf Sci. 23: 621-640.

AIKEN G.R., McKNIGHT D.M., WERSHAW R.L., MacCARTHY P., (Eds). (1985). Humic substances in soil, sediment and water, J.Wiley, New York.

ALLEN G.P., SALOMON J.C., BASSOULLET P., DU PENHOAT Y. and DE GRANDPRE C. (1980). Effects of tides on mixing and suspended sediment transport in macrotidal estuaries. Sedimentary Geology, 26, 69-90.

AMOS C.L. (1987). Fine grained sediment transport in Chignecto Bay, Bay of Fundy, Canada. Cont. Shelf Res., 7, Nos. 11-12, 1295-1300.

ANDERSON H.and RUSSELL J., (1976) Possible relationships between soil fulvic acid and polmaleic acid; Nature Vol. 260, 552.

AVOINE J. and LARSONNEUR C., (1987) Dynamics and behaviour of suspended sediment in macrotidal estuaries along the south coast of the English Channel. Cont. Shelf Res., Vol. 7. Nos. 11/12, pp. 1301-1305.

AVOINE J., ALLEN G.P., NICHOLS M., SALOMON J.C., LARSONNEUR C., (1981) Suspended-sediment transport in the Seine Estuary, France: effect of man-made modifications on estuary-shelf sedimentology. Marine Geology, 40, 119-137

BAIER R.W., CUCCI T.L. and YENTSCH C.M. (1989). Flow cytometry for observing the distribution of adsorption sites on particles. Limnol. Oceanogr., 34(5), 947-952.

BALE, A.J., (1987). The characteristics, behaviour and heterogeneous chemical reactivity of estuarine suspended particles. Ph.D. Thesis, Plymouth Polytechnic, 216pp.

BALE A.J., BARRETT C.D., WEST J.R. and ODUYEMI K.O.K. (1987). Use of in-situ laser diffraction particle sizing for particle transport studies in estuaries, paper presented at the 17th EBSA meeting, University of Dundee, Scotland.

BALE A.J. and MORRIS A.W. (1987). In-situ measurement of particle size in estuarine waters, Estuarine and Coastal Shelf Science., 24, 253-263.

BALE, A.J., MORRIS, A.W. and HOWLAND, R.J.M. (1985). Seasonal sediment dynamics in the Tamar Estuary. *Oceanologica Acta*, 8, 1-6.

BALE A.J., MORRIS A.W., WEST J.R., DARBYSHIRE E. and BARTON M. (1988). Measurement of cohesive sediment transport parameters in estuaries.Paper presented at tha Chapman Conference on Sediment Transport in Estuaries, AGU, Bahia Blanca. Argentina.

BARTON M.L., (1992). Sediment transport processes in the Tamar Estuary. Ph.D. Thesis, University of Birmingham, 242pp.

BARTON M.L., STEPHENS J.A., UNCLES R.J. and WEST J.R. (1991). Particle fall velocities and related variables in the Tamar Estuary. In: Proceedings ECSA 19 Symposium on Estuaries and Coasts: Spatial and Temporal Intercomparisons.

BEEN K. and SILLS G.C. (1981). Self-weight consolidation of soft soils: An experimental and theoretical study. Geotechnique, Vol 31, No 4, pp519-535.

BIGGS R.B., SHARP J.H., CHURCH T.M., TRAMONTANO J.M., (1983). Optical properties, suspended sediments, and chemistry associated with the turbidity maxima of the Delaware estuary
Proc. of Symp. on the Dynamics of turbid coastal environments., Can J. Fish. Aquat. Sci., Vol. 40, No. Suppl.1, pp. 172-179.

BLACK K.S. (1994). The erosion of cohesive marine sediments in shallow water environ ments: A Review. Ph. D. Thesis. University College of North Wales. pp 194.

BOWDEN K.F. (1983). Physical Oceanography of Coastal waters. Wiley.

BROCHE P., DEMAISTRE J.C. and FORGET P. (1986). Use of HF Doppler radars for the investigation of the wind-current relationship. International Journal of Remote Sensing, 7(3), 325-337.

BUFFLE J, ZALI O, ZUMSTEIN J, and DEVITRE R, (1987). Analytical methods for the direct determination of inorganic and organic species - Seasonal changes of Iron, Sulphur and Pedogenic and Aquogenic organic constituents in the Eutrophic Lake Bret, Switzerland, Science of the Total Environment, Vol. 64 (1-2), 41-59.

BULLER A.T. and MCMANUS J. (1976). Fluctuations of suspended sediment in estuaries: A descriptive review. Tay Estuary Research Centre, St. Andrews University.

BURKILL P.H. (1987a). Analytical flow cytometry and its application to marine microbial ecology. *In Microbes in the sea* (ed.M.A. Sleigh), pp. 139-166. Chichester: Ellis Horwood.

BURKILL P.H. (1987b). Shipboard flow cytometry: sea trials and analysis with sorting of photosynthetic picoplankton in the Celtic Sea. *Cytometry* S1, 94.

BURKILL P.H. and MANTOURA R.F.C., (1990). The rapid analysis of single marine cells by flow cytometry. Phil. Tans. R. Soc. Lond.A. 333, pp. 99-112

BURROUGHS W.A. (1983) Direct determination of hydraulic equivalence using fluorescent sand tracers in the beach nearshore zone. Sci. & Eng., Vol. 43, No. 9, pp. 148

BURT T.N., (1984). Field settling velocities of estuary muds. Lecture notes and coastal and estuarine studies, Vol. 14: Estuarine cohesive sediment dynamics. Ch. VII, 126-50. Mehta A.J. (Ed).

BURT T.N. and PARKER W.R. (1984). Settlement and density in beds of natural mud during successive sedimentation. Hydraulics Research Ltd., Wallingford, England. Report No. IT 262.

CARPER G.L. and BACHMANN R.W. (1984). Wind resuspension of sediments in a prairie lake. Can. J. Fish. Aquat. Sci., Vol.41, 1763-1767.

CAREY J.H. (1989). The influence of a salt wedge and tidal flow dynamics on contaminant pathways in the Fraser River Estuary, British Columbia. In: Coastal and Estuarine Studies, Vol. 36: Esruarine Water Quality Management, (ed. W.Michaelis), Chap. IV, 202-224.

CHOI W. and CHEN K.Y. (1976). Associations of chlorinated hydrocarbons with fine particles and humic substances in nearshore surficial sediments. Environ. Sci. Tech., Vol 10, 8, pp782-786.

COARD M.A. (1987). Palaeolimnological study of the history of Loe Pool, Helston, and its catchment. Ph.D. Thesis, Polytechnic Southwest. pp 251.

COARD M.A., COUSEN S.M., CUTTLER A., DEAN H.J., DEARING J.A., EGLINTON T.I., GREAVES A.M., LACEY K.P.B., O'SULLIVAN P.E., PICKERING D.A., RHEAD M.M., RODWELL J.K. and SIMOLA H. (1983). Palaeolimnological studies of annually-laminated sediments in Loe Pool, Cornwall, U.K. In: Merilainen J, Huttunen P, and Batterbee R W (eds.). Palaeolimnology (Developments in Hydrobiology) Dr. W Junk bv. The Hague.

CRICKMORE M.C. (1976). Tracer techniques for sediment studies; their use, interpretation and limitations. In: Diamond Jubilee Symp. on Modelling Techniques in Hydraulic Eng. Vol. 1. Central Power and Water Research Station, Paper A13.

CRICKMORE M.J., and LEAN G.H. (1962). The measurement ofsand transport by the Time Integration Method with radioactive tracers. Proc. Roy. Soc. A 270, 27.

CSANADY G.T. (1978). Water circulation dispersal mechanisms. In: Lerman A.(ed.) Lakes: Chemistry, Geology, Physics. Springer, pp. 21-64.

CUCCI T.L., PHINNEV D.A., TOPINKA J.A., BOWMAN M.J., YENTSCH C.M. and PETERSON W.T. (eds). (1986).Real time characterization of individual marine particles at sea: Flow cytometry. Tidal mixing and plankton dynamics., Lect. Notes Coast. Estuar. Stud., Vol. 17, pp. 414-448

DARBYSHIRE E.J.and WEST J.R. (1991). Spatial and temporal turbulence characteristics in the Tamar Estuary. In: Proceedings ECSA 19 Symposium on Estuaries and Coasts: Spatial and Temporal Intercomparisons. pp. 37-41.

DAVIS M.B. and FORD M.S. (1982). Sediment focussing in Mirror Lake, New Hampshire. Limnol. Oceanogr. Vol. 27 (1), 137-150.

DAVIS J.A. (1982). Adsorption of natural dissolved organic matter at the oxide/water interface. Geochim. Cosmochim. Acta, 46, 2381-2393.

DELO, E.A., (1988a). Estuarine muds manual. Hydraulics Research Ltd., Wallingford. Unpubl. Report SR164, February 1988.

DELO E.A. (1988b) The behaviour of estuarine muds during tidal cycles. An experimental study and mathematical model, Hydraulics Research Ltd., Wallingford, England, Report No. SR 138. pp.31

DELO E.A. and BURT T.N. (1991). Distribution of heavy metals at a disposal site for contaminated estuarine dredged material. In: Proceedings CATS Conference, Belgium.

DITMARS J.D., MCCOWN D.L., PADDOCK R.A. (1986) Movement of tagged dredged sand at thalweg disposal sites in the Upper Mississippi River., Argonne, IL (USA), 10 pp.

DOWNING J.A. and RATH L.C,. (1988). Spatial patchiness in the lacustrine sedimentary environment. Limnol. Oceanogr., Vol. 33 (3), 447-458.

DRAAIJER A., TADEMA WIELANDT R. and HOUPT P.M. (1984). Investigations on the applicability of fluorescent synthetic particles for the tracing of silt. Netherlands Organisation for Applied Scientific Research, Report R 84/152 (in Dutch).

DRAKE D E, and CACCHIONE D A, (1986). Field observations of bed shear stress and sediment resuspension on continental shelves, Alaska and California. Cont. Shelf Res., Vol.6, 415-429.

DUINKER J.C. (1980). Susupended matter in estuaries: adsorption and desorption processes. In: Chemistry and Biochemistry of Estuaries. (Olaussen E., and Cato I., eds). John Wiley, Chichester. pp121-151

DYER K.R. (1973). Estuaries: A physical introduction. Wiley. pp. 140.

DYER K.R. (1986). Coastal and estuarine sediment dynamics. Wiley.pp. 342.

DYER K.R. (1988). Fine sediment particle transport in estuaries. In: Physical processes in estuaries. Dronkers J. and Van Leussen W. (eds). Springer-Verlag. pp. 560.

DYER K.R. (1989). Sediment Processes in Estuaries: Future Research Requirements. *Journal of Geophysical Research*, 94, 14327-14339.

EISMA D. (1986) Flocculation and de-flocculation of suspended matter in estuaries. Neth. J. Scales, 20. 183-199

EISMA D., KALF J.and VEENHUIS M. (1980). The formation of small particles and aggregates in the Rhine estuary. Neth. J. Sea Res. Vol. 14(2), 172-191.

ENGSTROM D.A. and WRIGHT H E jr., (1984). Chemical stratigraphy of lake sediments as a record of environmental change. In: Haworth E Y, and Lund J W G (eds.). Lake sediments as environmental history. Leicester University Press, 11-69.

GIBBS R.J. (1983). Effect of natural organic coatings on the coagulation of particles. Environ. Sci. Technol., 17, 237-240.

GIBBS R.J. (1985) Estuarine flocs: Their size settling velocity and density. J. Geophys. Res., 90(C2): 3249-3251.

GINGER C.M. (1987). Simulation and experimental determination of a consolidating mud deposit. Hydraulics Research, Wallingford, England, Report: SR 95.

GRIEVE J. and FLETCHER K. (1977). Interactons between zinc and suspended sediments in the Fraser River estuary, British Columbia. Est. coast. mar. Sci., 5; 415-419.

HAKANSON L, and JANSSON M. (1983). Principles of Lake Sedimentology. Springer.

HANSEN N.E.O. (1979). Effects of boundary layers on mixing in small lakes. Hydrodynamics of Lakes. Proceedings of a Symposium, Lausanne, Switzerland. W.H. Graf and C.H. Mortimer (Eds).

HANSEN D.V. and RATTRAY M. (1966). New dimensions in estuary classification. Limnol. Oceanogr., 11: 319-326.

HOLME-HANSEN O., LORENZEN C.J., HOLMES R.W. and STRICKLAND J.D.H. (1984).Fluorometric determination of chlorophyll. J. Conseil 30, 3-15.

HUBBEL D.W. and SAYER W.W. (1964). Sand transport studies with radioactive tracers. Journ. of the hydraulics division., ASCE, vol. 90, no.HY3, part 1.

HUNTER K.A. (1983). On the estuarine mixing of dissolved substances in relation to colloid stability and surface properties.*Geochimica Cosmochimica Acta. 47, 467-473*

HUNTER K.A. and LISS P.S. (1979). The surface charge of suspended particles in estuarine and coastal waters. Nature, 282, 823-825.

HUTTULA T. and KROGERUS K. (1991). One-dimensional vertical resuspension model for lakes. International Symposium on the Transport of Suspended Sediments and its Mathematical modelling, Florence (Italy).pp647-663.

JAHNKE J. and MICHAELIS W. (1990). Laser fluorometer for the detection of Rhodomine-B in estuarine waters. In: Coastal and Estuarine Studies, Vol. 36: Estuarine Water Quality Management, (ed. W.Michaelis), Chap. IV, 225-235.

JOPLING A V, (1960). An experimental study on the mechanisms of bedding. Ph.D. Thesis, Harvard Univ., Cambridge, Mass..

JORGENSEN . E. (1980). Lake management. Pergamon.

KNOX S., TURNER D.R., DICKSON A.G., LIDDICOAT M.I., WHITFIELD M. and BUTLER E..I. (1981). Statistical analysis of estuarine profiles: Application to manganese and ammonia in tha Tamar Estuary. Estuarine, Coastal and Shelf Science 13, 357-371.

KOLB M. and FRANZ H. (1990) Transport of Rhodamine-B following a slug release into the River Elbe above the Port of Hamburg. In: Coastal and Estuarine Studies Vol. 36: Estuarine Water Quality Managemant Michaelis W. (Ed). Chap. IV. pp. 188-202.

KOMAR P D, MILLER M C, (1973). The threshold of sediment movement under oscillatory water waves. Jour. Sed. Petrology, Vol. 43 (4), 1101-1110.

KRANCK K. (1975). Sediment deposition from flocculated suspensions. Sedimentology, 22 (1), 111-123.

KRANCK K. (1979). Dynamics and distribution of suspended particulate material in the St. Lawrence estuary. Naturaliste Can., 106, 163-173.

KRANCK K. (1981). Particulate matter grain-size characteristics and flocculation in a partially mixed estuary. *Sedimentology*, 28 (1), 107-114.

KRANCK K. (1982) The role of flocculation in the filtering of particulate matter in estuaries. The estuary as a filter (ed.) Kennedy V.S. pp. 159-175. Academic Press Inc., New York.

KRANCK K., (1984). Settling behaviour of cohesive sediment. (As above, p. 151-169).

KRAUS N.C., FARINATO R.S., HORIKAWA K. (1981). Field experiments on longshore sand transport in the surf zone: Time dependent motion, on-offshore distribution, and total transport rate. Coast. Eng. Japan., vol. 24, pp. 171-194.

KRONE R.B. (1962). Flume studies of the transport of sediment in estuarial shoaling processes, Final Report. Hydraulic Engineering and Sanitary Engineering Research Laboratory, University of California, Berkeley (CA). p 110.

KRONE R.B. (1972). A field study of flocculation as a factor in estuarial shoaling processes. Technical Bulletin 19. Committee on tidal hydraulics, Corpos of Engineers, U.S. Army. 114 pp.

LAKE J.L., NORWOOD C., DIMOCK C. and BOWEN R. (1979). Origins of polycyclic aromatic carbons in estuarine sediments. Geochimica et Cosmochimica Acta 43, 1847-1854.

LAMERE HENNESSEE, E., BLAKESLEE, P.J. and HILL, J.M., (1986). The distributions of organic carbon and sulfur in surficial sediments of the Maryland portion of Chesapeake Bay. *Sedimentary Petrology*, 56, 674-683.

LEE D.Y., LICK W., and KANG S.W., (1981). The entrainment and deposition of fine-grained sediment in Lake Erie. J. Great Lakes Res., Vol. 7, 224-233.

LEHMAN J.T. (1975). Reconstructing the rate of accumulation of lake sediment: The effect of sediment focussing. Quat. Res., V. 5, 541-550.

LEMMIN U. and IMBODEN D.M., (1987). Dynamics of bottom currents in a small lake. Limnol. Oceanogr., Vol. 32 (1), 62-75.

LESHT B.M., CLARKE T.L., YOUNG R.A., SWIFT D.J.P. and FREELAND G L. (1980). An empirical relationship between the concentration of resuspended sediment and near bottom wave-orbital velocity. Geophys. Res. Lett., V. 7, 1049- 1052.

LIKENS G.E. and DAVIS M.D. (1975). Post-glacial history of Mirror Lake and its watershed in New Hampshire, USA: An initial report. Int. Ver. Theor. Angew. Limnol. Verh., Vol. 19, 982-993.

LINLEY E.A.S. and FIELD J.G. (1982). The natural and ecological significance of bacterial aggregation in a nearshore upwelling ecosystem. Estuarine Coastal Shelf Sci., 14:1-11.

LITTLE D.I., HOWELLS S.E., ABBISS T.P., ROSTRON D., COUGHTREY P.J., MARTIN M.H., (1987).Some factors affecting the fate of estuarine sediment hydrocarbons and trace metals in Milford Haven 1978-82. In: Pollutant transport and fate in ecosystems., Spec. Publ. Br. Ecol. Soc., Vol. 6, pp. 55-87.

LODER T.C. and LISS P.S. (1982). The role of organic matter in determining the surface of suspended particles in estuarine and oceanic waters. Thalassia. Jugosl., 18 ,433-447.

LODER, T.C. and LISS, P.S. (1985). Control by organic coatings of the surface charge of estuarine suspended particles. *Limnology and Oceanography*, 30, 418-421.

LORING D.H., RANTALA R.T.T., MORRIS A.W., BALE A.J. and HOWLAND R.J.M. (1983). Chemical composition of suspended particles in an estuarine turbidity maximum zone, Can. J. Fish. Aquat. Sci., 40, suppl. 1, 201-206.

LOUISSE C.J., AKKERMAN R.J., SUYLEN J.M., (1986). A fluorescent tracer for cohesive sediment. Papers presented at the International Conference on Measuring Techniques of Hydraulics Phenomena in Offshore, Coastal and Inland Waters. London, England: 9-11 April, 1986., pp. 367-390.

LUETTICH R.A jr., HARLEMANN D.R.F. and SOMLYODY L. (1990). Dynamic behaviour of suspended sediment concentrations in a shallow lake perturbed by episodic wind events. Limnol. Oceanogr., Vol. 35 (5), 1050-1067.

MADSEN O S, GRANT W D, (1986). The Continental-shelf bottom boundary layer. Ann. Rev. Fluid Mech., V. 18, 265-305.

MAHAUT M.L. and GRAF G. (1987). A luminophore tracer technique for bioturbation studies.*Oceanol. Acta.* Vol 10, 3.

MARSH J.K., BALE A.J., UNCLES R.J. and DYER J.R. (1991). A tracer technique for the study of suspended sediment dynamics in aquatic environments. In: Proceedings of the International Association for Hydraulic Research, International Symposium on the Transport of Suspened Sediments and its Mathematical Modelling, Florence, Italy, 2-5 September. pp665-682.

MARSH, J.K., BALE, A.J., UNCLES, R.J., DYER, K.R. (1993). A particle tracing experiment in a small, shallow lake: Loe Pool. Submitted to British Geomorphological Research Group Symp.: Geomorphology and Sedimentology of Lakes & Reservoirs.Chap. 10, pp.139-153.

MARTINDILL M. (1993). Fluorescent and Phosphorescent Pigments. Polymers Paints Colour Journal, Vol. 183, no. 4333.

McCABE J.C., DYER K.R., HUNTLEY D.A. and BALE A..J. (1993). The variation of floc sizes within a turbidity maximu at spring and neap tides. Proceedings 23rd International Conference on Coastal Engineering, Venice. Chap.243, pp. 3178-3183.

McCARTHY J.F., JIMENEZ B.D. and BARBEE T. (1985). Effect of dissolved humic material on accumulation of polycyclic aromatic hydrocarbons: Structure-activity relationships. Aquat. Toxicol. , 7, 15-24.

MEADOWS P.S. and CAMPBELL J.I. (1988). An Introduction to marine science (2nd edition). Blackie, Glasgow, 285pp.

MEHTA A.J., PARCHURE T.M., DIXIT J.G. and ARIATHURAI R. (1982). Resuspension potential deposited cohesive sediment beds. In: Kennedy V.S. (Ed), Estuarine Comparison, Academic Press, New York, pp. 591-609.

MEHTA A.J. (1984). Characterisation of Cohesive Sediment Properties and Transport processes in estuaries. In: Lecture Notes on Coastal and Estuarine Studies, Vol. 14: Estuarine Cohesive Sediment Dynamics. (ed. A.J.Mehta). Springer-Verlag, New York, Chap. XV, 290-325.

MEHTA A J, and PARTHENIADES E, (1975). An investigation of the depositional properties of flocculated fine sediments. J. Hydraul. Res., Vol. 13, 361- 381.

MICHLER G., SIMON K., WILHELM F. and STEINBERG C. (1980). Vertical distribution of metals in a sediment core of a subalpine lake indicating stages in the development of civilization. Archives for Hydrobiology, Vol. 88, 24-44.

MIGNIOT C., (1968). A study of the physical properties of various fine sediments and their behaviour under hydrodynamic action. La Houille Blanche, 23,17,7, 591-620.

MOINE J, CAILLOT A., HOSLIN R., LARSONNEUR C., MASSIAS L., QUESNEY M., (1985)., (The use of radioactive tracers for the study of sediment movements in the Seine Bay.). (The Seine Bay. CNRS National Colloquium, Caen, 24-26 April 1985.)., Actes Colloq. Ifremer., No. 4, pp. 211-218

MONTAGUE C.L. (1984). Influence of biota on erodability of sediments. From: Lecture notes on coastal and estuarine studies. vol. 14: Estuarine cohesive sediment dynamics. Mehta A.J. (ed) pp. 251-267.

MORRIS A.W. (ed.). (1983). Practical procedures for estuarine studies. Natural Environmental Research Council, Swindon, 266 pp.

MORRIS A.W. (1986). Removal of trace metals in the very low salinity region of the Tamar Estuary, England. Sci. Total Environ., 49, 297-304.

MORRIS A.W., BALE A.J. AND HOWLAND R.J.M. (1982a) The Dynamics of Estuarine Manganese Cycling. Estuarine and Coatal Shelf Science., 14, 175-192.

MORRIS A.W., BALE A.J. and HOWLAND R.J.M. (1982b). Chemical variability in the Tamar Estuary, southwest England. Estuar. Coast. Shelf Sci., 14, 649-661.

MORRIS A.W., BALE A.J. et al. (1987). Controls of the chemical composition of particle populations in a macrotidal estuary. (Tamar Estuary, U.K.). Paper presented at the EBSA16 symposium: The dynamics of turbid coastal estuaries. Plymouth, Sept. 1986. Presented to Cont. shelf res.Sci., 7, Nos. 11/12, 1351-1355.

MORRIS A.W., BALE A.J., HOWLAND R.J.M., MILLWARD G.E., ACKROYD D.R., LORING D.H. and RANTALA R.T.T. (1986). Sediment mobility and its contribution to trace metal cycling and retenrion in an estuary. Wat. Sci. Tech., 18, 111-119.

NEWMAN D.E. (1964). The production of fluoescent tracers for detecting the movement of sand and shingle. Hydraulics Research Station. International Report, no. 41.

NEWMAN K.A., MOREL F.M.M. and STOLZENBACH K.D. (1990a). Settling and Coagulation Characteristics of Fluorescent Tracer Particles Determined by Flow Cytometry and Fluorometry. *Environmental Science and Technology*, 24, 506-513.

NEWMAN K.A., FRANKEL S.L. and STOLZENBACH K.D. (1990b). Flow Cytometric Detection and Sizing of Fluorescent Tracer Particles Deposited at a Sewage Outfall Site. *Environmental Science and Technology*, 24, 513- 519.

NICHOLS M.M., (1984). Effects of fine sediment resuspension in estuaries. pp. 5-42. In: Mehta A.J., Characteristics of cohesive sediment processes in estuaries. pp(151-169).

NUERNBERG H.W. (ed) (1985). Estuarine processes and river borne pollutants. Pollutants and their ecotoxicological significance., pp 227 - 238. Tl: Text language.

OCKENDEN M.C. and DELO E A. (1988). Consolidation and erosion of estuarine mud and sand mixtures. Hydraulic Research Ltd., Wallingford, England. Report No. SR149, February, 1988.

OFFICER C.B. (1976). Physical oceanography of estuaries(and associated coastal waters.). John Wiley, Chichester, Sussex. 465pp.

OFFICER C.B. (1981). Physical dynamics of estuarine suspended sediments. Marine Geology, 40, 1-14.

OFFICER C.B. and NICHOLS M.N. (1980). Box model application to a study of suspended sediment distribution and fluxes in partially mixed estuaries. In: Estuarine Perspectives (ed. V.S.Kennedy). Academic Press, New York, 329-340.

O'MELIA C.R. (1985). The influence of coagulation and sedimentation on the fate of particles, associated pollutants and nutrients in lakes, pp.207-224. In: W Stumm (Ed) , Chemical processes in lakes. Wiley-Interscience.

O'SULLIVAN P E, (1989). Microcystis blooms in the South West - Agriculture or Sewage? Paper presented at River and Lake Pollution in the South West, South West Environmental Protection Agency, 14 October, 1989.

O'SULLIVAN P E, (1990). The eutrophication of shallow coastal lakes in Southwest England - understanding, and recommendations for restoration based on palaeolimnology, historical records, and the modelling of changing phosphorus loads. Paper presented at 40th Anniversary Congress of the Finnish Limnological Society, Helsinki, Finland, 5-11 August, 1990.

O'SULLIVAN P.E., COARD M.A. and PICKERING D.A. (1982). The use of laminated sediments in the estimation and calibration of erosion rates. In: Recent developments in the explanation and prediction of Erosion and Sediment Yield (Proceedings of the Exeter Symposium, July 1982). I.A.H.S. Publ.No. 137, 385-396.

O'SULLIVAN P.E., HEATHWAITE A.L., FARR K.M. and SMITH . P. (1989). South West England and the Shropshire-Cheshire meres. Guide to Excursion A, Vth International Symposium on Palaeolimnology, Ambleside, Cumbria, UK, 1-6 September, 1989.

OTTESEN-HANSEN N E, (1977). Effects of boundary layers on mixing in small lakes. In: Graf W H and Mortimer C H (eds.). Hydrodynamics of Lakes, Proc. Sym. 12-13 October 1978, Lausanne, Switzerland. Elsevier.

OWEN, M.W. (1970a). A detailed study of the settling velocities of an estuary mud. Hydraulics Research Station, Wallingford. Unpubl. Report No. INT 78.

OWEN M.W. (1970b). Properties of a consolodating mud. Hydraulics Research, Wallingford, England, Report no. INT 83.

OWEN M.W. (1971). The effect of turbulence on the settling velocities of silt flocs. Proceeding of the 14th. Congress of I.A.H.R., Vol. 4, Paris. August, 1971, pp. 27-32.

OWEN M.W. (1976). Erosion of Avonmouth Mud. Hydraulics Research Station, Wallingford, England. September, 1975.Report No. INT 150.

PARCHURE T M, and MEHTA A J, (1985). Erosion of soft cohesive sediment deposits. J. Hydraul. Eng. (Am. Soc. Civ. Eng.), Vol. 111, 1308-1326.

PARK J.K. and JAMES A. (1990). Mass flux estimation and mass transport mechanism in estuaries. *Limnol. Oceanogr.*, 35(6), 1301-1313.

PARTHENIADES E.,1964). A summary of the present knowledge of the behaviour of fine sediment in estuaries. Massachussets Institute Technology Hydraulics Laboratory, Technical Note 8, 47 pp.

PARTHENIADES E. (1972). Results of recent investigations on erosion and deposition of cohesive sediments. In: Shen H W (ed.). Sedimentation symposium to honour Prof. H A Einstein, Colorado State Univ., Fort Collins, pp. 20-1 to 20-39.

PEJRUP M. (1986). Parameters affecting fine-grained suspended sediment concentrations in a shallow micro-tidal estuary, Ho Bugt, Denmark. Estuarine, coastal and shelf science, 22, 241-254.

PETHICK J. (1984). An introduction to coastal geomorphology. Arnold. pp. 260

PHARO C.H. and CARMACK E.C. (1979). Sedimentation processes in a short residence-time intermontane lake, Kamloops Lake, British Columbia. Sedimentology, Vol. 26, 523-541.

PHILLIPS O.M. (1977). The dynamics of the upper ocean. 2nd. ed. Cambridge University Press.

PICKERING D.A. (1987). Chemical and physical analysis of laminated sediment formed in Loe Pool, Cornwall. Ph.D. Thesis, Polytechnic Southwest.

POND S. and PICKARD G.L. (1983). Introductory Dynamical Oceanography, 2nd Ed.. Pergamon.

POSTMA H., (1967) Sediment transport and sedimentation in the estuarine environment. In: G.H. Lauff (Editor), Estuaries. Am. Assoc. Adv. Sci., Publ., 83: 158-179.

PRITCHARD D.W., (1955). Estuarine circulation patterns. Proc. Am. Soc. Civ. Eng., 81: 1-11.

PULS W. and KUEHL H. (1986). Field measurements of the settling velocities of estuarine flocs. Proc. 3rd Int. Symp. River Sediment. Jackson, Mississippi, U.S.A., March 1986.

RAST W. and LEE G.F. (1983). Nutrient loading estimates for lakes. J. Env. Engineering, V. 109, 502-517.

RATTRAY M. and HANSEN A.G. (1962). Circulation in an estuary. J. Mar. Res., Vol. 20 (2), 119-133.

READMAN J.W., MANTOURA R.F.C., RHEAD M.M. and BROWN L. (1982). Aquatic distribution and heterotrophic degradation of polycyclic aromatic hydrocarbons(PAH) in the Tamar Estuary. In: Estuarine, Coastal and Shelf Science, 14, 369-389.

REYNOLDS C.S. (1979). The limnology of the eutrophic meres of the Shropshire-Cheshire Plain. Field Studies., Vol.5, 93-173.

REYNOLDS C.S. (1984). Phytoplankton periodicity: the interactions of form, function, and environmental variability. Freshwater Biol. 14: 111-142.

ROBERTS D.J., LINDELL T. and KVARNAS H. (1982). Environmental factors governing regional lake water quality differences. Natl. Swed. Environ. Prot. Board, SNV PM 1621, Uppsala, pp. 32.

RUCK K.W. (1972) Erfahrungenbeim praparieren von sand fur Liestoffuntersuchuungen, Dtsch. Verb. Wasserwirch. Mitteilungsbl., 33.

RUCK K.W., (1977). Experiences with the preparing of sand for tracer tests.

RYDING S.O. and FORSBERG C. (1977). Sediments as a nutrient source in shallow polluted lakes. In: Gotterman H L (ed.). Interactions between sediments and freshwater. Dr. W Junk bv, The Hague. pp. 227-234.

RYDING S.O. and FORSBERG C. (1980). Short-term, load response relationships in shallow, polluted lakes. Developments in Hydrology No. 2, Dr. W Junk bv, The Hague.

SALOMONS W. and MOOK W.G. (1987). Natural tracers for sediment transport studies. *Continental Shelf Research*, Vol. 7, Nos. 11/12, 1333-1343.

SALOMONS W., DE ROOIJ N., KERDIJK H. and BRIL J. (1987). Sediment as a source for contaminants. Hydrobiologia, Vol. 149, 13-30.

SCHUBEL J.R. (1969). Size distributions of the suspended particles of the Chesapeake Bay turbidity maximum. Neth. J. Sea Res., 4, 283-309.

SCHUBEL J.R. (1972). Distribution and transportation of suspended sediment in upper Chesapeake Bay in Nelson, B.W. (ed). Environmental framework of coastal plain estuaryies. Geol. Soc. Amer. Memoir 133: 91-117.

SHAPIRO H.M. (1988). Practical flow cytometry. New York: Alan R. Liss.

SHOLKOVITZ E.R. (1976) Flocculation of dissolved organic and inorganic matter during the mixing of river water and seawater. Geochimica et Cosmochimica Acta 40, 831-845.

SHRIVASTAVA P.P. (1975). Preparation of fluorescent tracers with indigenous dyes and binding media. Offshore mineral exploration and marine geology division. Geological Survey of India. pp. 93-95.

SIGG L., STRUM M. and KISTLER D. (1987). Vertical transport of heavy metals by settling particles in Lake Zurich. Limnol. Oceanogr. 32: 112-130.

SIMOLA H., COARD M.A. and O'SULLIVAN P.E. (1981). Annual laminations in the sediment of Loe Pool. Nature, V. 290 (5803), 238-241.

SLEATH J.F.A. (1984). Sea bed mechanics. Wiley.

SLY P.G. (1977). Sedimentary environments in the Great Lakes. In: Gotterman H L (ed.). Interactions between sediments and freshwater. Dr. W Junk bv, The Hague. pp. 76-82.

SLY P.G. (1978). Sedimentary processes in lakes. In: Lermann A (ed.). Lakes: Chemistry, Geology, Physics. Springer. pp. 65-89.

SMITH I R, and SINCLAIR I J, (1972). Deep water waves in lakes. Freshwater Biol., Vol. 2, 387-399.

SMITH V.H. (1979). Nutrient dependance of primary productivity in lakes. Limnol. Oceanogr., Vol.24, 1051-1064.

SOBEY R.J. (1986). Wind-wave prediction. Ann. Rev. Fluid Mech., Vol. 18, 149- 172.

SOMLYODY L. (1986).Wind induced sediment resuspension in shallow lakes. Proceedings of Int. Conference on Water Quality Modelling in the Inland natural Environment. Bournemouth, England, June 1983.

SOULSBY R.L. and SMALLMAN J.V. (1986). A direct method of calculating bottom orbital velocity under waves. Hydraulics Research Ltd., Wallingford, England. Report No. SR76, February, 1986.

SPANHOFF R. and SUIJLEN J.M. (1990a). Chemical Tracers - A new desirable technique? In:
Coastal and Estuarine studies, vol 36: Estuarine Water Quality Management, (ed. W. Michaelis), Chap. V, 235-238. .

SPANHOFF R. and SUIJLEN, J.M. (1990b). Feasibility of Tracer Studies of Large Scale Cohesive-Sediment Transport. In: Coastal and Estuarine Studies, Vol.36: Estuarine Water Quality Management,(ed. W. Michaelis), Chap. IV, 197-202.

STEPHENS J.A., UNCLES R.J., BARTON M.L. and FITZPATRICK F. (1992). Bulk properties of intertidal sediments in a muddy macrotidal estuary. Mar. Geol., 103: 445-460.

STEVENSON J.R. and BURT T.N. (1985). Further studies of the field settling velocities ot Thames mud. - Hydraul Res. Stn, Wallingford. Report SR 10.

STRUM M. and MATTER A. (1978). Turbidites and varves in Lake Brienz (Switzerland); deposition of clastic deposits by density currents. Modern and Ancient Lake Sediments Special Publication, V. 2, 147-168, Blackwell Scientific Publications, Oxford.

STUMM W.and MORGAN J.J. (1981)., Aquatic chemistry: An introduction emphasising chemical equilibria in natural waters. 780 pp. Wiley Interscience, New York. 599-684.

STURLEY D.R.M. (1990). Topographically induced internal waves and enhanced vertical mixing in an estuary. PhD Thesis, Polytechnic South West (CNAA). pp.222.

SUIJLEN J.M. and VAN LEUSSEN W. (1989). Recent developments in large-scale tracing by fluorescent tracers. In: Coastal and Estuarine Studies. Vol. 36: Estuarine Water Quality Management. MIchaelis W. (Ed). Chap. IV., pp. 188-202.

SVERDRUP H.U. and MUNK W.H. (1947). Wind, sea and swell: Theory of relations for forecasting. United States Hydrographic Office, Publ. No. 601, p.44.

THEIS T.L. and McCABE P.J. (1978). Water circulation and dispersal mechanisms. In: Lerman A (ed.). Lakes: Chemistry, Geology, Physics. Springer. pp. 21- 64.

THOMPSON S. and EGLINGTON G. (1978). Composition and sources of pollutant hydrocarbons in the Severn Estuary. Marine Pollution Bulletin, 9, 133-136.

THORN M.F.C.and PARSONS J.G. (1980). Erosion of cohesive sediments in estuaries: An Engineering Guide. Proceeding of the Third International Symposium on Dredging Technology, BHRA, Paper F1, Bordeaux, France, March, 1980, pp. 349-358.

TIPPING E., WOOF C. and COOKE D. (1981). Iron oxide from a seasonally anoxic lake. Geochim . Cosmochim. Acta, 45, 1411-1419.

TUREKIAN K.K. (1977). The fate of metals in the oceans. Geochimica et Cosmochimicha Acta 41, 1139-1144.

TWILLEY R.R. and WARD L.G. (1986). Seasonal distrsbutions of suspended particulate material and dissolved nutrients in a coastal plain estuary. Estaries. vol. 9, no. 3, pp. 156-168.

UNCLES R.J. (1982). Computed and observed residual currents in the Bristol Channel. Oceanol. Acta, Vol. 5 (1), 11-20.

UNCLES R.J., BALE A.J., HOWLAND R.J.M., MORRIS,A.W. and ELLIOTT R.C.A. (1983).Salinity of surface water in a partially-mixed estuary, and its dispersion at low run-off. *Oceanologica Acta*, 6 (3), 289-296.

UNCLES R.J., ELLIOTT R.C.A. and WESTON S.A. (1984). Lateral distribution of water, salt and sediment transport in a partly mixed estuary. Reprinted from the 19th Coastal Engineering Conference Proceedings,ASCE, Houston Texas.Chap. 204, pp. 3067-3077.

UNCLES R.J., ELLIOTT R.C.A. and WESTON S.A. (1985). Observed fluxes of water, salt and suspended sediments in a partially mixed estuary, Estuarine and Coastal Shelf Science, 20, 147-167.

UNCLES R.J. and STEPHENS J.A. (1989). Distributions of suspended sediment at high water in a macrotidal estuary, Journal Geophysical Research, 94, No. C10, 14395-14405.

UNCLES, R.J., STEPHENS, J.A. and BARTON, M.L. (1991a). The nature of near bed currents in the upper reaches of an estuary. In: Proceedings of ECSA 19th Symposium on Estuaries and Coasts: Spatial and Temporal Intercomparisons.

UNCLES, R.J., STEPHENS, J.A., MARSH, J.K. and BALE, A.J. (1991b). Synoptic observations of fine-sediment concentration and transport in the turbidity maximum region of an estuary. International Symposium on the transport of suspended sediments and its mathematical modelling. Florence, Italy. pp.389-402.

VALE C. and SUNDBY B. (1987). Suspended sediment fluctuations in the Tagus Estuary on semi-diurnal and fortnightly time scales. Estuarine, Coastal and Shelf Science, 25,495-508.

VAN LEUSSEN W.,(1988). Aggregation of particles, settling velocity of mud flocs: A review. In: J. Dronkers and W. Van Leussen (Editors), Physical processes in estuaries. Springer, Berlin, pp. 347-403.

VASS K.K. (1980). The Trophic statusand conservation of Kashmir Lakes. Hydrobiologia, Vol. 68 (1), 9-15.

VOLLENWEIDER R.A. (1968). Scientific fundamentals of the eutrophication of lakes and flowing waters with particular reference to nitrogen and phosphorus as factors in eutrophication. Organisation for Economic Co- operation and Development (OECD), DAS/CSI/68.27, Paris.

VOLLENWEIDER R A, (1975). Input-output models with special reference to the phosphorus-loading concept. Schweiz. Z. Hydrol., V. 37, 58-89.

VUKMIROVIC V. (1963). The application of radioactive tracers in the study of sand movements in rivers. Institute for Development of Water Resources, Jaroslav Cerni, Belgrade.

WAKEHAM S.G., SCHAFFNER C.and GIGER W. (1980). Polycyclic aromatic hydrocarbons in recent lake sediments - 1. Compounds having anthropogenic origins. Geochimica et Cosmochimica Acta, 44, 403-413.

WANKOWSKI L.Z. (1979). An environmental impact assessment of alternative sewage treatment strategies in the Loe Pool catchment, Cornwall. Unpublished undergraduate dissertation for the award of B.Sc. (Hons.) degree, Environmental Science, Plymouth Polytechnic.

WEILENMANN U., O'MELIA C.R. and STUMM W. (1990). Particle transport in lakes: Models and measurements. Limnol. Oceanogr., V. 34 (1), 1-18.

WEINER B.B., (1979). Particle and spray sizing using laser defraction SPIE (Optics in quality assurance II) Society of Photo-optical Instrumentation Engineers. 170, 53-62.

WEIRICH F.H. (1986). A study of the nature and incidence of density currents in a shallow glacial lake. Annals of the Association of American Geographers, Vol. 76 (3), 396-413.

WILEY J.R. (ed), (1985). Role of sediments in the accumulation and transport of radionuchlides in waterways. Waste management research abstracts. No. 16. Information on radioactive waste programmes in progress., Waste Manage. Res. Abstr., no. 16, p. 108

WILEY J.D., ATKINSON L.P. (1982) Natural fluorescence as a tracer for distinguishing between Piedmont and coastal plain river water in the nearshore waters of Georgia and North Carolina. Estuar. coast shelf sci., vol. 14, no. 1, pp. 49-59.

ZULLIG H. (1982). The development of the holiday resort of St. Moritz reflected in the sediment deposits of the lake of St. Moritz. Wasser, Energie, Luft, 74 Jahrgang, Heft 7-8, 177-183.

10 Particle Tracing Experiment in a Small, Shallow Lake: Loe Pool, UK

J. K. MARSH
Institute of Marine Studies, University of Plymouth
A. J. BALE and R. J. UNCLES
Plymouth Marine Laboratory
and
K. R. DYER
Institute of Marine Studies, University of Plymouth

ABSTRACT

A tracer particle experiment was undertaken in Loe Pool, a small, shallow lake in south-west England (50°4′N, 5°17′W). The tracer particles were injected into the main river inflow of the lake. High concentrations of tracer particles were deposited within two well defined maxima in the northern region of the lake; a budget of the tracer showed that approximately 90% by weight was recovered in this area. The pattern of tracer particle deposition observed during the experiment was interpreted using a depth-averaged hydrodynamic model of the wind-driven circulation within the lake. The model was run for the duration of the tracer experiment using measured wind speed and direction data; the winds were predominantly from the east and north during the first few days after injection of the tracer particles. The numerical model showed that the depth-averaged, wind-driven velocities in the lake were typically of the order of 0.1 m s^{-1} and that the winds set up a flow which generated a large gyre to the south-west of the river mouth. The centre of this gyre corresponded with the location of the tracer particle maximum in the bed sediment. The secondary tracer particle maximum in the northern area corresponded to a region of very slack currents to the south-east of the river mouth. Wave-induced stresses increased with wind speed during the few days following injection but never exceeded 0.2 Pa in the area of maximum concentration in the northern region or 0.4 Pa in the area of secondary concentration maximum. Remobilization of the tracer was unlikely at these stresses.

Geomorphology and Sedimentology of Lakes and Reservoirs. Edited by J. McManus and R. W. Duck
© 1993 John Wiley & Sons Ltd

INTRODUCTION

There is a growing awareness of the role that sediments play in pollutant transport dynamics and eutrophication within lakes (Michler *et al.*, 1980; Vass, 1980; Zullig, 1982; Buffle *et al.*, 1987; Lemmin and Imboden, 1987; Salomons *et al.*, 1987). An ability to predict cohesive sediment transport within lacustrine waters is, therefore, of great importance, both economically and ecologically. Unfortunately, the processes that influence lake sediment dynamics—for example, deposition, consolidation, erosion and subsequent transport—are at present only partially understood.

The purpose of this chapter is to present results of a particle tracing experiment in Loe Pool, a small, shallow lake in south-west England (50°4'N, 5°17'W, Figure 10.1).

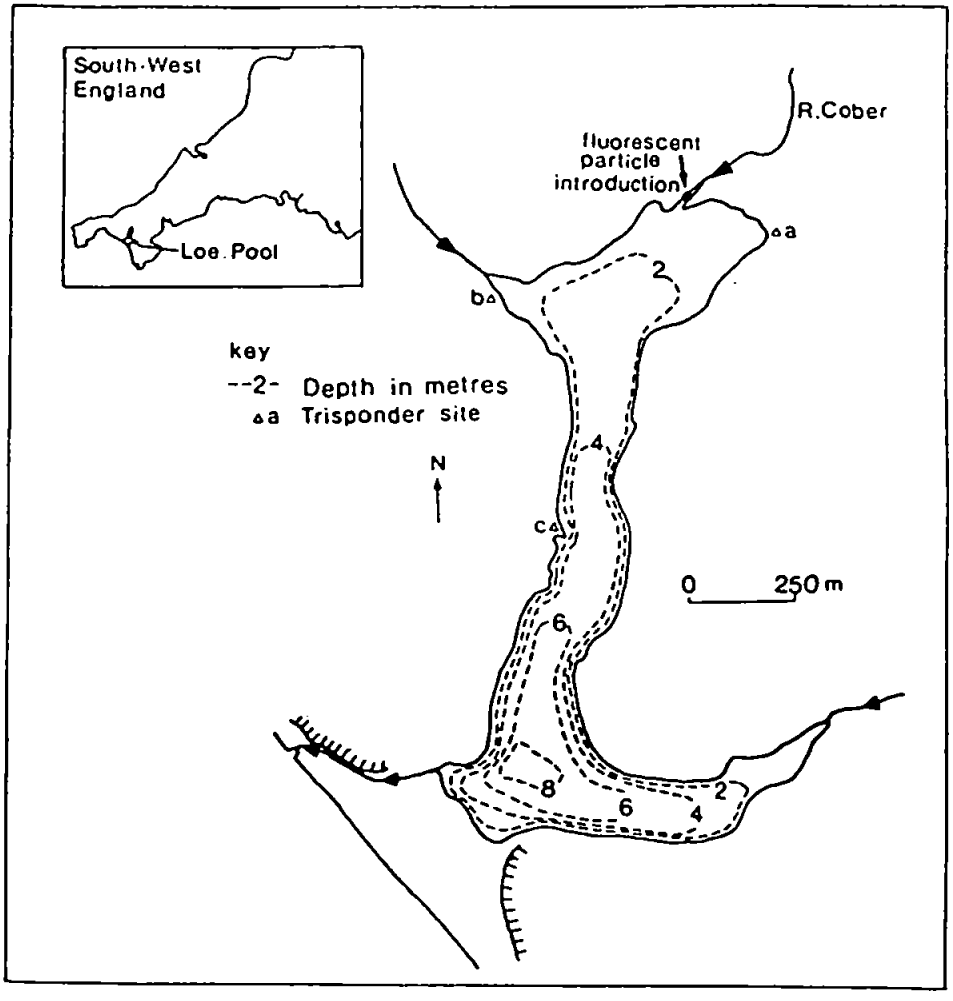

Figure 10.1 Location of Loe Pool and a chart of the bathymetry giving depths in metres. The injection site within the River Cober is shown, together with the locations of the positional trisponders (a, b, c)

A comprehensive examination of the lake sediments (O'Sullivan, Coard and Pickering 1982; Coard, 1987; Pickering, 1987; Coard, 1987) indicates that Loe Pool has become increasingly eutrophic throughout the 20th century due to nutrient enrichment, particularly from agricultural and sewage waste (O'Sullivan, 1990). Nutrients are adsorbed within the bed sediment due to the high adsorptive capacity of the cohesive sediment, and are remobilized during storm events (Ryding and Forsberg, 1977; Gelencser *et al.*, 1982; Ryding and Forsberg, 1977; Luettich, Harlemann and Somlyody, 1990). Reynolds (1979) has suggested that algal blooms often follow a period of windy weather; it is a reasonable hypothesis that the nuisance algal blooms experienced in Loe Pool since 1968 are related to wind-induced resuspension of nutrient-rich bed sediment.

STUDY SITE

Loe Pool is a shallow, eutrophic, freshwater coastal lake on the south coast of Cornwall, south-west England (Figure 10.1). The surface area of the lake is approximately 5.8×10^6 m^2 and the average depth is 3.3 m. During this study the average depth was 3.6 m and the lake volume was 2.1×10^6 m^3. The shallowness of the lake in conjunction with wind-induced mixing prevents prolonged thermal stratification.

The bathymetry of Loe Pool is such that bed slopes are of low gradient (Figure 10.1), whereas the hills surrounding the pool are steep in places, rising to 60–70 m. This suggests that Loe Pool was originally a deep lake with steep sides and that it has infilled with both marine and fluvial sediments. In the upper basin, deltaic deposits occur at the river mouth. There is an increase in depth with distance from the river mouth, to a maximum of 10 m immediately north of Loe Bar.

The lake catchment is drained by three main rivers of which the River Cober drains 73% and provides 93% of the water entering the lake. The average rate of flow of the Cober between 1972 and 1988 was 1.0 m^3 s^{-1}. The residence time of the lake waters (defined as the lake volume divided by the rate of river inflow assuming complete mixing) varies from a minimum of eight days during winter to a maximum of 150 days during summer.

The lake bed surface consists of a 0.2–0.6 m layer of unconsolidated brown, intermittently laminated, highly bioturbated sediment. It is a highly organic gyttja, with light and dark brown laminations just below the surface (top 0–0.05 m). The density is $1.1–1.2 \times 10^3$ kg m^{-3}, with a water content of 80–90%. The sedimentation rate is 1 kg m^{-2} yr^{-1} (Pickering, 1987). A red clay—brown gyttja boundary beneath the surface sediment marks the end of tin mining in this area and can be used to determine long term sedimentation patterns (O'Sullivan, Coard and Pickering, 1982; Pickering, 1987).

Contours of the thickness of the surface sediment layer estimated from 36 cores are indicated in Figure 10.2 (O'Sullivan et al., 1982), Coard and Pickering; 1982) This shows that there has been increased sediment deposition at the north end of the lake, where the lake width begins to narrow, suggesting a hydrodynamic control in this area. Sediment deposition rates are generally lower elsewhere in the lake, although there is a localized maximum in the deepest part of the lake.

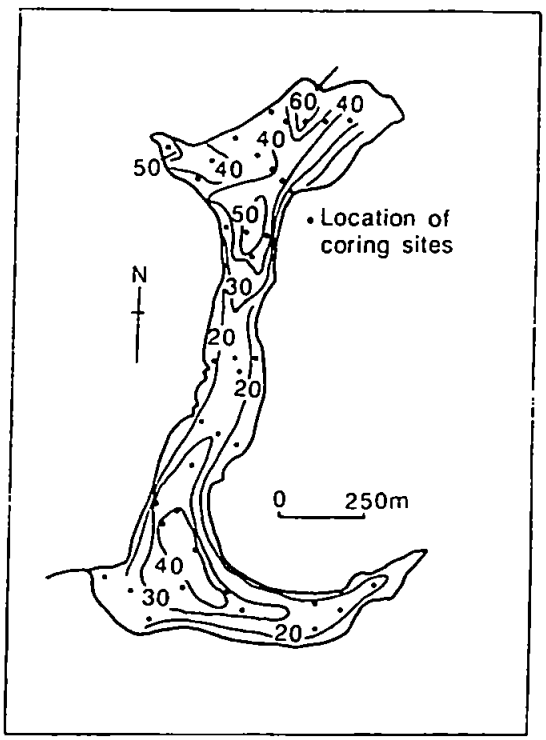

Figure 10.2 Isopach map of the brown-clay surface sediment of Loe Pool produced by multiple coring. Units in centimetres (From O'Sullivan, Coard and Pickering (1982) by permission

PARTICLE TRACING EXPERIMENT

Before the tracing programme, the transmitters of a Trisponder navigational system were installed at positions a, b and c in Figure 10.1 to allow the precise determination of sampling sites. Samples were taken to determine the intensity of background fluorescence in the water and bottom sediment before the experiment. An injection of 5.3 kg of tracer particles in a slurry of a detergent and Loe Pool water was made at the mouth of the River Cober (Figure 10.1) at 2000 hours on 28 April 1990 under windless conditions and with an absence of surface waves. The particle size range was from 0.1 to 20mm with a mode of 3μm.

The system was then left for three days before the surface layer (about the top 0.2 m) of the lake bed was systematically cored using a small gravity corer. As the tracer particles are negatively buoyant with a still-water settling time within the lake of the order of several hours, sampling was undertaken with much greater frequency in the area immediately surrounding the River Cober inlet and along the northernmost stretch of the lake (typically one sample per 25 × 25 m grid). Fewer samples were taken in the south of the lake (typically one sample per 35 × 35 m grid). Over 760 core samples were collected during the subsequent 20 day study period and returned

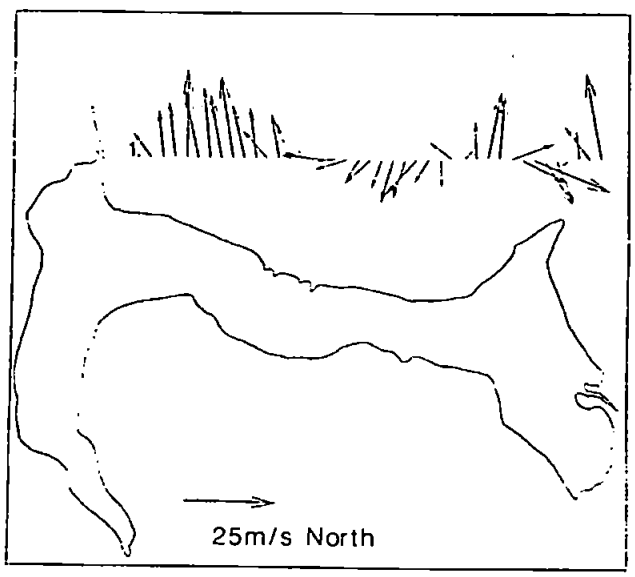

Figure 10.3 Twelve hour averaged wind velocity vectors, one for each half-day period following injection for the duration of the experiment. Note that west is vertically upwards on this diagram; wind arrow 1 relates to the first 12 hour period after injection.

for laboratory analysis using an analytical flow cytometer (AFC). Details of the tracer material and the analytical methods are given in Marsh *et al.* (1991).

The river flow and water level decreased steadily during the study period from 20 April onwards. The decrease in river flow caused the residence time for the water to increase from 50 to 130 days. The estimated river flow at Helston fell from a maximum of 0.52 $m^3 s^{-1}$ at the beginning of the study period to 0.19 $m^3 s^{-1}$ at the end. The wind speed and direction were measured during the experiment 1 km away at a military airfield, RNAS Culdrose, at a height of 100 m above sea level. However, these data provided only a rough guide to the prevailing winds at Loe Pool as the local topography modified the wind. The wind vectors, averaged over half-day periods for the duration of the study period, are shown in Figure 10.3. For the first week the wind was predominantly from the ENE and reached 15 m s^{-1}. Wind arrow 1 in Figure 10.3 relates to the first 12 hour period after injection.

A hydrodynamic model of the circulation was used to interpret the tracer particle movements. The model is described in the Appendix, together with the relationships used to estimate wave-induced shear stresses at the bed. As a result of the shallowness of the lake, particularly in the northern region (Figure 10.1) a depth-averaged circulation model was used.

RESULTS

Contours representing the number of tracer particles found per square centimetre of lake bed are presented in Figure 10.4. These show that two well defined concentration

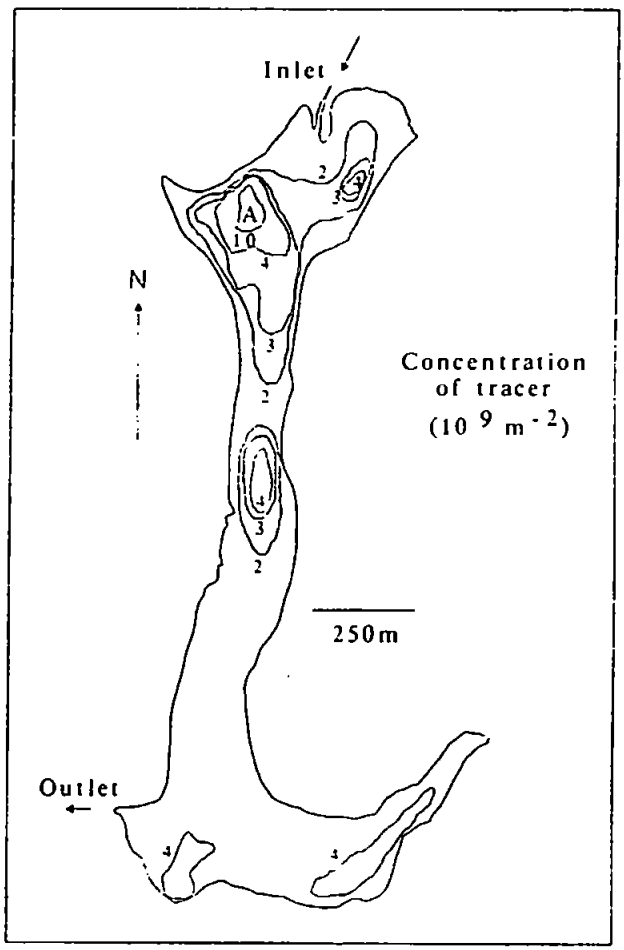

Figure 10.4 Measured tracer particle concentrations in the bed sediment of Loe Pool. The units are 10^9 particles per m^2 of bed. A denotes the main area of accumulation

maxima occurred in the northern part of the lake. The dominant region of accumulation was south-west of the river inlet and is marked as A in Figure 10.4; here, concentrations were in excess of 1×10^{10} particles m^{-2}. The secondary area of accumulation in the northern region occurred to the south-east of the river inlet; here, concentrations reached 4×10^9 particles m^{-2}. Most of the tracer particles were accumulated between 150 and 225m from the injection site.

A third less prominent region of accumulation occurred approximately half-way along the lake; here, concentrations reached 4×10^9 particles m^{-2}. Concentrations in the southern area of lake bed, close to Loe Bar (Figure 10.1), were typically 3×10^9 particles m^{-2}, but no clear patterns could be observed.

Tracer particle size and fluorescence were determined simultaneously using analytical flow cytometry, (Marsh *et al.*, 1991). Tracer particle size varied with distance from the mouth of the River Cober (Figure 10.5). There was a significant spatial

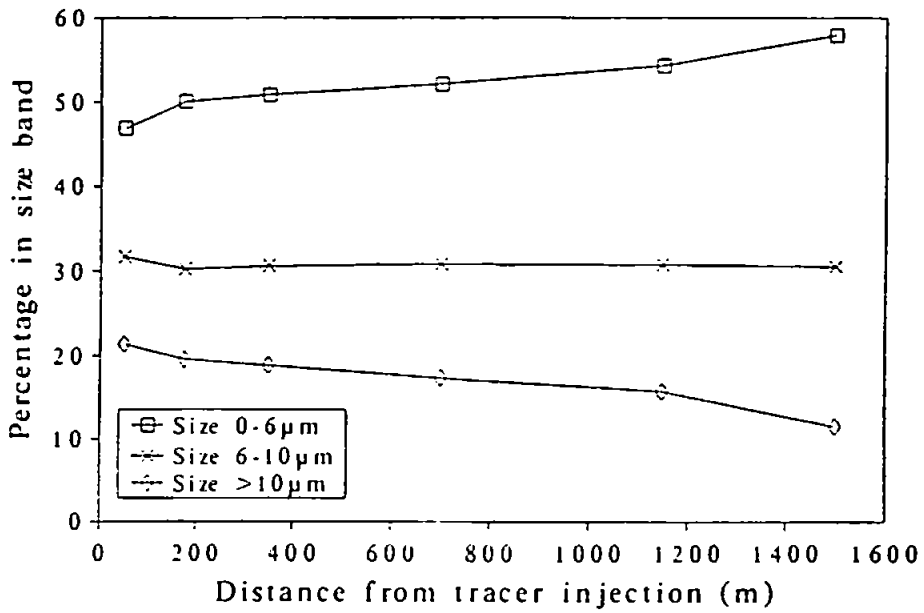

Figure 10.5 Tracer particle size distribution (percentage weight in size bands 0–6, 6–10 and 10–20 μm of the recovered bed sediment tracer) as a function of distance from injection point

sorting of the smallest tracer particles from the injection site, with the percentage by weight recovered in the smallest size band (0–6 cm) increasing by 11% over the 1600 m distance from the tracer injection site. Associated with this was an 11% decrease in the percentage recovered in the largest size band (>10 μm).

A budget of recovered tracer particles showed that approximately 90% by weight of the total 3.8×10^{14} recovered particles were found in the northern area. Initially, 5.3 kg of tracer particles were injected. Microscopy and analytical flow cytomet indicated that the main particle population consisted of particles in the size range 2–4 μm (smaller than the manufacturer's specified size of 4–6 μm) and possessing an angular and platy structure. Microscopy analysis of several samples indicated an average length of 3.25 μm and a volume of 10–15 μm^3.

The tracer particle density was 1.37×10^3 kg m^{-3}. Therefore, 5.3 kg of injected tracer particles (where one particle weighed 1.8×10^{-14} kg) was equivalent to 2.9×10^{14} particles. The difference between this number and the estimated recovered number of 3.8×10^{14} was consistent with the errors associated with the sampling and analytical technique.

DISCUSSION

Both the recent sedimentology of Loe Pool (Figure 10.2) and the observed tracer particle concentrations (Figure 10.4) showed enhanced deposition rates in the northern region, although the detailed patterns of accumulation were different. However,

the tracer represented an instantaneous injection, whereas the brownclay surficial sediment was an accumulation that had occurred over more than 40 years. In addition, much of the natural sediment entering the lake would have done so during spate conditions when water circulation patterns might have been very different from those experienced during the tracer experiment.

During the first few days following the injection of the tracer particles, the winds were predominantly from the east and north (Figure 10.3). The depth-averaged, wind-driven circulation in the lake, predicted by the hydrodynamic model for a 15 m s^{-1} northerly wind and a 13 m s^{-1} easterly wind are shown in Figure 10.6. Maximum

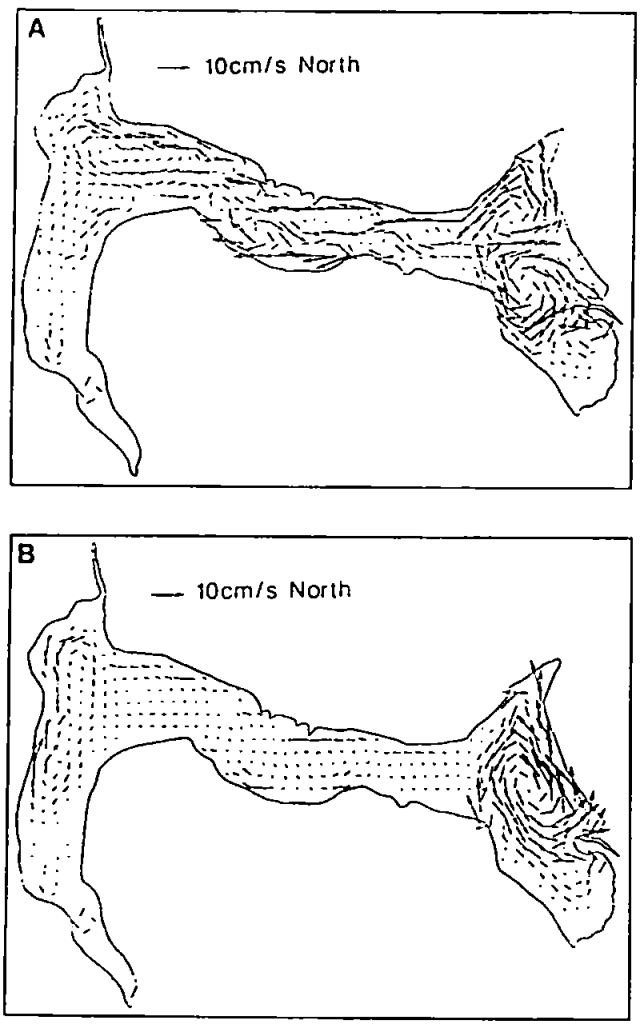

Figure 10.6 Modelled depth-averaged, wind-driven water circulation within Loe Pool for a 15 m s^{-1} northerly wind (A) and a 13 m s^{-1} easterly wind (B). Note that west is vertically upwards on these diagrams

current speeds were of the order of 0.1 m s^{-1} and the shallow northern part of the lake showed a particularly strong circulation.

In the case of a northerly wind, the circulation within the norther area of the lake consisted of two strong, opposing gyres, one almost due south of the river inlet and the other southeast of the inlet. For an easterly wind, there was a strong gyre to the south-west of the river inlet and a much weaker gyre to the east of the river inlet. It is likely that an easterly wind, recorded on high ground, will be deflected in the river valley and will tend to have a significant northerly component locally. Therefore, we expect that winds from the north and east will tend to generate a double-gyre circulation pattern in this northern area similar to that shown in Figure 10.6A.

Reversing the wind directions (i.e. southerly or westerly winds) tends to reverse the currents generated by northerly and easterly winds shown in Figure 10.6. Ignoring advective accelerations in the hydrodynamic equations (see Appendix), then multiplying these equations throughout by -1 leads to the same equations and solutions, but with reversed velocities and surface elevations, providing the wind stress is also reversed.

The model was run for the duration of the tracer experiment using measured river run-off and wind speed data. The calculated circulation patterns for the first two half-days following the injection of the tracer particles, when the wind was mainly easterly (Figure 10.3), are shown in Figure 10.7. A large gyre existed to the south-west of the river mouth. The centre of this gyre corresponded with the location of the tracer particle maximum observed in the bed sediment (A in Figure 10.4). The secondary tracer particle maximum in the northern area corresponded to the region of very slack currents predicated by the model close to the shoreline, south-east of the river mouth.

The settling time of the tracer particles, assuming Stokes settling, was of the order of several hours in this shallow, northern area. Thus, particles leaving the river inlet, following the injection, were carried westwards in the northern section of the gyre (Figure 7A) and advected back around to the east in the gyre arms. Particles sinking in the arms of the gyre were swept into the centre because centrifugal forces on the tracer particles within the gyres dominated both frictional forces and Coriolis forces. Therefore, the pressure gradients drove the water and tracer particles into the gyre centre near the bed because of the reduced centrifugal accelerations in the slower, near-bed currents. This occurred regardless of the sense of rotation of the gyre.

The circulation patterns remained similar but increased in strength during the first few days after injection, so that the tracer particles experienced a fairly stable flow field for a much longer period than their settling time. Those particles which advected to the south before settling to the bed experienced a number of gyres (Figure 10.7B). The first major gyre outside of the northern region, approximately half-way down the lake, corresponded with the concentration maximum shown in Figure 10.4.

The wave-stress model (presented in the Appendix) was used to simulate bed shear stresses due to waves during the course of the experiment. Bed shear stresses for the first and second half-days following injection are contoured in Figure 10.8 A comparison with Figure 10.4 shows that the tracer particle maxima in the northern region occurred in those areas where accumulation was expected due to water circulation and where modelled bed shear stresses were less than 0.1 Pa. Stresses in very shallow water (less than 0.5 m) were much higher and of the order of 1 Pa.

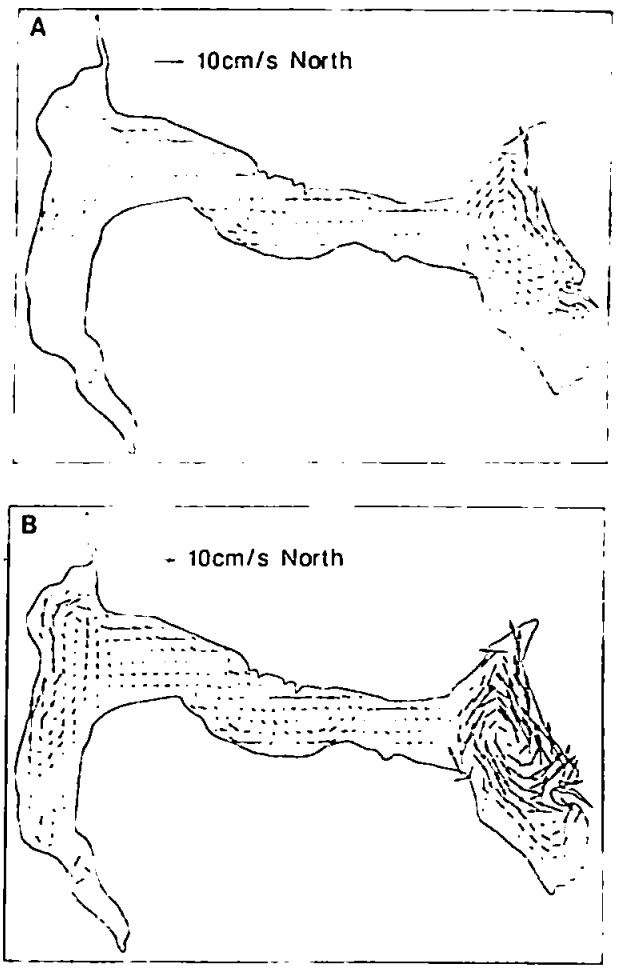

Figure 10.7 Modelled depth-averaged, wind-driven water circulation within Loe Pool for the first half-day following injection (A) and the second half-day following injection (B). Note that west is vertically upwards on these diagrams

The wave-induced stresses increased with wind speed during the few days following injection but never exceeded 0.2 Pa in the area of maximum tracer concentration (A in Figure 10.4) or 0.4 Pa in the area of the secondary concentration maximum in the northern region. Even if resuspension of deposited tracer particles had occurred due to strong winds and wave activity, the wind-driven flow patterns would have tended to maintain tracer particles in the northern region becoming concentrated within the gyre system.

Maximum wave-induced bed shear stresses occurred near the end of the sampling period (Figure 10.3) when a 25 m s^{-1} wind blew from the south-west and the fetch was at a maximum. Stresses reached 0.4 Pa in the area of maximum concentration and 0.8 Pa in the area of secondary maximum concentration.

sediment) would be predicted for a considerable period of time following the initial deposition. However, some resuspension was likely to have occurred near the end of the sampling period.

CONCLUSIONS

A tracer particle experiment has been undertaken in Loe Pool, a small shallow lake in south west England. The particles were injected into the main river inflow to the north of the lake and the resultant pattern of particle deposition interpreted using a depth-averaged hydrodynamic model of the wind-driven circulation within the lake. The following conclusions were drawn.

1. High concentrations of tracer particles (particles per m^2 of bed sediment) occurred in the northern region with two well defined maxima. The accumulation of the natural, brown clay sediment of Loe Pool showed some similarity to the tracer particle concentrations in the northern region of the lake, although differences existed. However, most of the natural sediment would have entered the lake during spate conditions when the circulation might have been different from that predicted for the experiment.
2. Most of the tracer particles were deposited between 150 and 225 m from the injection site. There was a significant spatial variation for the particle size range <20 μm along the lake. The percentage by weight in the smallest size band increased by 11% over the 1600 m distance from the tracer injection site, with an 11% decrease in the percentage in the largest size band. The smallest particles tended to travel furthest from the injection site before deposition.
3. A budget of recovered tracer particles showed that approximately 90% by weight were found in the northern region. The estimated number of 'recovered' particles was 3.8×10^{14}. The estimated number of injected tracer particles was 2.9×10^{14} The difference is consistent with the errors associated with sampling and the analytical technique.
4. The winds were predominantly from the east and north during the first few days after injection of the tracer particles. A numerical model showed that the depth-averaged, wind-driven circulation in the lake was typically of the order of 0.1 m s^{-1} and that the shallow, northern part of the lake had a particularly strong circulation.
5. During the first two half-days following the injection of the tracer particles, when the wind was mainly easterly, a large gyre existed to the south-west of the river mouth. The centre of this gyre corresponded with the location of the tracer particle maximum in the bed sediment. The secondary tracer particle maximum in the northern region corresponded to a region of very slack currents to the south-east of the river inlet. These circulation patterns remained similar but stronger during the first few days after injection, so that the tracer particles experienced a fairly stable flow field for a much longer period than their settling time.
6. Simulated bed shear stresses for the first and second half-days following injection indicated that the tracer particle maxima occurred in areas of hydrodynamic

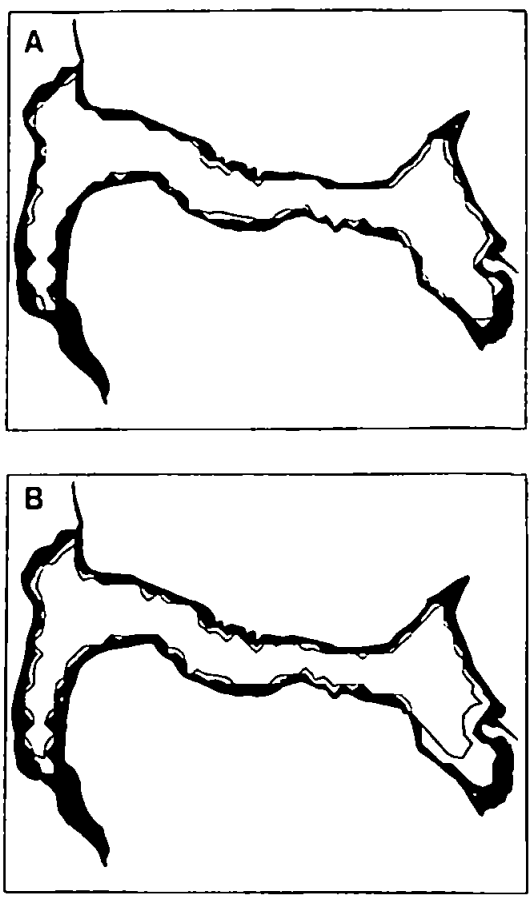

Figure 10.8 Modelled wave-induced, bed shear stress within Loe Pool for the first half-day following injection (A) and the second half-day following injection (B). The shaded area denotes the region where predicted shear stresses are equal or greater than 1 Pa due to the shallow water. The 0.1 Pa contour is shown when it is distinguishable from the higher shear stresses. Note that west is vertically upwards on these diagrams

The surface sediments within Loe Pool typically have water contents of 80–90% (Coard, 1987). The corresponding dry density is approximately 100–230 kg m^{-3} and the critical bed shear strength for erosion is estimated to be 0.3–0.8 Pa (Delo, 1988). However, these data should be viewed with caution because the bed sediments are likely to be viscoelastic (and bioturbated) and their strength properties dependent on factors other than simply dry density. Moreover, the strength of the natural sediment will increase dramatically beneath the top few millimetres.

It is likely that the deposited tracer particles became incorporated within the natural bed sediment, partly as a result of particle cohesion and occupation of interstices and partly because of bioturbation. On the basis of the wind–wave modelling and assuming that the tracer particles became incorporated within the natural surface sediment, minimal remobilization of the deposited tracer particles (and natural

accumulation where, in addition, the bed shear stresses were less than 0.1 Pa. These wave-induced stresses increased with wind speed during the following few days but, in the northern region, never exceeded 0.2 Pa in the area of maximum concentration or 0.4 Pa in the area of secondary concentration maximum.

7. Maximum wave-induced bed shear stresses occurred near the end of the sampling period when a 25 m s^{-1} wind blew from the south-west and the fetch was at maximum. Stresses reached 0.4 Pa in the area of maximum concentration and 0.8 Pa in the area of secondary maximum concentration. Assuming that the deposited tracer particles were incorporated within the natural sediment, minimal remobilization of the deposited sediment would be expected for a considerable period of time following the initial deposition.

REFERENCES

Buffle, J., Zali, O., Zumstein, J. and Devitre, R. (1987). Analytical methods for the direct determination of inorganic and organic species—seasonal changes of iron, sulphur and pedogenic and aquagenic organic constituents in the eutrophic Lake Bret, Switzerland, *Science of the Total Environment*, 64, 41–59.

Coard, M. A. (1987). Palaeolimnological study of the history of Loe Pool, Helston, and its catchment, *PhD Thesis*, Polytechnic Southwest.

Delo, E. A. (1988). Estuarine muds manual, *Report No. SR164*, Hydraulics Research Ltd.

Dyer, K. R. (1986). *Coastal and Estuarine Sediment Dynamics*; Wiley.

Gelencser, P., Szilagyi, F., Somlyody, L. and Lijklema, L. (1982). A study on the influence of sediment in the phosphorus cycle in Lake Balaton, *Collaborative Paper CP–82–44*; International Institute of Applied Systems Analysts.

Hakanson, L. and Jansson, M. (1983). *Principles of Lake Sedimentology*; Springer.

Komar, P. D. and Miller, M. C. (1973). The threshold of sediment movement under oscillatory water waves, *Journal of Sedimentary Petrology*, 43, 1101–1110.

Lemmin, U. and Imboden, D. M. (1987). Dynamics of bottom currents in a small lake, *Limnology and Oceanography*, 32, 62–75.

Luettich, R. A. Jr, Harlemann, D. R. F. and Somlyody, L. (1990). Dynamic behaviour of suspended sediment concentrations in a shallow lake perturbed by episodic wind events, *Limnology and Oceanography*, 35, 1050–1067.

Marsh, J. K., Bale, A. J., Uncles, R. J. and Dyer, K. R. (1991) A tracer technique for the study of suspended sediment dynamics in aquatic environments. In: *Proceedings of the International Association for Hydraulic Research, International Symposium on the Transport of Suspended Sediments and its Mathematical Modelling, Florence Italy, 2–5 September 1991*, pp. 665–682.

Michler, G., Simon, K., Wilhelm F. and Steinberg, C. (1980). Vertical distribution of metals in a sediment core of a subalpine lake indicating stages in the development of civilization; *Archives for Hydrobiology*, 88, 24–44.

O'Sullivan, P. E. (1990). The eutrophication of shallow coastal lakes in southwest England—understanding, and recommendations for restoration based on palaeolimnology, historical records, and the modelling of changing phosphorus loads, paper presented at the *40th Anniversary Congress of the Finnish Limnological Society, Helsinki, Finland, 5–11 August 1990.*

O'Sullivan, P. E. Coard, M. A. and Pickering, D. A. (1982). The use of laminated sediments in the estimation and calibration of erosion rates. In: *Recent Developments in the Explanation and Prediction of Erosion and Sediment Yield (Proceedings of the Exeter Symposium, July 1982)*: I.A.H.S. Publication 137, 385–396.

Pickering, D. A.. (1987). Chemical and physical analysis of laminated sediment formed in Loe Pool, Cornwall, *PhD Thesis*, Polytechnic Southwest.

Pond, S. and Pickard, G. L. (1983). *Introductory Dynamical Oceanography*. 2nd edn. Pergamon Press.
Reynolds, C. S. (1979). The limnology of the eutrophic meres of the Shropshire–Cheshire Plain. *Field Studies*, 5, 93–173.
Ryding, S. O. and Forsberg, C. (1977). Sediments as a nutrient source in shallow polluted lakes. In: *Interactions Between Sediments and Freshwater*. (Ed. H. L. Gotterman). Dr. W. Junk, pp. 227–234.
Salomons, W., de Rooij, N., Kerdijk, H. and Bril, J. (1987). Sediment as a source for contaminants. *Hydrobiologia*, 149, 13–30.
Sleath, J. F. A. (1984). *Sea Bed Mechanics*. Wiley.
Smith, I. R. and Sinclair, I. J. (1972). Deep water waves in lakes. *Freshwater Biology*, 2, 387–399.
Soulsby, R. L. and Smallman, J. V. (1986). A direct method of calculating bottom orbital velocity under waves. *Report No. SR76*. Hydraulics Research Ltd.
Sverdrup, H. U. and Munk, W. H. (1947). Wind, sea and swell: theory of relations for forecasting: *Publication No. 601*. United States Hydrographic Office, p.44.
Uncles, R. J. (1982). Computed and observed residual currents in the Bristol Channel. *Oceanologica Acta*, 5 11–20.
Uncles, R. J., Jordan, M. B. and Taylor, A. H. (1986). Temporal variability of elevations, currents and salinity in a well-mixed estuary. In: *Estuarine Variability* (Ed. D. A. Wolfe). Academic Press, 509pp.
Vass, K. K. (1980). The trophic status and conservation of Kashmir Lakes. *Hydrobiologia*, 68, 9–15.
Zullig, H. (1982). The development of the holiday resort of St. Moritz reflected in the sediment deposits of the lake of St. Moritz. *Wasser, Energie, Luft*, 74, 177–183.

APPENDIX: HYDRODYNAMIC MODEL OF WIND-DRIVEN CIRCULATION

Depth-averaged Equations of Flow

Wind stress drives a circulation of water within the lake which depends on the magnitude and direction of the stress, the shoreline shape and bathymetry. The near-surface waters and the whole water column in shallower areas will tend to move in the direction of the wind stress, the reverse being true in the near-bed waters, especially in the deeper areas. However, in a very shallow lake such as Loe Pool, it is reasonable to estimate the depth-averaged currents using a depth-integrated model of the flow. In small shallow lakes the earth's rotation (Coriolis force) is generally assumed to be negligible, with the principal driving force for bottom currents being wind setup (Lemmin and Imboden, 1987), although we include Coriolis force in this model.

Ignoring density differences within the lake and horizontal viscosity, the depth-averaged equations of continuity and momentum are, respectively (Uncles, 1982):

$$\partial\zeta/\partial t = -\nabla(hv)$$

and

$$\partial v/\partial t = -(v\nabla)v - g\nabla\zeta - fxv + \tau_w - Dv|v|/h$$

where t is time, g is the acceleration due to gravity, ζ is the surface elevation, h total depth, v is the depth-averaged velocity, f is the Coriolis parameter ($1 \times 10^{-4}\ s^{-1}$), D the bottom drag coefficient (2.5×10^{-3}), W the wind velocity and τ_w the surface wind stress, where:

$$\tau_w = \rho_a C_D W|W|$$

with ρ_a the density of air and $C_D = 3 \times 10^{-3} \pm 50\%$ (Uncles, Jordan and Taylor, 1986).

are largely dependent on the extent of preferential flood or ebb transport of SPM by the tidal currents (Uncles et al., 1985a,b,c; Uncles et al., 1988; Uncles and Stephens, 1989).

Intratidal variations in water-column SPM and salinity stratification, and therefore stability and vertical mixing, also play a role in fine-sediment transport and turbidity maximum formation (Hamblin, 1989; Uncles and Stephens, 1989; Sheng and Villaret, 1989; Wolanski et al., 1988; Dronkers, 1986; Kirby and Parker, 1977) as does the supply of fine sediment (Grabemann and Krause, 1989). The importance of tidal erosion-deposition mechanisms in the Tamar and the control exerted by the tidally-induced, bed-shear stresses has recently been reconfirmed by West and Sangodoyin (1991) who, in addition, found similar results for two other partially-mixed, macrotidal estuaries in the UK. West et al. (1991) have also shown from measurements of turbulence in the Tamar that vertical density gradients affect the velocity field, thereby confirming experimentally the theoretical expectation (Hamblin, 1989; Uncles and Stephens, 1989) that water-column stability does have the potential to modify fine sediment transport and turbidity maximum formation.

In this paper we attempt to further enhance our understanding of processes affecting fine-sediment transport and turbidity maximum formation by presenting the results of an experiment in which the salinity, longitudinal velocity, SPM concentration and transport of SPM were measured synoptically in the Tamar Estuary over a spring-tide tidal cycle during the summer of 1990.

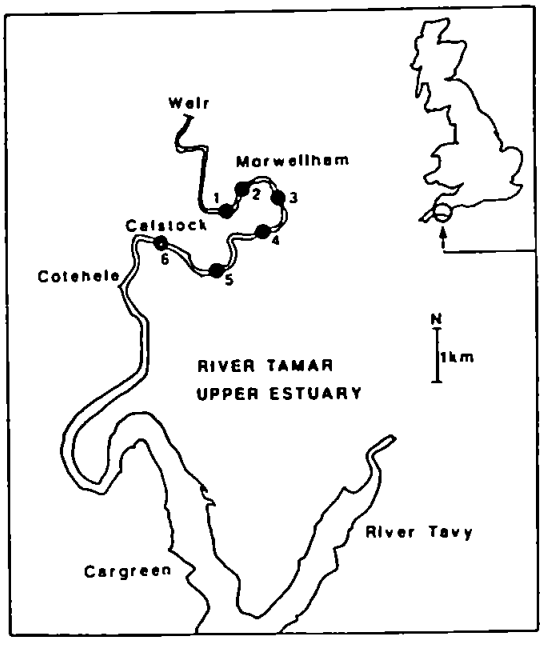

Figure 1. Map of the upper Tamar Estuary showing the locations of synoptic Stations 1 to 6 and those of the near-bed instrument packages at Stations 3 and 5.

International Symposium on
THE TRANSPORT OF SUSPENDED SEDIMENTS AND ITS MATHEMATICAL MODELLING
Florence (Italy), September 2-5, 1991

A TRACER TECHNIQUE FOR THE STUDY OF SUSPENDED SEDIMENT DYNAMICS IN AQUATIC ENVIRONMENTS

J.K. MARSH[†,‡], A.J. BALE[†], R.J. UNCLES[†] and K.R. DYER[‡]

† - Plymouth Marine Laboratory, West Hoe, Plymouth, UK

‡ - Institute of Marine Studies, Polytechnic Southwest, Plymouth, UK

SUMMARY

Two field experiments are described which use a fluorescent tracer particle possessing physical characteristics of mean size, particle fall velocity, density and surface charge similar to natural suspended particulate matter in many aquatic environments. The fluorescent tracer particles were detected using flow cytometry. In the freshwater environment of Loe Pool, the measured locations of the tracer particle maxima agreed closely with that predicted by a hydrodynamical model. Tracer particles injected into the Tamar Estuary were found to advect with the tidal currents and remained strongly associated with the saline intrusion. Some tracer particles were deposited on the inter-tidal mudflats in the upper reaches during the ebb and in the lower reaches at low-water slack. The freshwater residence time for the turbidity maximum region of the Tamar was approximately 3 days. However, the tracer was detectable during the neap tide one week after the initial injection, despite low rates of resuspension of bed sediment. This implies that some of the tracer particles had become incorporated within the natural flocs during the course of time and were associated with the turbidity maximum and the saline intrusion.

INTRODUCTION

Fine suspended sediments have a high adsorptive capacity for dissolved pollutants (Mehta, 1984; Lamere Hennessee *et al.*, 1986; Dyer, 1989). This knowledge has led, in recent years, to a proliferation of studies in aquatic environments examining the processes and mechanisms controlling sediment particle dynamics and cycling of contaminants. Despite extensive work these processes are still poorly understood.

Sediment dispersal can be examined using both natural and artificial tracer particle, enabling the locations of both contaminant sources and sinks to be identified (Salomons & Mook, 1987). Previous tracer work has predominantly used soluble fluorescent dyes for the study of water mass

transport. Radioactive or large fluorescent grains have been used for sediment particle tracing. Automated analysis and counting for tracer particle studies have in the past been both labour intensive and insensitive. A new tracing technique presented by Newman *et al.* (1990 a,b) and Spanhoff & Suijlen (1990) involved the use of Analytical Flow Cytometry (AFC) as a tool for fluorescent particle detection.

The work described here summarises two field studies initiated in Plymouth during 1988 as an integral part of a programme on coastal, cohesive sediment dynamics. AFC was used for the rapid characterisation of an artificial, fluorescent tracer particle in turbid suspensions in Loe Pool, a freshwater lake, and the Tamar Estuary, a macrotidal estuary.

Comparison of natural SPM with tracer particles

The size, density and concentration of sediment particles control their movement and settling behaviour. Clay particle sizes (less than 4μm) and silt (less than 63μm) particles characterise muddy, suspended particulate material (SPM) within many aquatic, dynamic environments (Dyer, 1986). In the turbidity maximum of the Tamar Estuary, fundamental SPM particle sizes fall within the range 0.1-37μm, with the mode between 5-10μm. The surface charge of these estuarine particles, determined by electrophoretic mobility measurements, is negative and agrees closely with values presented by Loder & Liss (1985) for aquatic environments. The main bulk of suspended sediment is transported as flocs, which have a density of approximately 1.1-1.8g cm^{-3} (Dyer, 1986).

The tracer particle used here is similar to that described by Newman *et al.*(1990a) and Spanhoff & Suijlen (1990). It is a highly fluorescent, inert, formaldehyde-resin particle, with a size-range of 0.1-20μm, a mode of 3μm and a density of 1.37g cm^{-3}. Microscopy indicates that the tracer particles have an irregular non-spherical structure with a modal volume of approx. 10-15μm^3.

Settling experiments were carried out in the laboratory using settling tubes similar to those described by Owen (1970), in order to examine the effectiveness of the tracer particle as a sediment analogue in the aquatic environment. Estuarine SPM (M in Figure 1) from the turbidity maximum region of the Tamar Estuary was used. The inclusion of fluorescent tracer particles (B in Figure 1) in the settling column suspensions caused a reduction in the median fall velocity at all salinities (Figure 1) with the effect being more pronounced at low salinities (H. Stevens, *pers. comm.*).

These data suggest that the tracer particles behave more like natural SPM at the higher turbidities which typify estuarine turbidity maxima regions. Barton *et al.* (1991) showed that the measured settling velocities of Tamar Estuary SPM were an order of magnitude less in laboratory than in field experiments. Therefore, the median settling velocities shown in Figure 1 can only be used as a rough guide, although they clearly indicate that the tracer particles have a limited effect on median fall velocities. The median fall velocities for the mud and tracer particle admixture in the laboratory is in the range $1x10^{-5}$m s^{-1} to $1x10^{-3}$m s^{-1} for turbidities 0.3-10.0kg m^{-3}, respectively, at salinities of 0-1ppt (Figure 1).

Detection and Methodology

Flow cytometry uses laser optics to determine the nature of a particle population on a particle-by-particle basis, in terms of light scattering (size) and fluorescence spectra. Extensive calibration and detection

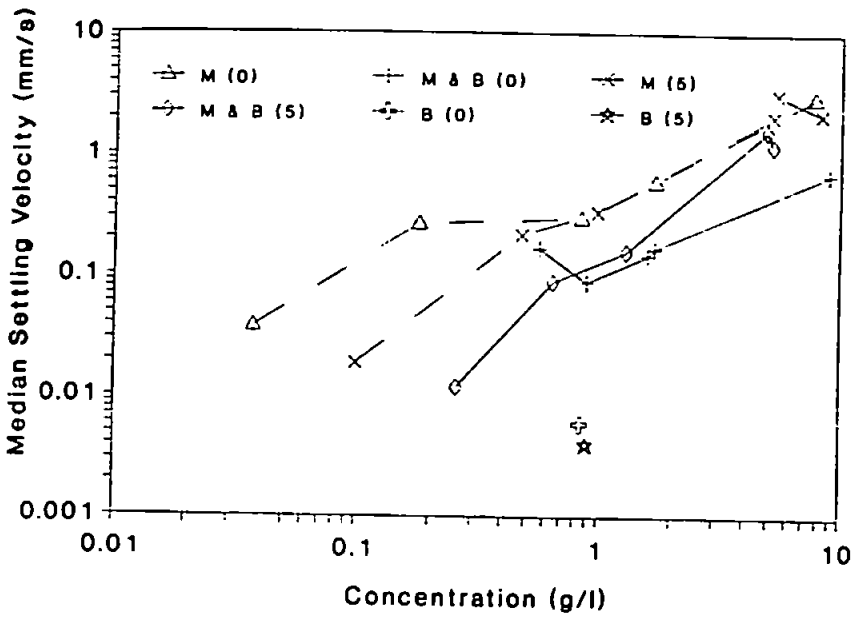

Figure 1. The effects of salinity and concentration on the median settling velocity of estuarine suspended sediment particle (M) and/or tracer particle (B) suspensions at different salinities (0 and 5ppt). Tracer particle suspensions were carried out without SPM at 2 salinities

experiments were carried out to ensure that the fluorescent tracer particle was detectable both in dilute tracer particle suspensions and, more importantly, in turbid sediment suspensions. Detection limits for tracer particles of 1:50,000 natural SPM particles were achieved with a reproducability of ±5%.

Sediment particles from both experimental sites were checked for background fluorescence. In the field the tracer was mixed thoroughly with a laboratory surfactant and diluted with water from the site thus ensuring neutral buoyancy on injection beneath the water surface. Samples of known volume were taken from the water column and (for Loe Pool) from the bed sediment. A gravity corer of known cross-section was used to remove the surface 2cm of sediment. The samples were stored at 4°C prior to analysis.

Samples were diluted, sonified, filtered, sonified again and analysed on the AFC. The total number of tracer particles with fluorescence above a specified background level were counted. The size of each tracer particle was determined simultaneously by reference to calibration beads.

THE LOE POOL EXPERIMENT

Loe Pool is a shallow, freshwater coastal lake (Figure 2) situated in southwest England (50°4'N, 5°17'W). The surface area is approximately 580m^2 and the average depth is 3.3m. The water volume is 2.1x10^{6}m^3. Bathymetry shows increasing depths away from the mouth of the River Cober,

maximizing at 10m in the south. The hills surrounding the Pool are steep in places, rising to 60-70m.

Tracer particles were injected into the lake and a hydrodynamical model used to interpret the observed distributions in terms of the wind-driven circulation measured during the experiment. The model and experimental procedure are described first, followed by an interpretation of the data.

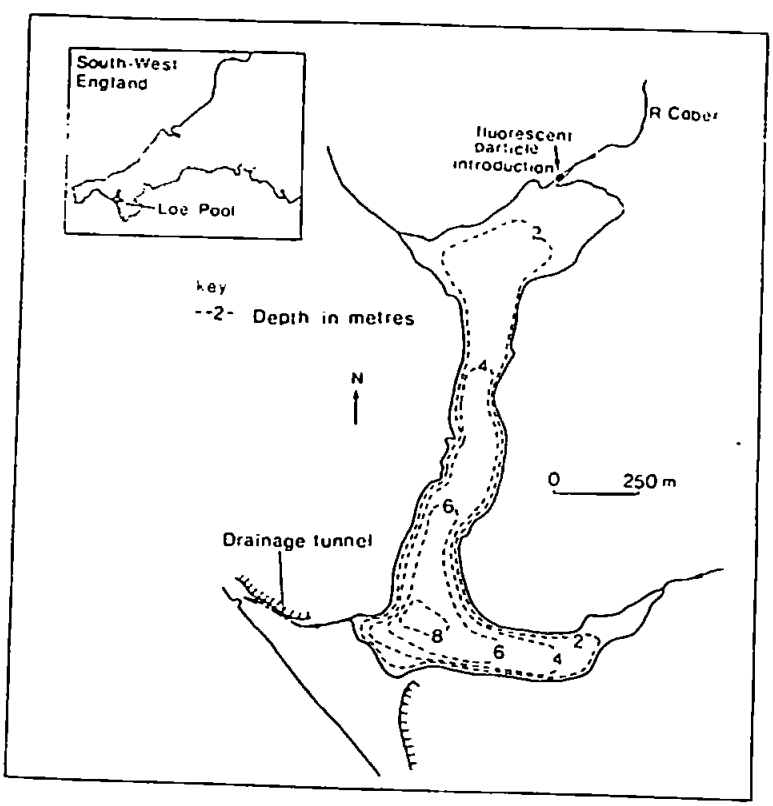

Figure 2. The location, bathymetry and tracer particle injection site for Loe Pool, S.W. Cornwall.

Hydrodynamical model

Wind stress drives the circulation of water within the lake. This circulation depends upon the magnitude and direction of the stress, shoreline shape and bathymetry. A two-dimensional, depth-averaged, hydrodynamical model was used to investigate the wind-driven circulation in Loe Pool. Vertical structure in the currents was ignored because of the shallowness of the lake. The model is fully nonlinear and includes Coriolis effects in the equations of continuity and momentum (Uncles, 1982; Marsh *et al.*, 1991). In addition to these equations, an estimate of the wave-induced shear was made using the simplified equations of Hakanson and Jansson

(1983). A spatially uniform wind speed was assumed. Equations representing the significant wave height, period and wave phase speed were taken to be functions of the fetch and wind speed (Sverdrup and Munk, 1947) and used to compute bed shear stress due to waves.

Experimental procedure

Sampling positions were accurately determined using microwave navigational trisponders. From laboratory determination (Figure 1), a typical tracer particle/SPM admixture at ambient concentrations would settle out in one day in the shallow northern region. Therefore, in the area immediately surrounding the River Cober inlet, sampling was undertaken with much greater frequency (typically one sample per $25m^2$). Fewer samples were taken in the southern part of the lake (typically one sample per 35-$40m^2$). 5kg of tracer particles were injected as a tracer particle/Loe Pool water slurry at the mouth of the River Cober (Figure 2) under windless conditions. The system was left for 3 days before the surface layer (approx. top 2cm) of bed sediment was systematically cored using a small gravity corer. A total of 756 cores were taken for analysis back at the laboratory.

Data on windspeed and direction, river flow and lake water level during the study period were obtained. The river flow decreased steadily during the experiment from a maximum of $0.52m^3\ s^{-1}$ at the beginning, to $0.19m^3\ s^{-1}$ at the end. The lake water residence time exceeded 100 days during the study. Figure 3 shows the wind vectors averaged over half-day periods for the duration of the study. For days 2-5 the wind was predominantly from the ENE. The wind speeds ranged between 10-15m s^{-1} from the east for the first few days after injection of the tracer. Wind arrow 1 in Figure 3 marks the first 12 hour period after injection (time increases from left to right in Figure 3).

Results of the tracer experiment

The high concentrations of tracer particles in the northern region of the lake exceeded $10^{10}m^{-2}$ (Area A in Figure 4) indicating localised accumulation close to the injection site. Tracer particles were detected over a the entire lake but were of low concentration and patchy in the southern area. In this region levels were less than $4x10^9m^{-2}$, except for the two 'hot-spots' shown in Figure 4. There was a significant spatial sorting of the smallest tracer particles with distance from the injection site, with a greater proportion of the smallest particles travelling furthest.

A budget of recovered tracer particles showed that approximately 90% by weight were found in the northern area (surrounding Area A in Figure 4). The estimated number of recovered tracer particles was $3.8x10^{14}$. Initially, 5.3 kg of tracer particles were injected, a total of $2.9x10^{14}$ particles which was within the errors associated with sampling and analytical technique. Assuming the tracer particles to be analogous to natural SPM, then our results imply that approximately 90% of the sediment entering Loe Pool will, in the short-term, remain in this northern area, and by inference many sediment-borne pollutants will accumulate within the deposited sediment there. This result is consistent with the long-term sedimentation data presented by Pickering (1987).

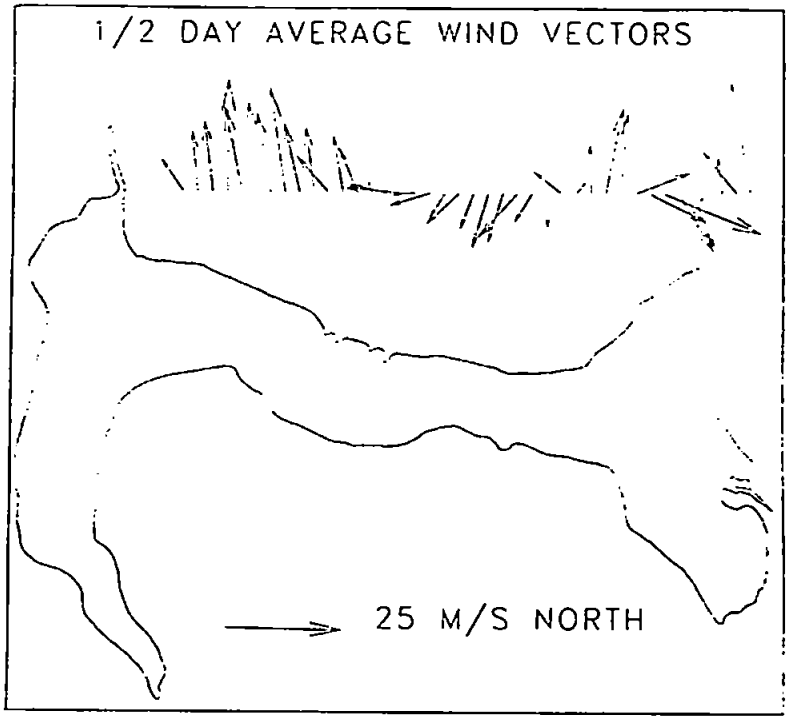

Figure 3. Half-daily wind vectors measured during the study period. Time increases from left to right.

Interpretation of results

Using the hydrodynamical model described above, the wind-driven water circulation patterns were determined for Loe Pool. The winds were predominantly from the east and north during the first few days after injection of the tracer particles (Figure 3). The modelled, depth-averaged, wind-driven circulation in the lake for a 15m s^{-1} northerly wind and a 13m s^{-1} easterly wind, are shown in Figures 5(A,B), respectively. Maximum current speeds are of the order of 0.1m s^{-1}. The shallow, northern part of the lake has a particularly strong circulation.

In the case of a northerly wind (Figure 5(A)), the depth-averaged, modelled circulation within the northern area consists of two strong, opposing gyres; one almost due south of the river mouth and the other to its west. For an easterly wind there is a strong gyre to the south and west of the river mouth and a much weaker gyre to the east of the river mouth.

The model was run for the duration of the experiment using river runoff and wind-speed data measured during the experiment. For the first few days following injection of the tracer particles the wind was mainly easterly (Figure 3) and the centre of the modelled wind-driven gyre corresponded with the location of the tracer particle maximum in the bed sediment (area A in Figure 4). The secondary tracer particle maximum in the region to the north-east of the R. Cober corresponded to the weak, wind-driven gyre in this area.

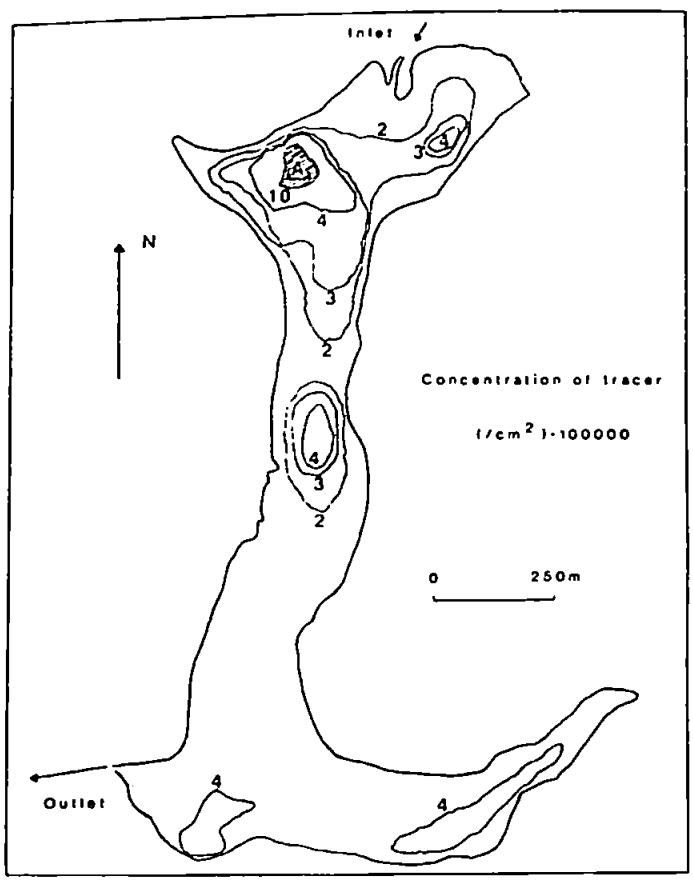

*Figure 4. Bed sediment tracer particle concentrations (units * 10^5 cm^{-2})*

Assuming the predicted currents to be similar to those which occurred during the experiment, then tracer particles leaving the river mouth were carried into the main gyre. These remained there whilst sinking. Particles sinking in the arms of the gyre were swept towards the centre near the bed because near-bed centrifugal forces are smaller than those due to pressure gradients. A convergence occurs, regardless of rotation direction, because the Rossby number, U/fR, is of the order of ten (Dyer, 1986), where R is the gyre radius of 150m, U the velocity of water in the arms of the gyre and f the Coriolis parameter.

The circulation patterns remained similar but stronger during the first few days after injection, so that the tracer particles experienced a fairly stable flow-field for a much longer period than the settling time. Therefore, the tracer particles were deposited on the bed of the lake due to the low bed shear stresses during the experiment.

The wave-stress model was used to simulate bed shear stresses during the course of the experiment. Bed shear stresses for the first day

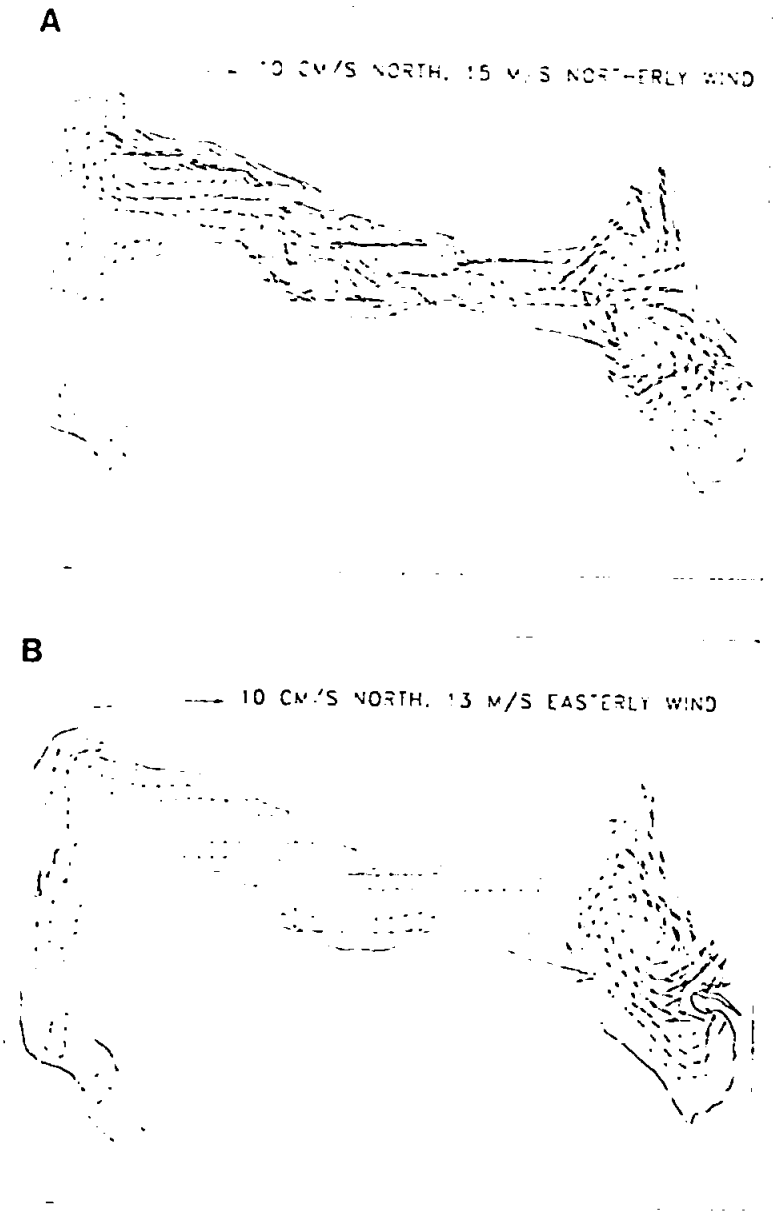

Figure 5. Predicted depth-averaged water circulation for a northerly 15m s^{-1} wind (A) and an easterly 13m s^{-1} wind (B).

following the injection indicated that the tracer particle maxima (area A in Figure 4) occurred where the stresses were less than 0.1Pa. Stresses in

very shallow water (less than 0.5m) were much higher and of the order of 1Pa. The wave-induced stresses increased with wind speed during the following few days but never exceeded 0.2Pa in area A (Figure 4). Maximum wave-induced bed shear stresses occurred near the end of the sampling period (Figure 3) when a 25m s^{-1} wind blew from the southwest (reversing the direction of gyre rotation) and the fetch was at a maximum; stresses then reached 0.4Pa in area A. However, if resuspension had occurred, the wind-driven flow patterns would still have maintained tracer particles in the same main gyre. Because the Rossby number was large, near-bed convergence occurred regardless of the direction of gyre rotation.

The surface sediments within Loe Pool typically have an 80-90% water content (Coard, 1987). The corresponding dry density is approximately 100-230kg m^{-3} and the critical bed shear-strength for erosion is estimated to be 0.3-0.8Pa (Delo, 1988). Assuming the tracer particles to be mixed within the natural sediment, then minimal remobilisation would have occurred for a considerable period following the initial deposition, although some resuspension was likely to have occurred near the end of the sampling period.

THE TAMAR ESTUARY EXPERIMENT

Cycles of sediment resuspension and deposition occur within the turbidity maximum with tidal, seasonal and longer time-scales. The turbidity maximum acts as temporary and long-term source and sink for both sediment and contaminants (Bale *et al.*, 1985; Dyer, 1989). The experiment described here was designed to assist our understanding of the mechanisms which control the chemical cycling of contaminants and to enhance knowledge of the retention, transport and mixing of SPM within the turbidity maximum.

The site chosen was the macrotidal Tamar Estuary (Figure 6). It is easily navigable to the limit of tidal intrusion and has been extensively studied over the last two decades. These studies have provided valuable information on the movement of sediment and pollutants (Bale, 1987; Barton *et al.*, 1991; Uncles *et al.*, 1991).

Field methodology

A tracing experiment was undertaken to examine the dynamics of the Tamar Estuary turbidity maximum. Axial surveys were carried out to determine the tidal range of the turbidity maximum in order to determine the optimum positions of the sampling sites within this region. Six stations (1 to 6 in Figure 6) were chosen and boats were moored in these positions. A mobile vessel was used to monitor the turbidity maximum migration and to carry out the tracer particle injection within the turbidity maximum. The injection took place at 1000h during high-water slack of a spring tide (tidal range: 4m ebb, 4.3m flood) and at 2.3km from the weir. The mass injected comprised 44.5kg of fluorescent tracer particles thoroughly mixed with estuarine water onboard. River flow for the week prior to the study was 5.0m^3s^{-1}, which was close to the average flow for the time of year.

The stationary sampling vessels pumped water samples from the surface, middle and bottom of the water column for tracer particle analysis. In addition, each vessel recorded current velocity and direction, salinity, depth, turbidity (determined gravimetrically) and temperature. Measurements were taken for a whole tidal cycle at 20 minute intervals.

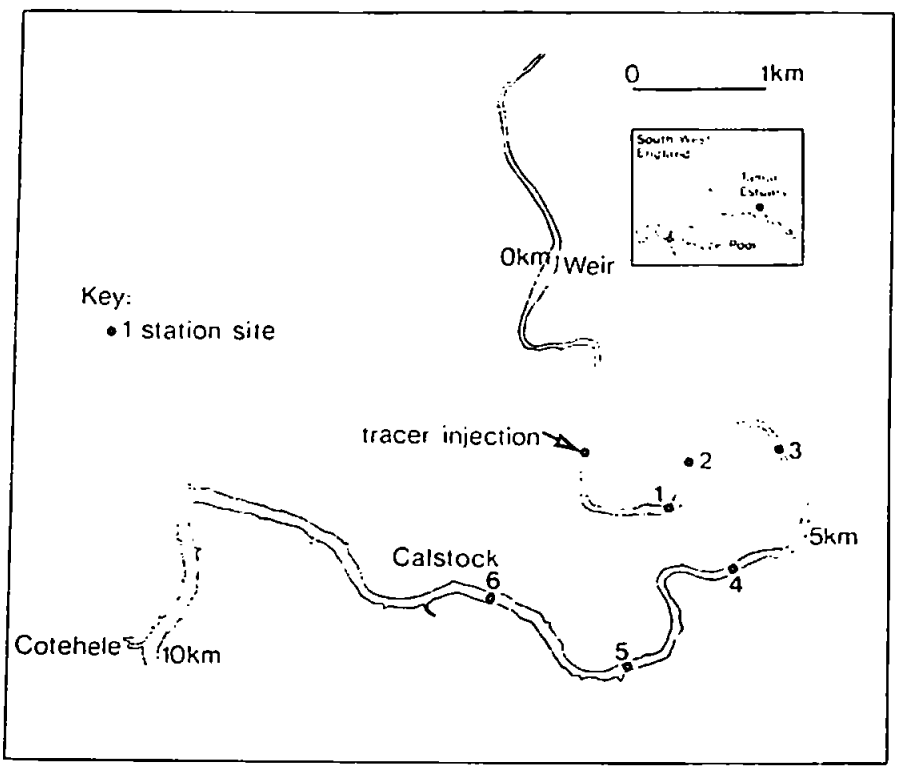

Figure 6. Location and water sampling stations 1 to 6 on the Tamar Estuary, Devon.

Data analysis

The mass budget of the tracer particles through each section of the estuary can be determined by considering the rate of water volume transport per unit width of estuary (Q):

$$Q = H\bar{U} \qquad (1)$$

where H is total depth and U (overbar) is the depth-averaged longitudinal current velocity. The instantaneous rate of transport of tracer particles over the cross-sectional area, A, is given by:

$$T_T = A\overline{UT} \qquad (2)$$

where T is the number of tracer particles per unit volume.

A mass budget for the tracer particles during the ebb and flood tidal flows can be calculated (shown in Table) by integrating the rate of transport (T_T) over the ebb and flood portions of the tide to give T_{TE} and

T_{TF}. The residual transport over the tide (that is, the net number of tracer particles passing the estuarine cross-section over the tidal period) is given by:

$$T_{TT} = T_{TE} + T_{TF} \quad (3)$$

The tracer particles were injected at the head of the saline intrusion at high-water slack and at a site up-estuary of stations 1-6. Therefore, during the early part of the tidal cycle they were advected down estuary with the ebb-flow of water through stations 1-6.

Results

The ebb, flood and tidally averaged synoptic data are presented in the Table, with up-estuary transport as negative, down-estuary transport as positive. Station identifiers (1-6) are shown in the Table followed by their distance from the estuary head and their tidally-averaged water depths, X and <H> respectively. $<\bar{U}>$ is the depth-averaged (overbar) and tidally-averaged (< >) current velocity at each station.

Table. Tidal average (< >) synthesis of longitudinal velocity ($\bar{U}$) and tracer particle data at stations 1-6. See text for an explanation of the symbols. G is the residual SPM flux (up-estuary transport is -ve).

Station	X	<H>	$<\bar{U}>$	T_{TE}	T_{TF}	T_{TT}	G
	km	m	m s^{-1}	No.(10^{14})	No.(10^{14})	No.(10^{14})	ppm m s^{-1}
1	3.0	1.97	0.14	50.2	-16.6	33.6	-49.3
2	3.7	2.06	0.16	9.6	-5.2	4.4	-9.7
3	4.6	2.13	0.21	12.3	-9.4	2.9	-15.9
4	5.6	2.42	0.29	6.2	-8.7	-2.5	107.6
5	7.0	3.28	0.10	18.5	-17.5	1.0	-62.8
6	8.5	2.34	0.04	2.2	-3.7	-1.5	-25.2

The residual currents were directed down-estuary at all stations, with the upper four stations having a current velocity of approximately 0.2m s^{-1} and the lower two stations having a slightly slower current. The residual (tidally averaged) rate of transport of tracer or SPM can be separated into components due to advection by the residual flow of water, vertical shear and tidal pumping (Uncles *et al.*, this volume).

Vertical shear was negligible compared with the other transport mechanisms for both SPM and tracer particles. Transport due to the residual flow of water (the freshwater inputs in steady conditions) was generally directed down-estuary for both SPM and tracer particles. Tidal pumping was dominant for both, but was generally directed up-estuary for SPM and down-estuary for tracer particles. Therefore, in the short-term (that is, for one tidal cycle following tracer particle injection) the SPM and tracer responded in a different way to the tidal processes of erosion, transport and deposition.

The fluorescent tracer particle transport (number of particles passing through a station) are presented for the ebb tide (T_{TE}), flood tide (T_{TF}) and their sum (T_{TT}) in the Table. The residual transport of SPM, G, is also

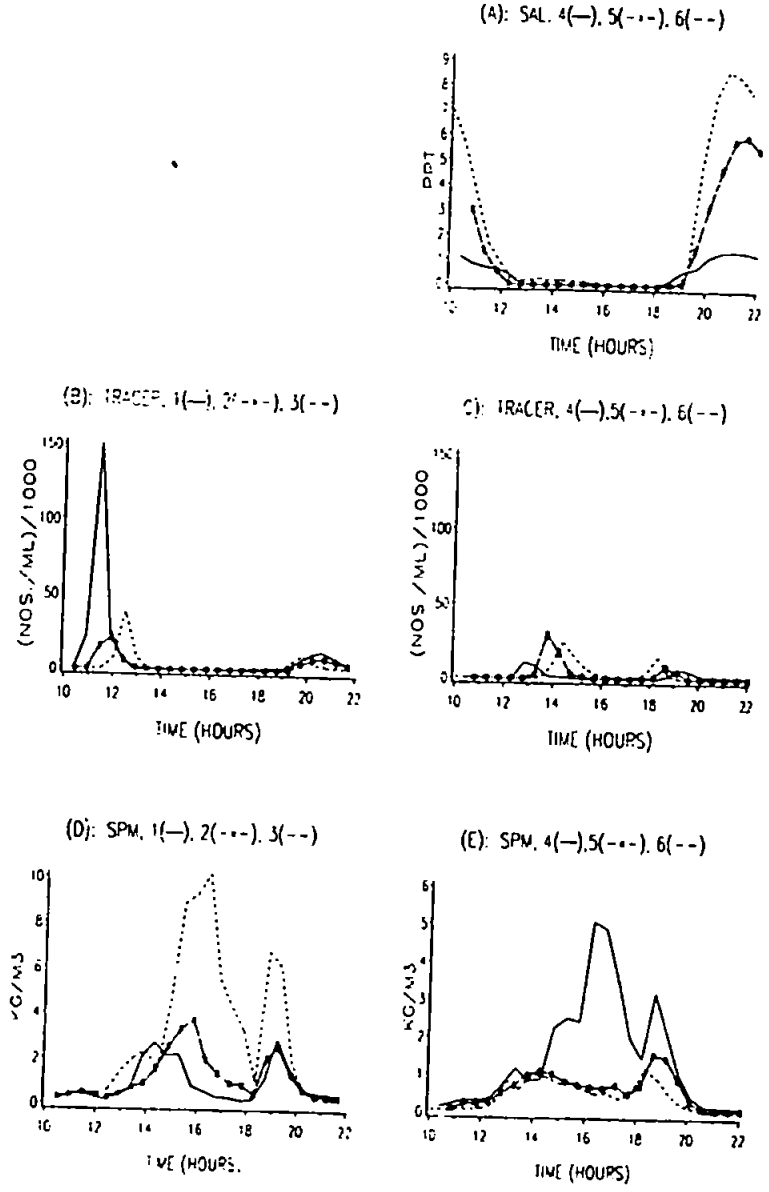

Figure 7. Time-series of depth-averaged salinity, tracer and SPM concentrations on 26/06/90.
(A): Salinity (ppt) at stations 4 (-), 5 (--) and 6 (- -). Salinity at stations 1 to 3, <0.3 and is not shown.*
*(B & C): Tracer concentration (no. * 10^3 ml^{-1}) at stations 1,4 (-), 2,5 (-*-) and 3,6 (- -).*
(D & E): SPM (kg m^{-3}) at stations 1,4 (-), 2,5 (--) and 3,6 (- -).*

shown. Relative to the ebb transport of particles at station 1 ($50.2x10^{14}$) the tidal sum, T_{TT} at each of the lower stations, stations 2-6, was very small, implying that most of the particles remained in the upper estuary. The fact that the ebb numbers did not decrease monotonically indicated the existence of significant sampling errors.

The residual flux of SPM, G, was generally directed up-estuary, implying continued transport of fine-sediment to the upper reaches (Uncles *et al.*, this volume). The residual numbers of tracer particles passing a station cross-section were either very small or directed down-estuary, so that the tracer particles were initially not behaving like SPM.

The depth-averaged, tracer particle concentrations (numbers ml^{-1}) are presented in Figure 7(B,C above) as time-series. The tracer particle/estuarine water slurry was introduced at the start of the ebb tide and 1.1 km up-estuary of station 1 (Figure 6). The tracer particles were advected down-estuary on the ebb flow as a very pronounced peak through each of the stations before returning on the flood tide to the vicinity of their original injection site. The depth-averaged time-series of SPM and salinity are presented in Figures 7(D,E,A above), respectively. SPM maximised at all stations as a result of resuspension due to peak ebb and flood current speeds (Uncles *et al.*, this volume) and the shallow depths near low-water (notably station 3 and 4 at 1620h). There is little correlation between the tracer particle and SPM concentrations, with advection dominating tracer particle behaviour and resuspension dominating SPM behaviour.

The depth-averaged salinity showed a reasonable correlation with the tracer particle advection, with the main tracer peak closely following the freshwater/saltwater interface (Salinity 0.1-0.5ppt). This implies that the tracer particles were largely advected with the tidal flow during the first tidal cycle following injection.

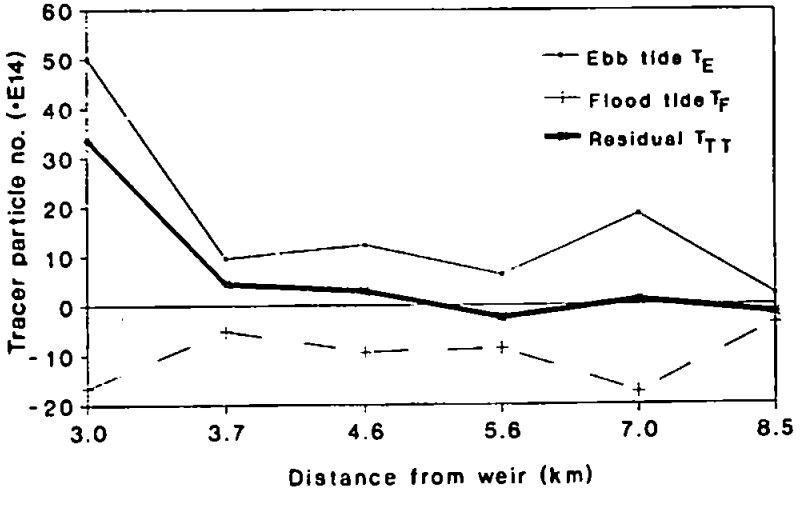

Figure 8. Ebb (T_E), flood (T_F) and residual (T_{TT}) tracer transport during the 26/06/90.

The ebb and flood tracer particle mass budgets (Table and Figure 8 above) indicate a large 'loss' of tracer from the water column on the ebb flow between stations 1 and 2. A possible explanation is that, despite increasing ebb current velocities in the main channel, the tracer particle (which was mixed homogeneously both laterally across the estuary and with depth by the boat's propellor immediately after injection) became trapped by the falling water levels and slow currents on the inter-tidal mudflats. The rising flood tide rapidly submerged the mudflats and caused resuspension and up-estuary transport of the tracer particle and a higher than expected peak in the flood-tide mass budget at station 1.

There is a measured, large net loss of tracer particle in the up-estuary region (Table and Figure 8 above). Approximately the same numbers of tracer particles were advected through stations 2-6 on the ebb as returned on the flood. The increased tracer particle number at station 5 suggests that the water sampling at stations 2-4 may have missed the tracer

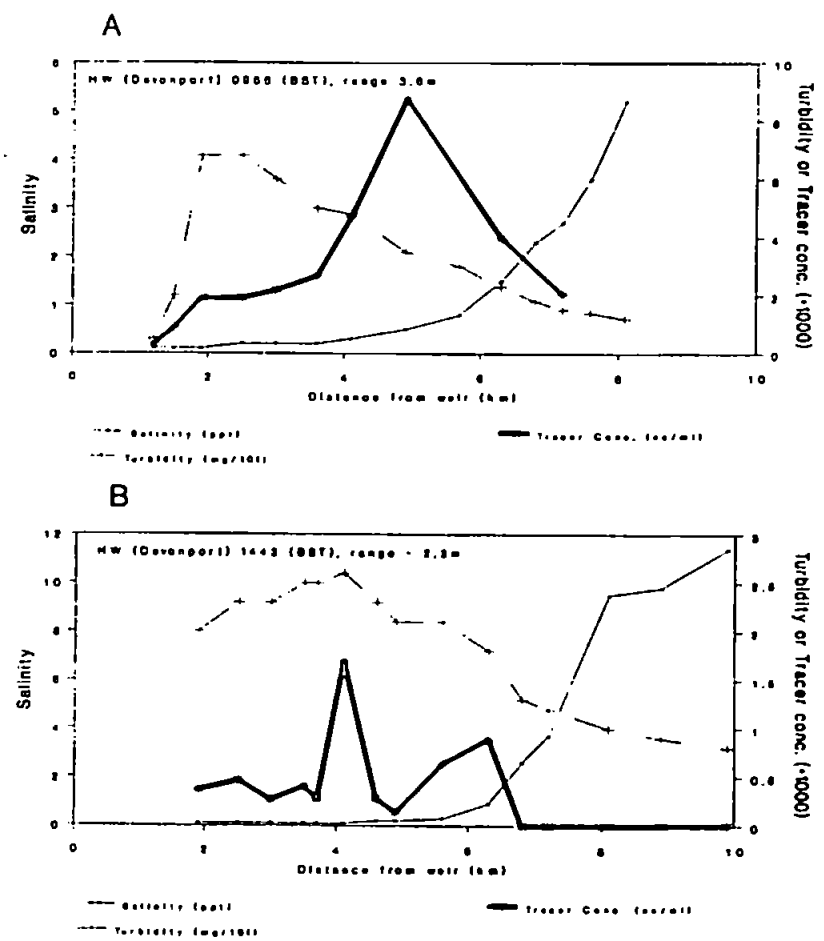

Figure 9. Tracer concentration, salinity and turbidity measurements taken during an axial survey of the turbidity maximum on 27/6/90 (A, the following day) and 3/7/90 (B, the following week).

particle maximum and that the sampling interval of 20 minutes was not sufficiently fine.

The tracer particle was detected in high concentrations 3.1km down-estuary of station 6 (a total migration of 11.1km) by the mobile vessel, immediately after low-water slack (which occurred at approx. 1720h at station 6). The returning tracer particle peak reached Calstock 15-30 minutes after slack water, suggesting that some of the tracer particle had settled out down-estuary of station 6 over low-water slack.

An axial survey of the surface water, carried out the following day (27/06/91), showed a large peak of tracer particles situated 5km from the weir at a salinity of approximately 0.5ppt and slightly down-estuary of the turbidity maximum (Figure 9A above). The tracer, having undergone 2 tidal cycles, had formed a more stable association with the natural suspended fine sediment. The tracer particles had also travelled further up-estuary than the original injection site. This indicates that an up-estuary residual transport of tracer particles had occurred.

A further axial survey was carried out one week later. The surface waters were again sampled, this time during a neap tide on 3/7/90. The tidal range was only 2.3m and because of the slower tidal currents the turbidity maximum SPM concentrations maximised at only 270mg l^{-1} (Figure 9B above). The tracer particles were closely associated with the turbidity maximum and had a well-defined peak in the same position as the SPM peak (Figure 9B above). Both peaks were clearly associated with the head of the saline intrusion at approximately 4km from the weir.

CONCLUSIONS

(1) A fluorescent tracer particle was investigated which had physical characteristics of mean size, fall velocity, density and surface charge similar to natural SPM in aquatic environments. The tracer particles were detected using flow cytometry.

(2) In the freshwater environment of Loe Pool, the locations of the bed-sediment, tracer particle maxima agreed closely with that expected from the predicted, water circulation patterns. Over 75% of the tracer particles were deposited within the perimeter of the main wind-driven gyre predicted by the hydrodynamical model. A further 15% were deposited in very close proximity to this gyre. Any sediment-borne pollutants will tend to accumulate within the deposited sediment there.

(3) Tracer particles injected into the Tamar Estuary, were found to advect with the tidal currents and remained strongly associated with the turbidity maximum at the saline intrusion. Some tracer particles were deposited on the inter-tidal mudflats in the upper reaches during the ebb and in the lower reaches at low-water slack.

(4) The freshwater residence time for the turbidity maximum was approximately 3 days (Uncles *et al.*, 1983). However, the tracer was detectable during the neap tide one week after the initial injection, despite low rates of resuspension of bed sediment. This implied that some of the tracer particles had become incorporated within the natural flocs during the course of time and were associated with the turbidity maximum.

(5) For both Loe Pool and the Tamar Estuary, the experiments described here

demonstrate that particles tend to accumulate in certain areas in response to hydrodynamical forcing. Organic contaminants and other pollutants are known to have an affinity for fine sediment. Such particle accumulation will lead to a build-up of contaminants. The present technique will enable patterns of accumulation to be described and aid both in the prediction of cohesive, sediment dynamics.

REFERENCES

Bale, A.J., (1987). The characteristics, behaviour and heterogeneous chemical reactivity of estuarine suspended particles. Ph.D. thesis, Plymouth Polytechnic, 216pp.

Bale, A.J., Morris, A.W. and Howland, R.J.M. (1985). Seasonal sediment dynamics in the Tamar Estuary. *Oceanologica Acta*, 8, 1-6.

Barton, M.L., Stephens, J.A., Uncles, R.J. and West, J.R. (1991). Particle fall velocities and related variables in the Tamar Estuary. In: Proceedings ECSA 19 Symposium on Estuaries and Coasts: Spatial and Temporal Intercomparisons.

Coard, M.A., (1987). Palaeolimnological study of the history of Loe Pool, Helston, and its catchment. Ph.D. thesis, Polytechnic Southwest.

Delo, E.A., (1988). Estuarine muds manual. Hydraulics Research Ltd., Wallingford. Unpubl. Report SR164, February 1988.

Dyer, K.R., (1986). Coastal and estuarine sediment dynamics. Wiley.

Dyer, K.R. (1989). Sediment Processes in Estuaries: Future Research Requirements. *Journal of Geophysical Research*, 94, 14327-14339.

Hakanson, L. and Jansson, M., (1983). Principles of Lake Sedimentology. Springer.

Lamere Hennessee, E., Blakeslee, P.J. and Hill, J.M., (1986). The distributions of organic carbon and sulfur in surficial sediments of the Maryland portion of Chesapeake Bay. *Sedimentary Petrology*, 56, 674-683.

.oder, T.C. and Liss, P.S. (1985). Control by organic coatings of the surface charge of estuaries suspended particles. *Limnology and Oceanography*, 30, 418-421.

ırsh, J.K., Bale, A.J., Uncles, R.J., Dyer, K.R. (1991). A particle-tracing experiment in a small, shallow lake: Loe Pool. Submitted to British Geomorphological Research Group Symp.: Geomorphology and Sedimentology of Lakes & Reservoirs.

Mehta, A.J. (1984). Characterisation of Cohesive Sediment Properties and Transport processes in estuaries. In: Lecture Notes on Coastal and Estuarine Studies, Vol. 14: Estuarine Cohesive Sediment Dynamics. (ed. A.J.Mehta). Springer-Verlag, New York, Chap. XV, 290-325.

Newman, K.A., Morel, F.M.M. and Stolzenbach, K.D. (1990a). Settling and Coagulation Characteristics of Fluorescent Tracer Particles Determined by Flow Cytometry and Fluorometry. *Environmental Science and Technology*, 24, 506-513.

Newman, K.A., Frankel, S.L. and Stolzenbach, K.D. (1990b). Flow Cytometric Detection and Sizing of Fluorescent Tracer Particles Deposited at a Sewage Outfall Site. *Environmental Science and Technology*, 24, 513-519.

Owen, M.W. (1970). A detailed study of the settling velocities of an estuary mud. Hydraulics Research Station, Wallingford. Unpubl. Report INT 78.

Pickering, D.A., (1987). Chemical and physical analysis of laminated sediment formed in Loe Pool, Cornwall. Ph.D. Thesis, Polytechnic Southwest.

Salomons, W. and Mook, W.G. (1987). Natural tracers for sediment transport studies. *Continental Shelf Research*, 7, 11/12, 1333-1343.

Spanhoff, R. and Suijlen, J.M. (1990). Feasibility of Tracer Studies of Large Scale Cohesive-Sediment Transport. In: Coastal and Estuarine Studies, Vol.36: Estuarine Water Quality Management,(ed. W. Michaelis) , Chap. IV, 197-202.

Sverdrup, H.U. and Munk, W.H., (1947). Wind, sea and swell: theory of relations for forecasting. United States Hydrographic Office, Publ. No. 601, p.44.

Uncles, R.J., (1982). Computed and observed residual currents in the Bristol Channel. *Oceanologica Acta*, 5 (1), 11-20.

Uncles, R.J., Bale, A.J., Howland, R.J.M., Morris, A.W. and Elliott, R.C.A. (1983). Salinity of surface water in a partially-mixed estuary, and its dispersion at low run-off. *Oceanologica Acta*, 6 (3), 289-296.

Uncles, R.J., Stephens, J.A. and Barton, M.L. (1991). The nature of near-bed currents in the upper reaches of an estuary. In: Proceedings of ECSA 19 Symposium on Estuaries and Coasts: Spatial and Temporal Intercomparisons.

Uncles, R.J., Stephens, J.A., Marsh, J.K. and Bale, A.J. (this volume). Synoptic observations of fine-sediment concentration and transport in the turbidity maximum region of an estuary.

Acknowledgements

The authors gratefully acknowledge the provision of data and assistance with analysis by P.Salmon and H. Stevens, and the numerous staff at PSW and PML who were involved in the Tamar Estuary experiment. Special thanks to N. Bowley and J. Stephens for technical assistance. J.K. Marsh gratefully acknowledges the receipt of a Natural Environment Research Council CASE Studentship.

International Symposium on
THE TRANSPORT OF SUSPENDED SEDIMENTS AND ITS MATHEMATICAL MODELLING
Florence (Italy), September 2-5, 1991

SYNOPTIC OBSERVATIONS OF FINE-SEDIMENT CONCENTRATIONS AND TRANSPORT IN THE TURBIDITY MAXIMUM REGION OF AN ESTUARY

R.J. UNCLES†, J.A. STEPHENS†, J.K. MARSH†,‡, and A.J. BALE†

†, Plymouth Marine Laboratory, Plymouth, PL1 3DH, U.K.

‡, Institute of Marine Studies, Polytechnic Southwest, Plymouth PL4 8AA.

SUMMARY

Results are presented of an experiment in which the salinity, longitudinal velocity, SPM concentration and transport of SPM were measured synoptically in the Tamar Estuary over a spring-tide tidal cycle during the summer of 1990. Six vessels were anchored in the turbidity maximum region of the Tamar and within the area containing the mobile stock of fine sediment. Vertical profiling for salinity, longitudinal velocity and SPM was carried out during one tidal cycle and data were obtained at 0.25m above the bed every 5 minutes during the synoptic measurements and for several days before and after. Vertical shear transport of SPM was insignificant compared with that due to tidal pumping. The tidal pumping of SPM was directed up-estuary at all stations and was generally opposed by the down-estuary transport of SPM due to advection by the residual (tidally averaged) water transport. The depth-averaged instantaneous currents were generally flood dominant. During the ebb, the SPM maxima were of the order of 1-10 kg m^{-3}. At the central station the fine-sediment suspensions reached concentrations of 26 kg m^{-3} near the bed during the flood and were highly stratified. The near-bed instrument packages demonstrated the growth of the turbidity maximum over the neap to spring-tide period and its dependence on both local resuspension and the presence of the freshwater-saltwater interface.

INTRODUCTION

A suspended particulate matter (SPM, or turbidity) maximum is a commonly observed feature in the low salinity reaches of many partly-mixed and well-mixed estuaries (Allen et al., 1977, 1980; Festa and Hansen, 1978; Officer and Nichols, 1980; Officer, 1981). In the Tamar Estuary it has been known for several years that tidally-induced resuspension is an essential mechanism for generating a strong, spring-tide turbidity maximum and that the location of the maximum and its associated stock of mobile bed sediment

The terms in the momentum equation represent the acceleration (equal to zero under steady-state conditions), which is equal to the inertial acceleration, the acceleration due to surface slope forcing, the Coriolis acceleration, the acceleration due to wind stress and the retardation due to the quadratic frictional drag at the bed.

The shoreline and bathymetry of Loe Pool were digitized and incorporated into the depth-averaged model using a 53 × 43 array of points with a spacing of 33 × 33 m to discretize the region.

Wave Model

In addition to these equations, an estimate of the wave-induced shear is made using the simplified equations in Hakanson and Jansson (1983). A spatially uniform wind speed is assumed. Equations representing the significant wave height, H, period, T, and wave phase speed, C, are taken to be functions of the fetch, F, and wind speed, $W = |W|$ (Sverdrup and Munk, 1947)

$$gH/W^2 = 0.0026(gF/W^2)^{0.47}$$

$$gT/W = 0.46(gF/W^2)^{0.28}$$

(Smith and Sinclair, 1972).

For sinusoidal waves

$$C = L/T$$

where L is wavelength and

$$C = [(gL/2\pi)\tanh(2\pi h/L)]^{0.5}$$

(Pond and Pickard, 1983; Dyer, 1986), so that C and L can be defined iteratively once T is known.

Knowing h, H and L, the horizontal displacement (d_o) at the bed due to the elliptical orbital motion of a surface wave (Komar and Miller, 1973) can be found

$$d_o = H/\sinh(2\pi h/L)$$

and the maximum horizontal velocity (U_m) can be calculated

$$U_m = \pi d_o/T$$

followed by the peak bed shear stress (τ_w) due to the wave (Sleath, 1984; Dyer, 1986; Soulsby and Smallman, 1986; Delo, 1988; Luettich, Harlemann and Somlyody, 1990).

$$\tau_w = f_w \rho (U_m)^2/2$$

In very shallow, fetch-limited conditions, such as occur in Loe Pool, a viscous, laminar wave boundary layer exists and the wave friction factor (f_w) is given by

$$f_w = 2(Re_w)^{-0.5}$$

and

$$Re_w = U_m d_o/\upsilon$$

where υ is the molecular viscosity (1×10^{-6} m^2 s^{-1}).

$$G_L = \langle Q \rangle \langle \bar{P} \rangle / \langle H \rangle \quad (7)$$

$$G_{TP} = \langle \bar{Q}\bar{P} \rangle / \langle H \rangle \quad (8)$$

and

$$G_V \doteq \langle \overline{HU'P'} \rangle / \langle H \rangle \quad (9)$$

Primes denote deviations from the depth average, such that:

$$P' = P - \bar{P} \quad \text{and} \quad U' = U - \bar{U} \quad (10)$$

RESULTS

Residual transport

A residual (tidal-average) synthesis of the synoptic data are presented in the Table. The convention used in the Table is that up-estuary transport is negative, down-estuary transport is positive. Station identifiers (1-6) are followed by their distances from the head (X, km) and their tidally averaged depths ($\langle H \rangle$, m).

Table. Tidal average (< >) synthesis of longitudinal velocity (U) and SPM (P) flux data at Stations 1-6. See text for an explanation of the symbols. Up-estuary transport is negative.

St.	X KM	$\langle H \rangle$ M	$\langle \bar{U} \rangle$ M/S	$\bar{U}_S$ M/S	$\bar{U}_L$ M/S	G_V PPM M/S	G PPM M/S	G_L PPM M/S	G_{TP} PPM M/S
1	3.0	1.97	0.14	-0.08	0.06	3.7	-49.3	90.3	-143.3
2	3.7	2.06	0.16	-0.06	0.10	0.5	-9.7	115.7	-125.9
3	4.6	2.13	0.21	-0.09	0.12	69.8	-15.9	358.1	-443.8
4	5.6	2.42	0.29	-0.13	0.15	19.0	107.6	225.6	-137.0
5	7.0	3.28	0.10	-0.06	0.05	2.8	-62.8	26.6	-92.2
6	8.5	2.34	0.04	-0.06	-0.02	-0.6	-25.2	-8.3	-16.2

The depth-averaged (overbar) and residual (tidally-averaged, < >) currents are $\langle \bar{U} \rangle$. These currents were directed down-estuary and were typically 0.2 m s^{-1} at the upper four stations near the head and decreased at the lower stations down-estuary. Currents corresponding to the residual, up-estuary water transport 'pumped' into the estuary by the tidal wave are denoted by $\bar{U}_S$ (equation 3) and these were typically 0.10 m s^{-1}. The summation of $\bar{U}_S$ and $\langle \bar{U} \rangle$ is denoted by $\bar{U}_L$ (equation 2), and this current is proportional to the residual, volume-transport of water per unit width (equation 2), which, in turn, is the result of down-estuary transport of

METHODS

Six vessels were anchored in the turbidity maximum region of the Tamar and within the area containing the mobile stock of fine sediment (see Figure 1 for the locations of Stations 1 to 6). Vertical profiling for salinity, longitudinal velocity and SPM was carried out during one tidal cycle on 26 June 1990. Pumped samples were taken for gravimetric analysis of the SPM concentrations and for onboard determination of salinity and temperature using portable salinometers.

Data were also obtained at 0.25m above the bed every 5 minutes during the synoptic measurements and for several days before and after. The instrument packages were modified versions of those discussed by Uncles et al. (1989). These data were obtained at Stations 5 and 3 (see Figure 1).

ANALYSIS

Q is the rate of water volume transport per unit width of estuary, with:

$$Q = H\bar{U} \tag{1}$$

where H is total depth, U the longitudinal velocity and the overbar denotes a depth average. The residual (tidally averaged) rate of water transport per unit width is:

$$\langle Q \rangle = \langle H\bar{U} \rangle = \langle H \rangle . (\langle \bar{U} \rangle + \bar{U}_s) = \langle H \rangle \bar{U}_L \tag{2}$$

where

$$\bar{U}_s = \langle \tilde{H}\tilde{\bar{U}} \rangle / \langle H \rangle \tag{3}$$

with the tilde defining a temporal deviation from the tidal average:

$$\tilde{\bar{U}} = U - \langle U \rangle \quad \text{and} \quad \tilde{H} = H - \langle H \rangle \tag{4}$$

The instantaneous transport of suspended sediment per unit width is given by:

$$Q_P = H\bar{U}\bar{P} \tag{5}$$

where P is SPM concentration and the residual transport per unit width, per unit tidally-averaged depth is:

$$G = \langle Q_P \rangle / \langle H \rangle = \langle H\bar{U}\bar{P} \rangle / \langle H \rangle = G_L + G_{TP} + G_V \tag{6}$$

where G_L is the suspended sediment transport due to the residual flow of water, $\langle Q \rangle$, and G_{TP} and G_V are due to tidal pumping and vertical shear, respectively, with:

fresh, riverine water in steady, laterally homogeneous conditions.

The SPM fluxes are divided into their four constituent parts in the Table. The first part, G_V, is the vertical shear (equation 9) which is the transport due to deviations of the SPM concentration and longitudinal velocity from their respective depth-averaged values. The second term, G, is the total flux (equation 6), the third is advective transport by the residual water flow, G_L (equation 7), and the fourth the tidal pumping term, G_{TP} (equation 8).

Vertical shear transport, G_V, was insignificant compared with that due to tidal pumping, G_{TP}. The tidal pumping of SPM was directed up-estuary at all stations and was generally opposed by the down-estuary transport of SPM due to advection by the residual water transport, G_L. The up-estuary transport of SPM due to up-estuary residual water flow, U_L, at Station 6 is a consequence of the measurements having been obtained in the deep channel, where density-driven currents can be important (Uncles et al., 1986). These findings are consistent with earlier measurements in the upper reaches of the Tamar (Uncles et al., 1985a,b,c).

Apart from Station 4, the total residual flux of SPM, G, was directed up-estuary, which implies continuing transport of mud to the upper reaches with some localised readjustment of sediment at Station 4. The residual flux was of the order of 1-2% of the maximum instantaneous fluxes.

Instantaneous SPM fluxes

Apart from Station 4, the depth-averaged instantaneous currents were flood dominant (Figure 2(a,b)). The low-water slack period existed for just a short time and occurred later moving up-estuary from Stations 6 to 1. Therefore, over the measurement area, the flood current began to flow first at Station 6 and last at Station 1. Ebb currents began to flow first at Station 1 and last at Station 6. The duration of slack currents was much longer at high than at low-water (Figure 2(a,b)).

Maximum ebb currents occurred around 1400h. At Stations 1 to 3 the ebb velocity was fairly constant from about 1500h until shortly before low-water slack when the flow in the upper estuary was riverine and water levels fell only slightly. The ebb current speed increased at Station 4 over this period (Figure 2(b)), indicating that the channel cross-section at that station was decreasing significantly in response to the slow fall in water level as low-water slack approached.

The depth-averaged SPM concentrations at Stations 1 to 6 (Figure 2(c,d)) showed that highest levels were reached at Station 3. Each station had well-defined ebb and flood SPM maxima. During the ebb, these maxima were of the order of 1 kg m^{-3} at Stations 5 and 6, 3-4 kg m^{-3} at Stations 1 and 2, and 5-10 kg m^{-3} at Stations 3 and 4.

The ebb-tide, SPM maxima tended to exceed the flood maxima at Stations 1 to 4 (Figure 2(c,d)), despite the general, flood dominance of current speeds in the upper estuary (Figure 2(a,b)). This apparent anomaly was a consequence of the large depth variations over the tidal cycle. A measure of the sediment loading of the water column, per unit surface area of estuary, is the depth-averaged SPM concentration multiplied by depth, $\overline{PH}$. This quantity is shown in Figure 3(a,b) for Stations 1 to 6. At all stations the SPM loading of the water column per unit surface area of estuary during maximum flood SPM concentrations (around 1900h) was significantly larger than that during maximum ebb SPM concentrations.

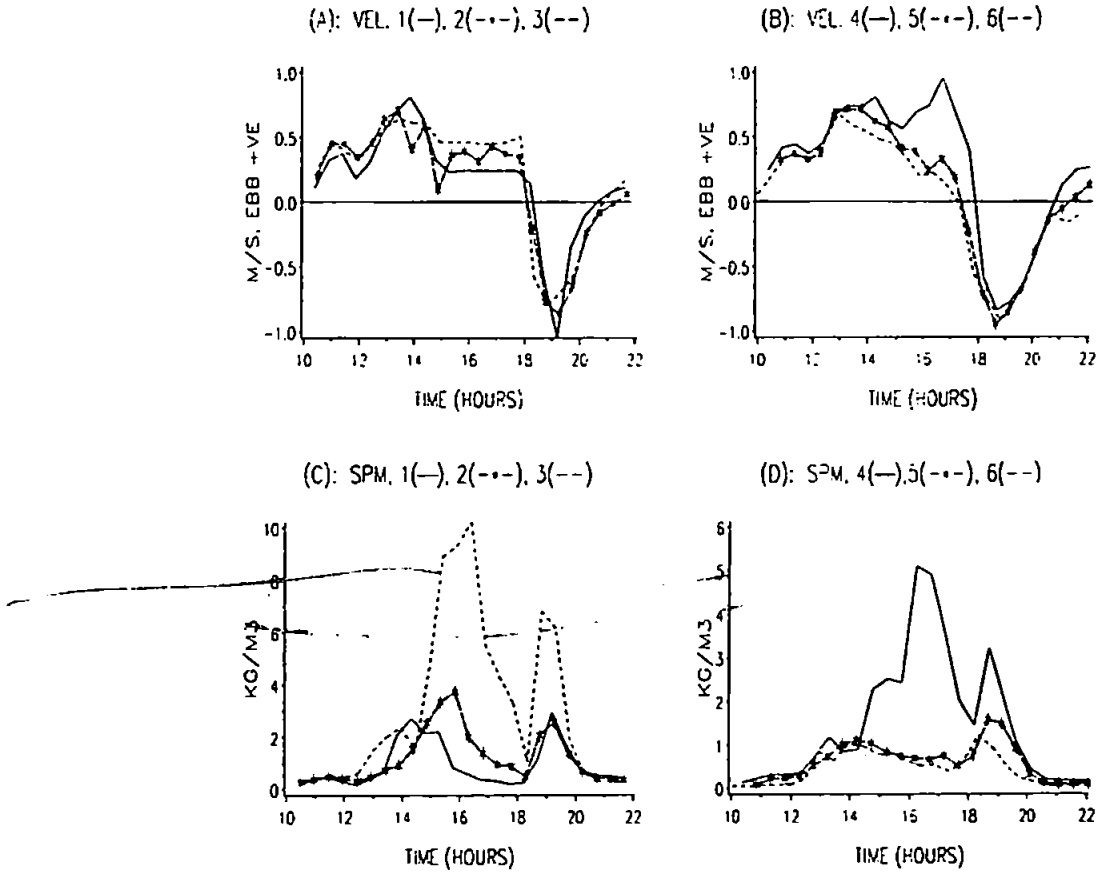

Figure 2. Depth-averaged velocity and SPM concentrations as functions of time in hours (BST) during 26/06/90 at synoptic Stations 1 to 6.
(A): Velocity (m s^{-1}) at Stations 1 (-), 2 (--) and 3 (- -).*
(B): Velocity (m s^{-1}) at Stations 4 (-), 5 (--) and 6 (- -).*
(C): SPM (kg m^{-3}) at Stations 1 (-), 2 (--) and 3 (- -).*
(D): SPM (kg m^{-3}) at Stations 4 (-), 5 (--) and 6 (- -).*

The SPM transport per unit width of estuary (equation 5) for Stations 1 to 6 is shown in Figure 3(c,d). Maximum flood transport occurred around 1900h at all stations. Typical peak, depth-averaged current speeds were less than about 1 m s^{-1} (Figure 2(a,b)), so that the time required to advect SPM the 5.5km from Station 6 to Station 1 on the flood was greater than about 1.5h, in contrast to the 45 min. time delay observed between the SPM peaks. Moreover, this 45 min. delay can be attributed to the time-lag between the occurrence of peak flood currents at Stations 6 and 1. Therefore, although advection of SPM occurred throughout the region, local resuspension and advection of locally resuspended sediment dominated the transport during the flood.

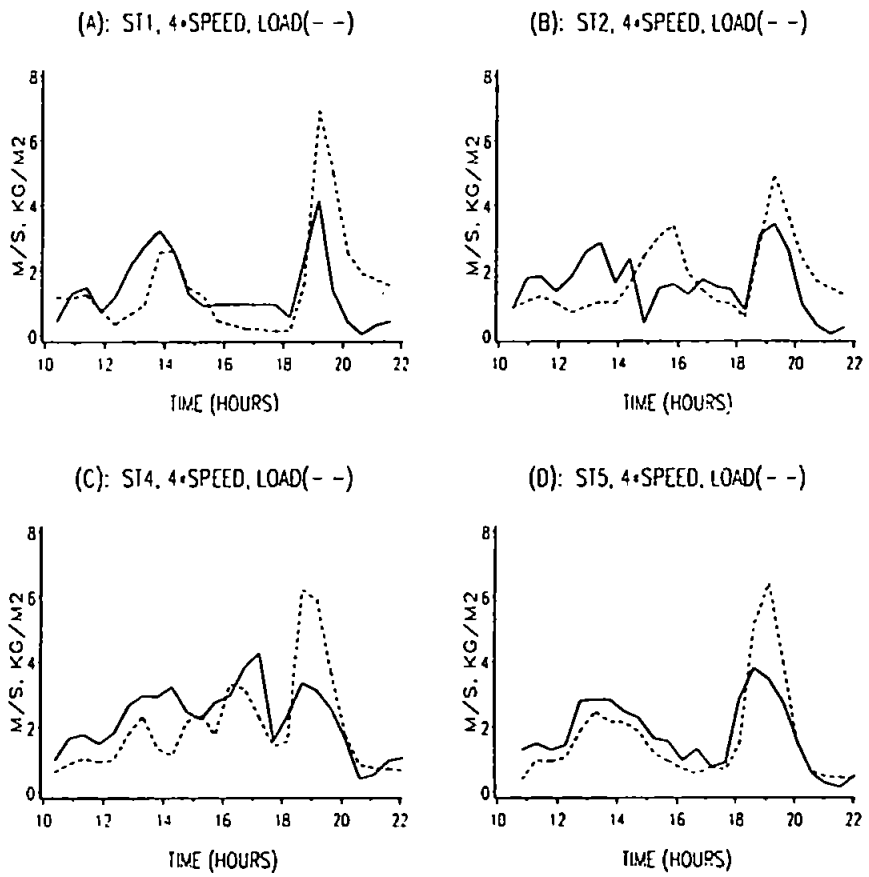

Figure 4. SPM load per unit surface area and depth-averaged water speed as functions of time in hours (BST) during 26/06/90 at synoptic Stations 1, 2, 4 and 5.
(A): SPM load (kg m^{-2}, - -) and speed (m s^{-1}, -, multiplied by 4 for clarity) at Station 1.
(B): SPM load (kg m^{-2}, - -) and speed (m s^{-1}, -, multiplied by 4 for clarity) at Station 2.
(C): SPM load (kg m^{-2}, - -) and speed (m s^{-1}, -, multiplied by 4 for clarity) at Station 4.
(D): SPM load (kg m^{-2}, - -) and speed (m s^{-1}, -, multiplied by 4 for clarity) at Station 5.

The correlations between flood current speeds and SPM concentrations at each station were strong, which implies that local resuspension and transport from mud-sources over the entire station area and down-estuary of Station 6 were the dominant processes influencing SPM levels. Figure 4 shows the depth-averaged velocity and SPM loading of the water column per unit surface area for Stations 1, 2, 4 and 5. Correlations between SPM

loading and ebb velocities were poor for Stations 1-3, reasonable at Station 4 and good for Stations 5 and 6.

Highest, ebb-tide SPM loads occurred at around 1400h, immediately following maximum, depth-averaged currents at Station 1 and around 1600h, roughly 2h after maximum depth-averaged currents at Stations 2 and 3 and close to low-water. This implies that both current speed and water depth played a critical role in determining the onset of bulk erosion and upward mixing of bed sediment at the upper three stations, possibly through a Richardson Number dependence related to the SPM stratification. The good correlation between SPM levels and ebb currents at Station 4 to 6 implies that fine sediment was available for resuspension from these stations and from the whole area between, and immediately up-estuary of, Station 4.

The highest SPM concentrations occurred at Station 3 (see later). These fine-sediment suspensions reached concentrations of 26 kg m^{-3} near the bed during the flood, which can be categorised as fluid mud, and were highly stratified. It therefore appears that the central region, around Station 3, was the main, although temporary, storage area for the mobile stock of fine sediment associated with the turbidity maximum.

SPM - salinity contours

The longitudinal and vertical variations of SPM and salinity over the tidal cycle are shown in Figure 5. Figure 5(left panel) gives hourly data between 1040h and 1540h and Figure 5(right panel) hourly data between 1640h and 2140h. At 1040h the water was ebbing following high-water, which occurred at roughly 1000h. The SPM increased up-estuary but had a low value due to flocculation, settling and deposition over the long, high-water slack period. As the freshwater-saltwater interface (taken to be 0.5ppt) moved down-estuary the SPM concentration increased behind it (1140h).

At 1240h the freshwater-saltwater interface had moved down-estuary of the stations and SPM levels had increased due to local resuspension. The resuspension increased with increasing current speed and reached maximum ebb-tide values at around 1540h to 1640h (Figure 5(right panel)), after maximum currents but when vertical mixing was intense and the SPM was fairly well mixed through the shallow water column.

The fast flood currents followed soon after the brief, low-water slack period at around 1800h and very high concentrations occurred near the bed at 1840h. Maximum concentrations occurred at 1900h (not shown). Some of this SPM moved up-estuary following maximum flood (1940h) and settling and deposition occurred at 2040h approaching high-water, which occurred at roughly 2200h.

The salinity was zero throughout the synoptic measurement period at Stations 1-3, so that there were no vertical or longitudinal density gradients other than those due to SPM. The depth-averaged salinity reached roughly 9 ppt at Station 6 and stratification was several ppt during the early ebb. The stratification which occurred during the early ebb and enhanced mixing which resulted when the stratification was eroded during the subsequent strong ebb currents aided resuspension of SPM and its upward transport. Stabilisation of the water column during periods of stratification restricted upward mixing of eroded SPM.

The rate of freshwater input to the Tamar over the weir (Figure 1) during the several days before the synoptic measurements was higher than that experienced during the preceding two months. As a result, it is unlikely that the bed sediment distribution (which responds more slowly to runoff than salinity, Uncles et al., 1988) was in equilibrium with the

Bottom-mounted instrument packages

The near-bed, continuously monitored data at Stations 5 and 3 generally confirmed these synoptic, six-station findings. In addition, over the 12 day deployment period, the instruments recorded the growth of the intratidal, SPM concentration maxima over the neap to spring-tide period.

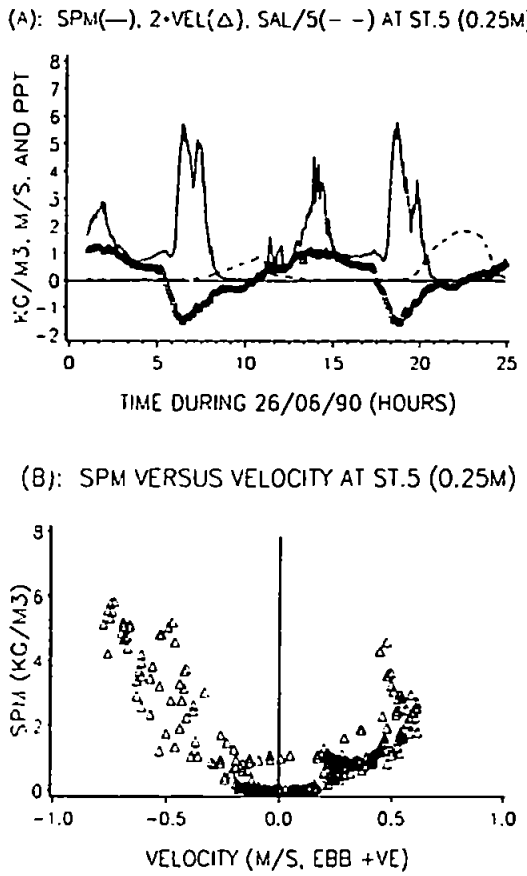

Figure 6. Time-series data for SPM concentrations, velocity and salinity at 0.25m above the bed during 26/06/90 at Station 5.
(A): SPM concentration (kg m^{-3}, -), velocity (m s^{-1}, - -, multiplied by 2 for clarity) and salinity (ppt, Δ, divided by 5 for clarity) against time in hours (BST).
(B): scatter plot of SPM concentration (kg m^{-3}) against velocity (m s^{-1}, ebb positive).

Figure 6(a) shows the time-series data for velocity, SPM and salinity at Station 5 for 26 June 1990. Peak flood currents exceeded peak ebb currents (Figure 6(a)) and flood SPM concentrations exceeded those on the ebb. The near-bed ebb and flood SPM concentrations correlated strongly with

salinity distribution. However, it is clear from Figure 5 (1040 and 2040h) that at high-water the freshwater-saltwater interface was located in the vicinity of the mobile stock of bed sediment.

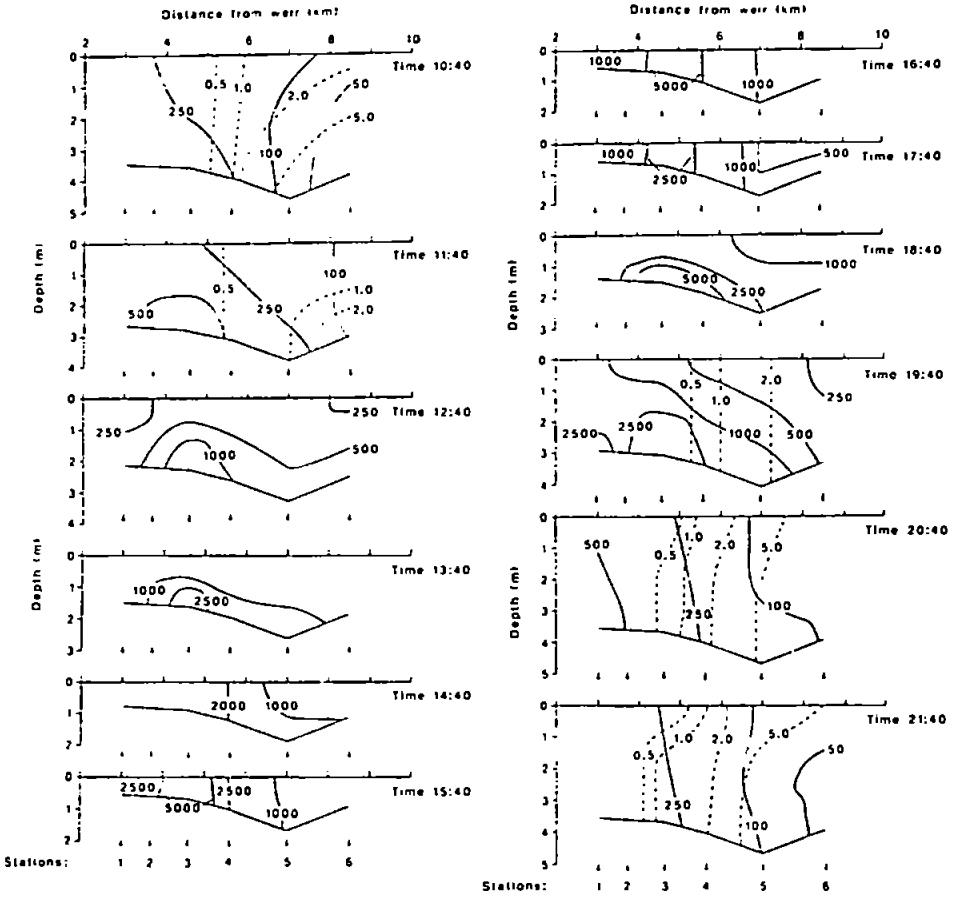

Figure 5. Longitudinal and vertical section of the upper Tamar between 2 to 10km from the weir, covering synoptic Stations 1 to 6, and showing contour plots for SPM concentrations (-) and salinity (- -) during 26/06/90. The left panel shows contours at times (BST) between 1040 and 1540 and the right panel times between 1640 and 2140.

The freshwater-saltwater interface had only a minor influence on SPM levels in these measurements (Figure 5) but, together with the tidal current speed and its flood-ebb asymmetry, it is known to have an important influence on the long-term location and localisation of the stock of mobile bed fine-sediment. The role of the freshwater-saltwater interface in the behaviour of the SPM transport is more evident from the bottom-mounted instrument packages.

near-bed ebb and flood current speeds (see scatter plot of SPM versus velocity in Figure 6(b)) but the ebb correlation was weaker, with SPM levels that continued to rise once maximum ebb currents had been reached. This implies that a large quantity of easily erodible sediment was advected into the vicinity of Station 5 from the major source areas around Stations 3 and 4.

The flood SPM levels were double-peaked. The first, major peak was associated with the maximum flood current speed whilst the second, minor peak was associated with the passage of the freshwater-saltwater interface (the advected water of longitudinally increasing salinity between 0 and 1 ppt). This secondary peak was possibly SPM resuspended by mixing in the fresh water immediately behind the interface during the ebb (see Figure 5, 1140h) and advected with the interface back up-estuary during the flood. Little time was available for settling and consolidation of SPM during low-water slack.

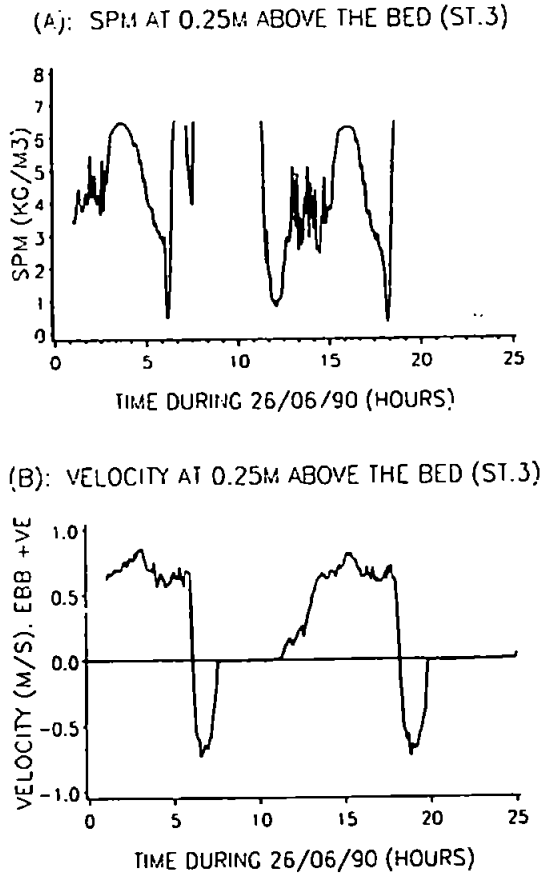

Figure 7. Time-series data for SPM concentrations and velocity at 0.25m above the bed during 26/06/90 at Station 3.
(A): SPM concentration (kg m^{-3}) against time in hours (BST).
(B): Velocity (m s^{-1}, ebb positive) against time in hours (BST).

At Station 3, in the fluid mud area, the near-bed SPM concentrations exceeded the calibration of the SPM sensor (8 kg m^{-3}) during the flood (Figure 7(a)). This was accompanied by a rapid decrease in longitudinal velocity as the fluid mud affected the near-bed flow field and 'stalled' the flow (Figure 7(b)).

A very strong correlation between near-bed SPM concentrations on the ebb and near-bed ebb currents implied the dominance of resuspension from nearby up-estuary areas and those in the vicinity of Station 3. However, maximum SPM levels were reached after maximum current speeds and at shallower water depths closer to the time of low-water, again implying the existence of a critical Richardson Number for erosion and resuspension of SPM. The salinity was very low throughout the day at Station 3 and there was no salinity-induced behaviour.

CONCLUSIONS

(1) The depth-averaged, residual currents were directed down-estuary and were typically 0.2 m s^{-1} at the upper four stations near the head and slower at the lower stations. Currents corresponding to the residual, up-estuary water transport 'pumped' into the estuary by the tide were typically 0.10 m s^{-1}.

(2) Vertical shear transport of SPM was insignificant compared with that due to tidal pumping. The tidal pumping of SPM was directed up-estuary at all stations and was generally opposed by the down-estuary transport of SPM due to advection by the residual water transport.

(3) Apart from Station 4, the total residual flux of SPM was directed up-estuary, which implies continuing transport of mud to the upper reaches with some localised readjustment of sediment at Station 4. The residual flux was of the order of 1-2% of the maximum instantaneous fluxes.

(4) Apart from Station 4, the depth-averaged instantaneous currents were flood dominant. The low-water slack period existed for just a short time and occurred later moving up-estuary from Stations 6 to 1.

(5) The depth-averaged SPM concentrations reached highest values at Station 3. Each station had well-defined ebb and flood SPM maxima. During the ebb, these maxima were of the order of 1 kg m^{-3} at Stations 5 and 6, 3-4 kg m^{-3} at Stations 1 and 2, and 5-10 kg m^{-3} at Stations 3 and 4.

(6) At all stations the SPM loading of the water column per unit surface area of estuary during maximum flood SPM concentrations was significantly larger than that during maximum ebb SPM concentrations. Local resuspension and advection of locally resuspended sediment dominated the transport during the flood.

(7) The SPM behaviour was more complicated on the ebb. Highest, ebb-tide SPM loads occurred immediately following maximum, depth-averaged currents at Station 1 and roughly 2h after maximum depth-averaged currents at Stations 2 and 3 and close to low-water. This implies that both current speed and water depth played a critical role in determining the onset of bulk erosion and upward mixing of bed sediment at the upper three stations.

(8) The highest SPM concentrations occurred at Station 3. These fine-sediment suspensions reached concentrations of 26 kg m^{-3} near the bed during the flood, which can be categorised as fluid mud, and were highly stratified. It therefore appears that the central region, around Station 3, was the main, although temporary, storage area for the mobile stock of fine sediment associated with the turbidity maximum.

(9) The longitudinal and vertical variations of SPM and salinity over the tidal cycle showed that the SPM increased up-estuary at high water, forming a turbidity maximum close to the weir, and had low concentrations due to flocculation, settling and deposition over the long, high-water slack period.

(10) Two instrument packages deployed at 0.25m above the bed in the turbidity maximum area demonstrated the growth of the turbidity maximum over the neap to spring-tide period and its dependence on both local resuspension, and therefore the location of the stock of mobile bed-source sediment, and the presence of the freshwater-saltwater interface.

(11) The flood SPM levels were double-peaked at Station 5. The first, major peak was associated with the maximum flood current speed whilst the second, minor peak was associated with the passage of the freshwater-saltwater interface.

(12) At Station 3, in the fluid mud area, the near-bed SPM concentrations exceeded the calibration of the SPM sensor, 8 kg m^{-3}, during the flood. This was accompanied by a rapid decrease in longitudinal velocity as the fluid mud affected the near-bed flow field and 'stalled' the flow. A very strong correlation between near-bed SPM concentrations on the ebb and near-bed ebb currents implied the dominance of resuspension from nearby up-estuary areas and those in the vicinity of Station 3. However, maximum SPM levels were reached after maximum current speeds and at smaller water depths nearer low-water, again implying the importance of both current speed and water depth.

REFERENCES

Allen, G.P., J.C. Salomon, P. Bassoulet, Y. Du Penhoat and C. De Grandpre, 1980: Effects of tides on mixing and suspended sediment transport in macrotidal estuaries, *Sedimentary Geology, 26*, 69-90.

Allen, G.P., G.Sauzay, P. Castaing and J.M. Jouanneau, 1977: Transport and deposition of suspended sediment in the Gironde Estuary, France, In: *Estuarine processes*, (ed. M Wiley), Academic Press, N.Y., 63-81.

Dronkers, J., 1986: Tide-induced residual transport of fine sediment, In: *Physics of shallow estuaries and bays*, (ed. J. van de Kreeke), Lecture notes on coastal and estuarine studies, 16, Springer-Verlag, 228-224.

Festa, J.F. and D.V. Hansen, 1978: Turbidity maxima in partially mixed estuaries: A two-dimensional numerical model, *Estuarine and Coastal Marine Science, 7*, 347-359.

Grabemann, I. and G. Krause, 1989: Transport processes of suspended matter derived from time-series in a tidal estuary, *J. Geophysical Research, 94*, No. C10, 14373-14379.

Hamblin, P.F., 1989: Observations and model of sediment transport near the turbidity maximum of the Upper Saint Lawrence Estuary, *J. Geophysical Research, 94*, No. C10, 14419-14428.

Kirby, R.A. and W.R. Parker, 1977: The physical characteristics and environmental significance of fine-sediment suspensions in estuaries, in: *Estuaries, Geophysics and the environment*, (ed. C.B. Officer), 110-120, National Academy Press, Washington, D.C.

Officer, C.B., 1981: Physical dynamics of estuarine suspended sediments, *Marine Geology*, 40, 1-14.

Officer, C.B. and M.N. Nichols, 1980: Box model application to a study of suspended sediment distributions and fluxes in partially mixed estuaries. In : *Estuarine Perspectives*, Academic Press, London, 329-340.

Sheng, Y.P. and C. Villaret, 1989: Modeling the effect of suspended sediment stratification on bottom exchange processes, *J. Geophysical Research, 94*, No. C10, 14429-14444.

Uncles, R.J., R.C.A. Elliott and S.A. Weston, 1985a: Observed fluxes of water, salt and suspended sediment in a partly mixed estuary, *Estuarine and Coastal Shelf Science, 20*, 147-167.

Uncles, R.J., R.C.A. Elliott and S.A. Weston, 1985b: Dispersion of salt and suspended sediment in a partly mixed estuary, *Estuaries, 8*, 256-269.

Uncles, R.J., R.C.A. Elliott and S.A. Weston, 1985c: Lateral distributions of water, salt and sediment transport in a partly mixed estuary, In : *Proc. of the 19th Int. Conf. on Coastal Engineering*, ASCE, Chapter 204, 3067-3077.

Uncles, R.J., R.C.A. Elliott and S.A. Weston, 1986: Observed and computed lateral circulation patterns in a partly mixed estuary, *Estuarine, Coastal and Shelf Science, 22*, 439-457.

Uncles, R.J., J.A. Stephens and T.Y. Woodrow, 1988: Seasonal cycling of estuarine sediment and contaminant transport, *Estuaries, 11*, 108-116.

Uncles, R.J. and J.A. Stephens, 1989: Distributions of suspended sediment at high water in a macrotidal estuary, *J. Geophysical Research, 94*, No. C10, 14395-14405.

Uncles, R.J., J.A. Stephens, R.H. Bruce, C.D. Barrett and N.J. Bloomer, 1989: Observations of temporal variability in a partly mixed estuary using a new instrument package, In: *Developments in estuarine and coastal study techniques* (eds. J. McManus and M. Elliott), Olsen and Olsen - International Symposium Series, Fredensborg, Denmark, 151-158.

West, J.R. and A.Y.A. Sangodoyin, 1991: Depth-mean tidal current and sediment concentration relationships in three partially mixed estuaries, *Estuarine, Coastal and Shelf Science*, *32*, 141-160.

West, J.R., Oduyemi, K.O. and K. Shiono, 1991: Some observations on the effect of vertical density gradients on estuarine turbulent transport processes, *Estuarine, Coastal and Shelf Science*, *32*, 365-384.

Wolanski, E., J. Chappell, P. Ridd and R. Vertessy, 1988: Fluidization of mud in estuaries, *J. Geophysical Research*, *93*, No. C3, 2351-2361.